Adaptace vlastností polymerních kompozitů na bázi uhlíkových nanotrubic z pohledu jejich možných senzorických vlastností

Robert Olejník

Disertační práce
2013

Univerzita Tomáše Bati ve Zlíně
Fakulta technologická

Disertační práce

ADAPTACE VLASTNOSTÍ POLYMERNÍCH KOMPOZITŮ NA BÁZI UHLÍKOVÝCH NANOTRUBIC Z POHLEDU JEJICH MOŽNÝCH SENZORICKÝCH APLIKACÍ

ROBERT OLEJNÍK

Fakulta technologická

Zlín červenec 2013

doktorský studijní program: 2808-V Chemie a technologie materiálů

28-03-9 Technologie makromolekulárních látek

Školitel: Doc*., Ing. Petr Slobodian, Ph.D.*

Obsah

Abstrakt

Stěžejním tématem je využití uhlíkových nanotrubic v kompozitních strukturách nebo i samostatně ve formě sítě z náhodně zapletených uhlíkových nanotrubic. Dále jsou zkoumány vlastnosti těchto struktur a to především jejich citlivost na tlak, ohyb či detekci par organických rozpouštědel.

Jedním z důležitých kroků je příprava membrány technologií elektrospinning. Tato membrána slouží k vytvoření sítě ze zapletených uhlíkových nanotrubic pomocí vakuové filtrace a také k vytvoření kompozitu s aktivní vrstvou na povrchu.

Další krokem je úprava povrchu uhlíkových nanotrubic tak, aby se zvýšila jejich citlivost. Vhodnou metodou je např. chemická oxidace nebo pokrytí uhlíkových nanotrubic polymerem.

Abstract

The main topic of this thesis is application of carbon nanotubes in composites or in the form of randomly entangled carbon nanotubes network. The properties of these structures, mainly their sensitivity to compression and elongation, sensitivity to the change of chemical surrounding in the course of detection of volatile organic compounds are further examined in this work.

One important step is in the preparation of the filtering membrane by technology electrospinning. This membrane is used to prepare network made of entangled carbon nanotubes by vacuum filtration technique. In this way, a polymeric composite structure with an active layer on the test specimen surface is prepared.

The following work was in carbon nanotubes surface modification to make them to be more sensitive. Suitable methods are for example chemical oxidation or polymer grafting of carbon nanotubes surface.

Keywords: carbon nanotubes, functionalization, sensing element, buckypaper, electrospinning

Publikační aktivity

Disertační práce obsahuje následující články označené římskými číslicemi:

I. R. Olejnik, P. Slobodian, P. Riha, and P. Saha, "An Electrically Conductive and Organic Solvent Vapors Detecting Composite Composed of an Entangled Network of Carbon Nanotubes Embedded in Polystyrene,"*Journal of Nanomaterials*, vol. 2012, Article ID 365062, 7 pages, **2012**. doi:10.1155/2012/365062 (IF=1,675), web of science, citace: 0

II. R. Olejnik, P. Slobodian, P. Riha and M. Machovsky, "Increased sensitivity of multiwalled carbon nanotube network by PMMA functionalization to vapors with affine polarity,". *Journal of Applied Polymer Science*. **2012**,vol. 126, iss. 1, s. 21-29. ISSN 0021-8995., (IF=1,2),web of science

III. P. Slobodian, P. Riha, R. Olejnik, U. Cvelbar, P. Saha, Enhancing effect of KMnO4 oxidation of carbon nanotubes network embedded in elastic polyurethane on overall electro-mechanical properties of composite, Composites Science and Technology, Volume 81, 14 June 2013, Pages 54-60, ISSN 0266-3538, 10.1016/j.compscitech.2013.03.023. (IF=3,144), web of science.

IV. P. Slobodian, P. Riha, R. Olejnik and P. Saha. "Electromechanical properties of carbon nanotube networks under compression, ", *Measurement Science and Technology*. **2011**, vol. 22, iss. 12, s. 1-7, (IF= 1,353), web of science

V. P. Slobodian, P. Riha, A. Lengalova, R. Olejnik, D. Kimmer and P. Saha. "Effect of compressive strain on electric resistance of multi-wall carbon nanotube networks, ". Journal of Experimental Nanoscience [online]. 2011, vol. 6, iss. 3, s. 294-304. ISSN 1745-8080, (IF= 1,011), web of science

VI. D. Kimmer, D. Petras, M. Zatloukal, R. Olejnik, P. Saha and P. Slobodian. "Polyurethane/MWCNT nanowebs prepared by electrospinning proces, " *Journal of Applied Polymer Science* [online]. **2009**, vol. 111, iss. 6, s. 2711-2714. ISSN 0021-8995, (IF=1,240), web of science, citace

VII. R. Olejnik, P. Slobodian, U. Cvelbar, P. Riha and P. Saha, "Plasma treatment as a way of increasing the selectivity of carbon nanotube networks for organic vapor sensing elements, " *Key Engineering Materials* Vol. 543 (2013) pp 410-413 (2013) Trans Tech Publications, Switzerland doi:10.4028/www.scientific.net/KEM.543.410, (IF=0,224), web of science

VIII. R. Olejnik, P. Slobodian and P. Saha, "Sensing element made of multi-wall carbon nanotube network for organic vapor detection, " *Key Engineering Materials*, Vol. 495 (2012), pp 355-358 Online available since 2011/Nov/15 (2012) Trans Tech Publications, Switzerland doi:10.4028/www.scientific.net/KEM.495.355, (IF=0,224), web of science

IX. D. Matejik, R. Olejnik, P. Slobodian and P. Saha, "Improved selectivity of oxidized multiwall carbon nanotube network for detection of ethanol vapor, " *Key Engineering Materials* Vol. 495 (2012) pp 83-86, doi:10.4028/www.scientific.net/KEM.495.83, (IF=0,224), web of science

X. D. Petras, P. Slobodian, R. Olejnik and P. Riha, "Temperature Dependence of Electrical Conductivity of Multi-Walled Carbon Nanotube Networks in a Polystyrene Composite," *Key Engineering Materials* Vol. 543 (2013) pp 356-359 (2013) Trans Tech Publications, Switzerland doi:10.4028/www.scientific.net/KEM.543.356, (IF=0,224), web of science

XI. A. Lengalova, P. Slobodian, R. Olejnik, P. Riha, "A pressure sensing conductive polymer composite with carbon nanotubes for biomechanical applications," *Key Engineering Materials* Vol. 543 (2013) pp 43-46 (2013) Trans Tech Publications, Switzerland doi:10.4028/www.scientific.net/KEM.543.43, (IF=0,224), web of science

XII. R. Boruta, R. Olejnik, P. Slobodian and P. Riha, "Different Kinds of Carbon-Based Material for Resistive Gas Sensing," *Key Engineering Materials* Vol. 543 (2013) pp 269-272, doi:10.4028/www.scientific.net/KEM.543.269, (IF=0,224), web of science

---

Disertační práce se dále odkazuje na další publikační aktivity, které přispívají k ucelenému přehledu adaptace polymerních kompozitů na bázi uhlíkových nanotrubic.

DALŠÍ PUBLIKAČNÍ AKTIVITY

ČLÁNKY BEZ IMPAKT FAKTORU

XIII. R. Olejnik, Petr Slobodian, P. Riha and P. Saha, "Selectivity of multi-wall carbon nanotube network sensoric units to ethanol vapors achieved by carbon nanotube oxidation," *Journal of Materials Science Research*, Vol. 1, No. 1; January 2012

XIV. R. Olejnik, P. Slobodian and P. Saha, "Multi-wall Carbon Nanotube Network Sensing Element for Organic Vapor Detection," *Journal of Materials Science and Engineering A1* (2012), Formerly part of Journal of Materials Science and Engineering, ISSN 1934-8959

KAPITOLA V KNIZE

XV P. Slobodian, P. Riha, R. Olejnik, "Electromechanical sensors based on carbon nanotube networks and their polymer composites," in *New Developments and Applications in Sensing Technology*, 1st Edition, Springer, 2011, 337 p., ISBN: 978-3-642-17942-6.

PATENTY A PRŮMYSLOVÉ VZORY

XVI. Užitný vzor s názvem "Tlakový senzor a způsob jeho výroby", podáno dne 25. 6. 2010 pod číslem PV 2010-506

XVII. Užitný vzor s názvem "Vysoce elastický plošný senzor určený k detekci tahové deformace", podáno dne 2. 11. 2012 pod číslem 2012-26935

XVIII. Funkční vzorek s názvem "Mikropásková anténa na bázi sítě z uhlíkových nanotrubic jako aktivní vrstva nanesená na skleněném substrátu"

ČLÁNKY VE SBORNÍKU S ISBN

XIX. R. Olejnik, P. Slobodian, P. Riha, D. Kimmer, P. Saha, "Multi-Wall Carbon Nanotube Networks Prepared From Pure MWCNT and Their Oxidised Forms Effect of Compressive Strain on Electric Resistance," 2. mezinárodní konference NANOCON 2010,12. - 14. 10. 2010, Olomouc, Czech Republic, ISBN: 978-80-87117-07-1

XX. R Olejnik., P. Slobodian, U. Cvelbar, "The Effect of Change Selectivity for Sensing Element Made from Multi-Wall Carbon Nanotube network Treated by Plasma," 3. mezinárodní konference NANOCON 2011, 21.-23. září 2011 Brno, Česká republika, ISBN: 978-80-87294-23- 9

XXI. R. Olejnik, P. Slobodian, U. Cvelbar, "Plasma surface modification of entangled multi-wall carbon nanotubes network for organic vapor detection," ICAPT 2011, 11-13 September *2011,* Strunjan, Slovenia. ISBN 978-961-92989-3-0

XXII. R. Olejnik, P. Slobodian, S. Almajdalawi, "Thin sensitive layer base on Multiwalled carbon nanotube/polypyrrole composite as a potential gas sensor," 5th WSEAS International Conference on SENSORS and SIGNALS (SENSIG '12), Sliema, Malta, September 7-9, 2012, ISBN: 978-1-61804-119-7

XXIII. R. Olejnik, P. Liu, P. Slobodian, M. Zatloukal,P. Sáha, "Characterization of Carbon Nanotube Based Polymer Composites Through Rheology," Novel trends in rheology III, July 28 -29, 2009, Zlín, Czech republic, ISBN 978-0-7354-0689-6

XXIV. D. Matejik, R. Olejnik, P. Slobodian, P. Saha, "Improved Selectivity of Oxidized Multiwall Carbon Nanotube Network for Detection of Ethanol Vapor," International Conference for Materials and Applications for Sensors and Transducers, ICMAST-2011, May 13-17, 2011,Kos Greece, ISBN-978-3-03785-292-7

XXV. P. Slobodian, R. Olejnik, P. Saha "Electrically Conductive High Elastic Polyurethane/Carbon Nanotube Entangled Network Film Composite with Strain Sensing Potential," 3. mezinárodní konference Nanocon 2011, 21.-23. září 2011, Brno, Česká republika, ISBN: 978-80-87294-23- 9

XXVI. P. Slobodian, R. Olejnik, P. Riha, P. Saha, "Effect of functionalized nanotubes with HNO_3 on electrical sensory properties of carbon nanotubes/polyurethane composite under elongation," WSEAS International Conferences, Catania, Sicily, Italy, November 3-5 2011. ISBN:978-1-61804-047-3.

XXVII. D. Petráš, P. Slobodian, R. Olejnik, P. Riha, "Improved electro-mechanical properties of carbon nanotubes network embeded in elastic polyurethane by oxidation," 5th WSEAS International Conference on SENSORS and SIGNALS (SENSIG '12), Sliema, Malta, September 7-9, 2012, ISBN: 978-1-61804-119-7

ČLÁNKY VE SBORNÍKU BEZ ISBN

XXVIII. R. Olejnik, P. Slobodian, U. Cvelbar, "Plasma treatment as a way of increasing the selectivity of carbon nanotube networks ofor organic vapor sensing elements," International Conference for Materials and Applications for Sensors and Transducers, ICMAST-2012, May 24-28, 2011,Budapest Hungary.

XXIX. P. Slobodian, P. Riha, R. Olejník, D. Petras, M. Machovsky, P. Sáha, “Electromechanical sensors based on carbon nanotube network,”, 4th International Conference on Sensing Technology, June 3-5, 2010, Lecce, Italy.

XXX. P. Říha, P. Slobodian,R. Olejník,D. Petráš,P. Sáha, “Development of manufacturing process for polymer/carbon nanotubes network composites,” 10th International Conference on Flow Processes in Composite Materials, July 11-15, 2010, Ascona, Switzerland

ABSTRAKTY Z KONFERENCÍ

XXXI. R. Olejník, D. Kimmer, P. Slobodian, P. Říha, P. Sáha, “Polyurethane/Carbon nanotube nanocomposite fibers prepared by electrospinning,” Carbon Nanoscience and Nanotechnology Nanotec09, August 26-29,2009, *Brussels, Belgium*

XXXII. R. Olejnik, P. Slobodian and P. Saha, “Carbon nanotube network embeded in high elastic polyurethane and its use for body kinematice and joint flexion sensing,” 4. ročník mezinárodní konference NANOCON 2012, 23. - 25. 10. 2010, Brno, Czech Republic,ISBN: 978-80-87249-32-1

XXXIII. R. Boruta, P. Slobodian, R. Olejnik, M. Machovsky and P. Riha, “Improvement of strain sensing element based on the carbon nanotube network by $KMnO_4$ oxidation,”International Conference for Materials and Applications for Sensors and Transducers, ICMAST-2012, May 24-28, 2011,Budapest Hungary

1. Úvod

Polymerní kompozity jsou pro praxi velmi zajímavé materiály především proto, že lze vlastnosti výsledného kompozitu upravit tak, aby odpovídaly požadavkům na jeho použití. Tyto vlastnosti z kompozitů dělají pro praxi užitečné materiály. Kompozity jsou složeny z matrice a plniva. V našem případě jsou použity různé druhy polymerů. Jako plnivo jsou použity uhlíkové nanotrubice, které jsou buď v neupraveném stavu, nebo jsou upraveny pro jejich lepší dispergovatelnost.

Práce popisuje přípravu kompozitních materiálů na bázi uhlíkových nanotrubic. Uhlíkové nanotrubice dávají materiálům lepší vlastnosti např. vyšší pevnost. Uhlíkové nanotrubice jsou ve formě vrstvy, která má velmi zajímavé vlastnosti. Tyto vlastnosti jsou charakterizovány různými metodami.

V průběhu práce bylo zjištěno, že síť ze zapletených uhlíkových trubic má jedinečné vlastnosti. Síť z náhodně zapletených uhlíkových nanotrubic, z kterých je vyrobena aktivní vrstva, je citlivá na mechanické podněty, a také na páry organických rozpouštědel. Aktivní vrstva může být samonosná, nebo nanesená na filtrační membráně a spojená s polymerní vrstvou, nebo ve formě sítě umístěné na elektrodách.

2. Elektrostatické zvlákňování

Proces výroby nanovláken byl patentován v roce 1934 Formasem [1-3], ten vymyslel způsob, jakým je možné připravit polymerní nanovlákna pomocí elektrostatických sil. Elektrostatické zvlákňování je efektivní metoda pro přípravu polymerních nanovláken obr. 1. Použité polymery můžou být jak přírodní [4], tak i syntetické [5,6]. Elektrostatickým zvlákňováním lze zpracovat

polymery ve formě roztoku [7] či taveniny [8] a lze vyrobit vlákna různých průměrů.

Podstatou této technologie je využití účinků elektrostatického pole na elektricky nabité viskoelastické kapaliny (obvykle roztok polymeru), kdy za optimálních podmínek dojde k vytvoření velmi tenkých vláken s průměrem v rozmezí od 2 nm do několika mikrometrů [9, 10].

Proces elektrostatického zvlákňování získal velkou pozornost vědců v posledních letech a to nejen kvůli svému univerzálnímu použití při zvlákňování nejrůznějších polymerních vláken, ale také vzhledem k možnosti vyrábět vlákna v submikronovém měřítku, které je jinak obtížné vyrobit pomocí běžně používaných zvlákňovacích metod [9].

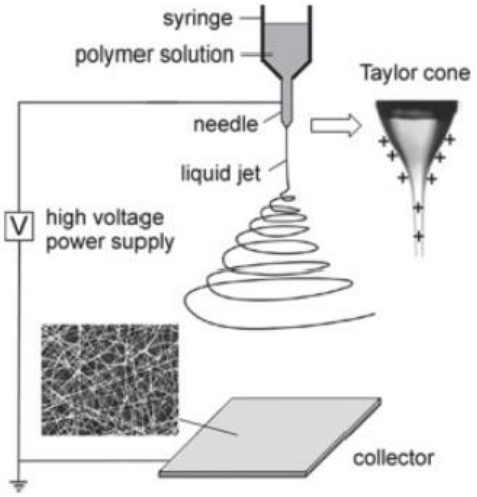

Obrázek 1 Schéme elektrostatického zvlákňování. [11]

Elektrostatické zvlákňování je metoda výroby nanovlákenných struktur pomocí působení elektrického pole velké intenzity na polymerní roztok nebo taveninu. Mezi elektrodami může být napětí až 75 kV. Zařízení pro elektrostatické zvlákňování se zpravidla skládá ze tří částí. Je to kapilára či jehla s malým průměrem naplněná roztokem polymeru, kovový sběrač a zdroj vysokého napětí. Roztok či tavenina polymeru je čerpán z konce pipety a vytahován ve formě vlákna v důsledku vysokého napětí [12]. Jedna elektroda je ponořena ve

zvlákňovaném roztoku nebo tavenině, na tu je přivedeno napětí a další je spojena s kolektorem. Ve většině případů je deska kolektoru uzemněná. Během procesu se na kolektoru sbírají vlákna z roztoku či taveniny o průměru řádově mikrometrů až nanometrů. Vlákna se pohybují vysokou rychlostí, více než 40 m s^{-1} směrem k uzemněné desce [13]. Pří pohybu vláken ke kolektoru dochází také k rotaci vláken.

Nanospider

Lze také vyrobit nanovlákna z volně otevřeného povrchu kapaliny [14]. Při tomto způsobu výroby nanovláken dochází k tvorbě trysek na povrchu rotujícího válce, částečně ponořeného do roztoku polymeru. Nanovlákna se vytváří náhodně ale pravidelně na povrchu válce a putují ke kolektoru, kde se náhodně ukládají a tvoří tak netkanou strukturu. Tato technologie je známá pod názvem Nanospider viz obr. 2.

Tato technologie byla vyvinutu na Technické univerzitě v Liberci, na katedře netkaných textilií a nanovlákenných materiálů a také byla patentována. Tuto komerční metodu pro výrobu polymerních nanovláken, která může být použita v průmyslovém rozsahu, byla zdokonalena profesorem Jirsákem.

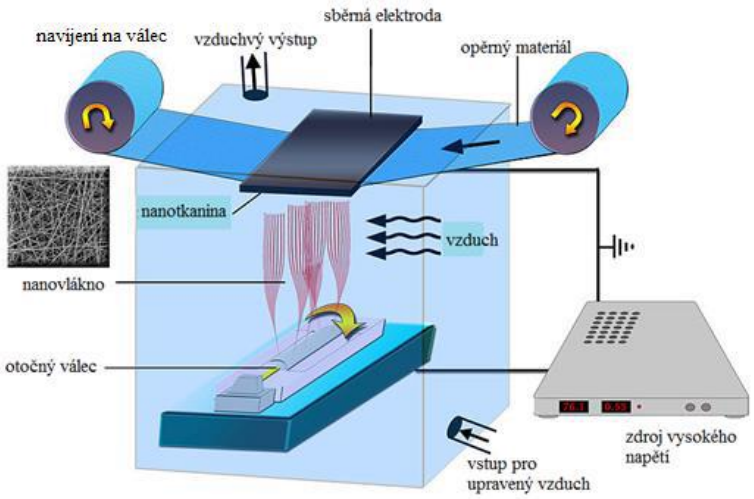

Obrázek 2 elektrostatické zvlákňování pomocí válce s hroty [16]

Nanospider má schopnost zpracovávat široké spektrum polymerů vytvářet vlákna o průměrech 50-300 nm do netkaných vrstev o plošné hmotnosti 0,1-10 g/m^2[17].

3. Uhlíkové nanotrubice

Uhlíkové nanotrubice jsou jednou z poměrně nových forem uhlíku. Uhlíkové nanotrubice byly objeveny v roce 1991 japonským operátorem elektronového skenovacího mikroskopu Sumiem Iimijimou, který zkoumal část uhlíkového materiálu na katodě vytvořeného pomocí výboje v elektrickém oblouku během přípravy fullerenů [18,19]. Nalezl, že střední část katody obsahuje různé druhy uzavřených uhlíkových struktur, jako jsou například uhlíkové nanotrubice. Tyto struktury nebyly nikdy dříve pozorovány.

Uhlíkové nanotrubice se staly předmětem zájmu vědců z mnoha odvětví, mezi která patří např. chemie, fyzika nebo materiálové inženýrství [20]. Uhlíkové nanotrubice nalézají v dnešní době mnoho praktických aplikací, jako jsou kompozitní materiály, senzorické členy, průhledné vodivé vrstvy a v mnoha dalších oblastech vědy a průmyslu [21-23].

Chiralita uhlíkových nanotrubic

Jak ukazuje obr. 3 uhlíkové trubice mají struktury složenou z benzenových kruhů, někdy v literatuře označované jako včelí plástve [28]. Nanotrubice jsou charakterizovány jejich průměrem, délkou a chiralitou.

Chiralita popisuje strukturu uhlíkových nanotrubic z pohledu orientace „grafénové“ vrstvy tvořené benzenovými kruhy obr. 3 b-d. Orientace „grafénového“ listu, respektive benzenových kruhů, je dána osou stočení definovanou jako chirální vektor $\overrightarrow{Ch}$ obr.3a. Základní rozdělení nanotrubic je

dáno pomocí její osy symetrie. Symetrické trubice jsou buď zig-zag nebo armchair, nebo nesymetrické chirální. Chirální vektor je rozlišen vektory $\overrightarrow{a_1}$ a $\overrightarrow{a_2}$ šestičlenných kruhů, rovnice 1.

$$\overrightarrow{Ch} = n\overrightarrow{a1} + m\overrightarrow{a2} \qquad (1)$$

V rovnici 1 jsou n a m celá čísla, která popisují tři různé situace, když n=m je to armchair struktura, když je m=0 je to struktura zig-zag v dalších případech jde o chirální strukturu [24]. Chiralita je velmi důležitá pro elektrickou vodivost uhlíkových nanotrubic. Struktura armchair má kovovou vodivost a ostatní dvě tedy zig-zag a chiralní jsou polovodivé.

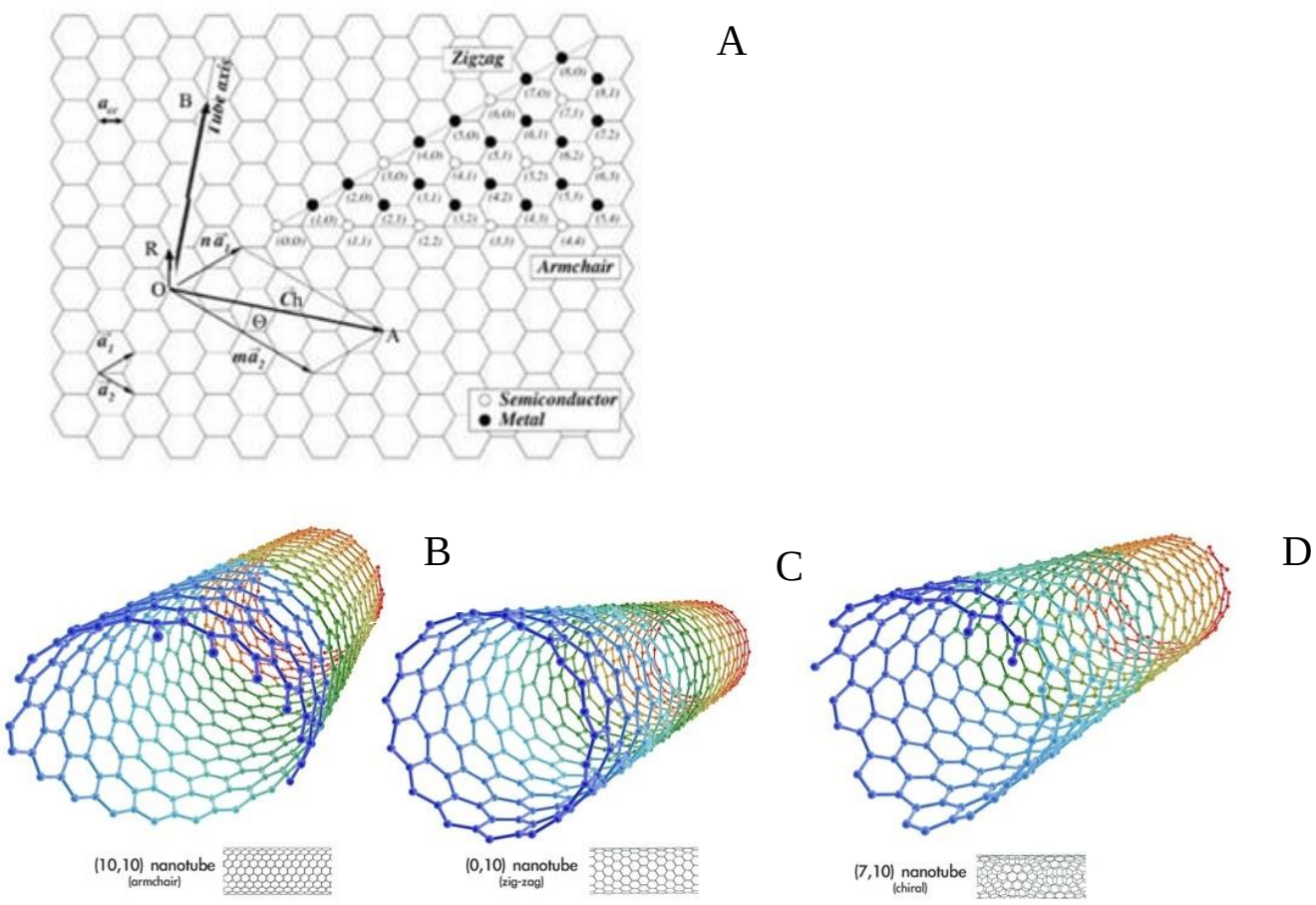

Obrázek 3 a) chirální vektor, b) armchair konfigurace, c) zig-zag konfigurace, d) chirální konfigurace [25].

Typy uhlíkových trubic

Existují dva základní typy uhlíkových nanotrubic a to jednostěnné a vícestěnné [18,19,26] Obr. 6. Jednostěnné uhlíkové nanotrubice jsou vytvořeny stočením grafenové vrstvy do formy trubiček, jak ukazuje obr. 4. Vícesměnné uhlíkové nanotrubice se skládají z mnoha trubic vložených do sebe jak je vidět na obr 6.

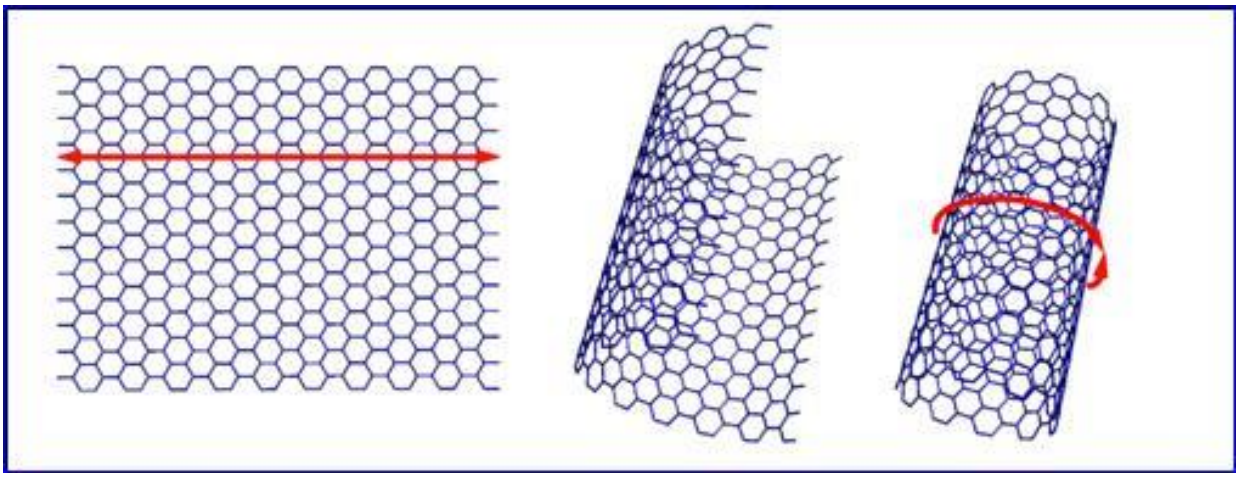

Obrázek 4 Sbalení grafenové vrstvy do formy uhlíkové nanotrubice. (šipka ukazuje směr sbalení.) [27]

3. 1. Jednostěnné uhlíkové nanotrubice

Uhlíkové nanotrubice jsou velmi pevným materiálem, který má vynikající mechanické vlastnosti, které ho předurčují k širokému použití. [31]. Lepší mechanické vlastnosti má jen grafen [32].

Youngův modul izolované nanotrubice je 1,4 TPa Hustota jednostěnných uhlíkových trubic je v rozmezí 1.2 – 1,4 g/cm^3. Většina jednostěnných uhlíkových nanotrubic má průměr mezi 0,8 – 1,2 nm a délku 100 až 1000 nm[33]. Jednostěnné uhlíkové nanotrubice mají užitné vlastnosti, mezi které patří např. tepelná vodivost, chemická odolnost a dobré elektrické vlastnosti. Výše zmíněné vlastnosti předurčují použití tohoto materiálu.

3. 2. Vícestěnné uhlíkové nanotrubice

Vícestěnné uhlíkové nanotrubice jsou na rozdíl od jednostěnných uhlíkových nanotrubic složeny z několika grafenových listů, které mají rozdílné průměry obr. 5. Vzdálenost mezi jednotlivými stěnami je 3,3 A. Vícestěnné uhlíkové nanotrubice mají menší aktivní povrch ve srovnání s jednostěnnými uhlíkovými nanotrubicemi. Průměr těchto trubic je v rozmezí 2 – 100 nm a délka je kolem 10 μm [34,35]. Youngův modul izolované vícesměnné nanotrubice je přibližně 1 TPa.

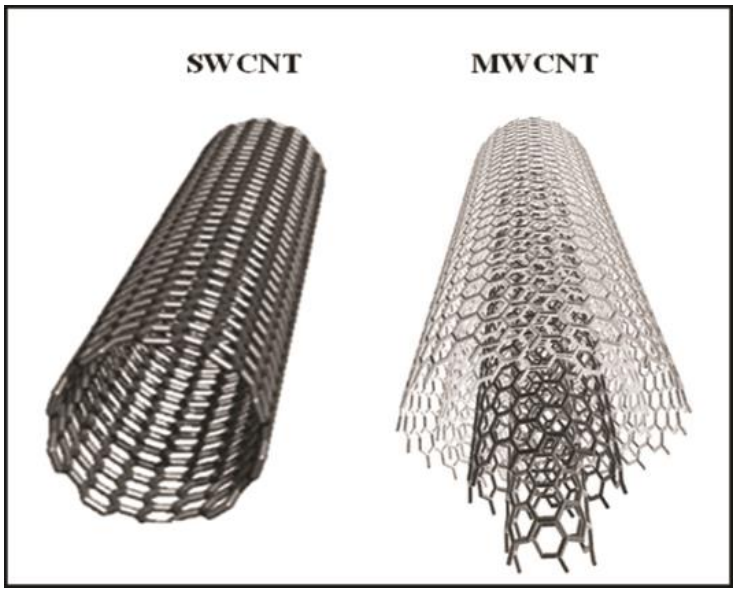

Obrázek 5 dva typické druhy uhlíkových nanotrubic. Jednostěnné (SWCNT) a vícestěnné) MWCNT) [36].

4. Výroba uhlíkových nanotrubic

Uhlíkové nanotrubice mohou být vyrobeny mnoha způsoby. Mezi základní typy syntézy patří výboj v elektrickém oblouku, laserové ablace a chemická depozice z plynné fáze.

4. 1. Výboj v elektrickém oblouku

Poprvé byla tato metoda využita pro výrobu fullerenů C_{60}. Jde o první metodu, která se používá k výrobě SWCNT, MWCNT. Tento výrobní postup spočívá ve vytvoření elektrického oblouku mezi dvěma grafitovými elektrodami v inertní atmosféře.

Jedna elektroda je naplněna kovovým práškem, který slouží jako katalyzátor. Množství katalyzátoru (železo, kobalt, nikl) ovlivňuje parametry vyrobených nanotrubic, především jejich průměr CNT [37-40]. CNT touto technologií vznikají tak, že při elektrickém výboji mezi elektrodami se vytvoří páry uhlíku, ze kterých se za přítomnosti katalyzátoru vytvářejí uhlíkové nanotrubice. Záporně nabitá elektroda se v průběhu reakce spotřebovává a na kladné elektrodě vznikají uhlíkové nanotrubice. V závislosti na podmínkách lze vyrábět buď SWCNT nebo MWCNT [37-41] obr. 6 b.

Schéma výrobního zařízení CNT metodou výboje v elektrickém oblouku je znázorněno na Obr. 6 a. Kladná elektroda je pevná s průměrem 6 – 7 cm. Záporná elektroda je posuvná a její průměr se pohybuje mezi 9 – 20 cm. Vzdálenost mezi elektrodami je několik milimetrů. K výrobě CNT je používáno stejnosměrného elektrického proudu v rozmezí 50 - 100 A. Napětí mezi elektrodami je mezi 25 – 35 V. Teplota v elektrickém oblouku se pohybuje od 3000 – 4000°C. Syntéza probíhá v inertní atmosféře. Nejčastěji se používá helium (He) nebo argon (Ar) o nízkém tlaku, který se pohybuje mezi 5 - 70 kPa. Pro helium (He) se nejčastěji používá tlak 66,7 kPa [42, 43,40].

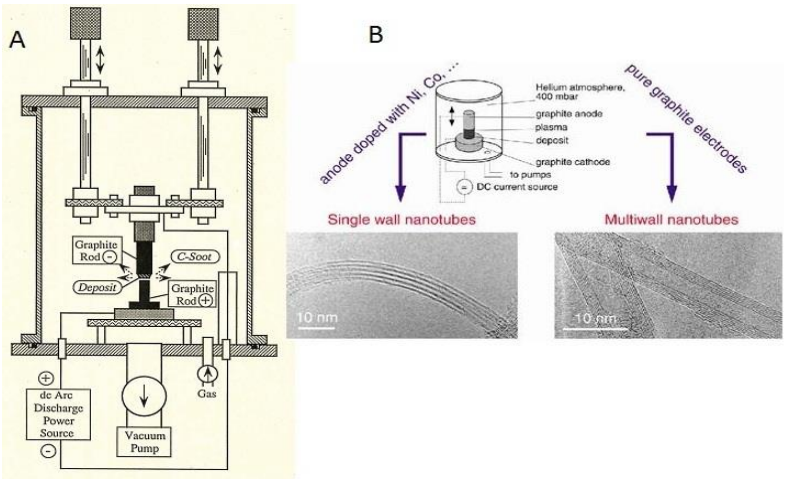

Obrázek 6 a) aparatura pro výroba uhlíkových nanotrubic v obloukovém výboji [43]. b) možnosti syntézy různých druhů nanotrubic [44]

4. 2. Laserová ablace

Tato metoda je založena na kondenzaci uhlíkových par, které se odpařují z grafitové elektrody. K odpaření se používá laserový impulz nebo kontinuální laserový paprsek v trubkové peci při teplotě 1200 °C Obr. 7. Hlavní rozdíl mezi pulzním a kontinuálním paprskem je v tom, že pulzní vyzařuje mnohem větší výkon 100 kW/cm^2. Kontinuální paprsek vyzařuje pouhých 12 kW/cm^2.

Pec je naplněna opět interním plynem a to heliem *He* nebo argonem *Ar* při tlaku kolem 66 kPa. Z povrchu se odpařují velmi horké páry. Páry v rychlém sledu expandují, při chladnutí kondenzují a tvoří složitější uhlíkové struktury, společně i s fullereny. Katalyzátory, které se váží na uhlíkové struktury, kondenzují pomaleji a brání jejich uzavírání do klecí. Katalyzátory, které se naváží, mohou dokonce takto uzavřené klecovité struktury otevírat. Z těchto základních struktur pak vyrůstají SWCNT do doby, dokud nejsou částečky katalyzátoru příliš velké nebo dokud okolí nezchladne natolik, že se uhlík nedostane na povrch katalyzátoru. Také je možné, že se katalyzátor pokryje takovým množstvím uhlíku, že jej již nemůže více přijmout, což zastaví růst nanotrubic.

Takto vzniklé nanotrubice jsou spolu drženy Van der Waalsovými silami. Vznikající materiál s vysokým podílem SWCNT je zachycen na měděném chladiči na konci pece. Výrobní postup laserové ablace je velmi podobný procesu obloukového výboje a reakce probíhají stejným způsobem. Proto je možné využít stejné atmosféry a směsi katalyzátorů [37,38,40-42,45].

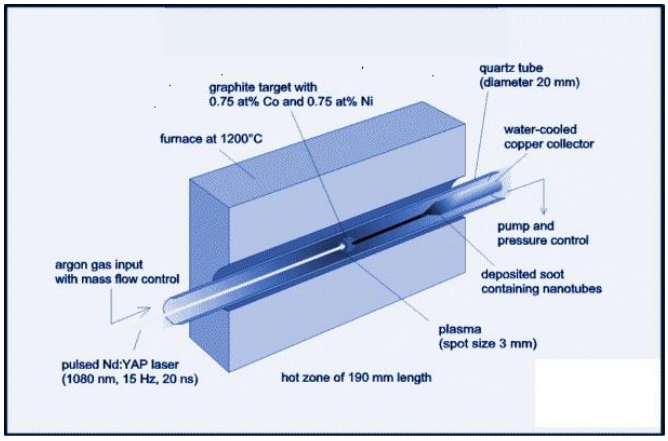

Obrázek 7 Aparatura pro výroba uhlíkových nanotrubic laserovou ablací [46].

4. 3. Chemická depozice z plynné fáze (CVD)

Třetí nejrozšířenější metodou přípravy CNT je syntéza pomocí CVD. Tato metoda se vyznačuje tím, že zdrojem uhlíku je plynná fáze v reaktoru a zdrojem energie je plazma Obr. 8. Zdrojem uhlíku je obvykle metan (CH_4), acetylen (C_2H_2) či oxid uhelnatý (CO). Zdroj energie je v procesu používán k rozštěpení molekul na reaktivní atomární uhlík, který poté difunduje na vyhřívaný substrát pokrytý vrstvou katalyzátorů (Fe, Co, Ni), na který se váže. Katalyzátor musí být vysoce porézní (zvyšuje růst CNT) s velkou aktivní plochou a silnou interakcí se substrátem. Tyto vlastnosti si musí uchovávat i za vysokých teplot. Uhlíkové nanotrubice se zde budou tvořit pouze tehdy, když zůstanou zachovány správné parametry. Typ CNT, jejich orientaci a průměr lze

kontrolovat vhodnou volbou katalyzátoru a reakčních podmínek [37, 39 - 42,]. Celá syntéza probíhá ve dvou krocích. Nejprve se připraví katalyzátor a následně se syntetizují nanotrubice. Katalyzátor se většinou nanáší na substrát pokovováním a následným chemickým leptáním či žíháním, které rozdělí katalyzátor na menší částečky. Teploty při syntéze nanotrubic metodou CVD se pohybují v rozmezí 650 – 900 °C. Výtěžek je kolem 30% [37, 39-42].

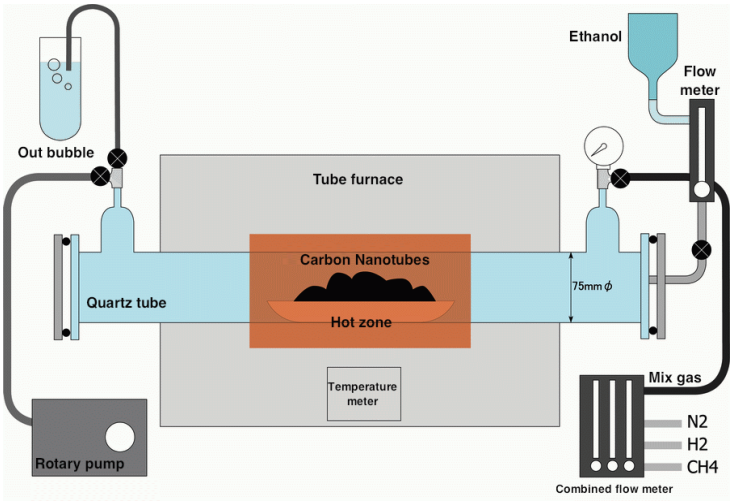

Obrázek 8 Aparatura pro výroba uhlíkových nanotrubic CVD technologii [47].

5. Dispergace uhlíkový nanotrubic

5. 1. Mechanická dispergace

Obecně jsou dvě možnosti jak dispergovat uhlíkové nanotrubice. A to buď mechanicky, nebo chemicky. U mechanické dispergace se jedná většinou o mletí, působení ultrazvukových vln, nebo jiné smykové působení.

Uhlíkové nanotrubice jsou drženy pohromadě působením Van der Waalsových sil, proto je zapotřebí působit na trubice vnější silou, aby se lépe separovaly a mohly být dispergovány [48].

Jedním ze způsobů je dispergace působením ultrazvukových vln na uhlíkové nanotrubice. Ultrazvukové vlny působí na trubice rozptýlené v organickém rozpouštědle, nebo ve vodě s přídavkem surfaktantu. K dispergaci se dá použít ultrazvuková lázeň, kde je navíc možné regulovat teplotu, což může pozitivně ovlivnit proces dispergace.

Druhým velmi často používaným způsobem je použití ultrazvukového hrotu, který má obvykle vyšší výkon než lázeň. Dá se měnit dispergovaný objem, ale není možné zahřívání. Proces sonikace je možné rozdělit na tři kroky: tvoření bublin a imploze, místní zahřátí a tvorba volných radikálů [49].

Další ze způsobů jak zlepšit dispergaci uhlíkových nanotrubic je mechanické mletí za použití kulového mlýnu. Tato technika snižuje množství agregátu, ale také zkracuje délku trubic a zvyšuje množství amorfního uhlíku. Tato metoda není k uhlíkovým nanotrubicím příliš šetrná [50]. Možnost, jak omezit drastické dopady na trubice, je mletí za pomocí tloučku a misky s malým množstvím toluenu. Tato možnost je šetrnější.

5. 2. Chemické úprava povrchu

Jak již bylo řečeno dříve, uhlíkové nanotrubice mají specifickou strukturu, která jim nedovoluje dobrou dispergaci v běžných organických rozpouštědlech, proto je vhodné použít metody, které zlepší jejich dispergovatelnost obr. 9.

Obecně jednou z možností jak zlepšit dispergaci nanotrubic je chemická úprava povrchu nanotrubic [51]. Vhodná funkcionalizace nanotrubic jim otevírá další možnosti zpracování. Chemická funkcionalizace zlepšuje dispergovatelnost a homogenitu rozptýlení nanotrubic v polymerní matrici. Tento typ funkcionalizme se dá také použít pro stabilizaci disperze uhlíkových nanotrubic.

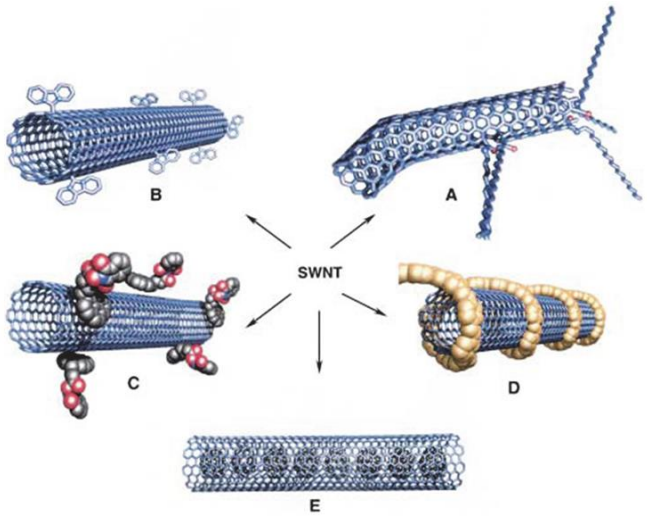

Obrázek 9 Možnosti funkcionalizace uhlíkových nanotrubic a) funkcionalizace na defektních místech nanotrubice, b) kovalentní funkcionalizace, c) nekovalentní funkcionalizace např. pomocí surfaktantů, d) obalení trubice polymerem, e) dopování nanotrubic [52].

Kovalentní funkcionalizace

Kovalentní funkcionalizace spočívá ve vytvoření kovalentních vazeb mezi trubicí a funkční skupinou nebo molekulami, které jsou na nanotrubice navázány. Chemické působení na povrch nanotrubice se děje především v místech kde jsou přítomny defekty, které umožňují funkcionalizaci. Tyto defektní místa jsou znázorněna na obr. 10 [53,54].

Obecně lze oxidaci uhlíkových nanotrubic provést působením např. $KMnO_4$, nebo směsí kyselin H_2SO_4/HNO_3. Působením těchto činidel se na povrchu trubic vytváří funkční skupiny v místech defektů nanotrubic. Oxidací se zlepší možnost dispergovatelnosti nanotrubic. Oxidace je také vhodná jako krok k vytvoření funkčních skupin pro následné navázání polymerních řetězců na povrch nanotrubice [55,56].

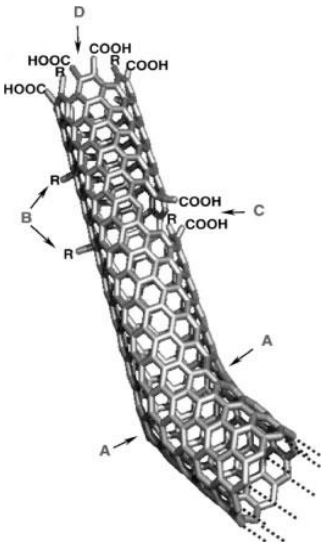

Obrázek 10 Typické místa na kterých můžou vzniknout defekty na povrchu uhlíkové nanotrubice a) pětičlenné a sedmičlenné uhlíkové kruhy, b) sp^3 defektní hybridizace (R=H a OH), c) narušení struktury nanotrubice oxidací –COOH, d) otevření konců nanotrubice končené – COOH skupinami [57].

Nekovalentní funkcionalizme

Obecně nekovalentní funkcionalizaci je možné provést za použití surfaktantů. Surfaktant vytvoří aktivní elektrostatickou vrstvu, která vyruší působení Van der Waalsových přitažlivých sil **[**58], které mezi nanotrubicemi obvykle působí. V dnešní době se používá mnoho různých druhů surfaktantů jako např. *SDS*, nebo *Triton X-100*. Problém však nastává, když surfaktanty musí být odstraněny [59-64].

6. Metody přípravy sítí z uhlíkových nanotrubic

Sítě z uhlíkových nanotrubic jsou zajímavou skupinou materiálů s dobrými elektrickými, mechanickými a optickými vlastnostmi, kterém můžou být využity v mnoha zařízeních. Tyto sítě mohou být jak vodivé tak i polovodivé a můžou být využity například v elektronice, optoelektronice a senzorických systémech citlivých na mechanické či jiné podněty.

Následující krátký přehled popisuje několik používaných technik pro přípravu sítí z náhodně zapletených uhlíkových nanotrubic.

6.1. Elektroforézní nanášení

Elektroforézní nanášení (*EPD*) obr. 11 je jedna z vhodných metod, které se dají využít pro výrobu vrstev uhlíkových nanotrubic. Touto metodou lze připravit makroskopicky homogenní vrstvu s řízenou tloušťkou. Tato technika je podstatě kombinací dvou procesů a to elektroforézy a nanášení. Uhlíkové trubice jsou hnány sílou elektrického pole, která je nutí se usazovat na elektrodě. Poté jsou trubice sbírány na elektrodě, kde vytvoří souvislou nanesenou vrstvu[65,66]. Základními parametry této metody je použité elektrické pole definované napětím a proudem. Dalším základním parametrem je čas nanášení.

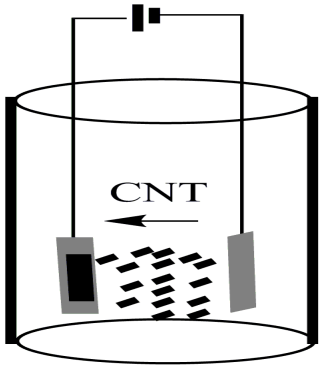

Obrázek 11 Elektro forézní depozice CNT vrstvy [67]

6.2. Rotační nanášení

Rotační nanášení obr. 12 je jednou z velmi jednoduchých a levných metod výroby vrstev z uhlíkových nanotrubic. Tyto vrstvy lze připravit za laboratorní teploty [68,69]. V případně rotačního nanášení lze substrát zahřát na vyšší teploty pro dosažení lepší kvality povrchu vzniklé vrstvy.

Jednou z nevýhod je nutnosti připravit homogenní disperze za použití např. ultrazvuku nebo úpravy povrchu trubic oxidací, nebo použití povrchově aktivních látek. Nanášení disperze je možné provést nakápnutím nebo nastříknutím disperze na rotující podklad. Podklad může být také ohřívaný 100-150 °C pro urychlení vypaření rozpouštědla.

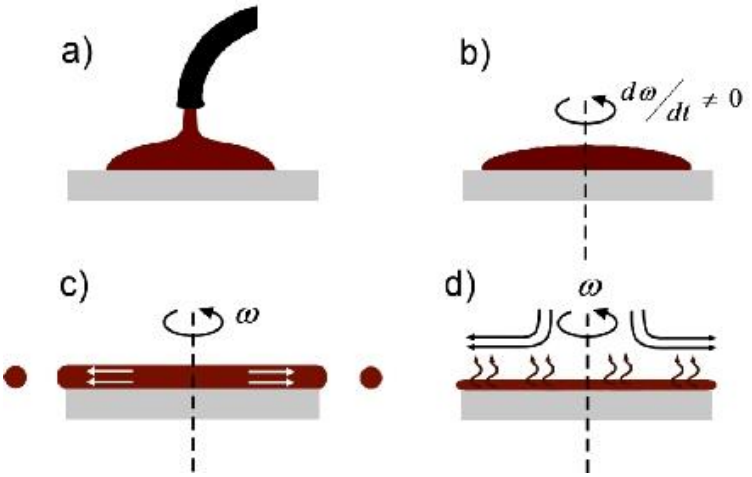

Obrázek 12 Rotační anášení a) nasení materiálu, roztočení substrátu s materiálem, c) vytvoření rovnoměrné vrstvy, d) sušení vzniklé vrstvy (šipky naznačují proudění vzduchu nad vzorkem [70]

6.3. Vakuová filtrace

Metoda vakuové filtrace obr. 13 je pravděpodobně nejjednodušší metoda přípravy vrstev uhlíkových nanotrubic a jejich sítí. Vytvořené vrstvy jsou homogenní, tenké, elektricky vodivé [71,72]. Proces filtrace se skládá ze tří kroků filtrace, odstranění povrchově aktivních látek a sušení filtrační membrány s vrstvou uhlíkových nanotrubic popřípadě rozpuštění filtrační membrány a získání sítě z uhlíkových nanaotrubic. Tato metoda má několik výhod: (I) během filtrace je vytvořen filtrační koláč samovolně. (II) Je zajištěna homogenita a dobré mechanické vlastnosti vzniklé vrstvy. (III) Tloušťka vrstvy je velmi dobře řízená pomocí objemu filtrované disperze.

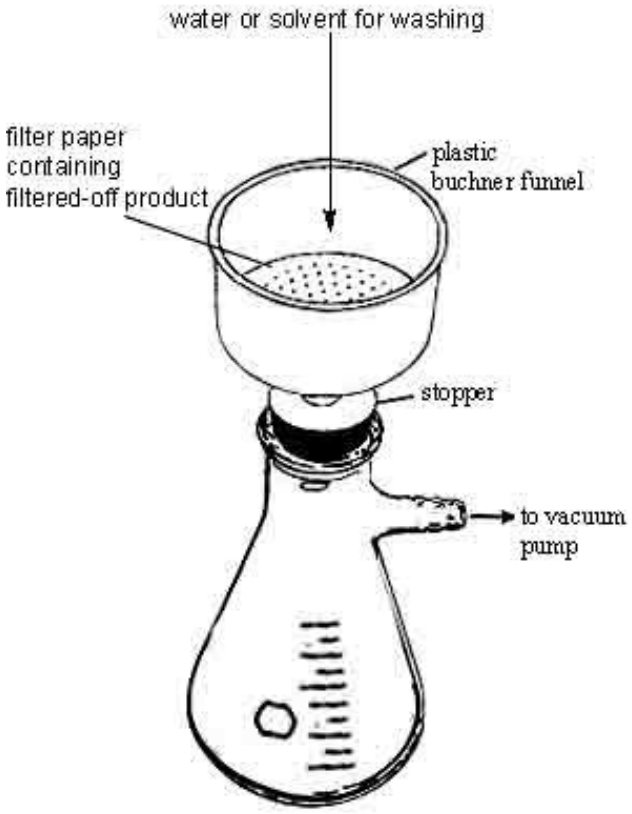

Obrázek 13 filtrační aparatura [72]

Uhlíkové nanotrubice mají, jak již bylo řečeno mnoho pro praxi zajímavých vlastnosti. Nanotrubice však mají tendenci tvořit agregáty [74], což znemožňuje jejich zpracování. Jednou z možností, jak tento problém vyřešit, je příprava disperze vhodného složení.

Tato disperze by měla být homogenní a stabilní [75,76]. Trubice by měly být co nejvíce dispergované. K tomu je zpravidla potřeba trubice, nebo vodnou disperzi upravit. V mnoha pracích se vyskytuje použití surfaktantů, hlavně SDS a Triton X-100 a jiné. Je také možné stabilizovat disperzi funkcionalizací nanotrubic pomocí kyselin nebo oxidačních činidel. Kyseliny zde předsatvují oxidující látky. Ke zlepšení dispergace se používá také ultrazvuku. Disperze se potom převede do formy tenkého filmu nebo vrstvy. Tenká vrstva může být součástí filtrační membrány, nebo může být odstraněn filtr, v případně když se vytvoří tlustší vrstva. Tato vrstva se nazývá síť z náhodně zapletených uhlíkových nanotrubic. Někdy je také nazývaná jako *buckypaper* [77,78]. Tato

síť je složena z náhodně zapletených uhlíkových nanotrubic. Je homogenní bez povrchových defektů nebo zlomů. Je to 3d objekt. Důležitým krokem je odstranění surfaktantů, které jsou po filtraci již nežádoucí příměsí. Odstranění surfaktantů může být provedeno například promytím filtrované vrstvy horkou vodou a poté metanolem.

Tato síť může být použita k vytvoření kompozitů, které budou mít specifické vlastnosti např. elektrickou vodivost, citlivost na mechanické podněty nebo citlivost na páry a plyny.

7. Kompozity na bázi polymer/CNT

Zajímavé vlastnosti uhlíkových nanotrubic z nich dělají vhodný materiál, který se dá využít jako nový systém pro výrobu kompozitu. Matrice můžou být z termoplastu nebo termosetu. Jeden z mnoha faktorů je kompatibilita uhlíkových nanotrubic s matricí. Efektivní systém funkcionalizace je klíčovým faktorem ovlivňující výsledné vlastnosti kompozitu. Uhlíkové nanotrubice se většinou používají jako částicové plnivo.

V této práci jsou však uhlíkové nanotrubice použity ve formě sítě z náhodně zapletených uhlíkových nanotrubic. Toto síť tvoří aktivní část kompozitního materiálu, která je citlivá na různé mechanické podněty a také na organické páry či plyny.

Polymerní kompozity na bázi uhlíkových nanotrubic *CNT* (carbon nanotubes) hrají roli v mnoha oblastech každodenního života. Kompozity jsou pro uživatele zajímavé především proto, že nabízí zlepšené vlastnosti anebo dokonce vlastnosti nové. Plnivo, jakým jsou uhlíkové nanotrubice přináší mnoho zajímavých vlastnosti výsledného materiálu a to především zvýšení pevnosti, tepelné vodivosti, elektrické vodivost a mnoho dalšího. V následující části kapitoly budou popsány způsoby, jakými lze připravit kompoty na bázi CNT.

7. 1. Roztoková metoda

Roztoková metoda přípravy polymerních kompozitů na bázi uhlíkových nanotrubic je velmi rozšířená. Jedná se o roztok polymeru obsahující uhlíkové nanotrubice o vhodné koncentraci. Míchání nanotrubic se provádí ultrazvukovými vibracemi, tento způsob je velmi efektivní. Trubice mohou být upravené oxidací či pokryté polymerem.

Důležitým faktorem je kompatibilita matrice a plniva, čehož se dosáhne zmíněnou úpravou povrchu (kapitola 5.2). Pro vznik polymerního filmu se nechá rozpouštědlo odpařit, a vznikne polymerní film různé tloušťky. Další možností je vytvoření roztoku polymeru s uhlíkovými nanotrubicemi, ve kterém jsou trubice dobře dispergovány. Poté je roztok s trubicemi vysrážen do rozpouštědla, ve kterém se polymer již nerozpouští.

7. 2. Zpracování ve formě taveniny

Zpracování termoplastických polymerů ve formě taveniny se provádí běžně dostupnými technikami, jako je míchání, vytlačování nebo vstřikování. Tyto techniky jsou jednoduché, rychlé a velmi využívané. Při tomto způsobu výroby kompozitů není nutné použít rozpouštědlo což je velká výhoda o proti předchozí metodě.

Tímto způsobem se zpracovávají termoplastické polymery, které je obtížné rozpustit v rozpouštědle a tato metoda se jeví jako vhodnější. Polymer je ve formě viskózní taveniny a plnivo je do této taveniny zamícháno. Tímto způsobem se připravují objemové kompozity stejně jako v předchozí metodě.

7. 3. Polymerace v přítomnosti CNT

Používají se uhlíkové nanotrubice upravené oxidací. Oxidací se na povrchu vytvářejí funkční skupiny. Tyto funkční skupiny se pak dále využívají pro navázání polymerních řetězců na povrch nanotrubic, v našem případě byl použit allyl isokyanát k následnému navázání volné vinylové skupiny a vzniku polymetylmetakrylátových řetězců na povrchu uhlíkových nanotrubic.

Polymerace za přítomnosti uhlíkových nanotrubic je efektivní metoda. Tato metoda zlepšuje dispergovatelnost a kompatibilitu nanotrubic s matricí.

8. Senzorické členy na plyny a páry

Uhlíkové nanotrubice, ať již jednostěnné nebo vícestěnné můžou být použity pro detekci plynů a par [79]. Tyto nanotrubice mohou být použity k výrobě miniaturních senzorů [80], které jsou schopné detekovat organické páry a plyny o nízkých koncentracích [81]. Toho může být využito také pro detekci zdravý škodlivých plynů či par, u kterých je detekce velmi důležitá [82-85].

Detekce plynů či par je na principu vnikání molekul analyzované látky do prostoru v síti a tvoření izolační vrstvy mezi jednotlivými nanotrubicemi. V síti se mění makroskopická vodivost, která je dána především křížením nanotrubic v síti. Zaznamenání této změny je velmi jednoduché pomocí měření změny odporu v našem případě dvoubodovou metodou.

Nanotrubice vykazují poměrně vysokou citlivost. Uhlíkové nanotrubice jsou schopné detekovat plyny např. CO, NO_2, NH_3, SO_2, NO [90] a mnohé další [86-88]. Nanotrubice jsou také schopné adsorbovat na svůj povrch molekuly par organických rozpouštědel. Uhlíkové nanotrubice také vykazují vyšší rychlost

odezvy (v řádech sekund) při detekci plynů a par a co víc, jsou schopné pracovat za pokojové teploty i za nízkých teplot.

Principem je vytvoření sítě z uhlíkových nanotrubic nakápnutím disperze vhodného složení a odpařením, síť se vytvoří samovolně. Příklad jedné takové elektrody je na obr.14 na které je vytvořena síť z těchto nanotrubic.

Komerční detektory na bázi polovodičů nejsou schopny pracovat za nízkých teplot. Tyto detektory pro svoji činnost potřebují vyšší teplotu v řádech stovek stupňů. Vlastní konstrukce těchto senzorů je mnohdy komplikovaná. V principu jde o vytvoření aktivní vrstvy, která je schopná detekovat molekuly. Mnohé vlastnosti komerčních detektorů jsou pro uživatelé nevýhodné a lze je s úspěchem nahradit detektory na bázi CNT.

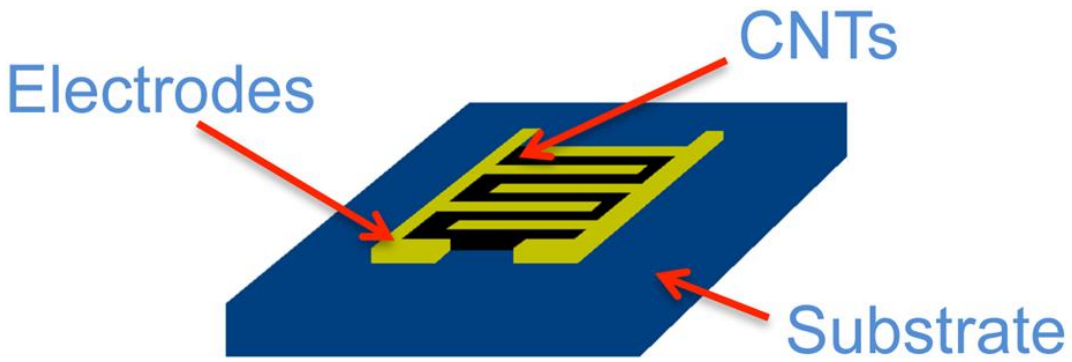

Obrázek 14 Elektroda pro senzorický člen [89]

Další z používaných metod je příprava aktivní vrstvy pomocí tisku disperze na papír nebo polymerní podklad např. PET folii.

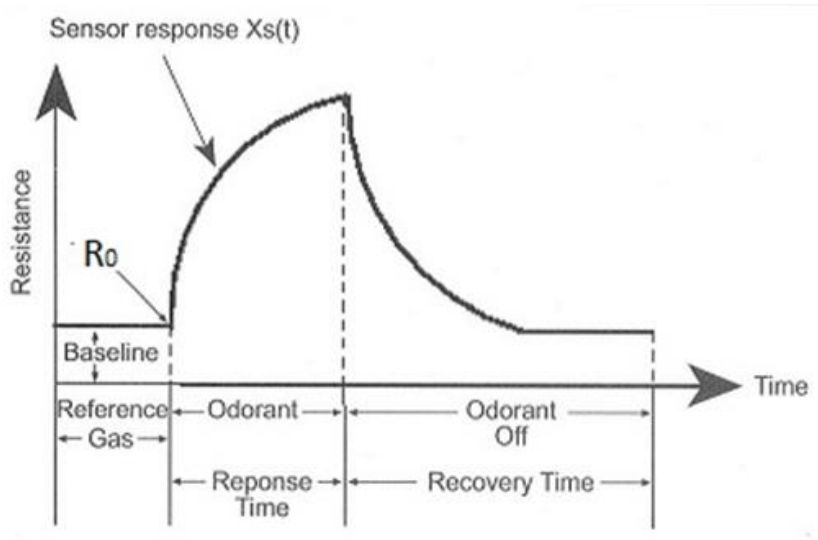

Obrázek 15 Typická odezva změny odporu na páry či plyny pro senzorický člen z uhlíkových nanotrubic [86]

Obr. 15 Představuje typickou odezvu pro páry a plyny senzoru z uhlíkových nanotrubic. Křivka má typický a tvar, kde lze sledovat několik částí. První část *baseline* je odezva bez přítomnosti plynu. R_0 je počáteční hodnota odporu. Poté je aplikován plyn a odpor se začíná růst sensor *response.* Po určitě době nastane na křivce maximum a změna odporu je na stejné hodnotě. V případě, že je senzor odstraněn z místa působení plynu, odpor pozvolna klesá a může se dostat na původní hodnotu (může to být i 90 % původní hodnoty) označeno na obrázku jako *recovery time*, respektive na hodnotu odezvy bez přítomnosti analyzované látky.

Princip změny odporu může být popsán jako vnikání molekul plynů nebo par do prostor v síti z uhlíkových nanotrubic a jejich interakce s povrchem trubic. Jde o fyzikální adsorpci, při které jsou molekuly vázány pomocí Van der Waalsových sil. Molekuly tvoří v síti nevodivou vrstvu, která snižuje vodivost při adsorpci a naopak vodivost se zvyšuje, když se molekuly ze sítě desorbují. Molekuly zkoumané látky mají mnoho možností jak interagovat s povrchem, jak ukazuje obr. 16.

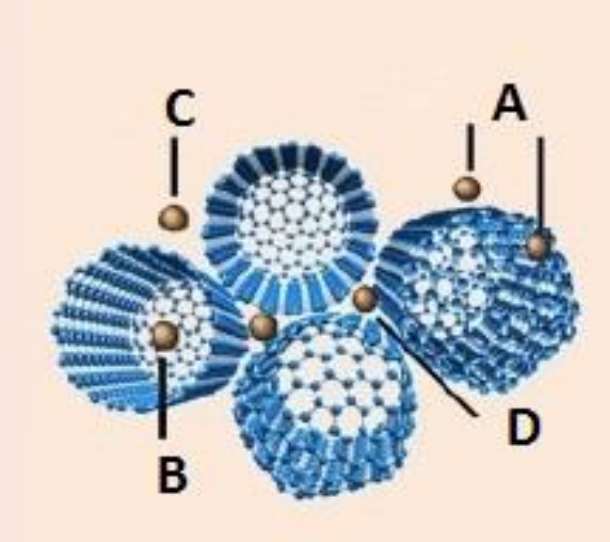

Obrázek 16 Adsorpční místa v uhlíkových nanotrubicích a) povrch, b) póry, c) venkovní prostor dotyku trubic, d) vnitřní prostor [91]

9. Senzorické členy na mechanické podněty

Pro zjištění stavu konstrukcí různých zařízení či staveb se používá monitorovacích zařízení, která se skládají ze senzorických členů většinou tenzometrů, které však nejsou schopné detekovat vysoký stupeň deformace, maximálně v řádech procent. Tento nedostatek může vyřešit senzor pro detekci deformace na bázi sítě z uhlíkových nanotrubic zakotvený ve vysoce elastickém polyuretanu.

Monitorování a diagnostika porušení konstrukcí je důležitým parametrem, který vypovídá o aktuálním stavu konstrukcí [92-94]. Výhoda tohoto systému je, že monitorování může probíhat pořád či v časových intervalech [9]. Síť pro monitorování je rozmístěna po konstrukci tak, aby zachytila všechny místa, které jsou nejvíce namáhána.

V dnešní době je snaha vytvořit hustou síť pro detekci a tím postihnout komplexně chování konstrukce. Je možné vytvořit tuto síť tak, aby signál byl

přenášen bezdrátově [95]. V dnešní době se také pokoušíme vytvořit síť podobnou nervové sítí s paralelním sběrem a zpracováním dat [96-98].

Materiály pro monitorování s poškození struktury nacházejí uplatnění již od 80. let 20. století, jak v civilní, tak kosmické sféře. Obecně jde o monitorování tvaru, vibrací a zdraví ve smyslu poškození struktury materiálů. Obr. 17 ukazuje jednu z možností jak sledovat poškození materiálu pomocí změny odporu senzorického členu.

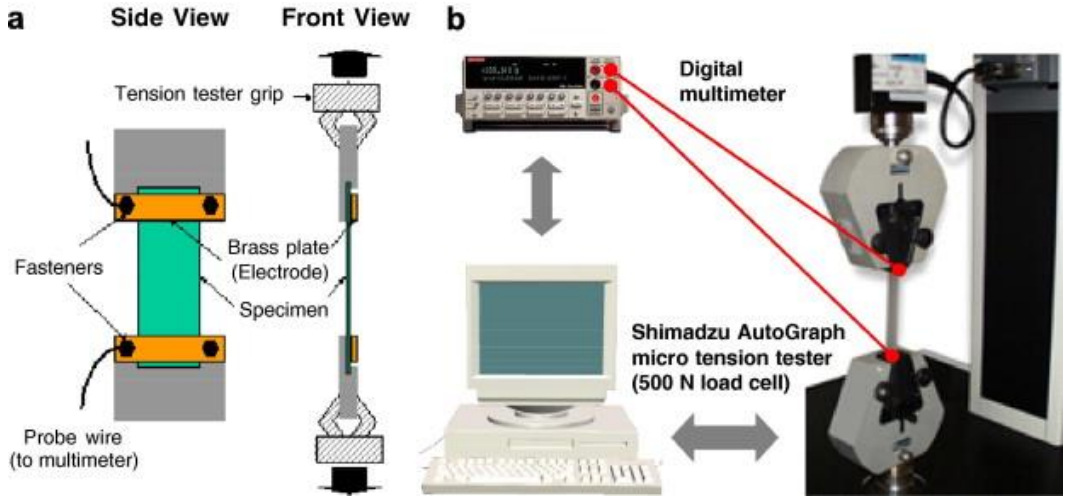

Obrázek 17 Ukázka senzorického členu citlivého na protažení vhodného k monitorování stavu konstrukcí. a) senzorický člen, b) Sběr a zpracování výsledků [99].

Pro monitorování poškození struktury se mohou využít uhlíkové nanotrubice ve formě zapletených sítí [97,100] např. jako sensor citlivý na protažení, ohyb či tlak. Je možné vytvořit polymerní kompozit, který je citlivý jak na statické tak dynamické mechanické namáhání [51].

Principem funkce senzorického členu na bázi uhlíkových nanotrubic a vysoce elastického polyuretanu je změna odporu sítě při aplikaci různých mechanických podnětů. Jedna se o vratnou deformaci vzniklé sítě díky vysoce elastickém polyuretanu který brání rozpojení kontaktů v sítě a pří odstranění deformačního podnětu se opět vrací téměř do původního stavu. Jedná se o nedestruktivní metodu monitorování.

Shrnutí nejdůležitějších publikací

Článek I

Článek popisuje přípravu kompozitu uhlíkových nanotrubic PS/CNT. Uhlíkové nanotrubice jsou filtrovány přes filtrační membránu, která je poté převedena lisováním do formy filmu. Uhlíkové nanotrubice jsou ve formě elektricky vodivé sítě. Elektrická vodivost resp. změna odporu byla měřena v závislosti na změně teploty a také byla zjištěna citlivost tohoto kompozitu na organické páry. Polystyrenová filtrační membrány zlepšila mechanické vlastnosti výsledného kompozitu.

Článek II

Článek popisuje přípravu uhlíkových nanotrubic, které jsou pokryty PMMA. Pokrytí nanotrubic bylo provedeno pomocí radikálové roztokové polymerace přes allyl izokyanát. Na uhlíkové nanotrubice byly navázány PMMA řetězce. Výsledný kompozit byl ve formě uhlíkového papíru s navázanými PMMA řetězci. Účelem je zvýšit selektivitu senzoru pro detekci par v závislosti na afinitě jednotlivých rozpouštědel k PMMA.

Článek III

Článek popisuje efekt, který je způsobený úpravou nanotrubic působením různých chemických činidel např. $KMnO_4$ a radiofrekvenční plazmou v O_2 atmosféře. Z takto upravených trubic byla připravena aktivní vrstva ukotvená ve vysoce elastickém polyuretanu. Takto vzniklý kompozit byl testován na cyklické mechanické namáhání. Bylo zjištěno, že vrstva z čistých nanotrubic velmi dobře interpretuje tvar vloženého impulzu oproti trubicím oxidovaným které vykazují mírné zkreslení. Oxidované trubice pomocí $KMnO_4$ mají však daleko vyšší změnu odporu pří deformaci, tudíž jsou více citlivé. Podobný trend změny odporu ukazuje měření postupného zatěžování a odlehčování vzorku z čistých a oxidovaných trubic. Oxidací se rapidně zvýšil faktor citlivosti.

Článek IV

Článek popisuje přípravu kompozitu na bázi PS/CNT přepraveného filtrování CNT disperze skrze PS membránu připravenou metodou elektrostatického zvlákňování. Kompozit byl stlačován a uvolňován a byla měřena napěťovo-deformační odezva. Bylo zjištěno, že po odlehčení zde zůstává zbytková deformace, která se však se zvyšujícími se počtem cyklů

nezvětšuje. Také byla měřena elektrická vodivost, která se zvyšuje, když se vzorek více deformuje.

Článek V

Článek popisuje přípravu sítě z uhlíkových nanotrubic pomocí filtrace. Tato síť je poté analyzována pomocí měření změny odporu při stlačování této struktury. Byly měřeny různé tloušťky těchto sítí a byla testována vratnost změny odporu při stlačení a uvolnění. Tyto vlastnosti přináší možnost využití v praktických aplikacích.

Článek VI

Článek popisuje přípravy nanovlánek pomocí elektrostatického zvlákňování. Jedná se o polyuretanové nanovlákna zvlákněná z roztoku DMF. Také byly připraveny nanovlákna s přídavkem uhlíkových nanotrubic. Byl studován efekt přídavku uhlíkových nanotrubic. Bylo zjištěno, že uhlíkové nanotrubic jsou přítomny v nanovláknech, a co víc, byly vytvořeny nanosíťky mezi jednotlivými vlákny.

Článek VII

Článek popisuje úpravu plazmou O_2 při tlaku 50 Pa. Citlivá vrstva pro detekci par organických rozpouštědel v tomto případě heptanu, byla vytvořena nakápnutím vodné disperze na elektrodu. Po odpaření vody byla elektroda vložena do plazmy a upravována různě dlouho. Bylo zjištěno, že nejefektivnější je plazmování po dobu 10 sec. Metoda je efektivní z pohledu její rychlosti a snadné aplikace na vzorek.

Článek VIII

Článek popisuje přípravu sítě z uhlíkových nanotrubic ve formě samonosné vrstvy pomocí vakuové filtrace, což je velmi efektivní metoda. Toto síť někdy také nazývaná *buckypaper* byla testována na odezvu pro organické páry pro několik vybraných rozpouštědel (tetrahydrofuran, methyl ethyl keton a etanol). Výsledky ukazují dobrou citlivost a selektivitu této struktury na organické páry. Selektivita je závislá na objemu nasycených par testovaných látek.

Článek IX

Článek popisuje přípravu sítě z uhlíkových nanotrubic ve formě samonosné vrstvy pomocí vakuové filtrace, což je velmi efektivní metoda. Sítě byly tentokrát upraveny oxidací pomocí

$KMnO_4$. Toto síť někdy také nazývaná *buckypaper* byla testována na odezvu pro organické páry pro několik vybraných rozpouštědel s ohledem na jejich polaritu. Byli vybráni zástupci polárních a nepolárních rozpouštědel. Výsledky ukazují dobrou citlivost a selektivitu této struktury pro organické páry. Oxidací se zvýšila selektivita. Odezva pro látky polární se zvýšila a naopak pro nepolární byl zaznamenám pokles v citlivosti. Procentuální zastoupení nasycených par při stejné teplotě byl přibližně stejný.

Článek X

Článek popisuje přípravu kompozitu na bázi sítě z uhlíkových nanotrubic a polystyrenové filtrační membrány. Bylo provedeno srovnání také se sítí bez polystyrénové membrány. Vrstva uhlíkových nanotrubic byla filtrována přes tuto membránu a poté lisována do formy tenkého filmu. Síť z trubic je elektricky vodivá. Byla měřena změna vodivosti v závislosti na teplotě, a zjistilo se, že v případě kompozitu s rostoucí teplotou vodivost roste lineárně.

Článek XI

Článek popisuje přípravu sítě z uhlíkových nanotrubic ve formě kompozitu na bázi PU/CNT vrstvy pomocí vakuové filtrace. Síť byla nalisována na povrch polyuretanové podložky vyrobené z velmi elastického polyuretanu. Podložka plní hned několik funkci: zlepšuje mechanické vlastnosti sítě z uhlíkových nanotrubic, umožňuje velký stupeň deformovatelnosti a vytvoření potřebného tvaru senzoru za použití běžných konvenčních metod. Článek ukazuje vyžití tlakového senzoru a senzoru na protažení při monitorování chůze.

Článek XII

Článek popisuje přípravu tenkých vrstev z několika různých materiálů v tomto případě jsou to vícestěnné uhlíkové nanotrubice, uhlíkové vlákna a saze. Tenká vrstva byla připravena na měděné elektrodě nakápnutím vytvořené vodné disperze a odpařením vody. Vrstvy byly testovány na odezvu pro páry etanolu. Bylo zjištěno, že všechny výše zmíněné materiály s nějakou mírou citlivosti reagují na tyto páry.

Poděkování

Na tomto místě bych rád poděkoval vedoucímu disertační práce doc. Ing. Petru Slobodianovi, Ph.D. za pomoc, cenné rady a připomínky, které vedly k sepsání disertační práce. Dále bych rád poděkoval Ing. Davidu Petrášovi a Ing. Dušanu Kimmerovi CSc. za výrobu nanovlákenných filtračních membrán. Poděkování patří také Ing. Michalu Machovskému, Ing. Pavlu Bažantovi a Doc. Ing. et Ing. Ivu Kuřitkovi, Ph.D et Ph.D za zhotovení SEM fotek a termogravimetrickou analýzu vzorků. Dále bych rád poděkoval všem, kteří se na vytvoření práce podíleli.

Reference

[1] Formhals, A., US Patent, 1,975,504 (1934)

[2] Formhals, A., US Patent, 2,160,962 (1939)

[3] Formhals, A., US Patent, 2,187, 306 (1940)

[4] Jamil A. Matthews,†, Gary E. Wnek,‡, David G. Simpson,§ and, and Gary L. Bowlin*,∥ Electrospinning of Collagen Nanofibers, *Biomacromolecules* 2002 *3* (2), 232-238

[5] Jayesh Doshi, Darrell H. Reneker, Electrospinning process and applications of electrospun fibers, Journal of Electrostatics, Volume 35, Issues 2–3, August 1995, Pages 151-160, ISSN 0304-3886

[6] Zhuo, H., Hu, J., Chen, S. and Yeung, L. (2008), Preparation of polyurethane nanofibers by electrospinning. J. Appl. Polym. Sci., 109: 406–411. doi: 10.1002/app.28067

[7] M.M Demir, I Yilgor, E Yilgor, B Erman, Electrospinning of polyurethane fibers, Polymer, Volume 43, Issue 11, May 2002, Pages 3303-3309, ISSN 0032-3861, 10.1016/S0032-3861(02)00136-2

[8] Cheryl L. Casper,†, Jean S. Stephens,†, Nancy G. Tassi,†, D. Bruce Chase,‡ and, anJohn F. Rabolt*,† Controlling Surface Morphology of Electrospun Polystyrene Fibers: Effect of Humidity and Molecular Weight in the Electrospinning Process, *Macromolecules* 2004 *37* (2), 573-578

[9] FANG, Jian, et al. Applications of Electrospun Nanofibers. *Chinese Science Bulletin*,2008, 53, 15, s. 2265-2286.

[10] Zhang, Yanzhong; Lim, Chwee Teck; Ramakrishna, Seeram; Huang, Zheng-ming, Recent development of polymer nanofibers for biomedical and biotechnological applications, Journal of Materials Science : Materials in Medicine 16. 10 (Oct 2005): 933-46.

[11] Li D. & Xia Y. 2004. Electrospinning of Nanofibers: Reinventing the Wheel,Advanced Materials,Vol. 16, No. 14, (July 2004), pp. 1151-70, ISSN 1521-4095

[12] HUANG, Zheng-Ming, et al. A Review on Polymer Nanofibers by Electrospinning and Their Applications in Nanocomposites . *Composites Science and Technology*.2003, 63, 15, s. 2223-2253.

[13] DEITZEL, J. M., et al. Controlled Deposition of Electrospun Poly(ethylene oxide) Fibers. *Polymer*. 2001, 42, 19, s. 8163-8170.

[14] YARIN, A. L.; ZUSSMAN, E. Upward Needleless Electrospinning of Multiple Nanofibers. *Polymer*. 2004, 45, 9, s. 2977-2980.

[15] LUKÁŠ, David; SARKAR, Arindam; POKORNÝ, Pavel. Self-organization of Jets in Electrospinning from Free Liquid Surface: A Generalized Approach. *Journal of Applied Physics*. 2008, 103, 8, s. 084309.

[16]Roller Electrospinning, [online], [cit. 16. 7. 2013]. Dostupný z WWW: Http://en.wikipedia.org/wiki/Roller_electrospinning, (n.d.).

[17] Z. Rożek, W. Kaczorowski, D. Lukáš, P. Louda, S. Mitura, Potential applications of nanofiber textile covered by carbon coatings, *Journal of Achievements in Materials and Manufacturing Engineering*. 27 (2008) 35–38.

[18] S. Iijma (**1991**) *Nature* 354,56

[19] S. Iijima, T. Icihashi, Single-shell carbon nanotubes of 1-nm diameter, *Nature* 363, 603-605, **1993**

[20] O. Breuer, Uttandaraman Sundararaj, Big returns from small fibres: a review of polymer/carbon nanotube composites, *polymer composites*, vol. 25, No. 6, december **2004**

[21] I. Oconnor, H. Hayden, S. Oconnor, J. N. Coleman, Yi K. Gunko, Polymer reinforcement with Kevlar-coated carbon nanotubes, *J. Phys. C* **2009**, 113, 20184-20192

[22] S. Chopra, K. McGuire, N. Gothard, A. M. Rao, Selective gas detection using a carbon nanotube sensor, *Applied physics letters*, volume 83,number 11, 15 semptember **2003**

[23] B-S Kong, H-T. Jung, S. H. Park, M-K. Park, Enhancement in electrical conductivity of transparent single-walled carbon nanotube films, Proceeding of the 2nd IEEE international conference on nano/micro engineered and molecular systems, January 16-19, **2007**, Bangkok, Thailand

[24] Institute of Engineering Innovation, School of Engineering, The University of Tokyo , Research:Chirality of single-walled carbon nanotubes,[on-line].[cit. 7.7.2012] http://ykkato.t.u-tokyo.ac.jp/nanotubechirality.en.html

[25] Chris Lee ,Arstechnica, A tangle of nanotubes make for great insulation, Mar 13 2009,[on-line].[cit. 7.7.2012] http://arstechnica.com/science/2009/03/a-tangle-of-nanotubes-in-your-roof-for-insulation/

[26] D. S. Betbune, C. H. Kinag, M. S. Devrics, G. Gorman, R. Savoy, J. Vascuez, R. Beyers, *Nature* 363, (**1993**), 605

[27] Electronic transition energies and vibrational properties of carbon nanotubes,Prof. Dr. Christian Thomsen, Institut für Festkörperphysik, TU Berlin, [on-line].[cit.1.11..2012],http://www.physik.uni-regensburg.de/aktuell/KollSS05/Thomsen-Vortrag.htm

[28] J. Prasek, J. Drbohlavova, J. Chomoucka, J. Hubalek, O. Jasek, V. Adam, R. Kizek, Methods for carbon nanotubes synthesis-review,*J. Mater. Chem.,* **2011**, 21,15872, doi: 10.1039./cjm12254a

[29] E. Mendoza, S.J. Henley, C.H.P. Poa, V. Stolojan, G.Y. Chen, C.E. Giusca, J.D. Carey, S.R.P. Silva, Dendrimer assisted catalytic growth of mats of multiwall carbon nanofibers, *Carbon*, 43, 2215-2234, **2005**

[30] E. Ghavanloo, S. A. Fazelzadeh, Vibration characteristics of single-walled carbon nanotubes based on an anisotropic elastic shell model including chirality effect , **2012**, *Applied Mathematical Modelling*, 36 (10) , pp. 4988-5000.

[31] E. T. Thostenson, Tsu-wei Chou, On the Elastic Properties of Carbon Nanotubebased Composites: Modeling and Characterization, *Journal of Physics D: AppliedPhysics*, 36, 573-576, **2003**

[32] J. Allen, Vincent C. Tung, and Richard B. Kaner ,Honeycomb Carbon: A Review of Graphene,Matthew,*Chemical Reviews* 2010 *110* (1), 132-145

[33] G. Dresselhaus, M.S. Dresselhaus, and P. Avouris, Carbon nanotubes: synthesis, structure, properties and applications, Springer Verlag, 1st edition, **2001**

[34] T. W. Ebbesen, P. M. Ajayan, H. Hiura, and K. Tanigaki, *Nature* 367, 519 **1994**.

[35] R. Saito, M. Fujita, G. Dresselhaus, and M.S. Dresselhaus, *Appl. Phys. Lett.*, 60, 2204, **1992**.

[36] V. Choudhary, A. Gupta, Carbon Nanotubes - Polymer Nanocomposites, Edited by Siva Yellampalli, ISBN 978-953-307-498-6, Published: August 17, **2011** under CC BY-NC-SA 3.0 license, in subject Polymers

[37] T. Prnka, K. Šperlink, Bionanotechnologie, Nanobiotechnologie, Nanomedicína, *vyd. Repronis*, 9/**2006**, Ostrava, ISBN 80-7329-134-7, p. 177.

[38] P Lhoták, Chemie fullerenů, Ústav Organické Chemie, VŠCHT Praha [on-line].[cit. 29.10.2012], p. 208. <http://ww.w.uochb.cas.cz/Zpravy/PostGrad2004/7_Lhotak.pdf>

[39] P. J. F. Harris, Carbon Nanotubes and Related Structures - New Materials for 21st Century, Departmen of Chemistry university of Reading, *1999*, Cambridge UK, ISBN 0-521-55446-2, p. 277.

[40] F. F. Komarov, A. M. Mironov, Carbon Nanotubes: Present and Future, *Physics and chemismy of solid state*, Vol. 5, No. 3, **2004**, p. 411 – 429

[41] M. Daenen, R. D. Fouw, B. Hamers, P. G. A. Janssen, K. Schouteden, M. A. J. Veld, The Wondrous World of Carbon Nanotubes (a review of current carbon nanotube technologies), Eindhoven University of Technology, *2003*, p. 89.

[42] H. Snášelová, Nanokompozit na bázi PVAc/MWNT připravený metodou roztoko-vé polymerace, příprava nanovláken technologií elektrospinning, Diplomová práce, FT UTB Zlín, **2008**, p. 106.

[43] Y. Ando, S. Iijima: *Jpn. J. Appl. Phys*. 32(**1993**), L107

[44] D. Gilbert Nessim, Properties, synthesis, and growth mechanisms of carbon nanotubes with special focus on thermal chemical vapor deposition, (Review Article) *Nanoscale*, **2010**, 2**,** 1306-1323, DOI:10.1039/B9NR00427K

[45] P. J. F. Harris, Solid State Growth Mechanisms for Carbon Nanotubes, *Carbon*, Vol. 45, **2007**, p. 229 – 239.

[46] Leibniz Institute for Solid State and Materials Research Dresden, [on-line].[cit.16.7..2013],< http://www.ifw-dresden.de/institutes/iff/research/Carbon/CNT/laser-ablation >

[47][online].[cit.16.7..2013],<http://www.nabond.com/Carbon%20Nanotube%20Production%20Device%20by%20Chemical%20Vapor%20Deposition_CVD751.htm>

[48] M. Yudasaka, Carbon nanotubes, environmentally benign new materials, Jidosha Gijutsukai Chubu Shibuho, 51, 48, **2002**

[49] J. Hilding, E. A. Grulke, Z. G.Zhang, and F. Lockwood, Dispersion of Carbon Nanotubes in Liquids, *Journal of Dispersion Science and Technology*, 24, 1, 1, **2003**

[50] M. Haluska, M. Hulman,; M. Hirscher,M. Becher, S. Roth, I. Stepanek, P. Bernier. Hydrogen storage in mechanically treated singlewall carbon nanotubes, AIP Conf. Proc., 591(Electronic Properties of Molecular Nanostructures), 603, **2001**

[51] A. Hirsch, Functionalization of single-walled carbon nanotubes, Angewandte Chemie International Edition, 41, 11, 1853, **2002**

[52] A. Hirsch, Functionalization of Single-Walled Carbon Nanotubes, *Angew. Chem.* 41 1853 1859 , 0044-8249, **2002**

[53] H. Huang, H. Kajiura, A. Yamada, M. Ata, Purification and alignment of arc synthesissingle-walled carbon nanotube bundles. *Chem. Phys. Lett*.**2002**, 356 (5,6), 567– 572.

[54] J.-M Moon, K. H. An, Y. H. Lee, Y. S. Park, D. J. Bae, G.S. Park, High-yield purification process of singlewalled carbon nanotubes. *J. Phys.Chem. B*, **2001**,105 (24),5677–5681.

[55] K. Esumi, M. Ishigami, A. Nakajima, K. Sawada, H. Honda, Chemical treatment of carbon nano-tubes. *Carbon* **1996**, 34 (2), 279–281.

[56] J. Chen, A. M. Rao, S. Lyuksyutov, M. E. Itkis, M. A. Hamon, H. Hu, R. W. Cohn,P. C. Eklund, D.T. Colbert, R.E. Smalley, R. C. Haddon, Dissolution of fulllength single-walled carbon nanotubes. *J. Phys. Chem. B* **2001**, 105 (13), 2525–2528.

[57] In-Yup Jeon, Dong Wook Chang, Nanjundan Ashok Kumar and Jong-Beom Baek, Functionalization of Carbon Nanotubes, Edited by Siva Yellampalli, ISBN 978-953-307-498-6, Published: August 17, 2011 under, CC BY-NC-SA 3.0 license, in subject Polymers

[58] R. J. Hunter, Foundations of Colloid Science; *Oxford University Press*: New York, **1986**; Vol. 1,600 pp.

[59] G. S. Duesberg, M. Burghard, J. Muster, G. Philipp, S. Roth, Separation of carbon nano-tubes by size exclusion chromatography. *Chem. Commun.* (Cambridge) **1998**, (3), 435–436.

[60] B. Vigolo, A. Penicaud, C. Coulon, C. Sauder, C. Pailler, R.; Journet, C.; Bernier, P.; Poulin, P. Dispersions and fibers of carbon nanotubes. Materials Research Society Symposium Proceedings **2001**, 633 *Nanotubes and Related Materials*, A12.1.1– A12.1.9.

[61] J. Liu, A .G. Rinzler, H. Dai, J. H. Hafner, R. K. Bradley, P. J. Boul, A. Lu, T. Iverson, K. Shelimov, C. B. Huffman, F. Rodriguez-Macias, Y.S. Shon, T. R. Lee, D. T. Colbert, R. E. Smalley, Fullerene pipes. *Science* (Washington, D. C.) **1998**, 280 (5367), 1253–1256.

[62] J. C. Lewenstein, T. P. Burgin, A. Ribayrol, L. A. Nagahara, R. K. Tsui, High yield selective placement of carbon nanotubes on pre-patterned electrodes. *Nano Lett*. **2002**, 2 (5), 443–446.

[63] M. Burghard, G. Duesberg, G. Philipp, J. Muster, S. Roth, Controlled adsorption of carbon nanotubes on chemically modified electrode arrays. *Adv. Mater*. (Weinheim, Germany) **1998**, 10 (8), 584–588.

[64] J.E. Riggs, D.B. Walker, D.L. Carroll, Y.P Sun, Optical limiting properties of suspended and solubilized carbon nanotubes. *J. Phys. Chem. B* **2000**, 104 (30), 7071– 7076.

[65] A. R. Boccaccini, J. Cho, J. A. Roether, B. J. C. Thomas, J. E. Minay, M. S. P. Shaffer,Carbon 2006, 44, 3149.

[66] O. O. Van der Biest, L. J. Vandeperre, Annu. Rev. Mater. Sci. 1999, 29, 327.

[67] Qiguan Wang and Hiroshi Moriyama (2011). Carbon Nanotube-Based Thin Films: Synthesis and Properties, Carbon Nanotubes - Synthesis, Characterization, Applications, Dr. Siva Yellampalli (Ed.), ISBN: 978-953-307-497-9, InTech, DOI: 10.5772/22021.

[68] J. U. Park, M. Hardy, S. J. Kang, K. Barton, K. Adair, D. K. Mukhopadhyay, C. Y. Lee, M. S. Strano, A. G. Alleyne, J. G. Georgiadis, P. M. Ferreira, J. A. Rogers, Nat. Mater. 2007, 6, 782.

[69] K. Kordas, T. Mustonen, G. Toth, H. Jantunen, M. Lajunen, C. Soldano, S. Talapatra, S. Kar, R. Vajtai, P. M. Ajayan, Small 2006, 2, 1021.

[70] S. L. Hellstrom,Basic Models of Spin Coating,October 28, 2007,submitted as coursework for Physics 210, Stanford University, Autumn 2007

[71] Z. C. Wu, Z. H. Chen, X. Du, J. M. Logan, J. Sippel, M. Nikolou, K. Kamaras, J. R. Reynolds, D. B. Tanner, A. F. Hebard, A. G. Rinzler, Science 2004, 305, 1273.

[72]][online].[cit.16.7..2013], http://speechinthesilence.com/web/2012/05

[74] A Thess R. Lee P. Nikolaev H. Dai, P. Petit P, Robert J, Xu C, et al.. Crystalline ropes of metallic carbon nanotubes. *Science* **1996**, 273: 483-487

[75]TV Sreekumar,T. Liu, S. Kumar, LM. Ericson, RH Hauge, RE Smalley, Singlewall nanotube film. *Chemistry of Materials*. **2003**, 15: 175-178

[76] Z. Wang, ZY. Liang, B. Wang, C. Zhang, L. Kramer, Processing and property investigation of single-walled carbon nanotube (SWNT) buckypaper/epoxy resin matrix nanocomposites. *Composites Part A: Applied Science and Manufacturing* **2004**, 35(10): 1225-1232

[77] AG. Rinzler, J. Liu, H. Dai, P. Nikolaev, CB. Huffman, FJ. Rodriguez-Macias, et al.. Large-scale purification of single-wall carbon nanotubes: process, product, and characterization. *Appl Phys A* **1998**, 67: 29-37

[78] AG. Rinzler, J. Liu, H. Dai, P. Nikolaev, C.B. Huffman, F.J. Rodriguez-Macias, P.J. Boul, A. H. Lu, D. Heymann, D.T. Colbert, R.S. Lee, J.E. Fischer, A.M. Rao, P.C.Eklund, R.E. Smalley, Large-scale purification of single-wall carbon nanotubes: process, product, and characterization, *Applied Physics A*, 67, 29-37, **1998**

[79] L. Valentini ,C. Cantalini, I. Armentano, J.M. Kenny, L. Lozly sensitive and selective sensorsbased on carbonnanotubesthin films for molecular detection, *Diamond and Related Materials*, Volume 13, Issues 4–8, April–August **2004**, Pages 1301–1305

[80] J. Suehiro, G. Zhou and M. Hara, Fabrication of a carbon nanotube-based gas sensor using dielectrophoresis and its application for ammonia detection by impedance spectroscopy ,2003 J. Phys. D: Appl. Phys. 36 L109 doi:10.1088/0022-3727/36/21/L01

[81] I. Sayago , M.J. Fernández, J.L. Fontecha, M.C. Horrillo, C. Vera, I. Obieta, I. Bustero Newsensitivelayers for surfaceacousticwavegassensors based on polymer and carbon nanotube composites, Procedia Engineering Volume 25, **2011**, Pages 256–259

[82] P. G. Collins, K. Bradley, M. Ishigami, and A. Zettl, *Science*, Vol. 287, 1801,**2000**.

[83] G. U. Sumanasekera, C. K. W. Adu, S. Fang, P. C. Eklund, *Phys. Rev. Lett.* Vol. 85, 1096,**2000**.

[84] S. Chopra, A. Pham, J. Gaillard, A.Parker, A. M. Rao, *Appl. Phys. Lett.* Vol. 80,4632,**2002**.

[85] K. G. Ong, K. Zeng, G. A. Grimes, *IEEE sens. J.* Vol. 2,82,**2002**.

[86] A. Huczko, Synthesis of aligned carbon nanotubes, *Applied Physics A materials Science Processing*, vol A74, pp 617-38, **2002**.

.

[87] W.S. Cho, S.I. Moon, Y. D Lee, Y.H. Lee, J.H. Park, B.K. Ju, *IEEE Electron. Dev. Lett*. 26 (**2005**) 498.

[88] S. Santucci et al., *J. Chem. Phys*. 119 (**2003**) 10904.

[89] J. Mauricio Marulanda, Carbon Nanotubes Applications on Electron Devices, Published: August 1, **2011** under CC BY-NC-SA 3.0 license, in subject Nanotechnology and Nanomaterials, ISBN 978-953-307-496-2

[90] K. Arshak, E. Moore, G.M. Lyons, J. Harris and S. Clifford, A review of gas sensors employed in electronic nose applications, *Sensor Review*, Volume 24 · Number 2 **2004** , 181–198

[91] [online].[cit.16.7..2013], http://bruceleeeowe.wordpress.com/2011/02/19/multifunctional-carbon-nanotubes-introduction-and-applications-of-multifunctional-carbon-nanotubes/

[92] A Mufti, Guidelines for Structural Health Monitoring, University of Manitoba, ISIS Canada, **2001**.

[93] C Silkorsky, Development of a Health Monitoring System for Civil Structures using a Level IV Non-Destructive Damage Evaluation Method, Proceedings of the 2nd International Workshop on Structural Health Monitoring, Stanford, CA, USA, **1999**.

[94] D. Balageas, C-P. Fritzen, A. Guemes, Structural Health monitoring, *ISTE Ltd*, **2006**

[95] J P Lynch and K Loh, A Summary Review of Wireless Sensors and Sensor Networks for Structural Health Monitoring, *Shock and Vibration Digest*, Vol 38, No 2, pp 91-128, **2006**.

[96] R A Shoureshi and A Shen, Analysis and Development of a Nervous System for Civil Structuring, Proceedings of the 4th International Conference on Earthquake Engineering, Taipei, Taiwan, **2006**.

[97] I Kang, M J Schulz, J H Kim, V Shanov and D Shi, A carbon nanotube strain sensor for structural health monitoring, *Smart Materials and Structures*, Vol 15, pp 737-748, **2006**.

[98] S Minakuchi, H Tsukamoto and N Takeda, 'Hierarchical sensing system for detecting impact damage in composite structures combining a fiber optic spinal cord network and distributed sensor nerve cell devices', Proceedings of the 7th International Workshop on Structural Health Monitoring, Stanford, CA, USA, pp 878-885, **2009**.

[99] T. Giang, Pham, Y-B. Park, Z. Liang, Ch. Zhang, B. Wang,Processing and modeling of conductive thermoplastic/carbon nanotube films for strain sensing,*Composites Part B: Engineering, Marine Composites and Sandwich Structures*,Volume 39, Issue 1, January **2008**, Pages 209–216

[100] P Dharap, Z Li, S Nagarajaiah and E V Barrera, Nanotube film based on single-wall carbon nanotubes for strain sensing, *Nanotechnology*, Vol 15, No 3, pp 379-382, **2004**.

Hindawi Publishing Corporation
Journal of Nanomaterials
Volume 2012, Article ID 365062, 7 pages
doi:10.1155/2012/365062

Research Article

An Electrically Conductive and Organic Solvent Vapors Detecting Composite Composed of an Entangled Network of Carbon Nanotubes Embedded in Polystyrene

R. Olejnik,[1,2] P. Slobodian,[1,2] P. Riha,[3] and P. Saha[1,2]

[1] *Polymer Centre, Faculty of Technology, Tomas Bata University in Zlin, 76001 Zlin, Czech Republic*
[2] *Centre of Polymer Systems, University Institute, Tomas Bata University in Zlin, Nad Ovcirnou 3685, 76001 Zlin, Czech Republic*
[3] *Institute of Hydrodynamics, Academy of Sciences, 16612 Prague, Czech Republic*

Correspondence should be addressed to P. Slobodian, slobodian@ft.utb.cz

Received 30 January 2012; Accepted 12 March 2012

Academic Editor: Sevan P. Davtyan

A composite composed of electrically conductive entangled carbon nanotubes embedded in a polystyrene base has been prepared by the innovative procedure, when the nonwoven polystyrene filter membrane is enmeshed with carbon nanotubes. Both constituents are then interlocked by compression molding. The mechanical and electrical resistance testing show that the polymer increases nanotube network mechanical integrity, tensile strength, and the reversibility of electrical resistance in deformation cycles. Another obvious effect of the supporting polymer is the reduction of resistance temperature dependence of composite and the reproducibility of methanol vapor sensing.

1. Introduction

Recent technology progress relies heavily on the use of materials that provide advanced structural and functional capabilities. In this respect, entangled carbon nanotube (CNT) network of buckypaper presents great promise for developing high-performance polymeric materials [1–3]. The networks can proportionally transfer their unique properties into composites and bring substantial improvements in structural strength, electrical and thermal conductivity, electromagnetic interference shielding, and so forth compared to polymer composites with carbon nanotube particulate filler.

The first polymer composite with CNT network was fabricated via filtering nanotube dispersion through fine filtration mesh [4]. Nanotubes stuck to each other and formed a thin entangled structure of pure nanotubes, later dubbed buckypaper. The network was then fixed by a polymer solution (epoxy [5, 6] or bismaleimide resin [1], polyvinyl alcohol, polyvinylpyrrolidone and polyethylene oxide water solutions [7]) to form composites.

However, the fabrication of CNT network-based polymer composite described above was rather laborious. Our idea is to circumvent polymer solution methods and to suggest a simple and easier manufacturing of multiwall carbon nanotube (MWNT) network-based polymer composites. The novel process consists in using nonwoven polystyrene (PS) filter as an integrating and supporting element on which nanotubes cumulate and form a network during MWNT suspension filtration. The nanotubes slightly infiltrate into the filter and adhere to it, finally forming a continuous layer. The obtained MWNT/PS-layered composite is compression molded above the melting temperature of PS, which causes transformation of the filter into flexible PS film. Repeating layering of MWNT/PS films enables producing bulky material.

The processing technique seems promising for continuous manufacturing of CNT networks/polymer composites since the filter support ensures the composite compactness. Peeling off MWNT layer from the membrane, which is common in previous methods, is eliminated here as well as network impregnation by polymer solutions.

In the present paper, the scanning electron microscopy (SEM) of a layered structure of MWNT network/polystyrene composite is carried out together with the tests of composite

tensile deformation and electrical resistance. The additional testing reveals the effect of the supporting polymer on the resistance temperature dependence of composite and the reproducibility of methanol vapor sensing.

2. Materials

Purified MWCNTs produced by chemical vapor deposition of acetylene which were supplied by Sun Nanotech Co. Ltd., China. According to the supplier, the nanotube diameter is 10–30 nm, length 1–10 μm, with a purity of ~90% and (volume) resistivity of 0.12 Ωcm. Further details on the nanotubes were obtained by means of the transmission electron microscopy (TEM) analysis presented in our previous paper [8]. From the corresponding micrographs, the diameter of individual nanotubes was determined to be between 10 and 60 nm, their length from tenths of micron up to 3 μm. The maximum aspect ratio of the measured nanotubes is thus about 300. The multiwall consists of about 15–35 rolled layers of graphene. Another analyses estimate oxygen content on CNT surface 5.5 at percentage with O/C ratio 0.06 measured by X-ray photoelectron spectroscopy, the high thermal stability measured by Thermogravimetric Analysis when only negligible degradation in the range of temperatures up to 700°C occurs, that is, a loss of mass ca 3 wt. % [9].

Polystyrene is a commercial polymer (Krasten 137, Kaucuk-Unipetrol Group, M_n = 102 530, and M_w/M_n = 2.75). Sodium dodecyl sulfate (SDS) and 1-pentanol were used as surfactant and cosurfactant, respectively. Methyl isobutyl ketone (MIBK) and dimethylformamide (DMF) were used as PS solvents, and tetraethylammonium bromide was used to adjust conductivity of PS solutions for electrospinning (filter preparation).

3. Experimental

MWNTs were used for the preparation of aqueous paste: 1.6 g of nanotubes and ~50 mL of deionized water were mixed with the help of a mortar and pestle. The paste was diluted in deionized water with SDS and 1-pentanol [10–12]. Then NaOH/water solution was added to adjust pH to the value of 10 [13]. The final nanotube concentration in the dispersion was 0.3 wt. % concentration of SDS and 1-pentanol 0.1 M and 0.14 M, respectively [10]. The dispersion was sonicated in Dr. Hielscher GmbH apparatus (ultrasonic horn S7, amplitude 88 μm, power density 300 W/cm^2, and frequency 24 kHz) under the temperature of ca 50°C for 2 hours.

Polystyrene nonwoven mats for filtration of nanotube dispersion were prepared by electrospinning from PS solution. The polymer was dissolved in a mixture of MIBK/DMF with the volume ratio 3 : 1 and PS concentration 15 wt. %. Electrical conductivity of the solution was adjusted to 75 μS/cm by tetraethylammonium bromide. PS nanofiber layer was manufactured using the NanoSpider (Elmarco, s.r.o.) equipped with a steel rotating electrode with needles and a steel cylindrical collecting electrode (more details in [14]). Electrospinning was carried out under the following conditions: electric voltage 75 kV (Matsusada DC power supply), temperature 20–25°C, relative humidity 25–35%, and the electrode rotation speed 8 min^{-1}. The motion rate of antistatic polypropylene nonwoven fabric which collects nanofibers was 0.16 m/min. To produce final PS nonwoven filters, the prepared nanofiber porous layer (thickness of about 1 mm) was subjected to hot pressing under 0.6 MPa and temperature 80°C.

In order to prepare entangled MWNT network on the supporting PS filter, a vacuum-filtration method was used. The formed disk-shaped network was washed several times by deionized water (to reach neutral pH) and methanol in situ. Subsequently, MWNT network with PS filter was placed between two acetone moistened filter papers and dried between two iron plates at room temperature for 24 hours. The final drying continued without iron plates at 40°C for another day. The thickness of the nonwoven PS filter was typically 0.5–0.8 mm, and the thickness of MWNT entangled network, according of the amount of dispersion filtered, was from 0.02 to 0.26 mm. The formed PS filter-supported MWNT network was then compression molded at 190°C. Thus, the originally porous PS filter was transformed into a film.

For comparison, pure carbon nanotube networks were prepared by filtration of dispersions through polyurethane nonwoven filters prepared again by electrospinning according to procedure described in [14]. After filtration, the MWNT sediment was washed by deionized water and methanol in situ and drained between dry filter papers for a moment before the entangled MWNT sediment was gently peeled off the filter and dried.

The structure of PS nonwoven filter as well as that of MWNT network was investigated with a scanning electron microscope (SEM) Vega LMU (Tescan s.r.o., Czech Republic). The sample was deposited on carbon targets and covered with a thin Au/Pd layer. The observation was carried out in the regime of secondary electrons.

The strength of the network was measured in a simple test. The sample materials (PS filter-supported MWNT network; pure entangled MWNT network) were cut into stripes (length 45 mm and width 10 mm) and stretched stepwise with 60 sec delay in deformation reading in each step.

To measure the dependence of electrical resistance on tensile deformation of MWNT/PS composite, the stripe (length 30 mm and width 5 mm) cut from the prepared MWNT/PS composite was fixed on PS tensile test specimen (dog bone shape) using 20 wt. % solution of PS in butanone. Two electrical contacts were fixed to the stripe by silver colloid electroconductive paint Dotite D-550 (SPI Supplies). The electrical resistance was measured lengthwise during 7 consecutive tensile cycles by a two-point technique with multimeter Sefram 7338.

MWNT/PS composite as a potential resistive gas sensor for organic vapor detection was identified by the electrical resistance measurement in a chemical vapor atmosphere. The resistance of network stripe cut out from the manufactured disks (length 15 mm, width 5 mm, and thickness

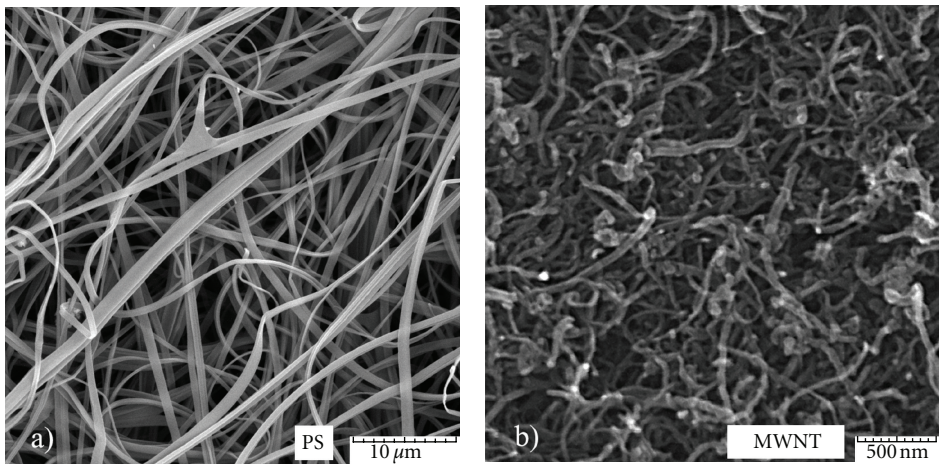

(a) (b)

Figure 1: SEM image of (a) PS filter prepared by electrospinning (displayed scaler 10 μm) and (b) surface of entangled MWNT network (scaler 500 nm).

ca 0.3 mm) was measured along the specimen length by the two-point technique using multimeter Sefram 7338. The stripe was placed on a planar holder with Cu electrodes fixed on both sides of the specimen. Time-dependent electrical resistance measurement was performed during adsorption and desorption cycles. In the former case the holder with the specimen was quickly transferred into an airtight conical flask full of methanol vapor, a layer of which was at the bottom. The measurement was conducted in the saturated vapor at atmospheric pressure, temperature 25°C and relative humidity 60%. After 6 minutes of measurement the holder was promptly removed from the flask, and for the next 6 minutes the sample was measured in the mode of desorption. This was repeated five times in consecutive cycles.

The temperature dependence of electrical resistance of MWNT networks and MWNT/PS composites were measured by a four-point method according to van der Pauw's idea [15]. The apparatuses used in the set up were Keithley K7002 scanner, Keithley K7011-S switching card, programmable current source Keithley K2410, Keithley K6517 electrometer and PC with GPIB cec488 and AD25PCI SE transducer cards and SVOR25TER connector. The resistance was measured at constant current 0.01 A in the course of heating from −40°C to 150°C (step 10°C) using thermostatic bath (Haake).

4. Results

4.1. SEM Results. The surface of PS filter prepared by technology of electrospinning and the upper surface of the MWNT network accumulated on the filter are shown as SEM micrographs in Figures 1(a) and 1(b), respectively. PS fibers are straight with smooth surface, submicron sizes with the average diameter of 0.6 ± 0.3 μm. The pores between them have an average size of about 0.5 μm. The apparent density of PS filter is $\rho_{\text{filter}} = 0.1\,\text{g/cm}^3$, thus its porosity ϕ for the measured PS density $\rho_{\text{PS}} = 1.04\,\text{g/cm}^3$ was calculated (from the relation below) to be about 0.9. The pores allow partial infiltration of MWNT into the filter at the beginning of filtration. When the pores are filled with nanotubes, the filter cake (pure nanotube entangled network) is formed above the filter surface, as shown in Figure 2.

The porosity of MWNT network was calculated to be $\phi = 0.67$ from relation $\phi = 1 - \rho_{\text{net}}/\rho_{\text{MWNT}}$, where $\rho_{\text{net}} = 0.56 \pm 0.03\,\text{g/cm}^3$ denotes the measured apparent density of the nanotube network ($n = 10$), and $\rho_{\text{MWNT}} = 1.7\,\text{g/cm}^3$ is the measured average density of nanotubes ($n = 3$). This density is very close to the theoretical value for MWNT, which is $1.8\,\text{g/cm}^3$ [16]. Also the network porosity corresponds to the published values for MWNT networks [17].

MWNT network was firmly embedded in PS filter by compression molding. The temperature of processing was 190°C, which is well above the glass transition temperature of PS used for experiments (T_g = 92°C, determined by differential scanning calorimetry technique). The melting phase was followed by cooling below PS glass transition temperature, when both layers were firmly linked.

Figure 3 shows composite arrangement after compression molding. The thickness of MWNT network was proportional to the volume of filtered MWNT dispersion and was typically from 26 μm to 260 μm. The arrangement of the layers of nanotube networks and PS is arbitrary. For instance, the structure prepared by double-sided filtration, MWNT-PS-MWNT composite, is shown in Figure 3(c). Other layer arrangements can be prepared by overlaying several MWNT/PS composite units prior to compression molding.

The role of MWCNT network thickness, that is, MWCNT, concentration in the conductive MWCNT network/PS composite, is not determining as in the case of particulate MWCNT/polymer composites. Though there is certainly an optimal and/or limiting MWCNT network thickness constituting resistive characteristics of the conductive

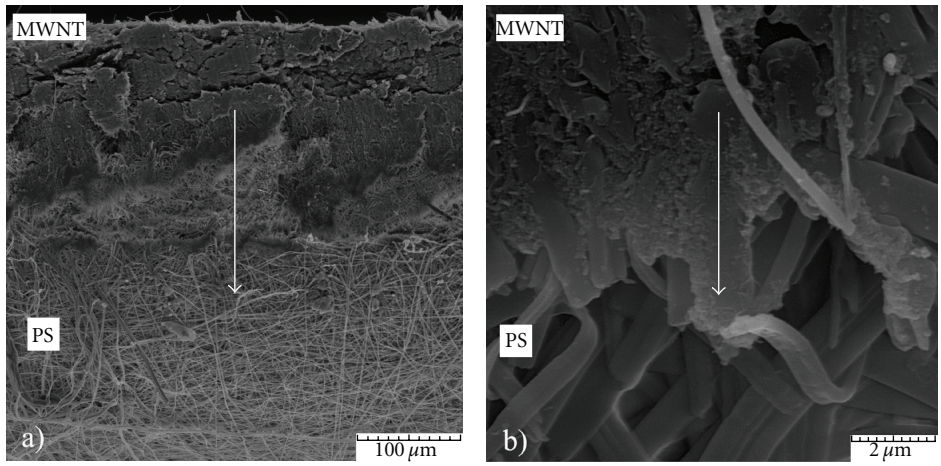

(a) (b)

Figure 2: (a) cross-section of composite consisting of MWNT network (upper part) and PS filter (lower part) before compression molding (scaler 100 μm). (b) the arrow indicates nanotube infiltration illustrated in detail in the enlarged image (scaler 2 μm).

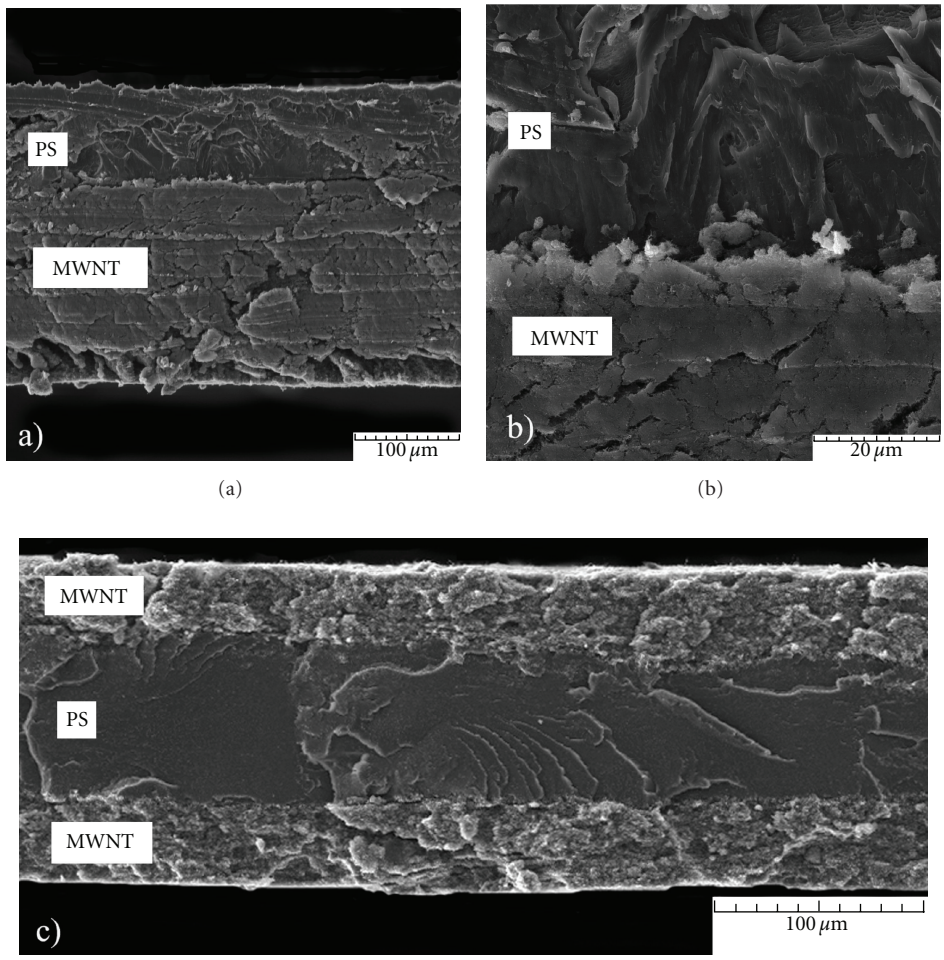

(a) (b)

(c)

Figure 3: SEM micrographs of layered MWNT network/PS composite after compression molding. (a) PS film (thicknesses about 80 μm) with attached nanotube network (260 μm) (scaler 100 μm), (b) the interface between nanotube network and PS film (scaler 20 μm), and (c) MWNT-PS-MWNT layer arrangement to decrease composite resistance (scaler 100 μm).

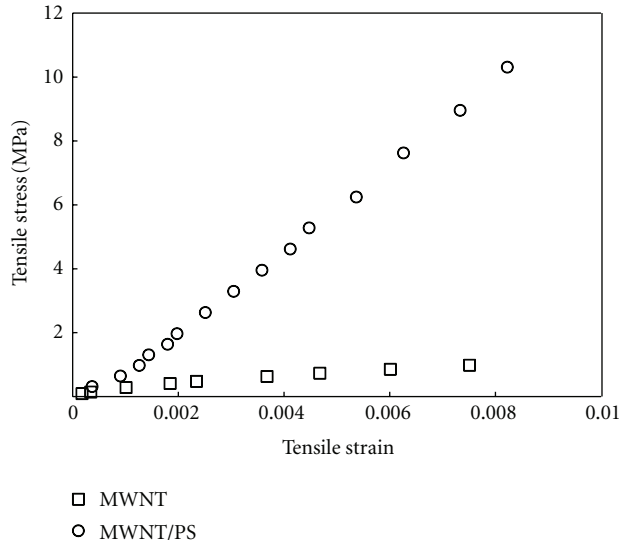

Figure 4: Tensile properties of MWNT network/PS composite (circles) and MWNT network (squares) in tensile test. Thickness of MWNT network is about 120 μm and MWNT/PS composite about 200 μm.

composite, this aspect is not investigated in this paper. Some informative results about this issue can be found in our paper [18].

To examine the length, thickness and multiwall arrangement of MWNT, TEM analysis was used. The obtained values slightly differ from the properties declared by the manufacturer. From TEM micrographs the diameter of individual nanotubes was determined to be between 10 and 60 nm, their length from tenth of micron up to 3 μm; the maximum aspect ratio is thus about 300. The number of coaxially rolled layers of graphene was typically from 10 till 35 with the interlayer distance of about 0.35 nm [8, 18].

4.2. Tensile Test Results. The results of tensile testing of MWNT network and PS filter supported MWNT network are shown in Figure 4. The measured stress/strain dependence for pure MWNT network indicates the tensile modulus of about 600 MPa and the ultimate tensile strength ~1 MPa. The values are relatively low, which corresponds to short nanotubes used for the research. PS filter support has a positive effect on the tensile strength of MWNT/PS composite, as can be seen in the same figure. The determined tensile modulus is about 1300 MPa and the ultimate tensile strength 10.3 MPa.

The electrical resistance change of MWNT network/PS composite is monitored by a two-point technique in extension/relaxation cycles. The results are shown in Figure 5 as the strain dependence of the relative resistance change $(R - R_0)/R_0$ due to the increasing tensile stress indicated in the figure. R and R_0 denote the measured and the initial resistance before the first extension/relaxation cycle, respectively. The resistance mechanism is apparently not reversible in the initial cycle, since the relaxation curve has a residual resistance increase in the offload state (Figure 6).

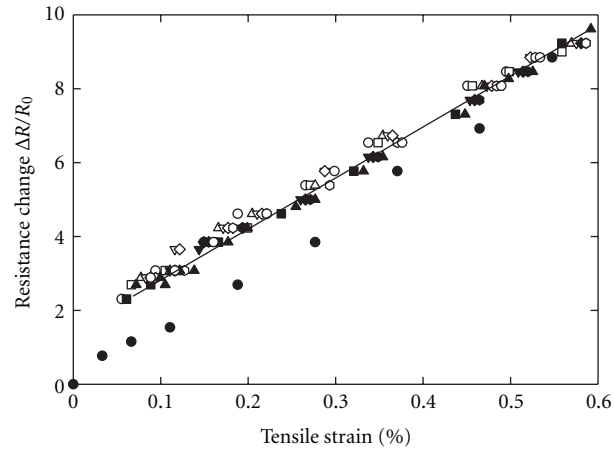

Figure 5: Relative change of electrical resistance versus tensile stress for MWNT network/PS composite subjected to 7 successive elongation/relaxation cycles (network thickness is about 20 μm; the filled and open symbols denote the extension part and the relaxation part of cycles, resp.). The solid circles represent the extension part of the first cycle and the full line the linear fitting of resistance change in subsequent cycles. The strain increase corresponds to the step increase of tensile stress 0.8, 1.9, 2.8, 4.3, 6.4, 9.2, 10.3, and 11.8 MPa, respectively.

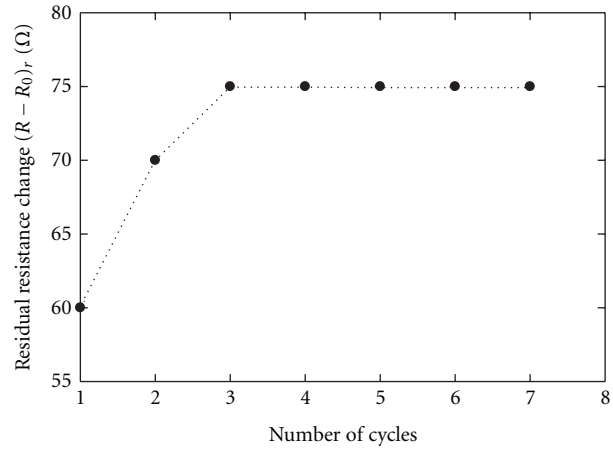

Figure 6: Residual resistance change versus number of cycles for MWNT network/PS composite subjected to 7 successive elongation/relaxation cycles.

Nevertheless, the ongoing extension cycles have a stabilizing effect on the resistance-elongation loops, and the normalized resistance change is fitted in Figure 5 by a linear dependence on tensile strain. The residual resistance change $(R - R_0)$, defined as the residual minimum resistance change during each cycle, tends to reach immediately to an asymptotic value (Figure 6). It indicates that during first deformations the nanotube network gets the structure which stays more or less the same regardless the number of deformation cycles. This mechanical stabilization is favorable for the use of the composite as a sensing element of elongation, especially when the network is suitably deformed in advance.

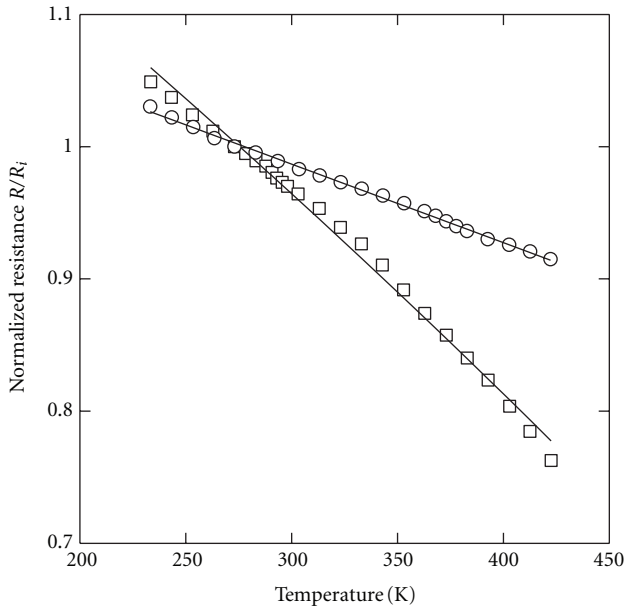

Figure 7: Temperature-dependent normalized resistance of MWNT network/PS composite (circles) and MWNT network (squares). The solid lines represent description by (1).

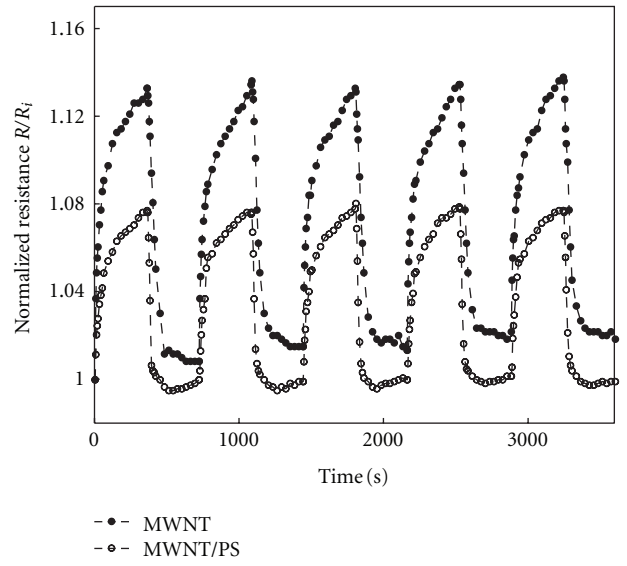

Figure 8: Time-dependent normalized resistance of MWNT network/PS composite (open circles) and MWNT network (filled circles) repeatedly exposed to methanol vapors at room temperature. The length of cycles of exposure and desorption is 360 sec.

The mechanism of resistance change during elongation combines probably a decrease of local contact forces between nanotubes as well as reduction of number of contacts. The decrease of contact forces restrains a contact of nanotubes, which in turn leads to the increase of contact resistance between crossing nanotubes. Besides that the extension straightens the nanotubes what may result in less contacts between them. Since the contact points act as parallel resistors, their decreasing number causes an enhancement of MWNT network resistance.

4.3. Electrical Resistance: the Effect of Temperature and Chemical Vapor. The effect of temperature and chemical vapor on the electrical resistance was also tested, and the results are presented in Figures 7 and 8, respectively. Figure 7 demonstrates that both the composite and pure MWNT network exhibit nonmetallic behavior ($d(R/R_i)/dT < 0$) over the investigated temperature range from 230 to 420 K. The negative slope indicates the presence of tunneling barriers, which dominate resistive behavior of the tested materials. The best description of the data presented in Figure 7 is obtained by the series heterogeneous model when the resistance is described as the sum of metallic (MWNT are regarded as metallic conductors) and barrier portions of the conduction path [19–22]:

$$\frac{R}{R_i} = aT + b\exp\left[\frac{c}{(T+d)}\right], \tag{1}$$

where a means the temperature coefficient arising from metallic resistance, and the second term (hopping/tunneling term) represents fluctuation-induced tunneling through barriers between metallic regions. T denotes temperature, b is constant depending on the geometrical factors from the effective fraction of the length for the barrier portion, and c; d are constants depending on the barrier to conduction parameters [19–22].

An obvious effect of the supporting polymer is a reduction of the temperature dependence of resistance. The resistance ratio R_{230}/R_{420} (values at the corresponding temperatures) is reduced from 1.35 in the case of MWNT network to 1.12 in the composite case.

The affinity of MWNT network with and without PS filter support to chemical vapor at room temperature is demonstrated in Figure 8. Results of repeated exposure to methanol vapors reveal that both materials response has good reproducibility. As stated in [9, 23], there are two possible mechanisms in which vapors can reversibly interact with nanotubes: physisorption, which does not involve charge transfer and chemisorption, which does. The short response time of the two materials to exposure to methanol and subsequent recovery suggests a physisorption mechanism. Methanol molecules could be absorbed to nanotube surface, which may cause a change in metallic/barrier conduction proportion resulting in the increase of resistance.

5. Concluding Remarks

Several techniques were applied to investigate a new type of composite: PS filter-supported entangled multiwall carbon nanotube network. The SEM observation indicates the penetration of carbon nanotubes into the nonwoven polystyrene filtering membrane and their tight bonding after the compression molding. The mechanical testing reveals the effect of elongation on the composite electrical resistance when a repeated stretching is exerted. The measurements have shown fivefold resistance increase at the maximum

strain as well as stability and linearity of resistance change. The sensitivity of the composite to an organic solvent vapor (methanol) has been investigated also by a resistance measurement. The resistance variation as a response to physisorption and desorption of a vapor during cycles was found to be reversible and reproducible. Thus, the testing indicates a good potentiality of the composite composed of electrically conductive entangled carbon nanotube network embedded in a polystyrene base to be applied as a sensing element for tensile deformation and organic vapors.

Acknowledgments

The work was supported by the Operational Program of Research and Development for Innovations cofunded by the European Regional Development Fund (ERDF), the National budget of Czech Republic within the framework of the Centre of Polymer Systems project (Reg. no.: CZ.1.05/2.1.00/03.0111), the Czech Ministry of Education, Youth and Sports project (MSM 7088352101). This paper was also supported by the internal grant of TBU in Zlín no. IGA/FT/2012/022 funded from the resources of specific university research and by the Fund of Institute of Hydrodynamics AV0Z20600510.

References

[1] Q. Cheng, J. Bao, J. Park, Z. Liang, C. Zhang, and B. Wang, "High mechanical performance composite conductor: multi-walled carbon nanotube sheet/bismaleimide nanocomposites," *Advanced Functional Materials*, vol. 19, no. 20, pp. 3219–3225, 2009.

[2] D. Wang, P. Song, C. Liu, W. Wu, and S. Fan, "Highly oriented carbon nanotube papers made of aligned carbon nanotubes," *Nanotechnology*, vol. 19, no. 7, Article ID 075609, 2008.

[3] S. Wang, Z. Liang, B. Wang, and C. Zhang, "High-strength and multifunctional macroscopic fabric of single-walled carbon nanotubes," *Advanced Materials*, vol. 19, no. 9, pp. 1257–1261, 2007.

[4] D. A. Walters, M. J. Casavant, X. C. Qin et al., "In-plane-aligned membranes of carbon nanotubes," *Chemical Physics Letters*, vol. 338, no. 1, pp. 14–20, 2001.

[5] J. Gou, "Single-walled nanotube bucky paper and nanocomposite," *Polymer International*, vol. 55, no. 11, pp. 1283–1288, 2006.

[6] Z. Wang, Z. Liang, B. Wang, C. Zhang, and L. Kramer, "Processing and property investigation of single-walled carbon nanotube (SWNT) buckypaper/epoxy resin matrix nanocomposites," *Composites A*, vol. 35, no. 10, pp. 1225–1232, 2004.

[7] G. Xu, Q. Zhang, W. Zhou, J. Huang, and F. Wei, "The feasibility of producing MWCNT paper and strong MWCNT film from VACNT array," *Applied Physics A*, vol. 92, no. 3, pp. 531–539, 2008.

[8] P. Slobodian, P. Riha, A. Lengalova, and P. Saha, "Compressive stress-electrical conductivity characteristics of multiwall carbon nanotube networks," *Journal of Materials Science*, vol. 46, no. 9, pp. 3186–3190, 2011.

[9] P. Slobodian, P. Riha, A. Lengalova, P. Svoboda, and P. Saha, "Multi-wall carbon nanotube networks as potential resistive gas sensors for organic vapor detection," *Carbon*, vol. 49, no. 7, pp. 2499–2507, 2011.

[10] C. S. Chern and L. J. Wu, "Microemulsion polymerization of styrene stabilized by sodium dodecyl sulfate and short-chain alcohols," *Journal of Polymer Science A*, vol. 39, no. 19, pp. 3199–3210, 2001.

[11] A. S. Patole, S. P. Patole, J. B. Yoo, J. H. Ahn, and T. H. Kim, "Effective in situ synthesis and characteristics of polystyrene nanoparticle-Covered multiwall carbon nanotube composite," *Journal of Polymer Science B*, vol. 47, no. 15, pp. 1523–1529, 2009.

[12] A. S. Patole, S. P. Patole, S. Y. Jung, J. B. Yoo, J. H. An, and T. H. Kim, "Self assembled grapheme/carbon nanotube/polystyrene hybrid nanocomposite by in situ microemulsion polymerization," *European Polymer Journal*, vol. 48, pp. 252–259, 2012.

[13] H. T. Ham, Y. S. Choi, and I. J. Chung, "An explanation of dispersion states of single-walled carbon nanotubes in solvents and aqueous surfactant solutions using solubility parameters," *Journal of Colloid and Interface Science*, vol. 286, no. 1, pp. 216–223, 2005.

[14] D. Kimmer, P. Slobodian, D. Petras, M. Zatloukal, R. Olejnik, and P. Saha, "Polyurethane/MWCNT nanowebs prepared by electrospinning process," *Journal of Applied Polymer Science*, vol. 111, pp. 2711–2714, 2009.

[15] L. J. van der Pauw, "A method of measuring specific resistivity and Hall effect of discs of arbitrary shape," *Philips Research Reports*, vol. 13, pp. 1–9, 1958.

[16] X. L. Xie, Y. W. Mai, and X. P. Zhou, "Dispersion and alignment of carbon nanotubes in polymer matrix: a review," *Materials Science and Engineering R*, vol. 49, no. 4, pp. 89–112, 2005.

[17] R. L. D. Whitby, T. Fukuda, T. Maekawa, S. L. James, and S. V. Mikhalovsky, "Geometric control and tuneable pore size distribution of buckypaper and buckydiscs," *Carbon*, vol. 46, no. 6, pp. 949–956, 2008.

[18] P. Slobodian, P. Riha, A. Lengalova, R. Olejnik, and P. Saha, "Effect of compressive strain on electric resistance of multi-wall carbon nanotube networks," *Journal of Experimental Nanoscience*, vol. 6, pp. 294–304, 2011.

[19] A. Allaoui, S. V. Hoa, P. Evesque, and J. Bai, "Electronic transport in carbon nanotube tangles under compression: the role of contact resistance," *Scripta Materialia*, vol. 61, no. 6, pp. 628–631, 2009.

[20] A. B. Kaiser, Y. W. Park, G. T. Kim, E. S. Choi, G. Düsberg, and S. Roth, "Electronic transport in carbon nanotube ropes and mats," *Synthetic Metals*, vol. 103, no. 1–3, pp. 2547–2550, 1999.

[21] M. Shiraishi and M. Ata, "Conduction mechanisms in single-walled carbon nanotubes," *Synthetic Metals*, vol. 128, no. 3, pp. 235–239, 2002.

[22] S. Kulesza, P. Szroeder, J. K. Patyk, J. Szatkowski, and M. Kozanecki, "High-temperature electrical transport properties of buckypapers composed of doped single-walled carbon nanotubes," *Carbon*, vol. 44, no. 11, pp. 2178–2183, 2006.

[23] S. G. Wang, Q. Zhang, D. J. Yang, P. J. Sellin, and G. F. Zhong, "Multi-walled carbon nanotube-based gas sensors for NH_3 detection," *Diamond and Related Materials*, vol. 13, no. 4–8, pp. 1327–1332, 2004.

Key Engineering Materials Vol. 543 (2013) pp 356-359

doi:10.4028/www.scientific.net/KEM.543.356

Temperature Dependence of Electrical Conductivity of Multi-Walled Carbon Nanotube Networks in a Polystyrene Composite

David Petras[1,a], Petr Slobodian[1,2,b], Robert Olejnik[1,2,c], Pavel Riha[3,d]

[1]Tomas Bata University in Zlin, Faculty of Technology, Polymer Centre, T.G.M. 275, 760 01 Zlin, Czech Republic

[2]Tomas Bata University in Zlin, Centre of Polymer Systems, University Institute, Nad Ovcirnou 3685, 760 01 Zlin, Czech Republic

[3]Institute of Hydrodynamics, Academy of Sciences, 166 12 Prague 6, Czech Republic

[a]petras.david@seznam.cz, [b]slobodian@ft.utb.cz, [c]rolejnik@volny.cz, [d]riha@ih.cas.cz

Keywords: Carbon nanotubes, polystyrene, electrical conductance, conductance model.

Abstract. The conductance properties of multi-walled carbon nanotube mats and their polystyrene composite were examined to investigate the mechanism of conduction and the specific role of the supporting polymer. By measuring the temperature dependence of the conductance, it was found that the conduction mechanism in carbon nanotube mat follows the series heterogeneous model when the conductance is described as the sum of metallic and barrier portions of the conduction path. This mechanism is affected by the polymeric portion of the composite, since the temperature dependence of the composite conductance is decreased.

Introduction

The first CNT network was made by dispersing nanotubes into a liquid suspension and then filtered it through a fine filtration mesh [1]. Consequently, the pure nanotubes stick to one another and form a thin intertwined freestanding structure, later dubbed "buckypaper". Consequently, numerous studies were aimed to reveal its mechanical, electrical and other properties. Nevertheless, the electrical conductance of the entangled multi-walled carbon nanotube (MWCNT) network structures of buckypaper embedded in polymer was not yet tested. Thus the aim of this study is to carry out such thermoelectrical tests on a polymer nanocomposite prepared by an innovative procedure when the non-woven polystyrene filtering membrane and the carbon nanotube filtration cake are integrated by compression molding [2].

Experimental

Purified MWCNTs produced by chemical vapor deposition of acetylene, which were supplied by Sun Nanotech Co. Ltd., China. According to the supplier, the diameter of the nanotubes are 10-30 nm, with a length of 1-10 μm, with a purity of ~90% and (volume) a resistivity of 0.12 Ωcm. Further details on the nanotubes were obtained by means of the transmission electron microscopy (TEM) analysis presented in our paper [3]. From the corresponding micrographs the diameter of individual nanotubes was determined to be between 10 and 60 nm, their length from tenths of micron up to 3 μm. The maximum aspect ratio of the measured nanotubes is thus about 300. The multi-wall consists of about 15-35 rolled layers of graphene.

The nanotubes were used for the preparation of an aqueous paste: 1.6 g of MWCNTs and ~50 ml of deionized water were mixed with a mortar and pestle. The paste was then diluted in deionized water with sodium dodecyl sulfate (SDS) and 1-pentanol. Consequently, an aqueous solution of NaOH was added to adjust the pH to 10. The final nanotube concentration in the suspension was 0.3 wt.%, concentration of SDS and 1-pentanol 0.1M and 0.14M, respectively. The suspension was sonicated in an apparatus from "Dr. Hielscher GmbH" (ultrasonic horn S7, amplitude 88 μm, power density 300 W/cm^2, frequency 24 kHz) for 2 hours and with temperature of ca 50°C.

Polystyrene (PS) non-woven mats for filtration of nanotube dispersion were prepared by electrospinning from a commercial polymer (Krasten 137, Kaucuk-Unipetrol Group, M_n = 102 530, M_w/M_n = 2.75). The polymer was dissolved in a mixture of methyl isobutyl ketone and dimethylformamide with the volume ratio 3:1 and PS concentration 15 wt. %. Electrical conductivity of the solution was adjusted to 75 μS/cm by tetraethylamonium bromide. PS nanofiber layer was manufactured using the laboratory apparatus SPIN-LAB (SPUR a.s., Czech Republic) equipped with an electrospinnig needle electrode and a steel planar collecting electrode (Fig. 1). Electrospinning was carried out under the following conditions: electric voltage 75 kV (Spellman DC power supply), temperature 20-25°C, relative humidity 25-35 %. Flow rate of polymer solution was 0.42 ml/min^{-1}. The motion rate of antistatic polypropylene non-woven fabric which collects nanofibers was 0.20 m/min. To produce final PS non-woven filters, the prepared nanofiber porous layer (thickness of about 1 mm) was subjected to hot pressing under 0.6 MPa and temperature 80°C.

In order to prepare entangled MWCNT network on the supporting PS filter, a vacuum-filtration method was used. The resulting disk-shaped network was washed several times with deionized water (to reach a neutral pH) and methanol in situ. Subsequently, the MWCNT network with PS filter was placed between two acetone moistened filter papers and dried between two iron plates at room temperature for 24 hours. The final drying continued, without the iron plates, at 40 °C for another day. The thickness of the non-woven PS filter was typically 0.5-0.8 mm and the thickness of the MWCNT entangled network, according of the amount of dispersion filtered, was from 0.02 to 0.26 mm. The formed PS filter-supported MWCNT network was then compression molded at 190°C. Thus the originally porous PS filter was transformed into a film.

For comparison, pure carbon nanotube networks were prepared by filtration of dispersions through polyurethane non-woven filters prepared again by electrospinning according to procedure described in [4]. After filtration, the MWCNT sediment was washed by deionized water and methanol in situ and drained between dry filter papers for a moment before the entangled MWCNT sediment was gently peeled off the filter and dried.

The temperature dependence of electrical conductance of MWNT networks and MWCNT/PS composites were measured by a four-point method according to van der Pauw idea [5]. The apparatuses used in the set up were Keithley K7002 scanner, Keithley K7011-S switching card, programmable current source Keithley K2410, Keithley K6517 electrometer and PC with GPIB cec488 and AD25PCI SE transducer cards and SVOR25TER connector. The conductance was measured at constant current 0.01 A in the course of heating from -40°C to 150°C (in steps of 10°C) using thermostatic bath (Haake).

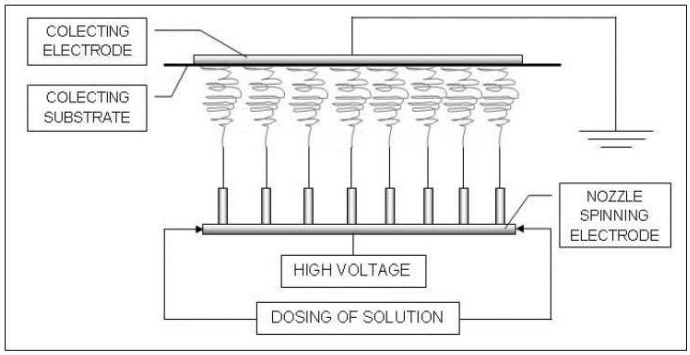

Fig. 1 Scheme of used electrospinning equipment Spin-lab (SPUR a.s., Czech Republic).

Results

The cross-section of PS filter prepared by technology of electrospinning and the MWCNT network accumulated on the filter are shown as SEM micrographs in Fig. 2. PS fibers are straight with smooth surface, submicron sizes with the average diameter of 0.6±0.3 μm. The pores between them have an average size of about 0.5 μm. The apparent density of PS filter is ρ_{filter} = 0.1 g/cm^3, thus its porosity ϕ for the measured PS density ρ_{PS} = 1.04 g/cm^3 was calculated to be about 0.9. The pores allow partial infiltration of MWCNT into the filter at the beginning of filtration. When the pores are filled with nanotubes, the filter cake (pure nanotube entangled network) is formed above the filter surface.

MWCNT network was firmly embedded in PS filter by compression molding. The temperature of processing was 190°C, which is well above the glass transition temperature of PS used for experiments (T_g = 92°C, determined by differential scanning calorimetry technique). The melting phase was followed by cooling below PS glass transition temperature, when both layers were firmly bonded.

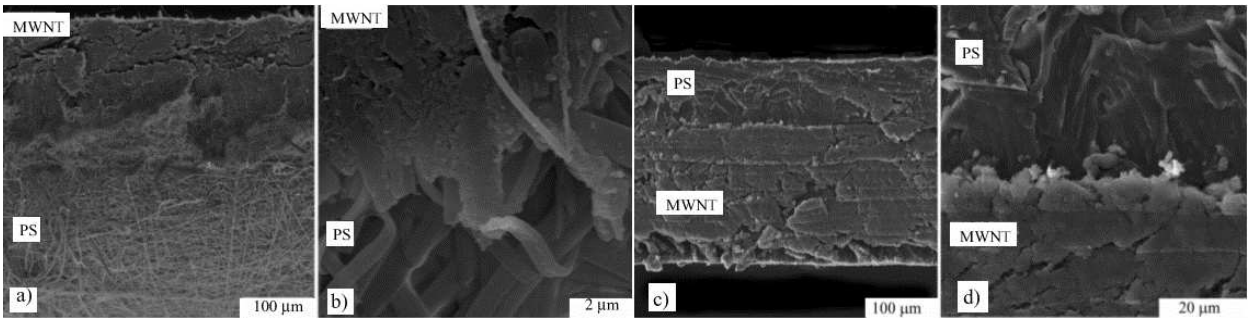

Fig. 2 a) Cross-section of composite consisting of MWCNT network (upper part) and PS filter (lower part) before compression molding (scaler 100 μm). b) The arrow indicates nanotube infiltration illustrated in detail in the enlarged image (scaler 2 μm). c) and d) Cross-section of composite after compression molding.

The effect of temperature on the electrical conductance was tested to find out the conduction mechanism in the carbon nanotube mat and polymeric composite. The results are presented in Fig. 3. The figure demonstrates that both the composite and pure MWCNT network exhibit non-metallic behavior ($d(G/G_i)/dT>0$) over the investigated temperature range from -40 to 150 ^{o}C. The positive slope indicates the presence of tunneling barriers, which dominate conductive behavior of the tested materials. The best description of the data presented in Fig. 3 is obtained by the series heterogeneous models when the resistance $R = 1/G$ is described as the sum of metallic (MWCNT are regarded as metallic conductors) and barrier portions of the conduction path [6-9],

$$R/R_i = aT + b\exp[c/(T)], \tag{1}$$

where a means the temperature coefficient arising from metallic conductance and the second term (hopping/tunneling term) represents fluctuation-induced tunneling through barriers between metallic regions. T denotes temperature, b is constant depending on the geometrical factors from the effective fraction of the length for the barrier portion and c is constants depending on the barrier to conduction parameters [6-9]. As follows from Fig. 3, Eq. 1 describes conductance data very well. The values of coefficients a, b, c for MWCNT network and MWCNT/PS composite are -0.0015, 1.4, 0.8 and -0.0005, 1.12, 4.86, respective.

An obvious effect of the supporting polymer is a reduction of the temperature dependence of conductance. The conductance ratio G_{150}/G_{-40} (values at the corresponding temperatures) is reduced from 1.38 in the case of MWCNT network to 1.11 in the composite case.

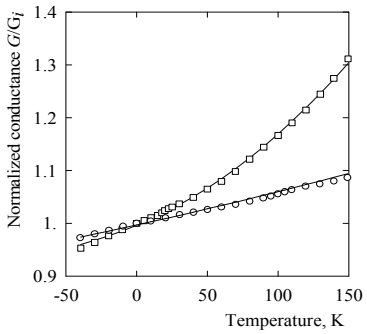

Fig. 3 Temperature-dependent normalized conductance of MWCNT network/PS composite (circles) and MWCNT network (squares). The solid lines represent description by Eq. 1.

Summary

Conduction properties of a multi-walled carbon nanotube mat and its polystyrene composite were investigated using a four-point measurement system over a broad range of temperatures. Both materials show an increase of conductance with rising temperatures contrary to the conductance of metals. The carbon nanotube mat shows nonlinear temperature dependence while a polystyrene carbon nanotube composite shows linear dependence and lower growth slope than the corresponding one of the pure nanotube system. The possible mechanism to explain this phenomenon is the effect of polymer on the electrical contacts between nanotubes leading to constrained increase of conductance of composites with temperature.

Acknowledgement

The work was supported by the Operational Program of Research and Development for Innovations co-funded by the European Regional Development Fund (ERDF), the National budget of Czech Republic within the framework of the Centre of Polymer Systems project (Reg. No.: CZ.1.05/2.1.00/03.0111). This article was also supported by the internal grant of TBU in Zlin No. IGA/FT/2012/022 funded from the resources of Specific University Research and by the Fund of Institute of Hydrodynamics AV0Z20600510. We also appreciate the support and help provided by the company SPUR a.s. (Czech Republic) in preparation of polystyrene non-woven filters.

References

[1] D.A. Walters, et al.: Chem. Phys. Lett. Vol. 338 (2001), p.14.

[2] R. Olejnik, P. Slobodian, P. Riha, P. Saha: J. Nanomaterials (2012). (In Press).

[3] Slobodian, P. Riha, A. Lengalova and P. Saha: J. Mat. Sci. Vol. 46 (2011), p. 3186.

[4] D. Kimmer, P. Slobodian, D. Petras, M. Zatloukal, R. Olejník and P. Saha: J. Appl. Polym. Sci. Vol. 111 (2009), p. 2711.

[5] L.J. van der Pauw: Philips Res. Repts Vol. 13 (1958) p. 1.

[6] A. Allaoui, S.V. Hoa, P. Evesque, J. Bai: Scripta Materialia, Vol. 61 (2009) p. 628.

[7] A.B. Kaiser, Y.W. Park, G.T. Kim, E.S. Choi, G. Dusberg, Synth. Met. Vol. 103 (1999) p. 2547.

[8] M. Shiraishi, M. Ata: Synth. Met. Vol. 128 (2002) p. 235.

[9] S. Kulesza, P. Szroeder, J.K. Patyk, J. Szatkowski, M. Kozanecki: Carbon Vol. 44 (2006) p. 2178.

Key Engineering Materials Vol. 543 (2013) pp 43-46

doi:10.4028/www.scientific.net/KEM.543.43

A pressure sensing conductive polymer composite with carbon nanotubes for biomechanical applications

Anežka Lengálová[1,a], Petr Slobodian[1,2,b], Robert Olejnik[1,2,c], Pavel Riha[3,d]

[1]Tomas Bata University, Centre of Polymer Systems, University Institute, 760 01 Zlin, Czech Republic

[2]Tomas Bata University, Polymer Centre, Faculty of Technology, 760 01 Zlin, Czech Republic

[3]Institute of Hydrodynamics, Academy of Sciences, 166 12 Prague 6, Czech Republic

[a]lengalova@fhs.utb.cz, [b]slobodian@ft.utb.cz, [c]rolejnik@volny.cz, [d]riha@ih.cas.cz

Keywords: Carbon nanotubes, polyurethane, pressure sensor, electrical resistance.

Abstract. A sensing element made of conductive composite created by an entangled network of electrically conductive carbon nanotubes embedded in polyurethane was used for simultaneous measurements of the pressure between the shoe and floor as well as the extension of the leg at the knee joint during marching. The results recorded as sensor resistance change show reasonable reversibility of the basic sensor characteristics, which gives potential for practical applications.

Introduction

Even if the area of nanomaterials has been lately in the centre of attention, its potential has not yet been exhausted. In case the preparation of the material is easy, the more attractive and promising its application is.

The objective of our paper is to explore properties of a pressure sensing element made of conductive composite consisting of entangled network of multi-walled carbon nanotubes (MWCNT) embedded in polyurethane (PU) and to apply the composite in dynamic pressure measurements. The composite was manufactured by a novel process which consists in using non-woven PU filter as an integrating and supporting element on which nanotubes cumulate and form a network during MWCNT suspension filtration. The nanotubes slightly penetrate into the filter and adhere to it, finally forming a continuous layer. Repeating layering of MWNT/PU films enables to produce bulk material.

The resulting composite can sustain very large deformations, which is promising for its practical use for high-strain sensing elements or highly deformable electromagnetic shielding [1]. In our paper, the composite is applied to detect the human knee flexion and its repeated movement as an example of cyclic strain load; this may be useful in orthopedics and rehabilitation [1]. The second issue addressed in the paper is compression deformation of the composite sensor, which can be practically used for footwear evaluation as well as gait analysis or other biomedical applications (plantar pressure assessment, foot ulceration, therapeutics, etc.).

Experimental

Purified MWCNT produced by acetylene chemical vapor deposition were supplied by Sun Nanotech Co. Ltd., China. According to the supplier, the nanotube diameter is 10-30 nm, length 1-10 μm, purity >90% and volume resistivity 0.12 Ωcm. The nanotubes were used for the preparation of aqueous paste: 1.6 g of MWCNT and ~50 ml of deionized water were mixed with the help of a mortar and pestle. The paste was then diluted in deionized water with sodium dodecyl sulfate (SDS) and 1-pentanol as surfactants. Consequently, NaOH aqueous solution was added to adjust pH to the value of 10 [2]. The final nanotube concentration in the suspension was 0.3 wt.%, concentrations of SDS and 1-pentanol were 0.1M and 0.14M, respectively. The suspension was sonicated in Dr. Hielscher GmbH apparatus (ultrasonic horn S7, amplitude 88 μm, power density 300 W/cm^2, frequency 24 kHz) for 2 hours at the temperature of ca 50°C.

To make an entangled MWCNT network on a polyurethane porous membrane [3], a vacuum filtration method was used. The formed disk-shaped network was washed several times with deionized water and methanol in situ. The structure of PU non-woven filtering membrane, prepared by the electro-spinning process, is shown as scanning electron microscope (SEM) picture in Fig. 1a). A detailed view of an individual nanotube structure is presented in Fig. 1b). As can be seen, the nanotube consists of about 15 rolled layers of graphene, with the interlayer diameter of ca 0.35 nm. The third micrograph, Fig. 1c), proves that MWCNT network is a porous structure created by entangled nanotubes. The structures were investigated with SEM produced by Vega LMU (Tescan s.r.o., Czech Republic).

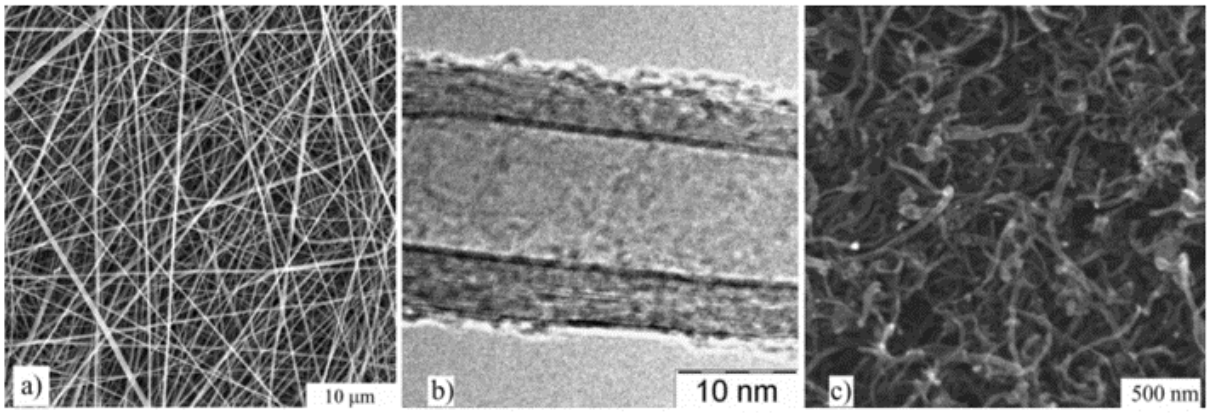

Fig. 1 a) SEM micrograph of polyurethane non-woven filtering membrane, b) TEM micrograph of nanotube structure, c) SEM micrograph of entangled MWCNT network surface.

To illustrate a potential practical use of the produced electrically conductive composite, plantar pressure detection and knee flexion were investigated. In the former case, a strip of MWCNT network/PU composite was pasted to a shoe sole, in the latter case to an elastic knee bandage, Fig. 2. The electrical contacts were fixed to the strip by a silver-colloid electro-conductive paint Dotite D-550 (SPI Supplies) and the resistance was measured lengthwise by the two-point technique using multimeter Sefram 7338. The time-dependent resistance change was monitored through the Vernier LabQuest Interface System connected to the Differential Voltage Probe and the Wheatstone bridge with sampling frequency 100 Hz.

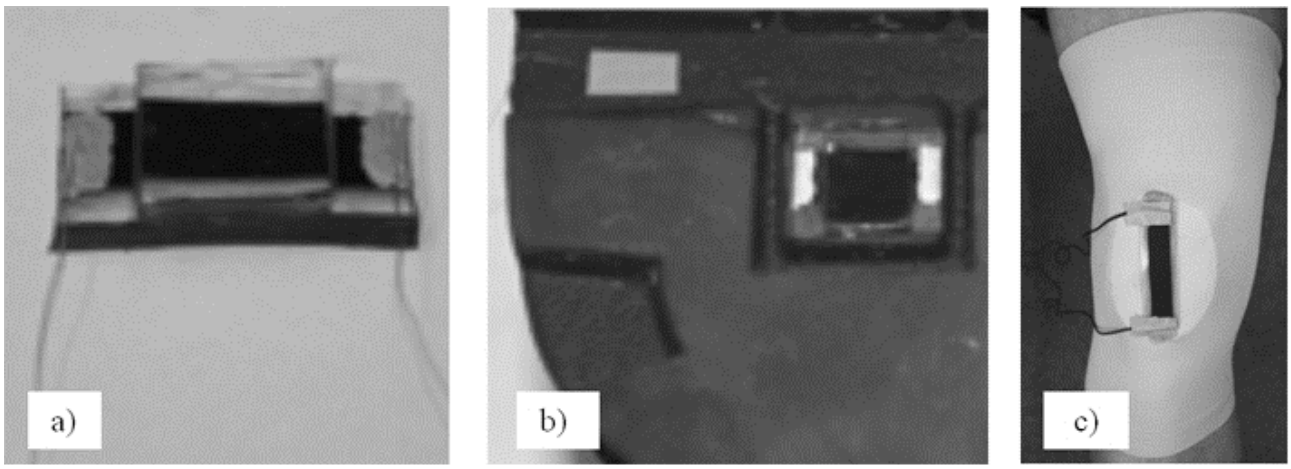

Fig. 2 a) Strip of MWCNT/PU composite as a pressure and extension sensor, b) sensor pasted on the shoe sole and c) on the knee bandage.

Results

To test the sensing abilities of the composite, we measured the pressure between the shoe sole and the floor during a volunteer's marching on the spot, and simultaneously extension of the leg at the knee joint was monitored. The waveforms recorded in terms of normalized resistance are shown in Fig. 3. It is apparent that both cycles (pressure on the sole and strain on the knee) are perfectly in phase, i.e. peaks corresponding to bended knee (the upper curve) appear at the time when the leg is lifted (the lower curve).

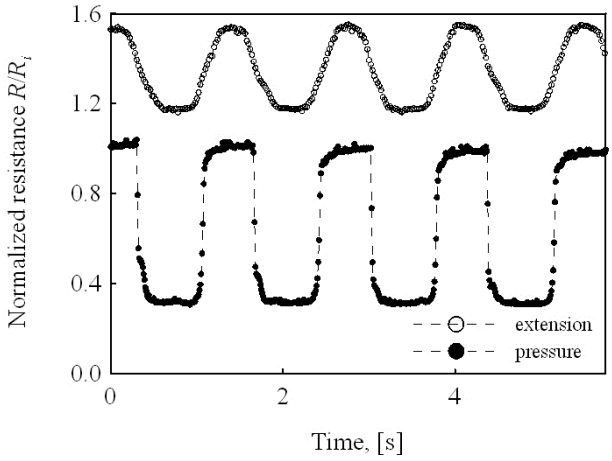

Fig. 3 Waveforms of the normalized resistance during volunteer's marching detected by MWCNT/PU sensor adhered to the knee bandage (empty symbols) and shoe sole (solid symbols).

The resistance of the sensors is reversible not only in the five cycles displayed above, but also over a long period, as follows from Fig. 4. The marching frequency was about 1 Hz, which resulted in 90 cycles during which, as can be seen in the figure, the sensor´s resistance is reproducible and no material property variation is observed. As a commercial sensor made of MWCNT/PU composite should withstand multiple test cycles, we believe that our composite has reasonable durability and reversibility of basic characteristics and is able to comply with practical application requirements. Moreover, during the volunteer's exercise, no obstructions or difficulties were subjectively noticed, which shows that the system is flexible enough to be used, for instance, for monitoring the human body movements.

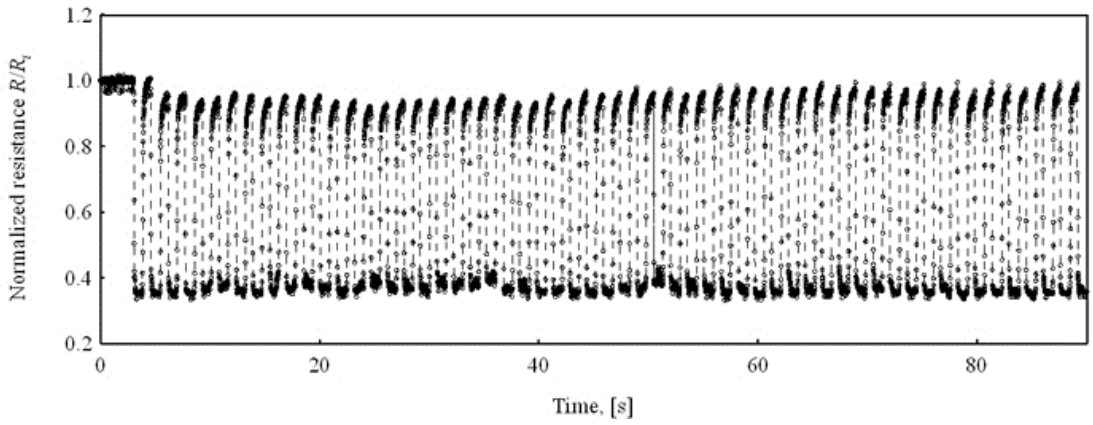

Fig. 4 The normalized resistance cycles in the course of plantar pressure measurement, showing the composite sensor repetitive properties.

Fig. 5 shows the resistance change during repeated forceful treads on the ground. As can be seen, the resistance decreases with the number of compression cycles, in each of which the compactness of MWCNT network increases, more contacts are created and the resistance slightly decreases.

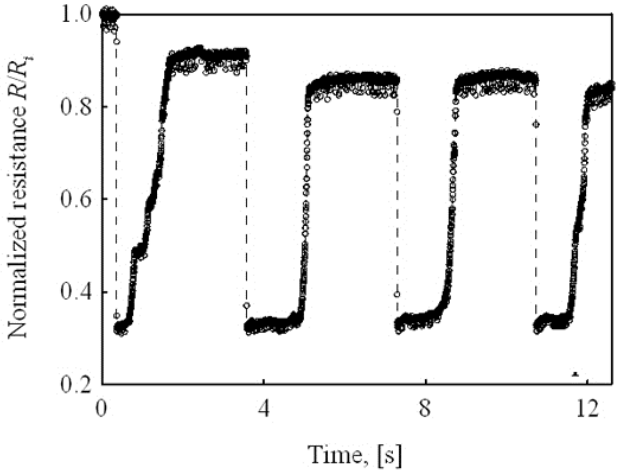

Fig. 5 The resistance change of the MWCNT/PU composite sensor after repeated forceful treads on the ground.

Summary

In the paper we have introduced a highly deformable composite created by a network of electrically conductive entangled carbon nanotubes embedded in elastic polyurethane. The composite was prepared from a non-woven polyurethane filtering membrane in which carbon nanotubes were enmeshed and sintered. As an example of the composite reliable application as a strain sensor, plantar pressure and human knee flexion during marching on the spot was measured. The results in terms of sensor resistance change are promising for potential application in orthopedics, rehabilitation and footwear design.

Acknowledgement

The work was supported by the Operational Program of Research and Development for Innovations co-funded by the European Regional Development Fund (ERDF), the National budget of the Czech Republic within the framework of the Centre of Polymer Systems project (Reg. No.: CZ.1.05/2.1.00/03.0111). This research was also supported by the internal grant of TBU in Zlin, No. IGA/FT/2012/022 funded from the resources of Specific University Research and by the Fund of the Institute of Hydrodynamics of the Academy of Sciences of CR, AV0Z20600510. The authors also appreciate the support and help provided by company SPUR a.s. (Czech Republic) during preparation of polyurethane non-woven filters.

References

[1] P. Slobodian, P. Riha and P. Saha: Carbon (2012). http://dx.doi.org/10.1016/.carbon. 2012.03.008.

[2] C.S. Chern, L.J. Wu: J. Polym. Sci. Part A: Polym. Chemistry Vol. 39 (2001) p. 3199.

[3] D. Kimmer, P. Slobodian, D. Petras, M. Zatloukal, R. Olejník and P. Saha: J. Appl. Polym. Sci. Vol. 111 (2009), p. 2711.

Key Engineering Materials Vol. 543 (2013) pp 269-272

doi:10.4028/www.scientific.net/KEM.543.269

Different Kinds of Carbon-Based Material for Resistive Gas Sensing

Roman Bořuta[1,a], Robert Olejnik[1,2b], Petr Slobodian[1,2c], and Pavel Riha[3,d]

[1]Tomas Bata University in Zlin, Faculty of Technology, nam. T. G. Masaryka 275, 762 72 Zlin Czech Republic

[2]Centre of Polymer Systems, Nad Ovčírnou 3685, 760 01 Zlin, Czech Republic

[3]Institute of Hydrodynamics, Academy of Sciences, 16612 Prague 6, Czech Republic

[a]roman.boruta@post.cz, [b]rolejnik@volny.cz, [c]slobodian@ft.utb.cz, [d]riha@ih.cas.cz

Keywords: Carbon-based mats, gas sensing, interdigitated electrode, organic vapors.

Abstract. Gas sensing properties of networks made of carbon black, carbon nanofibers and carbon multi-walled carbon nanotubes are tested. The networks' reaction to vapors of volatile organic compounds is measured through their change of electrical resistance. The measured resistance increase is up to 27.7 % for carbon black, 40% for carbon nanofibers and 47.7% for multi-walled carbon nanotubes.

Introduction

The carbon based materials such as carbon black (CB), carbon nanofibers (CF) and carbon nanotubes (CNT) can be potentially used as sensor materials for detection of organics vapors. For instance, both principal types of CNT – the multi-walled (MWCNTs) and single-walled nanotubes show remarkable sensitivity to the change of chemical composition of the surrounding environment. Gas and vapor adsorption as well as desorption usually proceeds at high rates and amounts [1]. This property is favorable for their use in the form of membranes [2], adsorbents [3] or gas sensors [4,5]. The adsorbed molecules influence the electrical properties of isolated CNT and also the resistance of inter-tube contacts [6,7]. The electrical resistance of CNT aggregates or network structures is predominantly determined by contact resistance of crossing tubes rather than by resistance of CNT segments. The tubes are usually much shorter than sensor dimension and inter-tube contacts act as parallel resistors between highly conductive CNT segments. The significant effect which has influence on the macroscopic CNT electrical resistance is a vapor adsorption at the contacts between nanotubes forming non-conductive layers between them [4]. Thus the resistance measurement is a simple and convenient method to register CNT response to vapor action.

The aim of the paper is to gain further experiences with carbon-based mats exposed to chemical vapors. Our recent results in this respect are summarized in papers [8-11]. The use of carbon black and carbon nanofibers for a vapor sensing represents further step to understanding of adsorption processes in the carbon-base networks.

Experimental

The purified MWCNT of acetylene type were supplied by Sun Nanotech Co. Ltd., China (diameter 10-30 nm, length 1-10 μm, purity >90% and volume resistance 0.12 Ωcm according to supplier). The complete information about the used pristine MWCNT can be found in our paper [12], where also the results of TEM analysis are presented. The carbon black (CB) VulcanXC-72, ISO classification of N472, was obtained from Cabot Corporation, USA. CB had density 1.67 g/cm^3, average particle diameter of 30 μm, nitrogen surface area 220 m^2/g, dibutyl phthalate (DBP) absorption value 200 cm^3/100 g and iodine absorption value 270 mg/g. The carbon fibers (CFs) with

trade name VGCF® (stands for Vapor Grown Carbon Fiber) were supplied by Showa Denko K. K (Japan). Their basic properties represent diameter 150 nm, length 10 μm, density 2.0 g.cm-3 and resistivity of 0.012 Ωcm.

There are several methods to integrate CTs to different gas sensor structures. Li et al. developed a resistive gas sensor by simply casting SWCNTs on interdigitated electrodes [14]. This method is used in this work. The interdigitated electrodes pattern was printed on the board with 35 μm Cu layer by etching with the resistance paint. The pattern was etched for 15 minutes by $FeCl_3$ at room temperature and the paint was removed by toluene. Finally, the electrodes were cleaned by absolute ethanol. The aqueous dispersion of carbon nanotubes (black or nanofibers) was then drop-deposited onto the electrode area and the carbon-based network was formed after water evaporation.

The structure of networks was investigated with a scanning electron microscope (SEM) made by Vega Easy Probe (Tescan s.r.o., Czech Republic). The sample taken from the electrode was first deposited onto carbon targets and covered with a thin Au/Pd layer. For the observations the regime of secondary electrons was chosen.

Results

Fig 1. shows SEM analysis of the surface of carbon black, multi-walled carbon nanotubes and carbon nanofibers networks, respectively. The networks were formed from the aqueous dispersion of CB, MWCNTs or CFs on the surface of the interdigitated electrode by a drop method. The obtained micrographs in Fig. 1 show some differences between CB, CF and MWCNT networks. The surface of CB seems to be more packed than surface of MWCNT network. On the other hand, the diameter of pores of CF network seems larger than the one of pristine carbon nanotubes suggesting smaller adsorption area for organic vapors.

The sensitivity of networks to organic vapors is measured here by the change of electrical resistance of carbon-based layer. The resistance of network increases when it is exposed to the organic solvent vapor and a reversible decrease is observed when the layer is removed from the vapor as seen in Fig. 2. The vapor of ethanol is inducing agent. The graph illustrates a time-dependent change of parameter S representing sensitivity of networks,

$$S = \frac{R_g - R_a}{R_a} = \frac{\Delta R}{R_a} \quad , \tag{1}$$

where R_a represents specimen resistance in air and R_g the resistance of specimen exposed to vapor, ΔR denotes the resistance change. The curves show specific course of adsorption/desorption, with an obvious on/off effect. An initial sharp increase in sensitivity is followed by a slower phase. Simultaneously, desorption is represented by a rapid decrease reaching a constant value in some cases, in others followed by further, slower decrease.

The obtained results show the increase of network sensitivity up to 27.7 % for carbon black, to 40% for carbon nanofibers and to 47.7% for multi-walled carbon nanotubes, when exposed to ethanol vapor. The highest sensitivity of MWCNT to organic vapor originates probably from their unique characteristics due to their hollow center, nanometer size and large surface area in comparison with CB and CF. Thus the ethanol molecules may be ore adsorbed to MWCNT surface and change the network resistance.

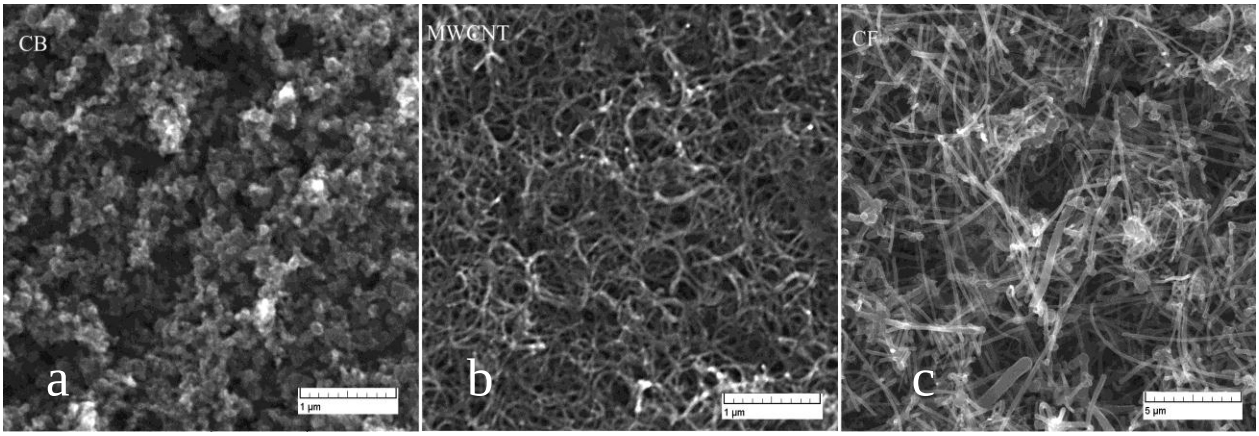

Fig.1 SEM analysis of the network surface made of three different materials a) carbon black, b) multi-walled carbon nanotubes, c) carbon nanofibres.

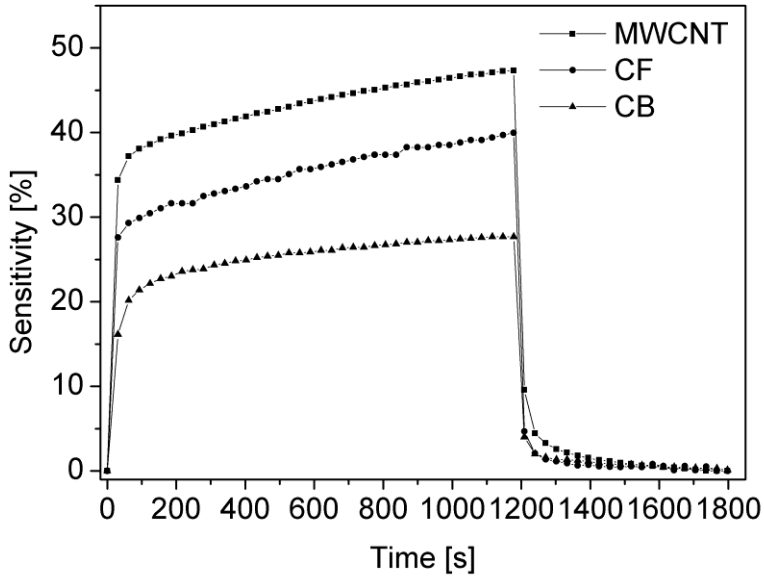

Fig. 2 Adsobtion/desorption cycle for tree different networks of carbon black, multi-walled carbon nanotubes and carbon fibres.

Conclusions

The interdigitated electrodes pattern was printed on the board by etching resistant paint. The pattern was etched for 15 minutes by $FeCl_3$ at room temperature and paint was removed by acetone. A resistive gas sensor was made by simply casting MWCNTs, CFs and CB on interdigitated electrodes. The aqueous dispersions of each carbon-based material were then drop-deposited onto the electrode area. These materials were then exposing to the ethanol vapors. Their response to adsorption/desorption cycles was determined as a change of macroscopic resistance. CNT network has good sensitivity and assumed selectivity defined by pressure of saturated vapors of the used organic solvent. Finally it was found that measured response has good selectivity. The measured resistance increase is up to 27.7 % for carbon black, 40% for carbon fibers and 47.7% for multi-walled carbon nanotubes.

Acknowledgement

The work was supported by the Operational Program of Research and Development for Innovations co-funded by the European Regional Development Fund (ERDF), the National budget of Czech Republic within the framework of the Centre of Polymer Systems project (Reg. No.: CZ.1.05/2.1.00/03.0111). This article was also supported by the internal grant of TBU in Zlin No. IGA/FT/2012/022 funded from the resources of Specific University Research and by the Fund of Institute of Hydrodynamics AV0Z20600510.

References

[1] C.M. Hussain, C. Saridara, S.J. Mitra: J. Chromatogr. A Vol. 1185 (2008) p. 161

[2] R. Smajda, A. Kukovecz, Z. Konya, I. Kiricsi: Carbon Vol. 45 (2007) p. 1176

[3] S. Agnihotri, J.P.B. Mota, M. Rostam-Abadi, M.J. Rood: J. Phys. Chem. B Vol. 110 (2006) p. 7640

[4] A.I. Romanenko, et al.: Sensor Actuat. A-Phys. Vol. 138 (2007) p. 350

[5] A. Qureshi, W.P. Kang, J.L. Davidson, Y. Gurbuz: Diam. Relat. Mater. Vol. 18 (2009) p.1401

[6] F. Tournus, S. Latil, M.I. Heggie, J.C. Charlier: Phys. Rev. B Vol. 72 (2005) p. 075431

[7] D.J. Mowbray, C. Morgan, K.S. Thygesen: Phys. Rev. B Vol. 79 (2009) p. 195431

[8] P. Slobodian, P. Riha, A. Lengalova, P. Svoboda, P. Saha: Carbon Vol. 49 (2011), p. 2499

[9] R. Olejnik, P. Slobodian, P. Riha, P. Saha: J. Mat. Sci. Res. Vol.1 (2012) p. 101

[10] R. Olejnik, P. Slobodian, P. Riha, M. Machovsky: J. Appl. Polym. Sci. (In Press). DOI 10.1002/app.36366

[11] R. Olejnik, P. Slobodian, P. Riha, P. Saha: J. Nanomat. (2012). (In Press)

[12] P. Slobodian, P. Riha, A. Lengalova, P. Saha: J. Mat. Sci. Vol. 46 (2011), p. 3186

[13] D. Kimmer, P. Slobodian, D. Petras, M. Zatloukal, R. Olejník, P. Saha: J. Appl. Polym. Sci. Vol. 111 (2009), p. 2711.

[14] J. Li, Y. Lu, Q. Ye, et al.: Nano Letters Vol. 3 (2003) p. 929

Selectivity of Multi-wall Carbon Nanotube Network Sensoric Units to Ethanol Vapors Achieved by Carbon Nanotube Oxidation

Robert Olejnik
Polymer Centre, Faculty of Technology, T. Bata University, T.G.M. 275, 76272 Zlin, Czech Republic
&
Centre of Polymer Systems, University Institute, T. Bata University
Nad Ovcirnou 3685, 76001 Zlin, Czech Republic
E-mail: rolejnik@volny.cz

Petr Slobodian (Corresponding author)
Polymer Centre, Faculty of Technology, T. Bata University, T.G.M. 275, 76272 Zlin, Czech Republic
&
Centre of Polymer Systems, University Institute, T. Bata University
Nad Ovcirnou 3685, 76001 Zlin, Czech Republic
Tel: 420 57 603 1350 E-mail: slobodian@ft.utb.cz

Pavel Riha
Institute of Hydrodynamics, Academy of Sciences, Pod Patankou 166 12 Prague, Czech Republic
E-mail: riha@ih.cas.cz

Petr Saha
Polymer Centre, Faculty of Technology, T. Bata University, T.G.M. 275, 76272 Zlin, Czech Republic
&
Centre of Polymer Systems, University Institute, T. Bata University
Nad Ovcirnou 3685, 76001 Zlin, Czech Republic
E-mail: saha@utb.cz

Received: October 8, 2011 Accepted: October 27, 2011 Published: January 1, 2012
doi:10.5539/jmsr.v1n1p101 URL: http://dx.doi.org/10.5539/jmsr.v1n1p101

This project was supported by the internal grant of TBU in Zlín No. IGA/3/FT/11/D funded from the resources of specific University research, the Operational Program Research and Development for Innovations co-funded by the European Regional Development Fund (ERDF) and national budget of the Czech Republic within the framework of the Centre of Polymer Systems project (reg.number: CZ.1.05/2.1.00/03.0111), the Fund of the Institute of Hydrodynamics AV0Z20600510 and the Czech Ministry of Education, Youth and Sports project (MSM 7088352101).

Abstract

Two kinds of multiwall carbon nanotubes (MWCNT) networks "Buckypaper" were made by the vacuum filtration method of MWCNT aqueous suspension. The first one was prepared from pure CNT and the second from its oxidized form. The CNT oxidation increase content of oxygen bonded to the surface of CNT. The sensitivity of MWCNT networks to organic solvent vapors (ethanol and heptane) has been investigated by

resistance measurements. The solvents had different polarities given by Hansen solubility parameters and nearly the same volume fractions of saturated vapors at the condition of experiment. CNT oxidation significantly increases the sensitivity of CNT resistive sensoric unit to vapors of ethanol and decrease response to heptane vapors.

Keywords: Carbon nanotube network, Buckypaper, Oxidation, Sensor, Electrical resistance

1. Introduction

Carbon nanotubes (CNTs) have raised much interest during the recent years due to their inherent extraordinary electrical and mechanical properties. Moreover CNTs show remarkable sensitivity to the change of chemical composition of the surrounding environment. Gas and vapor adsorption as well as desorption usually proceeds at high rates and amounts (Hussain et al., 2008). This property is favorable for their use in the form of membranes (Smajda et al., 2007), adsorbents (Agnihotri et al., 2006) or gas sensors (Romanenko et al., 2007; Qureshi et al., 2009; Brahim et al., 2009; Ouyang and Li, 2010).

The molecules are adsorbed on CNT surface by van der Waals attracting forces, which leads to remarkable changes in CNT electrical resistance. Physisorbed molecules influence the electrical properties of isolated CNT and also of inter-tube contacts (Mowbray et al., 2009; Slobodian et al., 2011). The resistance of macroscopic CNT objects like aggregates or network structures used in gas sensors is predominantly determined by contact resistance of crossing tubes, rather than by resistance of CNT segments. Here, the tubes are much shorter than sensor dimensions and inter-tube contacts act as parallel resistors between highly conductive CNT segments. It was found that so called “Buckypaper”, network prepared from entangled CNTs by vacuum filtration is capable to detect organic vapors in air (Kastanis et al., 2007).

Carbon nanotutubes can be used as resistive gas sensors for detection of volatile organics compounds (VOC). Several principles of sensing mechanisms can be employed. It goes from the change of intrinsic resistance of individual tubes by exposure to reducing methanol vapors (Li et al., 2007) (here fixed in PMMA matrixes) or in the form of thin polymeric film with percolating CNT network (Philip et al., 2003; Greenshields et al., 2011) or using of electrically conductive network structures made of carbon nanotubes with substantial role of inter-tube contacts (similar to present contend). Such carbon nanotube networks (“Buckypaper”) can be used for detection by variation of ways. It can be made from pure tubes (Kastanis et al., 2007) or their wet chemical oxidized forms (Slobodian et al.) enhancing selectivity to oxygenated kinds of VOC or by dry functionalization by oxygen or fluorine plasma (Liu et al., 2007) increasing response to ethanol. Another variation of this principle can be found in the literature like printing of CNT layer onto flexible PET foil (Parikh et al., 2007), conductive PMMA/CNT composite prepared as spray layered of PMMA microbeads decorated by CNT (Feller et al., 2011) next one can be mentioned as increasing of sensitivity to vapors with affine polarity by CNT covalent functionalization by PMMA (Olejnik et al., 2011) or CNT network made of adsorbed carbon nanotubes onto skeleton made of electrospuned nylon 6,6 nanofibers applied as sensor for low molecular weight alcohols (Choi et al., 2010).

The quality of aqueous dispersion of nanotubes, the porosity of formed networks as well as nanotube adherence, intercontact resistance, etc., can be suitably influenced by a nanotube surface functionalization such as oxidation (Kastanis et al., 2007). It was found that the oxidized CNTs form a network with more uniform pore structure and dense morphology with lower porosity in comparison with networks formed by pristine nanotubes. The network structure results from fine nanotube aqueous dispersion, and thus deposition of individual CNT and/or only small CNT agglomerates on filtrating membrane.

CNT oxidation in $KMnO_4/H_2SO_4$ mixture causes nanotube shortening, creation of defect sites and open ends (Rasheed et al., 2007; Hernadi, et al., 2001). Potassium permanganate ($KMnO_4$) produce carboxylic acid groups (-COOH) on CNT surface as well as a significant amount of other oxygenated functional groups such as hydroxyl (-OH) and carbonyl (=O) groups (Rasheed et al., 2007; Hernadi, et al., 2001). Small amount of amorphous carbon after the $KMnO_4$ oxidation process can be also expected (Hernadi, et al., 2001). Nevertheless, the other study shows that oxidation by $KMnO_4$ in an acidic suspension provides treated nanotubes free of amorphous carbon (Rasheed et al., 2007).

Even if carbon nanotubes are presently used for detection of gases the sensors are quite expensive and difficult to produce. Simpler and cheaper ways to detect gases can be reflected in practical application of CNT network structure. The present work describes increased sensitivity and achieved selectivity to vapors of ethanol by CNT oxidation in $KMnO_4/H_2SO_4$ solution.

2. Experimental

2.1 Materials

Multiwall carbon nanotubes (MWCNTs) Baytubes C150, produced by chemical vapor deposition were supplied by Bayer Material Science AG, Germany (diameter 5-20 nm, length 1-10 μm, C-purity > 99% and bulk density 140-230 kg/m^3 declared by supplier). The oxidized material was prepared by following procedure: glass reactor, 300 cm^3 of 0.5M H_2SO_4, 1.5g of $KMnO_4$ and 0.5g of MWCNTs, the dispersion was sonicated at 40°C using UP-400S Dr. Hielsher GmbH Apparatus (ultrasonic horn H7, amplitude μm, power density 300W/ cm^3, frequency 24 kHz) for one hour at 50% power of the apparatus and in 50% pulse mode, the product was filtered and washed with concentrated HCl to remove MnO_2.

MWCNT networks (Buckypaper) (MWCNT-N), were prepared by CNT dispersion vacuum filtration thought polyurethane membrane prepared by technology of electrospinning (Kimmer et al., 2009). Aqueous paste was prepared using a mortar and pestle. The paste was diluted in DI water with sodium dodecyl sulfate (SDS). The final nanotube concentration in the dispersion was 0.03 wt.%. The dispersion was sonicated in Dr. Hielscher GmbH apparatus (ultrasonic horn S7, amplitude 88 μm, power density 300 W/cm^2, frequency 24 kHz) for 2 hours and the temperature of ca 50°C. The final MWCNT dispersion was centrifuged in Hettich-Zentrifugen (Rotina 35) at 4000 rpm for 15 min. Supernatant was used for filtration. The formed disk-shaped networks were washed several times by deionized water and methanol in situ, then peel off the filtering membrane and dried between filter papers at RT.

2.2 Instruments

The structure of MWCNT networks was observed by means of scanning electron microscope (SEM) Vega LMU, produced by Tescan Ltd. The samples were deposited on carbon targets and covered with a thin Au/Pd layer. For the observations the regime of secondary electrons was chosen. The content of oxygen in both forms of MWCNT networks was detected with help of X-ray spectroscopy (EDX) which was in accessories of microscope.

2.3 Reactions

The stripes made of CNT networks (length 15 mm, width 5 mm, thickness ca 0.15 mm) were exposed to the vapors of two different solvents, namely ethanol and heptane. The electrical resistance of stripes was measured along the specimen length by the two-point technique using multimeter Sefram 7338. The stripe was placed on a planar holder with Cu electrodes fixed on both sides of the stripe. Time-dependent electrical resistance measurements were performed during adsorption and desorption cycles. The holder with the specimen was quickly transferred into an airtight conical flask full of vapors of the respective solvent a layer of which was at the bottom. The measurements were conducted in saturated vapors at atmospheric pressure, temperature 25°C and relative humidity 60%. After 6 minutes of measurement the holder was promptly removed from the flask and for the next 6 minutes the sample resistance was measured in the mode of desorption. Four different specimens were measured for each MWCNT network and solvent.

3. Results

SEM analyses of upper surfaces of different kind of papers prepared in the course of optimalization process to achieve the smoothest "Buckypaper" surface are presented in Fig. 1. In all cases it demonstrates CNT network as a porous structure created from entangled nanotubes with inter-tube pores. Fig. 1A shows a network fabricated from CNT dispersion prepared only by sonication, B) shows a network made after milling CNT agglomerates before sonication and finally C) shows a network when dispersion of milled and sonicated CNTs was centrifuged. Fig. 2D represents the upper surface of CNT network made from $KMnO_4$ oxidized tubes. The original MWCNT material is supplied in form of CNT granules. It seems that MWCNTs are not enough individualized from granules by sonication only, since MWCNT network surface is wrinkled by remaining MWCNT granules, Fig.1A. The wrinkles are partially eliminated by MWCNT milling using a mortar and pestle before sonication since MWCNT granules nearly disappears, Fig. 2B. However, there are probably still some MWCNT aggregated to submicron aggregates which can be eliminated by centrifugation, Fig. 1C. This MWCNT network is the most uniform, smooth and crack-free. Finally, the surface of the MWCNT network made of oxidized tubes seems to be smoother than all made of pure MWCNT with more densely packed tubes and a smaller diameter of inter-tube pores. Moreover, EDX measurements proved an increase of oxygen content on the surface of MWCNT from 4.86 at. % on pure MWCNT network to 21.26% on network made from $KMnO_4$ oxidized tubes.

The strips made of optimized MWCNT network (Fig. 1C) and the network of $KMnO_4$ oxidized tubes were exposed to the vapor of two different solvents. The solvents were chosen to have similar values of saturated

vapor pressure, p_i, which defines corresponding volume fractions of vapors in air, x_i, with considerably different polarities defined by Hildebrand solubility parameter, δ_i. As good candidates to satisfy these criteria the organics solvents heptane and ethanol were selected. Calculated values of x_i are 7.8 vol. % for ethanol and 6.0 vol. % for heptane at 25°C with δ_i = 15 $Mpa^{1/2}$ and δ_i = 26 $Mpa^{1/2}$ for heptane and ethanol, respectively.

The typical adsorption/desorption behavior of MWCNT networks exposed to/disposed from heptane and ethanol during two cycles are presented in Fig. 2. The experimental curves represents measured data for a pure MWCNT network, part a), and the network made of oxidized tubes, part b), as an average values (4 specimens) with standard deviations represented by error bars. Over all, the adsorption of organics molecules increase resistance with time, which is presented in the figure as sensitivity, S, defined by Eq. (1),

$$S = \frac{R_g - R_a}{R_a} = \frac{\Delta R}{R_a} \quad (1)$$

Here R_a represents specimen resistance in air and R_g resistance of the specimen exposed to vapor, ΔR stands for the resistance change. There is observed an initial sharp increase in S followed by a slower phase. Simultaneously, the organic molecules are removed in the course of desorption and the specimen resistance recovers the initial value. This desorption part starts again by a rapid sensitivity decrease followed by a slower decrease to a constant value within time of the measurement. The mechanism of macroscopic resistance change can be explained by formation of non-conducting layers between nanotubes (Romanenko et al., 2007). It lowers the quality of inter-tube contacts and also their number leading directly to change in macroscopic resistance of MWCNT strip. In any case, the studied macroscopic resistance response was found to be reversible and reproducible.

It can be recapped on basis of the measured data that used MWCNT networks are sensitive to the change of its surrounding for system like air/organics solvent. The measured sensitivities after 6 min of exposition are presented in Table 1. The network made of pure MWCNT seems to have the same sensitivity for heptane and ethanol when experimental errors are taken into account. On the contrary, the sensitivity values and their ratio, $S_{oxidised}/S_{pure}$, for oxidized form of MWCNT network demonstrates significant increase of sensitivity to polar ethanol compared to the sensitivity decrease for non-polar heptane. This is probably caused by the increased polarity of oxidized tubes and better affinity of ethanol molecules to the MWCNT surface.

4. Conclusions

Multiwall carbon nanotubes were used in their pure and oxidized form to prepare entangled networks (buckypaper) whose response to two organic solvent vapors was measured by their electrical resistance. The results show that the prepared networks are capable to detect vapors in the air. The MWCNT network can be considered as a suitable material for application as a cheap and easy to prepare micro-sized vapor sensing element, which is sensitive, selective and has reversible and reproducible properties. The sensor sensitivity to ethanol vapors was effectively improved by MWCNT oxidation by acidic $KMnO_4$.

References

Agnihotri, S., Mota, J. P. B., Rostam-Abadi, M., & Rood, M. J. (2006). Theoretical and experimental investigation of morphology and temperature effects on adsorption of organic vapors in single-walled carbon nanotubes. *Journal of Physical Chemistry B, 110*(15), 7640-7647. http://dx.doi.org/10.1021/jp060040a

Brahim, S., Colbern, S., Gump, R., Moser, A., & Grigorian, L. (2009). Carbon nanotube-based ethanol sensors. *Nanotechnology, 20,* 235502. http://dx.doi.org/10.1088/0957-4484/20/23/235502

Hernadi, K., Siska, A., Thien-Nga, L., Forro, L., & Kiricsi, I. (2001). Reactivity of different kinds of carbon during oxidative purification of catalytically prepared carbon nanotubes. *Solid State Ionics, 141*(1), 203-209. http://dx.doi.org/10.1016/S0167-2738(01)00789-5

Hussain, C.-M., Saridara, C., & Mitra, S. (2008). Microtrapping characteristics of single and multi-walled carbon nanotubes. *Journal of Chromatography A, 1185*(2), 161-166. http://dx.doi.org/10.1016/j.chroma.2008.01.073

Kastanis, D., Tasis, D., Papagelis, K., Parthertios, J., Tsakiroglou, C., & Galiotis, C. (2007). Oxidized multi-walled carbon nanotube film fabrication and characterization. *Advanced Composites Letters, 16*(6), 243-248.

Kimmer, D., Slobodian, P., Petras, D., Zatloukal, M., Olejnik, R., & Saha, P. (2009). Polyurethane/MWCNT nanowebs prepared by electrospinning process. *Journal of Applied Polymer Science, 111*(6), 2711-2714. http://dx.doi.org/10.1002/app.29238

Mowbray, D. J., Morgan, C., & Thygesen, K. S. (2009). Influence of O_2 and N_2 on the conductivity of carbon nanotube networks. *Physical Review B, 79*(19), Article Number 195431. http://link.aps.org/doi/10.1103/PhysRevB.79.195431

Ouyang, M., & Li, W. J. (2010). Performance of F-CNTs sensors towards ethanol vapor using different functional groups. Proceedings of the 5th IEEE International Conference on Nano/Micro Engineered and Molecular Systems, January 20-23, Xiamen, China. http://dx.doi.org/10.1109/NMDC.2010.5651960

Qureshi, A., Kang, W. P., Davidson, J. L., & Gurbuz, Y. (2009). Review on carbon-derived, solid-state, micro and nano sensors for electrochemical sensing application, *Diamond and Related Materials, 18*(12), 1401-1420. http://dx.doi.org/10.1016/j.diamond.2009.09.008

Rasheed, A., Howe, J. Y., Dadmun, M. D., & Britt, P. F. (2007). The efficiency of the oxidation of carbon nanofibers with various oxidizing agents. *Carbon, 45*, 1072-1080. http://dx.doi.org/10.1016/j.carbon.2006.12.010

Romanenko, A. I., Anikeeva, O. B., Kuznetsov, V. L., Buryakov, T. I., Tkachev, E. N., & Usoltseva, A. N. (2007). Influence of helium, hydrogen, oxygen, air and methane on conductivity of multiwalled carbon nanotubes. *Sensors and Actuators A, 138*(2), 350-354. http://dx.doi.org/10.1016/j.sna.2007.05.010

Smajda, R., Kukovecz, A., Konya, Z., & Kiricsi, I. (2007). Structure and gas permeability of multi-wall carbon nanotube buckypapers. *Carbon, 45*(6), 1176-1184. http://dx.doi.org/10.1016/j.carbon.2007.02.022

Slobodian, P., Riha, P., Lengalova, A., Svoboda, P., & Saha, P. (2011). Multi-wall carbon nanotube networks as potential resistive gas sensors for organic vapor detection. *Carbon, 49*(7), 2499-2507. http://dx.doi.org/10.1016/j.carbon.2011.02.020

Liu, C. K., Wu, J. M., & Shih, H. C. (2010). Application of plasma modified multi-wall carbon nanotubes to ethanol vapor detection. *Sensors and Actuators B-Chemical, 150*(2), 641-648. http://dx.doi.org/10.1016/j.snb.2010.08.026

Greenshields, MWCC, Meruvia, MS, Hummelgent, IA, Coville, NJ, Mhlanga, SD, Ceragioli, HJ, Quispe, JCR, & Baranauskas, V. (2011). AC-Conductance and Capacitance Measurements for Ethanol Vapor Detection Using Carbon Nanotube-Polyvinyl Alcohol Composite Based Devices. *Journal of Nanoscience and Nanotechnology*, *11*(3), 2384-2388. http://dx.doi.org/10.1166/jnn.2011.3518

Choi, J, Park, EJ, Park, DW, & Shim, SE. (2010). MWCNT-OH adsorbed electrospun nylon 6,6 nanofibers chemiresistor and their application in low molecular weight alcohol vapours sensing. *Synthetic Metals, 160*(23-24), 2664-2669. http://dx.doi.org/10.1016/j.synthmet.2010.10.022

Shih, Y. H., & Li, M. S. (2007). Adsorption of selected volatile organic vapors on multiwall carbon nanotubes *Journal of Hazardous Materials, 154*(1-3), 21-28. http://dx.doi.org/10.1016/j.jhazmat.2007.09.095

Parikh, K, Cattanach, K, Rao, R, Suh, DS, Wu, AM, & Manohar, SK. (2005). Flexible vapour sensors using single walled carbon nanotubes, *Sensors and Actuators B-Chemical*, *113*(1), 55-63. http://dx.doi.org/10.1016/j.snb.2005.02.021

Philip, B, Abraham, JK, Chandrasekhar, A, & Varadan, VK. (2003). Carbon nanotube/PMMA composite thin films for gas-sensing applications. *Smart Materials & Structures*, *12*(6), 935-939, Article Number: PII S0964-1726(03)68091-2. http://dx.doi.org/10.1088/0964-1726/12/6/010

Olejnik R., Slobodian P., Riha P., & Machovsky M. Increased sensitivity of multi-walled carbon nanotube network by PMMA functionalization to vapors with affine polarity. *Journal of Applied Polymer Science,* paper in press.

Feller, J. F., Lu, J., Zhang, K., Kumar, B., Castro, M., Gatt, N., & Choi, H. J. (2011). Novel architecture of carbon nanotube decorated poly(ethyl methacrylate) microbead vapour sensors assembled by spray layer by layer. *J Mater Chem*, *21*(12), 4142-4149. http://dx.doi.org/10.1039/c0jm03779f

Table 1. Increase of sensitivity of pure MWCNT network and the network made from oxidized tubes exposed to saturated vapors of heptane and ethanol

Organic solvent	S_{pure} [%]	$S_{oxidised}$ [%]	$S_{oxidised}/S_{pure}$
heptane	11.7±0.9	7.4±1.3	0.63
ethanol	11.3±0.8	34.0±2.0	3.0

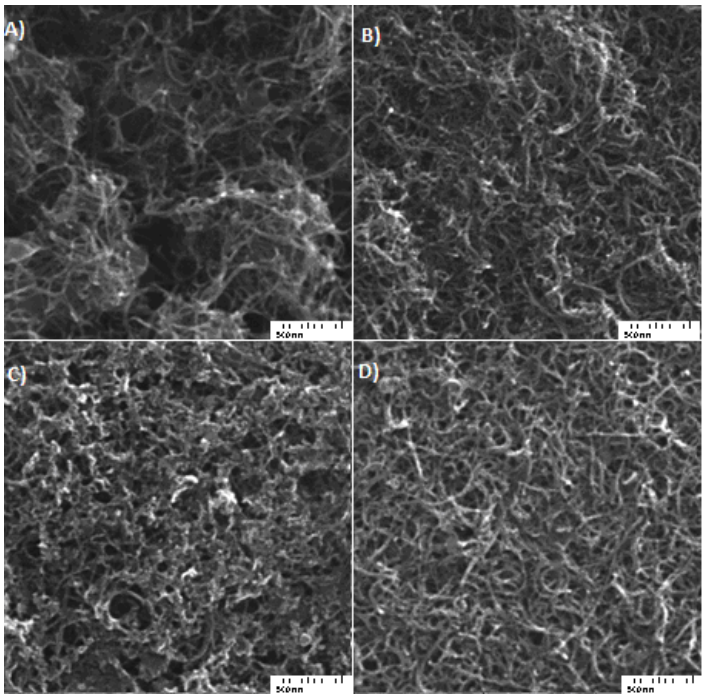

Figure 1. SEM analyses of upper surfaces of MWCNT networks. A) The network prepared from MWCNT dispersion treated by sonication only. B) The network prepared from milled and sonication treated MWCNT. C) The network prepared from dispersion of milled, sonicated MWCNT and centrifuged MWCNT. D) MWCNT network made from $KMnO_4$ oxidized tubes

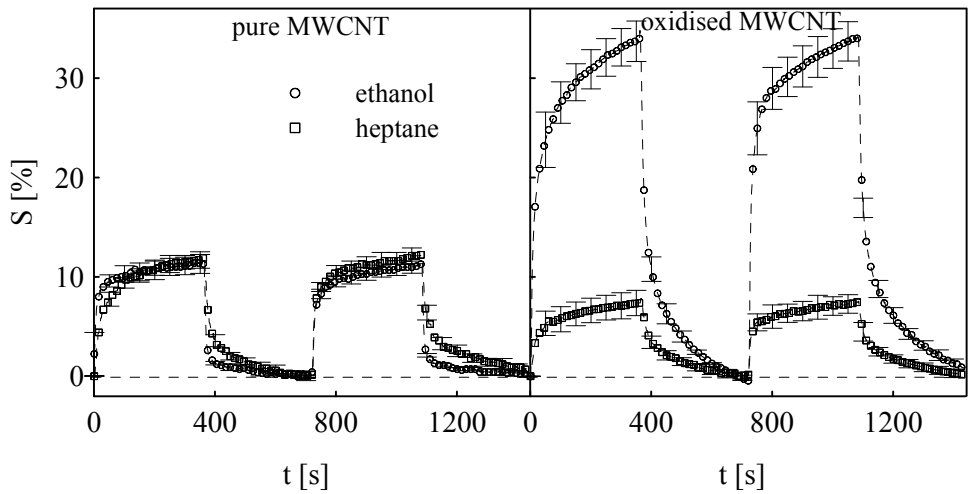

Figure 2. Two adsorption/desorption cycles for pure MWCNT and oxidized MWCNT networks exposed to vapors of heptane (filled circles) and ethanol (open circles)

ISSN 1927-0585 E-ISSN 1927-0593

Journal of Materials Science and Engineering A 1 (2011)
Formerly part of Journal of Materials Science and Engineering, ISSN 1934-8959

Multi-wall Carbon Nanotube Network Sensing Element for Organic Vapor Detection

Robert Olejnik[1, 2], Petr Slobodian[1, 2] and Petr Saha[1, 2]

1. Centre of Polymer Systems, University Institute, Tomas Bata University, Nad Ovcirnou 3685, Zlin 76001, Czech Republic

2. Polymer Centre, Faculty of Technology, Tomas Bata University in Zlin, T.G.M. 275, Zlin 76272, Czech Republic

Received: July 19, 2011 / Accepted: September 02, 2011 / Published: December 10, 2011.

Abstract: Multiwall carbon nanotubes (MWCNT) network "Buckypaper" was made by the vacuum filtration method of MWCNT aqueous suspension. The sensitivity of multi-wall carbon nanotube (MWCNT) networks of randomly entangled pure nanotubes to various organic solvent vapors (methyl ethyl ketone, tetrahydrofuran ethanol and heptane) has been tested by macroscopic resistance measurements. The results demonstrate that the network electrical resistance increases when exposed to organic solvent vapors, and a reversible reaction is observed when the sample is removed from the vapors. It was found that process is reproducible. The investigated MWCNT networks could be potentially used as sensing elements for organic vapor detection.

Key words: Carbon nanotube network, sensor, buckypaper, electrical resistance.

1. Introduction

Entangled carbon nanotube (CNT) network "Buckypaper" show a great potential for developing of new materials with advanced structural and functional capabilities. In this respect its application as different kind of sensoric units or as an active part of sensing structural composites can be mentioned. Both kind of CNT like Single-wall carbon nanotubes (SWCNT) and multi-wall carbon nanotubes (MWCNT) show remarkable sensitivity to the change of chemical composition of the surrounding environment and thereafter they can be applied in the file of gas sensors [1-3]. Gas and vapor adsorption as well as desorption usually proceeds at high rates and amounts [4]. The molecules are adsorbed on the carbon nanotube (CNT) surface by van der Waals attracting forces, which leads to remarkable changes in CNT electrical resistance.

Physisorbed molecules influence the electrical properties of isolated CNTs and also inter-tube contacts [5, 6]. The resistance of macroscopic CNT objects like aggregates or network structures is predominantly determined by contact resistance of crossing tubes, rather than by resistance of CNT segments. Here, the tubes are much shorter than sensor dimensions and inter-tube contacts act as parallel resistors between highly conductive CNT segments. The dominating process influencing macroscopic resistance is probably gas or vapor adsorption in the space between nanotubes, which forms non-conductive layers between the tubes. This process decreases both the quantity and quality of contacts between nanotubes and consequently increases macroscopic resistance [1]. Macroscopic conductivity measurement is then a simple and convenient method to register CNT response to vapor adsorption/desorption.

The present work describes preparation and testing of MWCNT network as a resistive gas sensor for organic vapors detection. The sensitivity, reversibility and reproducibility of MWCNT network "Buckypaper" strips to saturated vapors of four different organic solvents are tested. The preferential

Corresponding author: Robert Olejnik, Msc., research fields: nanotechnology and carbon nanotube. E-mail: rolejnik@volny.cz.

use of these resistors may be for sensitive, micro-sized, cheap and easy prepared organic vapors detectors or switches.

2. Experiment

The purified MWCNT of acetylene type were supplied by Sun Nanotech Co. Ltd., China (diameter 10-30 nm, length 1-10 μm, purity > 90% and volume resistance 0.12 Ω·cm according to supplier). The MWCNT aqueous paste was prepared using a mortar and pestle (1.6 g of MWCNT and ~ 50 mL of deionized water), then diluted by deionized water and SDS (sodium dodecyl sulfate) and 1-pentanol were added, pH was adjusted to the value of 10 using aqueous solution of NaOH. The final nanotubes concentration in the suspension was 0.3 wt%, concentration of SDS and 1-pentanol 0.1M and 0.14M, respectively. The dispersion was homogenized using Dr. Hielscher GmbH apparatus (ultrasonic horn S7, amplitude 88 μm, power density 300 W/cm^2, frequency 24 kHz) for 2 hours and the temperature of ca 50 °C. MWCNT networks, "Buckypaper" (MWCNT-N), were prepared by dispersion vacuum filtration thought polyurethane submicron size porous membrane. The formed disk-shaped network was washed several times by deionized water and methanol in situ, then removed and dried between filter papers at room temperature.

High-resolution transmission electron microscopy (HRTEM) using microscope JEOL JEM 2010 at the accelerating voltage of 160 kV was employed to characterize used brand of MWCNT. The sample for HRTEM was deposited on a copper grid with carbon film (SPI, USA) and dried. The structure of MWCNT networks was observed with the help of scanning electron microscope (SEM) Vega LMU, produced by Tescan Ltd. The samples were deposited on carbon targets and covered with a thin Au/Pd layer. For the observations the regime of secondary electrons was chosen. The MWCNT network was also analyzed by X-ray photoelectron spectroscopy (XPS) on TFA XPS Physical Electronics instrument [7, 8] at the base pressure in the chamber of about 6×10^{-8} Pa. The samples were excited with X-rays over a 400-μm spot area with a monochromatic Al $K_{\alpha 1,2}$ radiation at 1,486.6 eV. Photoelectrons were detected with a hemispherical analyzer positioned at an angle of 45° with respect to the normal to the sample surface. Survey-scan spectra were made at a pass energy of 187.85 eV, the energy step was 0.4 eV. Individual high-resolution spectra for C 1s were taken at a pass energy of 23.5 eV and 0.1 eV energy step. The concentration of elements was determined from survey spectra by MultiPak v7.3.1 software from Physical Electronics. Thermogravimetric analyses (TGA) of the samples were carried out using thermogravimeter Setaram Setsyt Evolution 1200. The samples were examined under inert atmosphere of helium (5.5 purity, SIAD TP); the gas flow was 30 cm^3/min at the pressure of 101.325 kPa (i.e., 30 sccm) for all experiments. A platinum crucible was used for the sample, the weight of which was about 4 mg. The temperature was increased from ambient up to 1,200 °C at the rate of 20 °C/min.

The strips made of CNT networks (length 15 mm, width 5 mm, thickness ca 0.3 mm) were exposed to the vapors of four different solvents, adsorbates, (tetrahydrofuran–THF, methyl ethyl ketone–MEK, ethanol–Et-OH and heptane). The electrical resistance of network stripes cut was measured along the specimen length by the two-point technique using multimeter Sefram 7338. The stripe was placed on a planar holder with Cu electrodes fixed on both sides of the specimen. Time-dependent electrical resistance measurements were performed during adsorption and desorption cycles. The holder with the specimen was quickly transferred into an airtight conical flask full of vapors of the respective solvent a layer of which was at the bottom. The measurements were conducted in saturated vapors at atmospheric pressure, temperature 25 °C and relative humidity 60%. After 6 minutes of measurement the holder was promptly removed from

the flask and for the next 6 minutes the sample was measured in the mode of desorption.

3. Results

A sample of the prepared free-standing MWCNT network is shown in Fig. 1 part a). The prepared discs were uniform, smooth and crack-free, with significant structural integrity allowing easy manipulation. Typical thicknesses were in the range of 0.15–0.65 mm according to the volume of aqueous MWCNT dispersion used in filtration (filtrating of 1.64 mL of dispersion per 1 cm^2 of filter area yields a network thickness 100 □m). The upper surface and cross-sections of the prepared MWCNT network as SEM micrographs are presented Fig. 1b). It demonstrates CNT network structure as porous structure created from entangled nanotubes with inter-tube pores. This structure is additionally electrically conductive. In our previous reports we presented results of analyses of the same CNT network such as; MWCNT network apparent density 0.56 ± 0.03 g/cm^3 leading to porosity 0.67 [9, 10], electrical resistivity 0.084 ± 0.003 Ωcm and contact resistance of the network 3.1 ± 0.3 kΩ [11] calculated according theory presented in [12].

The structure of an individual nanotube is demonstrated in Fig. 3a provided by HRTEM analyses. As can be seen, it consists of about 15 rolled layers of graphene, with the interlayer distance of ca 0.35 nm. Detailed TEM analyses brought more detailed characterization of used MWCNT [7] when diameter of individual nanotubes was determined to be between 10nm and 60 nm with average diameter and standard deviation to be 15 ± 6 nm, their length from tenths of micron up to 3 μm. The maximum aspect ratio of the measured nanotubes is thus about 300. From XPS graphs we read an oxygen content on the surface of MWCNT network to be 5.5 at.%, the O/C ratio was 0.06. Besides that, sample showed some impurities like Na, Si and S in very small amounts (tenths of percent). Their origin can probably be attributed to unwashed surfactant SDS (Na and S) and Si as an impurity from nanotubes production. Thermogravimetric analyses (TGA) shows hardly any degradation in the range of temperatures used (up to 700 °C); only very small mass loss of ca 3 wt.% was observed at the highest temperature. This is probably caused by decomposition of amorphous carbon contained in the original material together with functional groups like O-C=O or C-O, also included in crude material [13].

The typical adsorption/desorption behavior of CNT network exposed to/disposed from different organic vapors are presented in Fig. 2. The graph illustrates a time-dependent change of parameter *S* representing sensitivity of the nanotube networks, defined by Eq. (1).

$$S = \frac{R_g - R_a}{R_a} = \frac{\Delta R}{R_a} \tag{1}$$

where R_a represents specimen resistance in air and R_g resistance of the specimen exposed to gas/vapor, ΔR stands for the resistance change. The used solvents can be characterized by parameters like Hildebrand solubility parameter, δ_i, the saturated vapor pressures, p_i, as well as the corresponding volume fractions, x_i, presented in Table 1.

Journal of Materials Science and Engineering A 1 (2011)
Formerly part of Journal of Materials Science and Engineering, ISSN 1934-8959

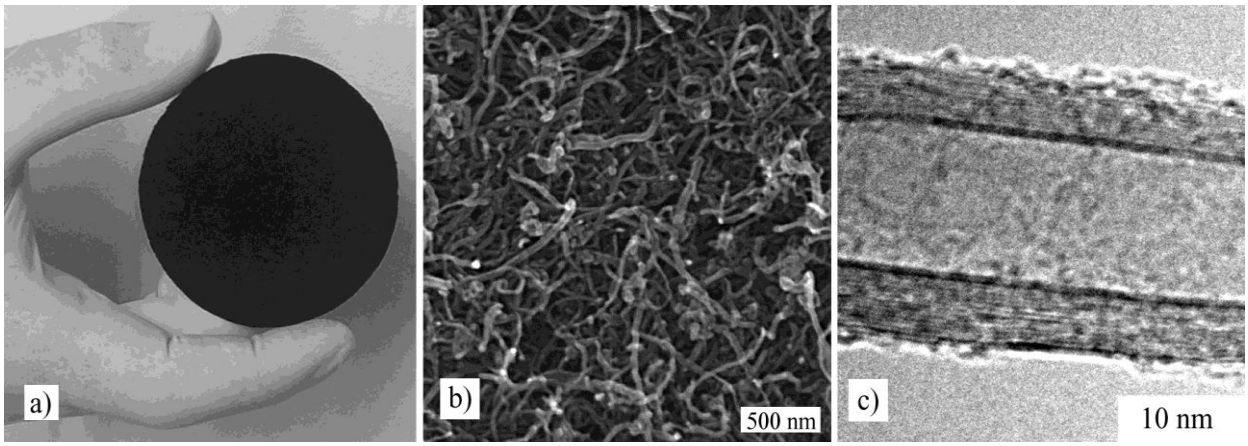

Fig. 1 Free-standing randomly entangled MWCNT (a), SEM micrograph of the surface of entangled MWNT network (b) and TEM micrograph of nanotube structure (c).

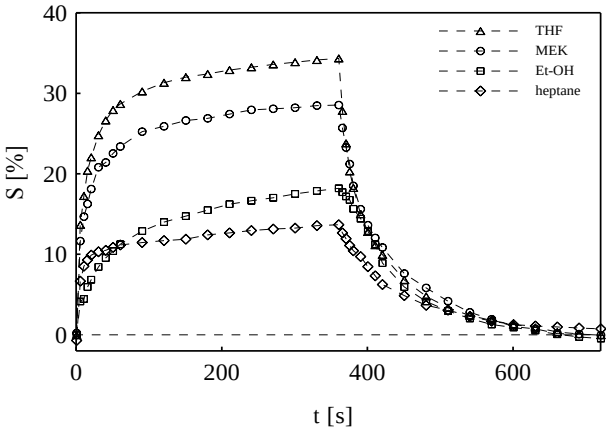

Fig. 2 One adsorption/desorption cycle for MWCNT network exposed to vapors of four different organic solvents (tetrahydrofuran, methyl ethyl ketone, ethanol and heptane).

In all cases, the adsorption of solvents molecules causes increase in resistance with time representing appropriate increase in values of sensitivity, *S*. It was found that the used MWCNT network is sensitive to the change of its surrounding for system like air/organics vapors. There is observed an initial sharp increase in *S* followed by a slower phase. Simultaneously, desorption cycle starts by a rapid sensitivity decrease followed by a slower decrease to a constant value within time of the cycle. The organic molecules are removed in the course of desorption and the specimen resistance recovers the initial value. Adsorption/desorption was found to be a reversible process. The assumed mechanism of macroscopic resistance change can be explained by formation of non-conducting layers between nanotubes and by pushing the tubes away from each other. It lowers the quality of inter-tube contacts and also their number leading directly to change in macroscopic resistance of MWCNT strip. The measured sensitivities after 360 s of adsorption are presented in Table 1. It was found that the highest value was measured for THF (34.4%) followed by MEK (28.6%), Et-OH (18.3%) and heptane (13.7%).

Sensitivity apparently depends on different experimental variables like type of network, vapor pressure and the polarity of the solvent. Although in our case the solvents with different polarities were used, the sensitivity seems to by mainly affected by x_i value, when *S* continuously increases.

Three consecutive cycles of MWCNT network adsorption/desorption in saturated vapors of THF measured again in 6-minute intervals are presented in Fig. 3. The data again presents sensitivity and reversibility of adsorption/desorption process and reasonable reproducibility presented by error bars calculated from the data measured for three different MWCNT network strips.

4. Conclusions

Multiwall carbon nanotubes were used to prepare MWCNT network (buckypaper) by vacuum filtration method of its aqueous dispersion when uniform, smooth and crack-free discs were formed. The

macroscopic resistance of strips made of MWCNT network were measured by two-point method when exposed to/disposed from different organic vapors. It was found that resistance of strips is sensitive to change of its surrounding in such air/organics vapors system. The exposition of network structure leads to increase of resistance on the contrary to resistance decrease when the strip is again removed from vapors atmosphere to

Table 1 Properties of tested organic solvents: total Hildebrand solubility parameter, δ_t, saturated vapor pressures, p_i, and corresponding volume fractions, x_i, at 25°C and atmospheric pressure. *S* represents sensitivity of the nanotube networks to vapors.

Solvent	δ_t (Mpa$^{1/2}$)	p_i (kPa)	x_i (vol. %)	*S* (%)
THF	19.5	20.66	20.4	34.4
MEK	19	12.67	12.5	28.6
Et-OH	26.5	7.86	7.1	18.3
heptane	15.3	6.13	6.0	13.7

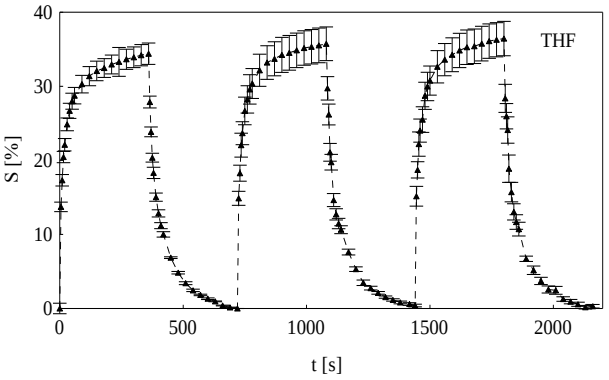

Fig. 3 Three adsorption/desorption cycles of MWCNT network exposed to saturated vapors of THF.

air. The process is immediate and reversible. The sensitivity increase mainly by volume fraction of used solvents rather than is influenced by their polarity. Further measurement of adsorption/desorption in air/THF system approved reasonable reproducibility of such measurements. There considered mechanism of macroscopic resistance change was explained by formation of non-conducting layers between appropriate crossing nanotubes decreasing quantity and quality of contact pushing the tubes away from each other. Finally, it was concluded that MWCNT network can be potentially used as sensing element for organic vapor detection.

Acknowledgements

This project was supported by the internal grant of TBU in Zlín No. IGA/3/FT/11/D funded from the resources of specific university research. This article was also created with support of Operational Programme Research and Development for Innovations co-funded by the European Regional Development Fund (ERDF) and national budget of Czech Republic within the framework of the Centre of Polymer Systems project (Reg. No.: CZ.1.05/2.1.00/03.0111) and by the Czech Ministry of Education, Youth and Sports project (MSM 7088352101).

References

[1] A.I. Romanenko, O.B. Anikeeva, V.L. Kuznetsov, T.I. Buryakov, E.N. Tkachev, A.N. Usoltseva, Influence of helium, hydrogen, oxygen, air and methane on conductivity of multiwalled carbon nanotubes, Sensor Actuat A: Phys. 138 (2) (2007) 350-354.

[2] A. Qureshi, W.P. Kang, J.L. Davidson, Y. Gurbuz, Review on carbon-derived, solid-state, micro and nano sensors for electrochemical sensing application, Diam. Relat. Mater. 18 (12) (2009) 1401-1420.

[3] P. Slobodian, P. Riha, A. Lengalova, P. Svoboda, P. Saha, Multi-wall carbon nanotube networks as potential resistive gas sensors for organic vapor detection, Carbon 49 (7) (2011) 2499-2507.

[4] C.M. Hussain, C. Saridara, S. Mitra, Microtrapping characteristics of single and multi-walled carbon nanotubes, J. Chromatogr A 1185 (2) (2008) 161-166.

[5] F. Tournus, S. Latil, M.I. Heggie, J.C. Charlier, pi-stacking interaction between carbon nanotubes and organic molecules, Phys. Rev. B 72 (7) (2005) 075431.

[6] D.J. Mowbray, C. Morgan, K.S. Thygesen, Influence of O-2 and N-2 on the conductivity of carbon nanotube

networks, Phys. Rev. B 79 (19) (2009) 195431.

[7] A. Vesel, M. Mozetic, A. Zalar, XPS characterization of PTFE after treatment with RF oxygen and nitrogen plasma, Surf Interface Anal 40 (3-4) (2008) 661-663.

[8] A. Vesel, M. Mozetic, A. Zalar, XPS study of oxygen plasma activated PET, Vacuum 82 (2) (2007) 248-251.

[9] P. Slobodian, P. Riha, A. Lengalova, P. Saha, Compressive stress-electrical conductivity characteristics of multiwall carbon nanotube networs, Journal of Materials Science 46 (9) (2011) 3186.

[10] P. Slobodian, P. Riha, A. Lengalova, R. Olejnik, P. Saha, Effect of compressive strain on electric resistance of multi-wall carbon nanotube networks, Journal of experimental nanoscience 6 (3) (2011) 294.

[11] P. Slobodian, P. Riha, A. Lengalova, P. Svoboda, P. Saha, Multi-wall carbon nanotube networks as potential resistive gas sensors for organic vapor detection, Carbon 49 (2011) 2499-2507.

[12] A. Allaoui, S.V. Hoa, P. Evesque, J. Bai, Electronic transport in carbon nanotube tangles under compression: The role of contact resistance, Scripta. Mater. 61 (6) (2009) 628-631.

[13] L. Licea-Jimenez, P.Y. Henrio, A. Lund, T.M. Laurie, S.A. Perez-Garcia, L. Nyborg, H Hassander, H. Bertilsson, R.W. Rychwalski, Compos Sci Technol 2007;67(5):844-854.

Electromechanical sensors based on carbon nanotube networks and their polymer composites

P. Slobodian[1], P. Riha[2], R. Olejnik[1]

[1]Polymer Centre, Faculty of Technology, Tomas Bata University in Zlin, Czech Republic
[2]Institute of Hydrodynamics, Academy of Sciences, Prague, Czech Republic

Abstract A network of entangled multiwall carbon nanotubes and the composite consisting of filter-supported multiwall carbon nanotube network are conductors whose conductivity is sensitive to compressive stress both in the course of monotonic stress growth and when loading/unloading cycles are imposed. The testing has shown as much as 100% network conductivity increase at the maximum applied stress. The entangled carbon nanotube networks are prepared by vacuum filtration method and peeled off from the filter. The carbon nanotubes are used in pristine condition or chemically functionalized. The filter-supported entangled networks are prepared by the nanotube dispersion filtration through a non-woven flexible polystyrene filter. The nanotubes infiltrate partly into the filter surface pores and link the accumulated filtrate layer with the filtering mat. The filter-support increases nanotube network mechanical integrity, the composite tensile ultimate strength and affects favorably the composite electrical resistance. Other obvious effect of the supporting polymer is reduction of the resistance temperature dependence. Moreover, the conductivity of carbon nanotube networks manifests also organic vapor dependence. The dependence is reversible, reproducible, selective as well as possibly influenced by nanotube oxidation.

Keywords Carbon nanotube network, Compression, Electrical conductivity, Stress sensor, Gas sensor.

1 Introduction

Recent technological progress heavily relies on the use of materials that can offer advanced structural and functional capabilities. In this respect, entangled carbon nanotube (CNT) network structures show a great potential for developing high-performance polymer composites and enhanced sensors. CNT networks can proportionally transfer their unique properties into reinforced composite materials and films for sensors and bring substantial improvements in structural strength, electrical and thermal conductivity, electromagnetic interference shielding and other properties [1,2].

The first carbon nanotube network was fabricated by Walters *et al.,* who dispersed nanotubes into a liquid suspension and then filtered through fine filtration mesh [3]. Consequently, pure nanotubes stuck to one another and formed a thin freestanding entangled structure, later dubbed buckypaper.

The fabrication of CNT network based polymer composite described above is rather laborious. A novel idea is to circumvent the laborious technology and to suggest a way leading to continuous and technologically easier manufacturing of CNT network based polymer composites. The novel process consists of using the non-woven polystyrene (PS) filter on which CNT collect and form a network during CNT suspension filtration, as integrating and supporting element. The CNT slightly infiltrate into the filter and adhere to it, finally forming CNT layer. The obtained CNT/PS composite is compression moulded above PS melting temperature when PS filter transforms into flexible PS polymer film. The repeated layering of CNT/PS units yields bulky forms.

A recent study [4] investigates the mechanical behavior of entangled mats of carbon nanotubes and several other fibers during compression and cyclic tests. The obtained hysteresis loop between loading and unloading was linked with mat morphology and motion, friction and rearrangement of fibers during compaction. However, the electric resistance of CNT networks at compression has only been measured in [5,6]. The obtained data were analyzed to get an estimate of the resistance of CNT tangles and the contact resistance between nanotubes [5]. The purpose to reveal the effect of surface-doping of multiwall carbon nanotubes (MWCNT) networks on their pressure sensitivity is pursued in [6].

The homogeneity of MWCNT dispersion, the porosity of final entangled network and tube-tube interactions can be purposely influenced by the proper surface functionalization. Kastanis et. al [7] tested three different oxidizing agent, that is, ammonium hydroxide/hydrogen peroxide, sulfuric acid/hydrogen peroxide and hot nitric acid. They found that the increasing oxygen content on the surface of CNT leads to CNT networks with more uniform pore structure and dense morphology with lower porosity. The modified structure enhances network mechanical properties owing to stress undertaking by more inter-tube contacts.

The aim of this contribution is to introduce carbon nanotube networks and their composites as electromechanical sensing elements. The electrical conductivity of MWCNT networks is studied both in the course of monotonic stress growth and when loading/unloading cycles are imposed. In addition to it, the stress dependent deformation, the effect of temperature and chemical vapors as well as the effect of chemical functionalization by $KMnO_4/H_2SO_4$ oxidizing system which significantly modifies properties of MWCNT networks, is introduced.

2 Multiwall carbon nanotube networks and composites

The purified MWCNT of acetylene type (Sun Nanotech Co. Ltd., China) are used for the preparation of aqueous paste: 1.6 g of MWCNT and ~ 50 ml of deionized water are mixed with the help of a mortar and pestle. The paste is diluted in deionized water with sodium dodecyl sulfate (SDS) and 1-pentanol. Then NaOH solved in water is added to adjust pH to the value of 10 [8]. The final nanotube concentration in the dispersion is 0.3 wt.%, concentration of SDS and 1-pentanol 0.1M and 0.14M, respectively [9]. The dispersion is sonicated in Dr. Hielscher GmbH apparatus (ultrasonic horn S7, amplitude 88 μm, power density 300 W/cm^2, frequency 24 kHz) for 2 hours and the temperature of ca 50°C.

Pristine MWCNT are oxidized by $KMnO_4$ in a glass reactor with a reflux condenser filled with 250 cm^3 of 0.5M H_2SO_4, 5g of $KMnO_4$ and 2g of MWCNT. The dispersion is

sonicated using thermostatic ultrasonic bath (Bandelin electronic DT 103H) at 85°C for 15 hours. The product is filtered and washed with concentrated HCl to remove the MnO_2 and then washed by deionized water and dried.

The polyurethane (PU) non-woven membranes for MWCNT dispersion filtration are prepared by technology of electrospinning from PU dimethyl formamide solution using NanoSpider (Elmarco, s.r.o.). For more details of PU chemical composition and particular process characteristics see reference [10]. To make entangled MWCNT network on PU porous filtration membrane, the vacuum-filtration method is used. The formed network of disk shape is washed several times by deionized water (till neutral pH) and methanol in situ, then gently peeled off the membrane and dried between filter papers. The thickness of the disks is typically 0.15-0.6 mm.

The PS non-woven filters for MWCNT dispersion filtration and composite formation are prepared by electrospinning from polymer solution. PS (commercial polystyrene Krasten 137, Kaucuk-Unipetrol Group, M_n = 102 530, M_w/M_n = 2.75 [11]) is solved in a mixture of MIBK/DMF with the volume ratio 3:1 and PS weight concentration 15 wt%. The solution electrical conductivity is adjusted to value 75 μS/cm using tetraethylamonium bromide. PS nanofiber layer is using NanoSpider (Elmarco, s.r.o.) The experimental conditions of the electrospinning process are the following: The electric voltage 75 kV (Matsusada DC power supply), the temperature 20-25°C, the relative humidity 25-35 %, the electrode rotation speed 8 r/min and the motion rate of antistatic polypropylene non-woven fabric which collects nanofibers is 0.16 m/min. To prepare final PS non-woven filters, the prepared nanofiber porous layer (thickness of about 1 mm) is subjected to hot pressing at pressure 0.6 MPa and temperature 80°C.

To make entangled MWCNT network on PS filter, the vacuum-filtration method is used. The MWCNT slightly infiltrate into the filter and adhere to it, finally forming MWCNT layer. The formed network is washed several times by deionized water (till neutral pH) and methanol in situ. Subsequently, PS filter-supported MWCNT network is placed between two filter papers moistened by acetone and dried between two iron plates at the room temperature for one day. The final drying continues without iron plates at 40 °C throughout another day. The thickness of the non-woven PS filter is typically 0.5-0.8 mm and the height of MWCNT entangled network according of used amount of dispersion from 0.02 to 0.4 mm. The formed PS filter-supported MWCNT network is then compression moulded above PS melting temperature (190°C) when PS filter transforms in flexible PS film.

3 Experimental techniques

The structure of both MWCNT networks prepared from pristine tubes and their oxidized form are investigated with a scanning electron microscope (SEM) made by Vega LMU (Tescan s.r.o., Czech Republic). The sample is deposited onto the carbon targets and covered with a thin Au/Pd layer. The observation is carried out in the regime of secondary electrons.

Pure MWCNT are also analyzed via transmission electron microscopy (TEM) using microscope JEOL JEM 2010 at the accelerating voltage of 160 kV. The sample for TEM is fabricated on 300 mesh copper grid with a carbon film (SPI, USA) from MWCNT dispersion in acetone prepared by ultrasonication, which is deposited on the grid and dried.

The MWCNT networks and composites are tested for deformation using a simple set-up. The samples (length 10 mm and width 8 mm) cut out from the manufactured disks of entangled nanotubes is first stepwise compressed between two glasses to the maximum value

with 20 s delay of strain reading in each step. Then the down-stress curve is measured in the same manner.

The conductivity characteristic of network stripes with dimensions given above is measured in a similar way as deformation. The loading area between glass plates is 8x8 mm. Two electrical contacts are fixed to the stripe by silver colloid electro-conductive paint Dotite D-550 (SPI Supplies) and the electrical conductivity is measured lengthwise by the two-point technique using multimeter Sefram 7338.

The temperature dependence of the electrical resistivity of MWCNT networks and MWCNT/PS composites are measured by the four point method according van der Pauw method [12]. The apparatuses used in a set up are the scanner Keithley K7002, the switching card Keithley K7011-S, the programmable source of current Keithley K2410, the electrometer Keithley K6517 and PC with transducer cards GPIB cec488 and AD25PCI SE with connector SVOR25TER. The resistivity is measured at constant current 0.01 A in the course of heating from -40°C to 150 using thermostatic box Haake SPEC SU241. The temperature increments are 10°C.

The chemical vapors dependence of networks electric resistance is measured along stripe length (length 15 mm, width 5 mm, thickness ~ 0.3 mm) by the two-point technique using the multimeter Sefram 7378. The stripe is fixed on a planar holder with Cu electrodes and put into the saturated vapors of an organic solvent. The resistance variation is measured during the cycles of sorption (6 min) and desorption (6 min) at the temperature 25^{o}C, the ambient pressure and relative humidity 40 %.

4 Results

4.1 Free-standing entangled MWCNT networks

To examine the length, thickness, waviness, multi-wall arrangement and possible structural defects of MWCNT, TEM analysis is used. The diameter of individual nanotubes is determined to be between 10 and 60 nm, their length from tenth of micron up to 3 μm. The number of coaxially rolled layers of grapheme is typically from 10 till 35 with interlayer distance about 0.35 nm. The used $KMnO_4$ oxidation procedure of MWCNT pristine material leads to significant tubes degradation. The effect of tubes shortening together with creating of smaller tubes bundles was determined using TEM analyses.

The both types of MWCNT aqueous dispersions (using MWCNT pristine tubes and their oxidized forms) are filtered thought PU non-woven membrane to form intertwined networks. As follows from Fig. 1 (left), PU fibers of the membrane are straight with average diameter 0.14±0.09 μm ranging between 0.05-0.39 μm. The fibers surface is smooth and the main pore size is around 0.2 μm. Prepared MWCNT layer is then peeled of the filter achieving self-standing MWCNT entangled network. The typical thickness of prepared (Fig. 2) is about 0.15-0.6 mm.

The SEM micrograph of PS filter prepared by technology of electrospinning is shown in Fig. 1 (right). PS fibres are straight with smooth surface and submicron sizes with average diameter 0.6±0.3 μm. The average pore size is about 0.5 μm. The apparent density of PS filter is ~ 0.1 g/cm^3 giving porosity of about 0.9 for the measured density of PS 1.04 g/cm^3 at 25°C. The prepared MWCNT layer is not peeled of the filter and remains as a part of PS/MWCNT composite.

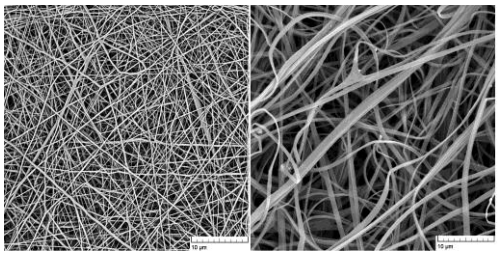

Fig. 1 SEM micrograph of PU (left) and PS non-woven filtering membrane at the same magnification (displayed scaler 10 μm).

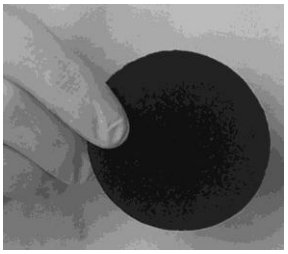

Fig. 2 Free-standing randomly entangled MWCNT network (disk diameter 75 mm, thickness 0.15 mm).

The upper surfaces of both principal MWCNT networks were studied, and their SEM micrographs can be seen in Fig. 3. The pictures show some differences between both structures. The surface of the network made of oxidized tubes seems to be smoother, with more densely packed tubes and a smaller diameter of inter-tube pores. Oxidation causes shortening of MWCNT (which was proved by TEM analyses), creation of defect sites and opened ends of the nanotubes. $KMnO_4$ produces mainly carboxylic acid groups (-COOH) with some amounts of other oxygenated functional groups, such as hydroxyl (-OH) or carbonyl (=O) groups, on the nanotube surface [13,14]. Functionalized nanotubes are better individualized from the bundles and aggregates since they are shorter and the functional groups tend to push away individual nanotubes from each other [15]. Commonly used high-energy ultrasound can also cause degradation of CNT when the aspect ratio of the tubes decreases and their ends open [16,17]. The differences in both CNT network structures appear also after network drying. Drying causes different shrinkage of the network, that is, about 7 % in the case of pure nanotubes but significantly higher in oxidized nanotubes reaching up to 20 %. The porosity ϕ of MWCNT network is calculated to be 0.67 and 0.56 for the pure and oxidized form, respectively. The results are obtained from relation $\phi = 1 - \rho_{net}/\rho_{MWCNT}$, where $\rho_{net} = 0.56 \pm 0.03$ g/cm^3 and $\rho_{net} = 0.75 \pm 0.03$ g/cm^3 denote measured apparent densities of the network made of pure and oxidized nanotubes, respectively. $\rho_{MWCNT} = 1.7$ g/cm^3 is the average density of MWCNT used in the research. This result is consistent with previously published findings that increasing oxygen content on the surface of CNT [7] or shortening of tubes [15] leads to the network with a more uniform pore structure and denser morphology, i.e., the lower porosity. It indicates better nanotubes dispersion in the aqueous

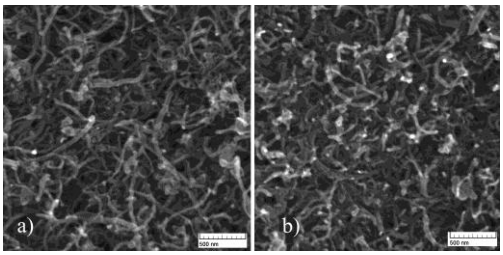

Fig. 3 SEM image of the surface of entangled MWCNT network of buckypaper made of a) pure, and b) oxidized MWCNT.

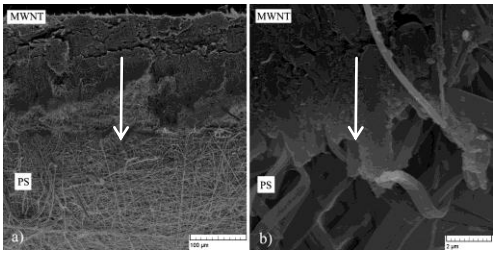

Fig. 4 Cross-section of composite consisting of MWCNT network (above) and PS filter before compression molding, part a) (scaler 100 μm). The arrow indicates nanotube infiltration illustrated in details in the enlarged image, part b) (scaler 2 μm).

suspension during filtration, when tubes are deposited as more individualized units or as smaller agglomerates. The resistivity of the networks is measured to be 0.084±0.003 Ω.cm for pristine and 0.156±0.003 Ω.cm for oxidized nanotubes, respectively.

4.2 PS filter-supported multi-wall carbon nanotube networks

The composite consisting of filter-supported entangled multiwall carbon nanotube networks were prepared by the nanotube dispersion filtration through a non-woven flexible polystyrene filter. The PS filter pores allows partial MWCNT infiltrating into the filter at the beginning of filtration as far as the pores are lined by nanotubes and pure nanotube network is formed above the filter surface, Fig. 4.

Fig. 5 shows composite arrangement after compression molding. The thickness of MWCNT network is proportional to volume of filtered MWCNT dispersion. The typical used dispersion volume is 0.26 to 4.07 cm^3/cm^2 (filter area) and the corresponding network

thickness is from 26 μm to 260 μm. The arrangement of nanotube networks and PS layers is arbitrary. MWCNT-PS-MWCNT composite layer arrangement is introduced in Fig. 4c. This composite is prepared by double-sided filtration. Other layer arrangements can be prepared by overlaying several MWCNT/PS composite units prior to compression molding.

The comparison of tensile tests for pure MWCNT network and composite are shown in Fig. 6. The measured stress/strain dependence for pure MWCNT network indicates the tensile modulus about 600 MPa and the ultimate tensile strength ~1 MPa. The PS filter-support has a positive effect on the tensile strength of MWCNT/PS composite as shown in Fig. 6. The measured tensile modulus is about 1300 MPa and the ultimate tensile strength is 10.3 MPa (thickness of PS film is 70 μm and MWCNT network 116 μm). The corresponding tensile values for pure PS film are 2100 MPa and 15.4 MPa (212 μm).

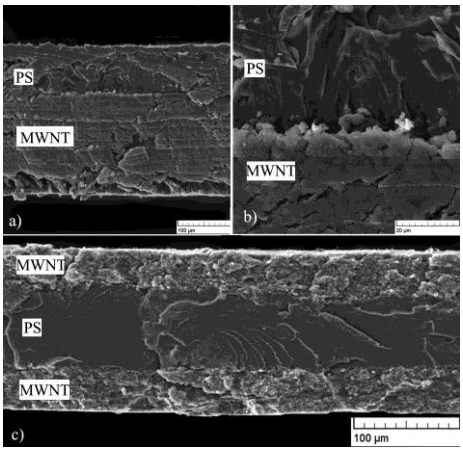

Fig. 5 SEM micrographs of MWCNT/PS composite after the compression molding. a) PS film (thicknesses about 80 μm) with attached nanotube network (260 μm), b) the interface between nanotube network and PS film, c) MWCNT-PS-MWCNT composite layer arrangement to decrease composite resistance.

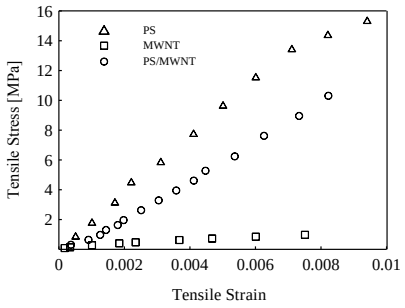

Fig. 6 Comparison of tensile properties of PS filter-supported MWCNT network (circles), MWCNT network (squares) and pure PS (triangles) in tensile test. The lines represent the power law fitting.

4.3 Effect of compressive strain/stress on electric resistance of multi-wall carbon nanotube networks

The resistance/compressive strain dependence is shown in Fig. 7 (compressive strain as well as compression is defined as positive deformation and loading, respectively). The measurement show that compression causes a decrease in MWCNT network resistance, as clearly visible in the figure. The plotted resistance values, R, are normalized with respect to the initial resistance, R_i, recorded at the start of the test at no load. For each network thickness, i.e. 0.23 and 0.38 mm, four samples are investigated. Their resistance is measured after each compression step to the preset deformation and for the subsequent unloaded state. The resistance in the unloaded states is reduced similarly to the resistance of compressed samples.

The observed effect of repeated compression on the network resistance is presented in Fig. 8. As can be seen, with increasing number of deformation cycles the resistance of

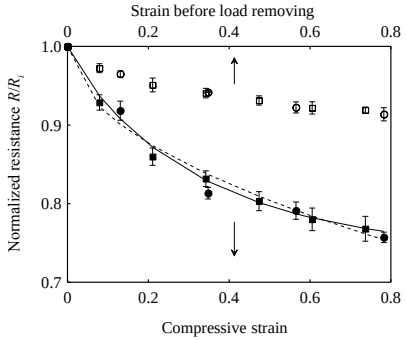

Fig. 7 Normalized resistance vs. strain dependence of entangled carbon nanotube network. The network thickness is 0.23 mm (squares) and 0.38 mm (circles). The full and open symbols denote the network with and without load, respectively. Data presented as a mean ± standard deviation, $n = 4$. The solid and dotted line represents the prediction given by equation (2) and the contact network model [5], respectively.

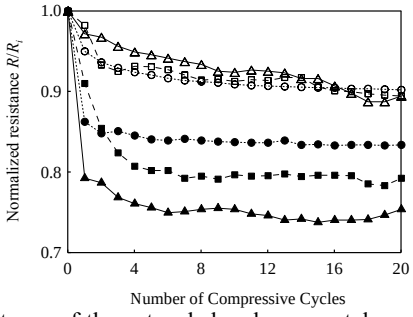

Fig. 8 Normalized resistance of the entangled carbon nanotube network vs. the number of compression/relaxation cycles; network thickness 0.38 mm. The applied compressive strain: 0.21 (circles), 0.47 (squares) and 0.74 (triangles). Full and open symbols denote the network with and without load, respectively.

MWCNT network first declines more steeply but after several cycles the decrease is very slight, and eventually no resistance change is observed. It indicates that the network rearrangement becomes steady what is favorable for MWCNT network use as the sensing element of compressive stress sensor when the network is suitably deformed in advance.

Electrical properties of manufactured structures are followed also in the course of twelve compression and relaxation cycles with cyclic accumulation of residual strain (compression as well as compressive strain is defined as positive loading and deformation, respectively). The measured data are shown in Fig. 9 as a plot of conductivity values σ vs. applied compressive stress τ. Compression causes a conductivity change during both the up-stress and down-stress periods due to specific deformation of porous structure. According to [5], the local contact forces increase during compression, allowing a better contact of nanotubes, which in turn leads to the decrease of contact resistance between crossing nanotubes; in release the dependence is just the opposite. At the same time, the possible effect of the distance between contacts on CNT tangle resistance is considered in [5]. The distance between contacts may decrease during compression owing to evoked relative motion of nanotubes, which corresponds to a lower intrinsic resistance of nanotube segments between contacts. Last but not least, compression may also bend the nanotubes sideways, which results in more contacts between nanotubes [19]. Since the contact points may act as parallel resistors, their increasing number causes an enhancement of MWCNT network conductivity.

The conductance mechanisms are apparently not reversible in the initial cycle since the down-stress curve indicates residual conductivity increase in the off-load state. Nevertheless, the ongoing compression cycles have a stabilizing effect on the conductivity-compression loops similarly to their effect on mechanical properties. The conductivity enhancement σ_r, defined as the residual minimum conductivity during each cycle, increases with the increasing number of cycles, and after about 7 cycles, σ_r tends to reach to an asymptotic value, Fig. 10.

Mechanical properties of manufactured structures are also followed in the course of twelve compression and relaxation cycles with cyclic accumulation of residual strain (compression as well as compressive strain is defined as positive loading and deformation, respectively). The results in the form of compressive stress vs. strain dependence are presented in Fig. 11.

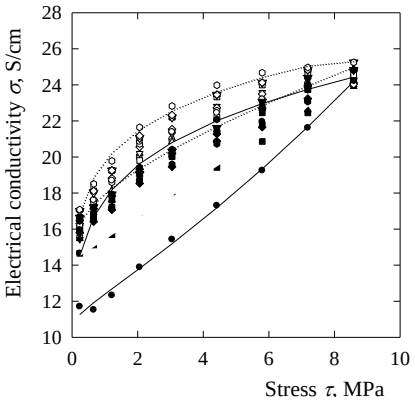

Fig. 9 Electrical conductivity-compressive stress loops for MWCNT network subjected to 12 successive compression/expansion cycles (network thickness 0.42 mm). The solid lines (first loading and unloading cycle) and dotted lines (twelfth cycle) represent the prediction given by Equation (2).

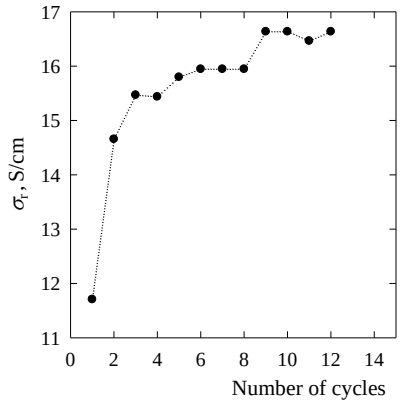

Fig. 10 Conductivity enhancement in each cycle vs. number of compression/expansion cycles.

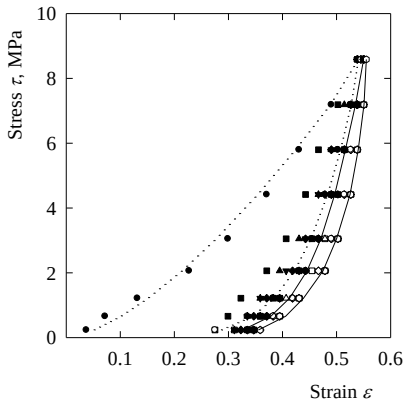

Fig. 11 Stress-strain loops in cyclic compression test for MWCNT network subjected to 12 compression/expansion cycles (the network thickness 0.42 mm). The dotted lines (first loading and unloading cycle) and solid lines (twelfth cycle) represent the power law fitting.

The accumulation of residual strain is often called ratcheting and the minimum strain in each cycle is defined as ratcheting strain, ε_r. In MWCNT network ratcheting strain appears after the first compression cycle, probably due to the initial deformation of porous structure and blocked reverse motion of nanotubes inside the compact network, as hypothesized in [5]. Thus the ability of the network to be repeatedly highly compressed is reduced. Moreover, during successive cycles of loading and unloading the change of ratcheting strain per cycle decreases and an asymptotic value of ε_r is obtained, as demonstrated in Fig. 12. Then stress-strain hysteresis loops reach a steady-state cyclic regime.

The oxidation of MWCNT modifies electrical conductivity of MWCNT networks under compression. It follows from Fig. 13 where the stress dependent conductivity of pristine and oxidized MWCNT networks is plotted for 4 compression and relaxation cycles. Compression causes a conductivity change during both the up-stress and down-stress periods due to specific deformation of porous structure. Nevertheless, the conductivity of nanotube network prepared from chemically functionalized MWCNT in $KMnO_4/H_2SO_4$ oxidizing system is lower and less deformation affected than pristine MWCNT network. It shows a stabilizing character of oxidation process.

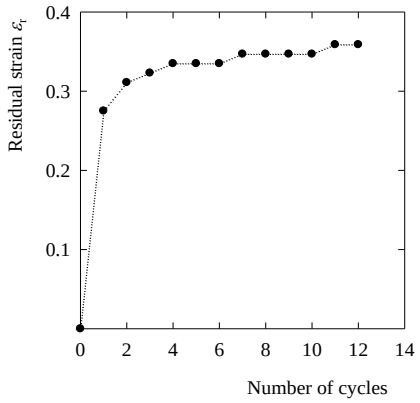

Fig. 12 Residual strain versus number of compression/expansion cycles.

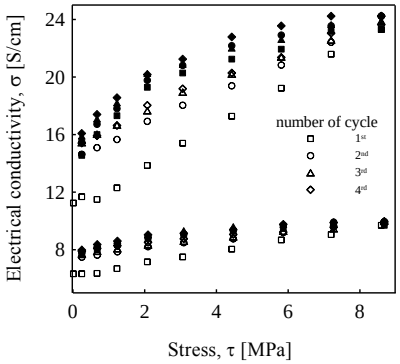

Fig. 13 Electrical conductivity-compressive stress loops for MWCNT and MWCNT ($KMnO_4$) network subjected to four successive compression/expansion cycles (the network thicknesses were 0.41 mm and 0.40 mm).

4.4 MWCNT network and contact resistance

The resistance of the CNT network is affected by many factors ranging from nanotube conduction mechanisms through their size to contact resistance between nanotubes and the network architecture [4-7]. However, according to the research carried out for short single wall carbon nanotube (SWCNT) network, the network resistance is dominated by the contact resistance between nanotubes while the intrinsic resistance of nanotubes is negligible [7]. Moreover, a uniform distribution of the intercontact resistances for unloaded SWNT network is supposed.

In accordance with the evidence given in [4], the local force between nanotubes increases during the compression. This allows better contacts between them, which consequently leads to the decrease of contact resistance. Besides electron transfer facilitated this way, the residual resistance decrease shown in Fig. 10 suggests an additional mechanism of

resistance/strain relation. As indicated in [13], compression may also buckle the nanotubes, which results in more contacts between them. Since the contact points act as parallel resistors, their increasing number cause reduction of overall network resistance. This structure reorganization, i.e. more contact points, probably partly remains when the compressive strength is released, which may be the reason for off-load resistance decrease.

If this more complicated picture of network electrical resistance change is assumed rather than the effect of contact resistance between nanotubes only [4,12], the possible distribution of individual intercontact resistances which is considered to govern the total resistance of the network [4] may change. In this regard, we assume that the distribution of intercontact resistances in compressed MWCNT network is such that the joint probability for this total network resistance change under strain ε is described by the cumulative distribution function $F(\varepsilon)$ for the two-parameter Weibull distribution,

$$\Pr(\varepsilon) = F(\varepsilon) = 1 - \exp\left[-(\varepsilon/\varepsilon_0)^m\right] \tag{1}$$

where $F(\varepsilon)$ is the cumulative distribution function of Weibull distribution. $F(\varepsilon)$ is an increasing function, $0 \le F(\varepsilon) \le 1$ and represents the probability of network resistance change $\Pr(\varepsilon)$ under strain no greater than ε. The two parameters of Weibull distribution are the shape parameter m and the normalizing factor ε_0. The shape parameter describes the spread in strain to change the resistance.

The assumption that the probability of the whole network resistance follows the Weibull distribution is substantiated in Fig. 15. The figure shows that all the experimental points very closely follow a straight line when plotted in Weibull coordinates $\ln(\ln(1/(1-P_i)))$ vs. $\ln \varepsilon$, where $P_i = (i\text{-}0.5)/n$ and i ranges from 1 to n, which is the number of tests. The goodness-of-fit to the straight line is reflected in the value of the correlation coefficient r = 0.99.

The tendency of the measured reduction of the macroscopic, i.e. network resistance with compressive strain is bound to the probability of network resistance change $\Pr(\varepsilon)$ under strain no greater than ε. Consequently, the following relation of the normalized network resistance R/R_i to function $F(\varepsilon)$ links appropriately the model prediction with the observed strain-dependent network resistance decrease

$$R/R_i = \alpha + \beta F(\varepsilon) = \alpha + \beta\left(1 - \exp\left[-(\varepsilon/\varepsilon_0)^m\right]\right) \tag{2}$$

where α and β are location parameters and R_i the initial network resistance at the start of experiments at no load. The reasonably good description of the measured data by the predictive relation (2) is shown in Fig. 5 (parameters α = 1, β = -0.26, m = 0.91, ε_0 = 0.33).

We exploit for data description in Fig. 5 also the contact network model despite of its original use to represent the electronic transport properties of carbon nanofiber/epoxy resin composites and CNT tangles of moderate CNT volume fractions (up to 0.2) [4,14]. Moreover, the contact resistance power law model $R_{CONTACT} = K\phi^n$ (see [4]) is used here also to evaluate the contact resistance between crossing MWCNT in our network (Fig. 16) though besides the contact resistance also the increase number of contacts in the course of compression owing to buckling of nanotubes may be expected.

As follows from Fig. 5, the contact network model describes the measured resistance data quite well similarly as Eq. 2 what may suggest also dominant effect of local contact resistance between MWCNT on the decrease of total resistance of entangled MWCNT network structures of buckypaper during the compression. The dependence of contact resistance $R_{CONTACT}$ on the network deformation expressed in terms of MWCNT volume fraction to compare it with similar data given in [4] is presented in Fig. x . The data show

that the contact resistance between the crossing MWCNT of entangled network structures of buckypaper (the considered average MWCNT diameter is 20 nm) is lower by up to two orders of magnitude in comparison to the contact resistance of powdery CNT layer [4]. The probable reason is higher MWCNT volume fraction and compactness of filtered MWCNT network with respect to powdery CNT layer investigated in [4].

The best description of the data in Fig.13 is obtained by the series heterogeneous model when the resistance is described as the sum of metallic (MWCNT are regarded as metallic conductors) and barrier portions of conduction path [17-19],

$$R/R_i = aT + b\exp\left[c/(T+d)\right], \tag{3}$$

where a the temperature coefficient arising from the metallic resistance and the second term (hopping/tunneling term) represents fluctuation-induced tunneling through barriers between metallic regions. T denotes temperature, whereas b, c, d the fitted parameters.

4.5 Effect of temperature on MWCNT and PS/MWCNT network resistance

The effect of temperature on the electric resistance is presented in Figs. 14. The composite as well as the pure MWCNT network exhibit non-metallic behavior ($\mathrm{d}(R/R_i)/\mathrm{d}T < 0$ over the investigated temperature range from 230 to 420 K. The negative $\mathrm{d}(R/R_i)/\mathrm{d}T$ indicates the presence of tunneling barriers, which dominate both the pure MWCNT network and the filter-supported network resistance. The obvious effect of the supporting polymer is reduction of the resistance temperature dependence. The resistance ratio R_{230}/R_{420} for resistances at the corresponding temperature is reduced form 1.35 in MWCNT network case to 1.12 in the composite case.

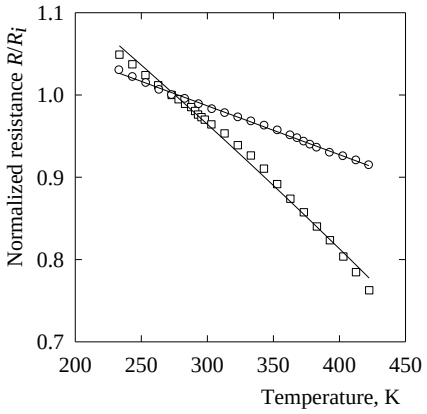

Fig. 14 Temperature-dependent normalized resistance of MWCNT/PS composite (circles) and MWCNT network (squares). The solid lines represent description by Eqn. (2).

4.6 Effect of organic vapors on MWCNT pure and oxidized networks

Single-wall carbon nanotubes and multi-wall carbon nanotubes (MWCNTs) show remarkable sensitivity to the change of chemical composition of the surrounding environment. This property is favorable for their use in the form of membranes [a], adsorbents [a] or gas sensors [c,d].

Gas and vapor adsorption as well as desorption usually proceeds at high rates and amounts [e]. The molecules are adsorbed on the carbon nanotube (CNT) surface by van der Waals attracting forces, which leads to remarkable changes in CNT electrical resistance. A smart application of this principle can eventually lead to development of CNT-based electrochemical biosensors and gas sensors with a useful ability to detect various gases and organic vapors. Conductivity measurement is then a simple and convenient method to register CNT response to vapor adsorption/desorption.

Previous research [f,g] found that physisorbed molecules influence the electrical properties of isolated CNTs and also inter-tube contacts. The resistance of macroscopic CNT objects like aggregates or network structures used in gas sensors is predominantly determined by contact resistance of crossing tubes rather than by resistance of CNT segments. Here, the tubes are much shorter than sensor dimensions and inter-tube contacts act as parallel resistors between highly conductive CNT segments.

Such CNT macroscopic objects contain four different adsorption sites: internal, interstitial channels, external grooves and external surfaces [b]. The dominating process influencing macroscopic resistance is probably gas or vapor adsorption in the space between nanotubes, which forms non-conductive layers between the tubes. This process decreases both the quantity and quality of contacts between nanotubes and consequently increases macroscopic resistance [c].

The strips made of both types of CNT networks were exposed to the saturated vapors of organic solvent - acetone (adsorbate), when the adsorption/desorption response cycles 6-minute intervals were measured, see Fig 15. The adsorption of acetone molecules causes increase in resistance with concentration and time, which is presented in the figure as sensitivity or gas response, S, defined as

$$S = \frac{R_g - R_a}{R_a} = \frac{\Delta R}{R_a} \tag{4}$$

where R_a represents specimen resistance in air and R_g resistance of the specimen exposed to gas/vapor, ΔR stands for the resistance change. As can be seen from the figure the responses are sensitive and reversible. The measurement performed for several specimens also proves its reproducibility. Finally, the response is significantly sensitive for oxidized nanotubes.

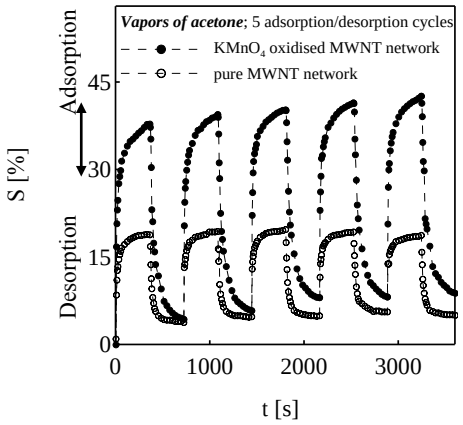

Fig. 15 Five adsorption/desorption cycles for MWCNT (empty symbols) and MWCNT-$N_{(KMnO4)}$ (full symbols) exposed to vapors of acetone.

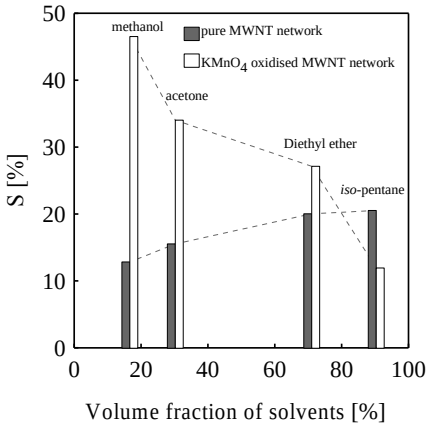

Fig. 16 Dependence of sensitivities of MWCNT-N and MWCNT-$N_{(KMnO4)}$ networks on volume fraction of four different organic solvents during adsorption/desorption cycles

Table 1 Sensitivity of pristine and oxidized MWCNT networks exposed to saturated vapors of different organic solvents.

Organic solvent	S_1 [%] MWCNT-N	S_2 [%] MWCNT-$N_{(KMnO4)}$	S_2/S_1
iso-pentane	20.6±1.4	12.0±0.3	0.6
diethyl ether	20.1±0.8	27.2±0.6	1.4
acetone	15.6±0.5	34.1±0.6	2.2
methanol	12.9±0.7	46.6±1.8	3.6

The effect of different adsorbates (iso-pentane, diethyl ether, acetone and methanol) is tested. The chosen solvents cover a broad range of Hansen solubility parameters overall defining the total Hildebrand solubility parameters, δ_t. The polarity of solvents increases in order iso-pentane, diethyl ether, acetone and methanol with values of δ_t, δ_t = 13.7 $MPa^{1/2}$, δ_t = 15.6 $MPa^{1/2}$, δ_t = 20.0 $MPa^{1/2}$ and δ_t = 29.6 $MPa^{1/2}$, respectively. The saturated vapor pressures of the solvent defining volume fractions of saturated vapors at defined conditions decreases in the same order from values 90.2 vol. % for iso-pentane, 70.9 vol. % for diethyl ether, 30.1 vol. % for acetone and 16.5 vol. % for methanol. Adsorption/desorption cycles for other solvents are measured under the same conditions as for acetone. The sensitivities S1 and S2 calculated for pure MWCNT-N (S1) and its oxidized form MWCNT-$N_{(KMnO4)}$ (S2) are presented in Fig. 15 and Table 1. Finally, to follow the selectivity of networks made of functionalized (oxidized) tubes, the ratio of S_2/S_1 was calculated for each solvent vapor. The only case when this value is lower than one, i.e., the oxidized nanotubes have lower sensitivity than their pure form, is for the non-polar solvent iso-pentane (S_2/S_1 = 0.6). On the other hand, the sensitivities to other solvents tested (those containing oxygen functional groups) are found higher for the oxidized form of MWCNTs, the ratio of sensitivities ranging from 1.4 (diethyl ether) to 3.6 (methanol). Thus S_2/S_1 may be correlated with δ_t, which means that the ratio is typical of each individual solvent.

5 Concluding remarks and discussion

The conductivity-compression characteristics for entangled CNT network structures of buckypaper produced by filtering a nanotube suspension have not been studied in details so far. Thus the primary aim of our research was to find out the effect of compression on network electrical conductivity when a simple and repeated loading is exerted. The measurements have shown over 100% network conductivity increase at the maximum applied compressive stress. It indicates a good potentiality of MWCNT entangled network to be applied as a compression sensing element. The conversion of compressive stress into improved conductivity is achieved by deformation of porous structure. The structure recovering mechanism projects into the ratcheting strain, the change of which decreases with the increasing number of applied cycles, and finally an asymptotic value of this residual strain is reached. During successive cycles of loading and unloading the nanotubes rearrangement becomes steady and MWCNT network reaches a stable stress-strain hysteresis loop shape. This mechanical stabilization is reflected also in conductivity data. The conductivity-stress loop is stable during the same number of cycles as in the mechanical cyclic loading. It shows that the entangled carbon nanotube network structure of buckypaper can be used as a sensing element of compressive stress, especially when the network is suitably deformed in advance.

A new type of composite consisting of PS filter-supported entangled multiwall carbon nanotube network is introduced as a conductive and/or sensoric polymeric material. PS filter-support increases nanotube network mechanical integrity and eliminates the laborious process of peeling off the nanotube network from the usual micro-porous (polycarbonate, nylon) filter followed by the network impregnation to increase its compactness. The prepared composite is flexible allowing its bending (radius up to 5-10 mm) without damage of

MWCNT layer. The combined mechanical and electrical properties as well as vapor sensing open new opportunities for the composite use as polymer composite conductors, pressure and vapor sensing elements as well as an electromagnetic interference shielding and lightning strike protection. A hot press molding process can produce solid bulk composites consisting of multiple-layers of PS filter-supported MWCNT network.

Acknowledgement

Two authors (Slobodian, Olejnik) would like to express that this project was supported by the internal grant of TBU in Zlín No. IGA/12/FT/10/D funded from the resources of specific university research. Finally Dr. Riha thanks the Grant Agency of the Academy of Sciences (GAAV IAA200600803) and the Institute of Hydrodynamics Fund AV0Z20600510.

6 References

1. Thostenson ET, Li CY, Chou TW (2005) Nanocomposites in context, Compos. Sci. Technol. Vol. 65, 2005, pp. 491-516
2. Cao Q, Rogers JA (2009) Ultrathin films of single-walled carbon nanotubes for electronics and sensors: A review of fundamental and applied aspects, Adv. Mater. Vol. 21, 2009, pp. 29-53
3. Walters DA et al. (2001) In-plane-aligned membranes of carbon nanotubes, Chem. Phys. Lett. Vol. 338, 2001, pp. 14-20
4. Poquillon D, Viguier B, Andrieu E (2005) Experimental data about mechanical behaviour during compression tests for various matted fibres, J. Mat. Sci. Vol. 40, 2005, pp. 5963-5970
5. Allaoui A, Hoa SV, Evesque P, Bai J (2009) Electronic transport in carbon nanotubes tangles under compression: The role of contact resistance, Scripta Mater. Vol. 61, 2009, pp. 628-631
6. Kukowecz A, et al. (2008) Multiwall carbon nanotubes films surface-doped with electroceramics for sensor applications, Phys. Stat. Sol. Vol. 245, 2008, pp. 2331-2334
7. Kastanis D, Tasis D, Papagelis K, Parthertios J, Tsakiroglou C, Galiotis C (2007) Oxidized multi-walled carbon nanotube film fabrication and characterization, Adv. Compos. Lett. Vol. 16, 2007, pp. 243-248
8. Ham HT, Choi YS, Chung IJ (2005) An explanation of dispersion states of single-walled carbon nanotubes in solvents and aqueous surfactant solutions using solubility parameters, Colloid Interf. Sci. Vol. 286, 2005, pp. 216-223
9. Chern CS, Wu LJ (2001) Microemulsion polymerization of styrene stabilized by sodium dodecyl sulfate and short-chain alcohols, J. Polym. Sci. Part A: Polym. Chem. Vol. 39, 2001, pp. 3199-3210
10. Kimmer D, et al. (2009) Polyurethane/MWCNT nanowebs prepared by electrospinning process, J. Appl. Polym. Sci. Vol. 111, 2009, pp. 2711-2714
11. Slobodian P, Kralova D, Lengalova A, Novotny R, Saha P, Adaptation of Polystyrene/Multi-Wall Carbon Nanotube Composite Properties In Respect of its Thermal Stability, Polym Composite Vol. 31(3) 2010, pp. 452-458.

12. Pauw LJ (1958) A method of measuring specific resistivity and Hall effect of discs of arbitrary shape, Philips Res. Repts Vol. 13, 1958, pp. 1-9
13. Rasheed A, Howe JY, Dadmun MD, Britt PF (2007) The efficiency of the oxidation of carbon nanofibers with various oxidizing agents, Carbon Vol. 45, 2007, pp. 1072-1080
14. Hernadi K, et al. (2001) Reactivity of different kinds of carbon during oxidative purification of catalytically prepared carbon nanotubes, Solid State Ionics Vol. 141, 2001, pp. 203-209
15. Wang XB, et al. (2007) Radical functionalization of single-walled carbon nanotubes with azo(bisisobutyronitrile), Appl. Surf. Sci. Vol. 253, 2007, pp. 7435-7437
16. Li Q, Ma Y, Mao C, Wu C (2009), Grafting modification and structural degradation of multi-walled carbon nanotubes under the effect of ultrasonics sonochemistry, Ultrason. Sonochem. Vol. 16, 2009, pp. 752 -757
17. Shelimov KB, et al. (1998) Purification of single-wall carbon nanotubes by ultrasonically assisted filtration, Chem. Phys. Lett. Vol. 282, 1998, pp. 429-434

a) Smajda R, Kukovecz A, Konya Z, Kiricsi I. Structure and gas permeability of multi-wall carbon nanotube buckypapers. Carbon 2007;45(6):1176-1184.
b)Agnihotri S, Mota JPB, Rostam-Abadi M, Rood MJ. Theoretical and experimental investigation of morphology and temperature effects on adsorption of organic vapors in single-walled carbon nanotubes. J Phys Chem B 2006;110(15):7640-7647.
c) Romanenko A I, Anikeeva OB, Kuznetsov VL, Buryakov TI, Tkachev EN, Usoltseva AN. Influence of helium, hydrogen, oxygen, air and methane on conductivity of multiwalled carbon nanotubes. Sensor Actuat A-Phys 2007;138(2):350-354.
d)Qureshi A, Kang WP, Davidson JL, Gurbuz Y. Review on carbon-derived, solid-state, micro and nano sensors for electrochemical sensing application. Diam Relat Mater 2009;18(12):1401-1420.
e)Hussain CM, Saridara C, Mitra S. Microtrapping characteristics of single and multi-walled carbon nanotubes. J Chromatogr A 2008;1185(2):161-166.
f)Tournus F, Latil S, Heggie MI, Charlier JC. pi-stacking interaction between carbon nanotubes and organic molecules, Phys Rev B 2005;72(7):Article Number 075431.
g)Mowbray DJ, Morgan C, Thygesen KS. Influence of O-2 and N-2 on the conductivity of carbon nanotube networks. Phys Rev B 2009;79(19): Article Number 195431.

ČESKÁ REPUBLIKA
ÚŘAD PRŮMYSLOVÉHO VLASTNICTVÍ

OSVĚDČENÍ

O ZÁPISU UŽITNÉHO VZORU

J. Kratochvíl

Josef Kratochvíl
předseda
Úřadu průmyslového vlastnictví

Číslo zápisu: **21352** Datum zápisu: 11.10.2010

Číslo přihlášky: **2010-22906** Datum přihlášení: 25.06.2010

Právo přednosti podle mezinárodní smlouvy
(bylo-li uplatněno a uznáno) od:

MPT: ***G 01 L 1/18*** (2006.01)
G 01 L 1/00 (2006.01)

Název: Tlakový senzor

Majitel: Univerzita Tomáše Bati ve Zlíně, Zlín, CZ

Původce: Slobodián Petr doc. Ing. Ph.D., Zlín, CZ
Olejník Robert Ing., Zlín, CZ
Říha Petr Ing. CSc., Praha, CZ
Kimmer Dušan Ing. CSc., Zlín, CZ
Petráš David Ing., Zlín-Malenovice, CZ

V Praze dne 11.10.2010

Úřad průmyslového vlastnictví v zápisném řízení nezjišťuje, zda předmět užitného vzoru splňuje podmínky způsobilosti k ochraně podle § 1 zák. č. 478/1992 Sb.

UŽITNÝ VZOR

(11) Číslo dokumentu:

21352

(13) Druh dokumentu: **U1**

(51) Int. Cl.:

G01L 1/18 (2006.01)
G01L 1/00 (2006.01)

(19) ČESKÁ REPUBLIKA

ÚŘAD PRŮMYSLOVÉHO VLASTNICTVÍ

(21) Číslo přihlášky: **2010 - 22906**
(22) Přihlášeno: **25.06.2010**
(47) Zapsáno: **11.10.2010**

(73) Majitel:
Univerzita Tomáše Bati ve Zlíně, Zlín, CZ

(72) Původce:
Slobodián Petr doc. Ing. Ph.D., Zlín, CZ
Olejník Robert Ing., Zlín, CZ
Říha Petr Ing. CSc., Praha, CZ
Kimmer Dušan Ing. CSc., Zlín, CZ
Petráš David Ing., Zlín-Malenovice, CZ

(74) Zástupce:
Ing. Dana Kreizlová, UTB ve Zlíně, Nám. T. G. Masaryka 5555, Zlín, 76001

(54) Název užitného vzoru:
Tlakový senzor

CZ 21352 U1

Tlakový senzor

Oblast techniky

Technické řešení se týká tlakového senzoru, který je určen pro měření tlaku, převedším pro miniaturní a méně exponované aplikace.

Dosavadní stav techniky

Snímače hodnoty mechanického tlaku působícího na plochu jsou v podstatě založeny na vyvolání mechanické deformace referenční plochy snímače a související ekvivalentní změně jiné dobře měřitelné veličiny, zpravidla elektrické. Základním požadavkem přitom je reprodukovatelnost, spolehlivost a dostatečná přesnost procesu měření, přičemž důležitou roli hraje také životnost snímače a v souvislosti s tím i jeho cena.

Jednoduchý princip tlakového senzoru lze vyjádřit následujícím způsobem: pružná deformace membrány, která je součástí tlakového senzoru, vyvolá deformaci odporového drátku a tím změnu jeho elektrického odporu. Velikost této změny pak reprezentuje odpovídající hodnotu tlaku. Tento jednoduchý princip však předpokládá opakované mechanické namáhání odporového drátku a s tím související omezenou životnost snímače. Proto byla vyvinuta řada typů tlakových senzorů, u nichž je odezva na mechanickou deformaci řešena zprostředkovaně - například tak, že pružný člen je tvořen vlnovcem, k němuž je připojeno jádro cívky, axiálně pohyblivé proti cívce. Při mechanické deformaci vlnovce se posunem jádra cívky změní její indukce a tuto změnu vyhodnotí elektrický obvod jako relevantní k dané hodnotě působícího tlaku. V analogickém provedení může úlohu vlnovce nahradit stočená deformační trubice, která se pod vlivem tlaku narovnává a její konec ovládá jádro cívky. Obě uvedená řešení představují určité zdokonalení předchozího základního principu, konstrukčně i objemově jsou však již poněkud náročnější. Jsou vhodná pro větší prostory a robustnější aplikace.

Vzhledem k rozmanitosti požadavků na tlakové senzory byly vyvinuty další typy, z nichž je třeba zmínit senzory na piezoelektrickém principu. Tlak působící na pružnou membránu přenese její prohnutí na piezoelektrický trn, který po stlačení vysílá odpovídající napěťový signál. Výhodou tohoto snímače je vedle robustnosti i jednoduchá konstrukce; je vhodný pro průmyslové aplikace. Pružná membrána však nemusí být v tlakovém senzoru aplikována ve své tradiční podobě, ale také může být vytvořena například vnější izolací kabelu (pryž, hliníkový nebo měděný oplet). Mezi opletem a jádrem tvořeným měděným vodičem je piezopolymer nebo piezogranule, spojené přes jádro a oplet s elektrickým obvodem. Působením tlaku na vnější plášť kabelu dochází následně ke stlačování piezopolymeru a vzniku odpovídajícího napěťového signálu, který je zaznamenán elektrickým obvodem. Výhodou tohoto typu senzoru je opět robustnost a jednoduchá konstrukce. Využívá se jako senzor pro indikaci přítomnosti a pohybu vozidel. Kabely jsou zabudovány do vozovky a senzor je schopen odlišit od sebe hmotnost pohybujících se vozidel.

Vedle dosud uvedených typů tlakových senzorů je v současné době k dispozici i několik typů s odlišnou technickou koncepcí, určených pro menší až miniaturní aplikace. Pružná plocha vystavená působení tlaku může být vytvořena z křemíkové membrány zhotovené monoliticky jako integrovaný senzor tlaku s malými rozměry a dobrými dynamickými vlastnostmi. Průhyb křemíkové membrány vyvolá změnu jejího odporu a tím změnu napětí v odporovém můstku. Jinou alternativou tohoto technického principu je tvarovaná křemíková mikromembrána přitlačovaná na nosič z izolantu (skla) přes dvě elektrody tvořící mikrokondenzátor. Zatížení mikromembrány přiblíží k sobě elektrody a změní tím kapacitu mikrokondenzátoru, jejíž měření vypovídá o hodnotě měřeného tlaku. Membrána je vybavena dorazovou plochou, která brání jejímu přetížení. Další alternativou této řady je pružná mikromembrána, na kterou je přilepen malý permanentní magnet, proti němuž je na pevné desce plošného spoje připevněn Hallův senzor spojený s měřicím přístrojem. Jiné z řešení na tomto technickém principu využívá tvarovanou křemíkovou mikromembránu s povrchem upraveným jako zrcadlo, připevněnou na nosiči z polopropustného skleněného zrcadla. Dutina mezi zrcadly tvoří FP interferometr, nad polopropustným zrcadlem je

světelný zdroj - LED a vyhodnocovací fotodiody. U všech těchto řešení se průhyb křemíkové mikromembrány transformuje ve změnu elektrické veličiny zaznamenané obvodem senzoru.

Popsané senzory na bázi křemíkové membrány jsou citlivé a jsou vhodné pro malé až miniaturní aplikace. Vyžadují však linearizaci výstupních hodnot při vyhodnocování vzhledem k hodnotám vstupního tlaku. Jejich nevýhodou je dále náročnost na použité konstrukční prvky a s tím spojená cena.

Podstata technického řešení

Uvedené nedostatky a nevýhody dosavadních snímačů tlaku do značné míry odstraňuje tlakový senzor podle technického řešení. Podstata technického řešení spočívá v tom, že soudržná laminátová struktura tlakového senzoru je tvořena plošným nosičem o tloušťce v rozmezí desítek až tisíců μm, vytvořeným na bázi termoplastického polymeru, na němž je ukotvena senzorická vrstva tloušťky v rozmezí jednotek až stovek μm, sestávající z navzájem propletených vícevrstevnatých uhlíkových nanotrubiček s průměrem 5 až 100 nm a délkou 1 až 20 μm, s porozitou 0,5 až 0,9 a měrným odporem 0,01 až 1 Ω/cm, a tato senzorická vrstva je zapojena do elektrického obvodu vybaveného snímačem odporu připojeným na výstup opatřený relevantní signalizací hodnoty tlaku.

Materiál senzorické vrstvy je elektricky vodivý - podle druhu použitých vícevrstevnatých uhlíkových nanotrubiček (MWCNT) dosahuje vodivosti v řádu 10^3 S/m. Vodivost zprostředkovává jednotlivá trubička přenosem náboje různými mechanismy. Trubičky však nemají nekonečnou délku a tak důležitým parametrem je jejich vzájemný dotyk a křížení. Tato místa pak zprostředkovávají přenos náboje mezi jednotlivými nanotrubičkami. Pro celkovou vodivost vzorku jsou nejslabšími místy a jejich četnost prakticky určuje výslednou vodivost vzorku.

Vzhledem k popsané struktuře vodivost senzorické vrstvy citlivě reaguje na deformační podmět. Při tlakové deformaci dochází k snižování porozity vzorku a naopak narůstá počet kontaktů mezi jednotlivými trubičkami, čímž se makroskopická vodivost vzorku zvětšuje - odpor klesá. Další mechanismus zvýšení makroskopické vodivosti je ve zvýšení přítlačné síly v místech kontaktu mezi jednotlivými trubičkami, což vede k snížení kontaktních odporů mezi jednotlivými trubičkami. Tyto změny jsou převážně vratné, kdy deformace je elastická. Zpočátku však dochází k akumulaci deformace nevratné, zbytkové, kdy se po odlehčení nevrátí struktura do počátečního stavu, zpětný pohyb trubiček je částečně blokován zhutněnou síťovou strukturou. Hodnoty nevratné složky se přibližně pohybují kolem 20 % při celkové kompresní deformaci 80 %. Tento efekt je stabilizován po cca deseti cyklech, kdy již hodnota nevratné deformace dále nenarůstá. Tento nedostatek lze také snadno odstranit jednorázovým stlačením senzorické vrstvy vyšším tlakem, než pro jaký se bude senzor používat.

Takováto senzorická vrstva je použita na detekci působícího napětí skrze velikost vyvolané deformace. Při zakotvení senzorické vrstvy do plošného nosiče na bázi termoplastického polymeru se výrazně sníží podíl nevratné složky deformace a získaná soudržná laminátová struktura může být opakovaně používána jako tlakový senzor. Prováděné testy ukázaly dostatečnou citlivost senzoru a vratnost změn mezi zatíženým/odlehčeným stavem v řádu provedených stovek kompresních cyklů.

Výhodou tlakového senzoru podle technického řešení je především jeho konstrukční jednoduchost, odolnost vůči poruchám, možnost miniaturizace a nízká cena.

Přehled obrázků na výkrese

Uskutečnitelnost a účinky technického řešení jsou dokumentovány na přiloženém výkrese, kde značí:

Obr. 1 - změna elektrického odporu normalizovaného k počáteční hodnotě odporu v závislosti na měrném stlačení v průběhu cyklu zatěžování/uvolňování pro tlakový senzor podle technického řešení tvořený plošným nosičem na bázi polystyrenu a senzorickou vrstvou z navzájem proplete-

ných vícevrstevnatých uhlíkových nanotrubiček. Plné body dokumentují pokles odporu vrstvy po stlačení na hodnotu příslušné deformace, body prázdné pak hodnoty po odlehčení.

Obr. 2 - dokumentuje využitelnost principu pro opakované stlačování. Jedná se o sto cyklů mezi hodnotami tlaku 0,3 a 5,4 MPa.

Příklady provedení technického řešení

Příklad 1

Plošný nosič na bázi PVAc filtrační membrány má tloušťku 45 μm. Na tomto plošném nosiči je nanesena senzorická vrstva o tloušťce 116 μm z uhlíkových nanotrubiček (použité nanotrubičky byly: MWCNT, acetylénový typ, Sun Nanotech Co. Ltd., China, průměry trubiček 10 až 30 nm a délky 1 až 10 μm, čistota 90 %). Tato soudržná laminátová struktura má šířku 8,3 mm a délku 32,0 mm. Absolutní odpor senzorické vrstvy po zapojení do elektrického obvodu, měřený ve směru délky bez stlačení, je 23,33 Ω. Tato struktura při stlačování tlakem 3,5 MPa vykazuje pokles absolutního odporu senzorické vrstvy na hodnotu 22,41 Ω. Rozdíl absolutního odporu připadající na zatížení tlakem 1 MPa je (23,33 - 22,41) : 3,5 Ω = 0,263 Ω. Tato hodnota je na ohmmetru/tlakoměru označena jako 1 MPa.

Příklad 2

Plošný nosič na bázi termoplastické filtrační membrány má tloušťku 87 μm. Na tomto plošném nosiči je nanesena senzorická vrstva o tloušťce 247 μm z uhlíkových nanotrubiček stejného typu jako v příkladě 1. Tato soudržná laminátová struktura má šířku 10 mm a délku 39 mm, absolutní odpor senzorické vrstvy měřený ve směru délky bez stlačení je 11,08 Ω. Tato struktura při stlačování tlakem 0,7 MPa vykazuje pokles absolutního odporu senzorické vrstvy na hodnotu 9,62 Ω. Rozdíl absolutního odporu připadající na zatížení tlakem 1 MPa je (11,08 - 9,62) : 0,7 = 2,086 Ω. Tato hodnota je na ohmmetru/tlakoměru označena jako 1 MPa.

Příklad 3

Plošný nosič na bázi termoplastické filtrační membrány má tloušťku 87 μm. Na tomto plošném nosiči je nanesena senzorická vrstva o tloušťce 247 μm z uhlíkových nanotrubiček stejného typu jako v příkladě 1. Tato soudržná laminátová struktura má šířku 6,5 mm a délku 12 mm, absolutní odpor senzorické vrstvy měřený ve směru délky bez stlačení je 5,16 Ω. Tato struktura při stlačování tlakem 4 MPa vykazuje pokles absolutního odporu senzorické vrstvy na hodnotu 4,39 Ω. Rozdíl absolutního odporu připadající na zatížení tlakem 1 MPa je (5,16 - 4,39) : 4 = 0,193 Ω. Tato hodnota je na ohmmetru/tlakoměru označena jako 1 MPa.

Příklad 4

Plošný nosič na bázi termoplastické filtrační membrány má tloušťku 89 μm. Na tomto plošném nosiči je nanesena senzorická vrstva o tloušťce 31 μm z uhlíkových nanotrubiček stejného typu jako v příkladě 1. Tato soudržná laminátová struktura má šířku 10 mm a délku 33 mm, absolutní odpor senzorické vrstvy měřený ve směru délky bez stlačení je 71,37 Ω. Tato struktura při stlačování tlakem 0,5 MPa vykazuje pokles absolutního odporu na hodnotu 62,51 Ω. Rozdíl absolutního odporu připadající na zatížení tlakem 1 MPa je (71,37 - 62,51) : 0,5 = 17,720 Ω. Tato hodnota je na ohmmetru/tlakoměru označena jako 1 MPa.

Příklad 5

Plošný nosič na bázi termoplastické filtrační membrány má tloušťku 450 μm. Na tomto plošném nosiči je nanesena senzorická vrstva o tloušťce 410 μm z uhlíkových nanotrubiček stejného typu jako v příkladě 1. Tato soudržná laminátová struktura má šířku 10,7 mm a délku 7,0 mm, absolutní odpor senzorické vrstvy měřený ve směru délky bez stlačení je 1,19 Ω. Tato struktura při stlačování tlakem 8,6 MPa vykazuje pokles absolutního odporu na hodnotu 1,06 Ω. Rozdíl abso-

lutního odporu připadající na zatížení tlakem 1 MPa je (1,19 - 1,06) : 8,6 = 0,015 Ω. Tato hodnota je na ohmmetru/tlakoměru označena jako 1 MPa.

Jako materiál plošného nosiče jsou v příkladech 2 až 5 použity další polymery, zejména polystyren (PS), polymetylmethakrylát (PMMA), případně další termoplastické polymery. Použitý polymer neovlivňuje charakteristiky senzorické vrstvy z uhlíkových trubiček. Z tohoto pohledu mohou být použity i jiné termoplastické polymery, například semikrystalické polymery. Funkční tloušťka vytvořeného plošného nosiče může být již od desítek mikrometrů. Zvyšování jeho tloušťky nemění konstrukční princip tlakového senzoru, jen forma plošného nosiče přechází od filmu až po polymerní desku.

Průmyslová využitelnost

Tlakový senzor podle technického řešení lze snadno vyrobit i v malých rozměrech a aplikovat u celé řady tradičních i zcela nových výrobků v nejrůznějších oblastech použití.

NÁROKY NA OCHRANU

1. Tlakový senzor, **vyznačující se tím**, že jeho soudržná laminátová struktura je tvořena plošným nosičem o tloušťce v rozmezí desítek až tisíců μm, vytvořeným na bázi termoplastického polymeru, na němž je ukotvena senzorická vrstva tloušťky v rozmezí jednotek až stovek μm, sestávající z navzájem propletených vícevrstevnatých uhlíkových nanotrubiček s průměrem 5 až 100 nm a délkou 1 až 20 μm, s porozitou 0,5 až 0,9 a měrným odporem 0,01 až 1 Ω/cm, a tato senzorická vrstva je zapojena do elektrického obvodu vybaveného snímačem odporu připojeným na výstup opatřený relevantní signalizací hodnoty tlaku.

1 výkres

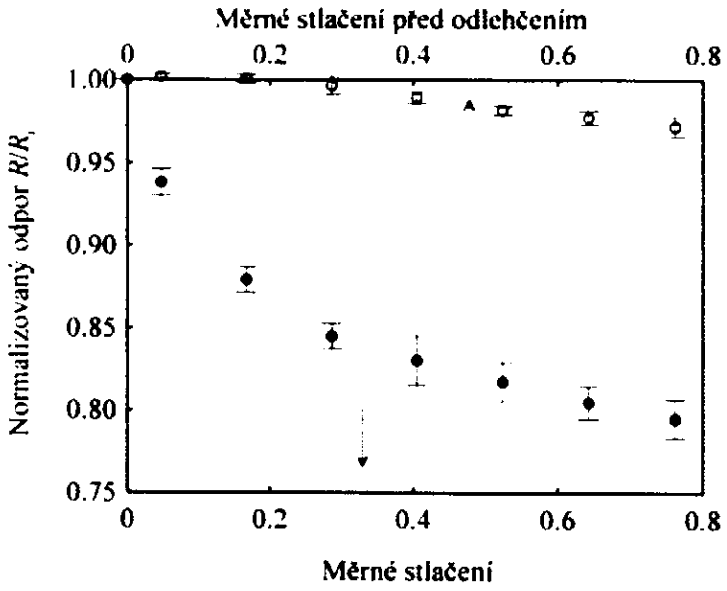

Obr. 1

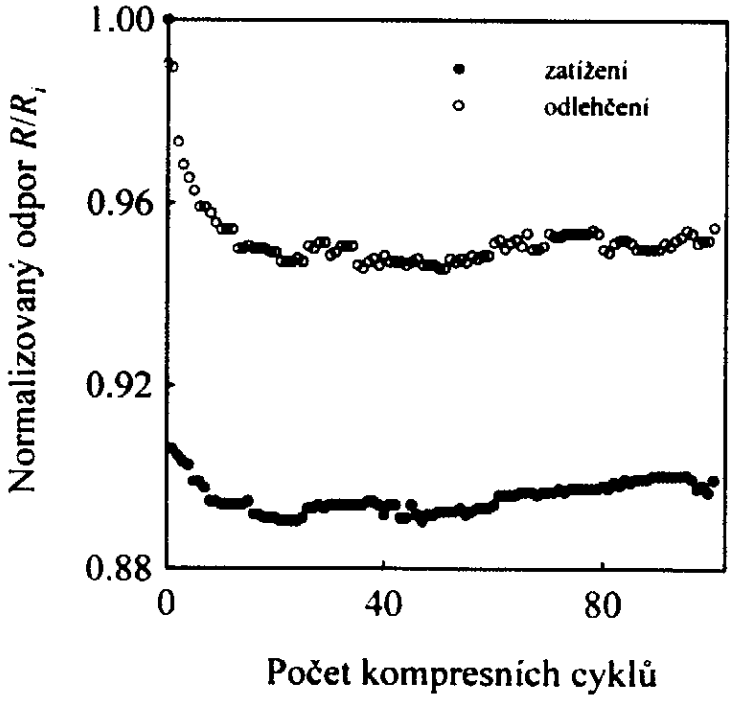

Obr. 2

Konec dokumentu

Úřad průmyslového vlastnictví

zapsal podle § 11 odst. 1 zákona č. 478/1992 Sb., v platném znění, do rejstříku

UŽITNÝ VZOR

číslo

24767

na technické řešení uvedené v přiloženém popisu.

V Praze dne 2.1.2013

Za správnost:

Ing. Jan Mrva
vedoucí oddělení rejstříků

Číslo zápisu: **24767** Datum zápisu: 2.1.2013

Číslo přihlášky: **2012-26935** Datum přihlášení: 02.11.2012

Právo přednosti podle mezinárodní smlouvy
(bylo-li uplatněno a uznáno) od:

MPT: ***G 01 N 3/08*** (2006.01)
G 01 N 3/32 (2006.01)
G 01 N 27/04 (2006.01)

Název: Vysoce elastický plošný senzor určený k detekci tahové deformace

Majitel: Univerzita Tomáše Bati ve Zlíně, Zlín, CZ

Původce: Slobodian Petr doc. Ing. Ph.D, Zlín, CZ
Olejník Robert Ing., Zlín, CZ
Říha Pavel Ing. CSc., Praha, CZ

UŽITNÝ VZOR

(19) ČESKÁ REPUBLIKA

ÚŘAD PRŮMYSLOVÉHO VLASTNICTVÍ

(21) Číslo přihlášky: **2012 - 26935**
(22) Přihlášeno: **02.11.2012**
(47) Zapsáno: **02.01.2013**

(11) Číslo dokumentu:
24767
(13) Druh dokumentu: **U1**
(51) Int. Cl.:
G01N 3/08 (2006.01)
G01N 3/32 (2006.01)
G01N 27/04 (2006.01)

(73) Majitel:
Univerzita Tomáše Bati ve Zlíně, Zlín, CZ

(72) Původce:
Slobodian Petr doc. Ing. Ph.D, Zlín, CZ
Olejník Robert Ing., Zlín, CZ
Říha Pavel Ing. CSc., Praha, CZ

(74) Zástupce:
UTB ve Zlíně, Univerzitní institut, Ing. Dana Kreizlová, nám. T.G. Masaryka 5555, Zlín, 76001

(54) Název užitného vzoru:
Vysoce elastický plošný senzor určený k detekci tahové deformace

Vysoce elastický plošný senzor určený k detekci tahové deformace

Oblast techniky

Technické řešení se týká vysoce elastického plošného senzoru, určeného pro detekci tahové deformace zejména většího rozsahu, ale schopného detekovat i opakované deformační podněty včetně cyklických deformací.

Dosavadní stav techniky

Dosud se k detekci deformace a jejímu převodu do elektrických veličin používají mnohé konvenční principy. Ty se odlišují na jedné straně převážně svojí citlivostí a na straně druhé náročností a cenou. Jednoduchou metodou detekce deformace je použití kovových vodičů, které při deformaci, při které se mění jejich délka a průřez, mění i svoji vodivost. Jsou to kovové vodiče vyrobené na bázi mědi, hodnocené faktorem citlivosti okolo 2,5, nebo klasický kovový drátkový tenzometr ve formě vlnovce v elastické fólii, vykazující faktor citlivosti okolo 2 - 5.

Existují však i sofistikovanější řešení používaná pro detekci deformace, založená na bázi polovodičů využívající piezoelektrický jev a mající faktor citlivosti až 130. Použití uvedených senzorů je však omezeno relativně malými deformacemi okolo 20 %. Měření velkých deformací nad 100 % vyžaduje použití senzorů vyrobených z nových netradičních materiálů.

V současnosti se objevují nové typy senzorů pro vyšší deformace, využívající k detekci sítě volně zapletených uhlíkových nanotrubiček, kdy faktor citlivosti dosahuje hodnot 7. Tyto typy senzorů však dosud nejsou k dispozici pro měření velkých tahových deformací. Elastický kompozit, vytvořený na bázi polydimethylsiloxanu s jednostěnnými uhlíkovými nanotrubičkami, umožňuje sice měřit deformaci až 280 %, nevýhodou zde ovšem je nízký faktor citlivosti - okolo 1.

Podstata technického řešení

Uvedené nevýhody a nedostatky dosud známých typů senzorů pro měření deformace odstraňuje vysoce elastický plošný senzor určený k detekci tahové deformace podle technického řešení. Podstata technického řešení spočívá v tom, že senzor je tvořen kompozitní vrstvenou strukturou sestávající z vysoce elastického polymerního nosiče na bázi termoplastického polyuretanu o tloušťce řádově tisíců μm a na něm zakotvené senzorické vrstvy o tloušťce až desítky μm, tvořené sítí uhlíkových nanotrubiček. Přitom pórozita této sítě je 60 až 90 %, průměr nanotrubiček 7 až 30 nm, jejich délka 300 nm až 10μm a měrná vodivost 10 až 20 S/cm. Tato senzorická vrstva je pomocí přechodové nanokompozitní vrstvy zakotvena v polymerním nosiči a zapojena do elektrického obvodu vybaveného snímačem změny její vodivosti podle deformace senzorické vrstvy.

Přechodová nanokompozitní vrstva je s výhodou tvořena sítí uhlíkových nanotrubiček prosycených termoplastickým polyuretanem a má s výhodou tloušťku 2 až 4 μm.

Vysoce elastický plošný senzor podle technického řešení představuje novou generaci deformačně - elektricky citlivých senzorů-převodníků, a to na bázi materiálů z oblasti nanotechnologií, konkrétně s využitím uhlíkových nanotrubiček. Jde o detekci deformace v tahu, kdy je detekovaná deformace převedena na deformaci senzorické vrstvy, jež citlivě reaguje na tento impuls změnou své makroskopické vodivosti. Vysoce elastický plošný senzor podle technického řešení pracuje tak, že uvedená elektrická odezva přesně zaznamenává velikost a charakter deformace. Tento senzor je schopen detekovat i opakované deformační podněty, např. při cyklické deformaci, a to v mnoha cyklech ($\sim 10^4$) bez znatelných změn svých materiálových vlastností. Senzor je schopen zachycení i velmi rychlých opakovaných dějů, jako jsou například vibrace. Senzor podle technického řešení dále vyniká velmi dobrou citlivostí. Tu je možno vyjádřit pomocí faktoru citlivosti senzoru, definovaného jako změna vodivosti senzoru vztažená k relativní deformaci senzoru. Je tedy žádoucí, aby senzor vykazující vyšší citlivost dosahoval co nejvyššího poměru těchto

hodnot. Senzor podle technického řešení poskytuje faktor citlivosti okolo 30 pro deformaci 10 %. To je velmi slibná hodnota při srovnání například s klasickým tenzometrem na bázi odporového drátku s hodnotami faktoru citlivosti v rozmezí 2 až 5. Hodnoty faktoru citlivosti navrhovaného senzoru bylo dosaženo rovněž díky chemické úpravě uhlíkových nanotrubiček, kdy při relativní deformaci 15,5 % senzor vykazoval faktor citlivosti 175. Vysoce elastický plošný senzor podle technického řešení se dále vyznačuje jednoduchou a levnou přípravou, možností snadné sériové výroby a snadnou aplikací na měřené předměty s jednoduchým vyhodnocením deformační odezvy měřením vodivosti senzoru.

Princip detekce senzoru podle technického řešení se od všech dosud známých srovnatelných řešení liší tím, že se zde jedná o vysoce elastický celek - polymerní nosič s přechodovou nanokompozitní vrstvou a senzorickou vrstvou uhlíkových nanotrubiček, která je prostřednictvím přechodové nanokompozitní vrstvy velmi pevně fixována v polyuretanovém polymerním nosiči. Rozsah možných deformací, při nichž si tento vysoce elastický plošný senzor zachovává nejen integritu, ale i funkční spolehlivost, je až 400 %. Při deformaci polyuretanového polymerního nosiče dochází k přenosu deformace na přechodovou nanokompozitní vrstvu a přes ni pak na senzorickou vrstvu, kterou tvoří síť z volně zapletených uhlíkových nanotrubiček (CNT). Při deformaci dochází u senzorické vrstvy k rozpraskání volně zapletené vrstvy CNT, a tím klesá počet elektricky vodivých kontaktů a odpor roste. Při odlehčení se polyuretanový polymerní nosič vrací zpět do původního tvaru, čímž dochází v senzorické vrstvě opětovně ke vzniku vodivých cest a odpor opět klesá. Senzor může být takto cyklicky namáhán při zachování své senzorické funkčnosti. Senzor podle technického řešení snese vysoké deformace, aniž by došlo k náhlému skokovému nárůstu odporu (elektrické perkolaci), protože vzniklé mikrotrhliny jsou stále v průběhu deformace propojeny trubičkami orientovanými ve směru deformace senzoru.

Plošný senzor pro detekci tahové deformace podle technického řešení vykazuje vysoký potenciál pro detekci různých druhů uvedených deformací a pohybů. Senzor může detekovat deformaci v mnoha cyklech beze změny svých materiálových vlastností. Detekce je funkční jak v běžném čase, tak i při měření rychlých dějů. Plošný senzor pro detekci tahové deformace podle technického řešení může proti stávajícím senzorům nabídnout měření mimořádně vysokých deformací s velkou citlivostí. Další jeho předností je finanční nenáročnost, snadný přenos jeho přípravy do technologických parametrů průmyslové výroby a snadnost jeho užití a vyhodnocování detekovaného signálu.

Příklady provedení technického řešení

Příklad 1

Senzorická vrstva sestávající z uhlíkových nanotrubiček zakotvená na přechodové nanokompozitní vrstvě byla nalisována (nad teplotou tání použitého polyuretanu) na polyuretanové zkušební tělísko typu lopatka pro tahovou zkoušku. Zkušební tělísko bylo umístěno do zařízení pro měření krípové tahové deformace. Senzorická vrstva byla opatřena dvěma měděnými elektrodami a její odpor byl měřen dvoubodovou metodou. Při deformování takto vytvořeného plošného senzoru dochází k adekvátní odezvě v elektrických vlastnostech. Odezva je citlivá, vratná, opakovatelná a reprodukovatelná.

Příklad 2

Vysoce elastický plošný senzor podle příkladu 1 byl umístěn do excentru vyvozujícího cyklickou sinusovou deformaci. Vzorek byl namáhán ve frekvenčním rozmezí 0,1 až 1,0 Hz. Elektrická odezva sleduje deformační podnět a je opět sinusová. Je patrné malé fázové posunutí, které je dáno především viskoelastickými vlastnostmi polyuretanového polymerního nosiče. Vzorek byl testován až do rozsahu 10^4 cyklů v rozmezí do 20 % deformace bez známek poklesu senzorické schopnosti.

Příklad 3

Plošný senzor dle příkladu 1 byl namáhán na trhacím stroji konstantní rychlostí deformace 1 mm/s. Senzorická vrstva si zachovává svoji měřitelnou vodivost, nedojde k perkolaci ani při velmi vysokých deformacích (400 %) blížících se limitní deformaci použitého polymerního nosiče. Změny jsou navíc po odlehčení vratné, a to v rámci vzniklé elastické deformace polyuretanového polymerního nosiče.

Příklad 4

Senzor z příkladu 1 byl na jednom konci vetknut a byla vyvozena vibrace s charakterem samovolného útlumu. Detekovaný signál přesně popisuje fyzikální podstatu děje a byly zaznamenány přesně odlišené vlny vibrace (např. 8 vln v jedné sekundě).

Příklad 5

Střední část senzoru z příkladu 1 byla přilepena na elastickou bandáž na koleni dobrovolníka. Senzorická část vzorku byla při ohybu kolena namáhána vždy na ohyb, protože ta leží nad neutrální osou polyuretanového polymerního nosiče. Tímto způsobem lze určit úhel ohybu kolena nebo provádět časová měření. Senzor dobře popisuje a tvarově rozlišuje různé typy pohybu kolena jako je běh, chůze, pochod, dřep, poskoky, seskoky, atd. Testování na rotopedu ukázalo opět trvanlivost tohoto senzoru, kdy při více než 10^4 cyklech (šlápnutí) nebyly pozorovány změny vlastností materiálu senzoru.

Průmyslová využitelnost

Vysoce elastický plošný senzor pro detekci tahové deformace podle technického řešení je využitelný v mnoha technických oblastech, kde je třeba detekovat různé typy deformací či pohybů zatížených tahovou deformací (tah, ohyb, změna polohy atd.). Může být aplikován jako samostatný senzor, popřípadě se stát senzorickou částí konstrukčního „samodetekujícího se" celku. Pomocí senzoru podle technického řešení může být snímána deformace nosníků, nádob, staveb, atd., jejich vibrace a konstrukční stav. Dále je možné takto indikovat skryté nebezpečí selhání apod. K technickým aplikacím senzoru podle technického řešení lze zařadit také sledování například hladiny kapalin v nádrži, ovládání robotické ruky, popřípadě detekce pohybu a polohy součástí elektronických hraček. Slibná je i oblast možné detekce pohybu částí lidského těla nebo ovládání přístrojů invalidními osobami (rukavice se senzory pro obsluhu PC).

NÁROKY NA OCHRANU

1. Vysoce elastický plošný senzor určený k detekci tahové deformace, **vyznačující se tím**, že je tvořen kompozitní vrstvenou strukturou sestávající z vysoce elastického polymerního nosiče na bázi termoplastického polyuretanu o tloušťce řádově tisíců μm a na něm zakotvené senzorické vrstvy o tloušťce až desítky μm, tvořené sítí uhlíkových nanotrubiček, přičemž pórozita sítě je 60 až 90 %, průměr nanotrubiček 7 až 30 nm, jejich délka 300 nm až 10μm a měrná vodivost 10 až 20 S/cm, a tato senzorická vrstva je pomocí přechodové nanokompozitní vrstvy zakotvena v polymerním nosiči a zapojena do elektrického obvodu vybaveného snímačem změny její vodivosti s deformací senzorické vrstvy.

2. Vysoce elastický plošný senzor podle nároku 1, **vyznačující se tím**, že přechodová nanokompozitní vrstva je tvořena sítí uhlíkových nanotrubiček prosycených termoplastickým polyuretanem a má tloušťku 2 až 4 μm.

Konec dokumentu

Evidenční formulář výsledku výzkumu a vývoje

nepodléhající zápisnému řízení u ÚPV ČR

Název výsledku:

Mikropásková anténa na bázi sítě z uhlíkových nanotrubic jako aktivní vrstva nanesená na skleněném substrátu

Microstrip antenna on the base of carbon nanotubes network as the active layer applied on the glass substrate

Kategorie výsledku:

☐ poloprovoz	☐ certifikovaná metodika
☐ ověřená technologie	☐ software
☐ prototyp	☐ jiné výsledky
☒ funkční vzorek	

Autor výsledku:

Jméno, příjmení a titul:	Matyáš Jiří, Ing.
Adresa bydliště:	Petrov 14, 69 65 Petrov u Hodonína
Telefon:	+420 57 603 2830
Email:	matyas@fai.utb.cz
Fakulta (org. složka UTB):	Fakulta aplikované informatiky
Ústav (katedra):	Ústav počítačových a komunikačních systémů
Datum narození:	30.11.1985
Osobní číslo:	A10516
Podíl (%) na řešení:	40%

1. Spoluautor: [1)]

Jméno, příjmení a titul:	Robert Olejnik, Ing.
Adresa bydliště:	Vršava I 1494, 76001 Zlín
Fakulta (org. složka UTB):	FT/UNI
Ústav (katedra):	Centrum polymerních materiálů/CPS
Datum narození:	20.04.1983
Osobní číslo:	01001055
Podíl (%) na řešení:	40%

2. Spoluautor:

Jméno, příjmení a titul:	Petr Slobodian, doc., Ing., Ph.D.
Adresa bydliště:	Podvesná XIV/1455, 760 01, Zlín
Fakulta (org. složka UTB):	FT/UNI
Ústav (katedra):	Centrum polymerních materiálů/CPS
Datum narození:	1.3.1971
Osobní číslo:	01096876
Podíl (%) na řešení:	10%

3. Spoluautor:

Jméno, příjmení a titul:	Vlček Karel, Ing.
Adresa bydliště:	Pod Vodojemem 2717, 76001 Zlín
Fakulta (org. složka UTB):	Fakulta aplikované informatiky
Ústav (katedra):	Ústav počítačových a komunikačních systémů
Datum narození:	23.03.1948
Osobní číslo:	
Podíl (%) na řešení:	10%

Je uzavřena smlouva o využití výsledku V a V externím subjektem? ~~**ANO**~~**/NE** [3)]
Licenční či jinou analogickou smlouvu je třeba doložit.

Stručný popis výsledku a jeho umístění v rámci UTB:
Mikropásková anténa na bázi sítě z uhlíkových nanotrubic jako aktivní vrstva nanesená na skleněném substrátu. Funkční vzorek byl vytvořen na Fakultě technologické a na Fakultě aplikované informatiky. Vzorek je umístěn na UTB na Fakultě aplikované informatiky na ÚPKS (Ústav počítačových a komunikačních systémů).

Microstrip Antenna based on network of carbon nanotubes as the active layer applied to the glass substrate. Functional sample was created by the Faculty of Technology and the Faculty of Applied Informatics. The sample is placed on the TBU Faculty of Applied Science at ÚPKS (Department of Computer and Communication Systems).

Technické parametry výsledku (technické a jiné parametry charakterizující výstup):
Byla vytvořena anténa na bázi sítě z uhlíkových nanotrubic, jako aktivní vrstvy zakotvené v polyuretanu a umístěné na substrát v tomto případě na skleněný podklad. V prvním kroku byla vytvořena vodná disperze uhlíkových nanotrubic, která byla filtrována přes membránu z polyuretanových nanovláken. Membrána byla poté spojena lisování s nosnou vrstvou tvořenou polyuretanem. Tímto způsobem byla vytvořena elektricky vodivá vrstva, která splňuje předpoklady pro použití ve sdělovací technice. Její složení je na Obr. 1. Funkční vzorek má odpor 180 Ω.

Anténa může být umístěna na různých podkladech, které splňují předpoklady vhodného izolačního substrátu (plasty, sklo, plexisklo).

Ekonomické parametry výsledku (např. roční zvýšení objemu výroby, zisku, exportu, výhoda oproti stávajícímu či srovnatelnému řešení apod.):
Výhoda inovativního řešení této mikropáskové antény spočívá v možnosti efektivní aplikace aktivní vrstvy na povrchy (substráty), mezi které patří zejména sklo a polymery. Tvarová rozmanitost umožňující vyrobit požadovaný tvar mikropáskové antény spolu se schopností miniaturizace a možnosti přizpůsobení na konkrétní výrobek, zvyšuje konkurenceschopnost této antény. Ekonomickou výhodu je možné spatřit v možnosti úspor na materiálu a velikosti antény, z něhož se vyrábějí dosavadní provedení mikropáskových antén, což umožňuje lepší implementaci do plastových krytů přenosných zařízení využívajících anténu (pouze některá frekvenční pásma) např. u RFID tagů.

Oblast průmyslové využitelnosti výsledku:
Sdělovací technika

Projekt aplikovaného výzkumu, experimentálního vývoje a inovací či jiná aktivita aplikovaného VaVaI, v rámci něhož výsledek vznikl:

The work was supported by the Operational Program of Research and Development for Innovations co-funded by the European Regional Development Fund (ERDF), the National budget of Czech Republic within the framework of the Centre of Polymer Systems project (Reg. No.: CZ.1.05/2.1.00/03.0111).

Využití neobvyklých materiálů pro konstrukci antén - IGA/FAI/2012/031

Fotografie, výkres či jiné podpůrné dokumenty:
Podrobný popis a obrazová dokumentace
Byla vytvořena mikropásková anténa na bázi sítě z uhlíkových nanotrubic jako aktivní vrstvy zakotvené v polyuretanu. V prvním kroku byla vytvořena vodná disperze uhlíkových nanotrubic, která byla filtrována přes membránu z polyuretanových nanovláken. Membrána byla poté spojena lisování s nosnou vrstvou tvořenou polyuretanem. Tímto způsobem byla vytvořena elektricky vodivá vrstva citlivá na příjem a vysílání signálu. Na obr. 1 můžeme vidět vrstvu tvořící anténu, skládající se z následujících části:

Aktivní vrstva z uhlíkových nanotrubic

Rozhraní

Polyuretanová nosná vrstva

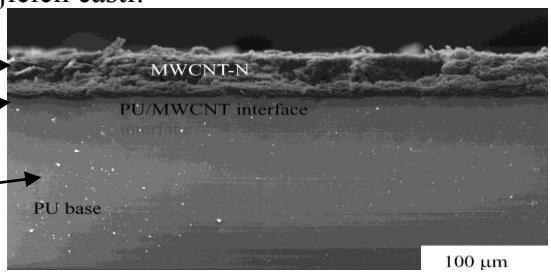

Obr.1 SEM analýza složení vrstvy antény .

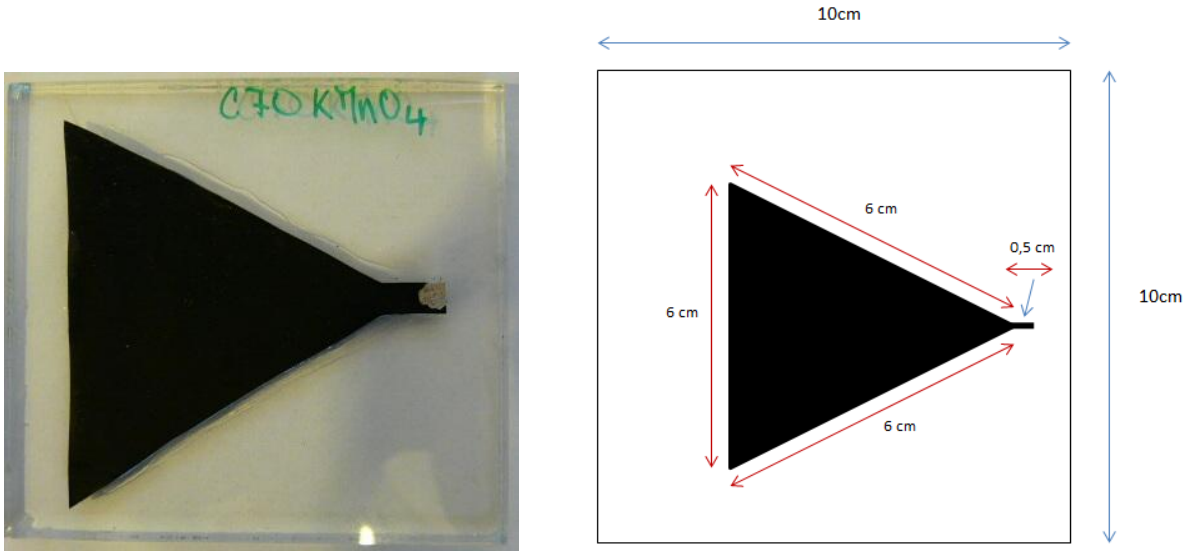

a) b)

Obr.2 a) foto mikropáskové antény na bázi sítě z uhlíkových nanotrubic jako aktivní vrstva nanesená na skleněném substrátu b) technický nákres antény (černé části představují anténu)

Přímý nadřízený (jméno, příjmení, titul): prof. Ing. Vladimír Vašek, CSc.

……..
Podpis přímého nadřízeného

……..
Podpis autora

Ve Zlíně dne……

……..
Podpis 1. spoluautora [4)]

Ve Zlíně dne……

[1)] doplňte jména všech spoluautorů, zkopírujte příslušnou část formuláře
[2)] doplňte názvy všech spolupracujících externích subjektů, zkopírujte příslušnou část formuláře
[3)] nehodící se škrtněte
[4)] v případě potřeby zkopírujte příslušnou část formuláře a doplňte jména všech spoluautorů

MULT-WALL CARBON NANOTUBE NETWORKS PREPARED FROM PURE MWCNT AND THEIR OXIDISED FORMS EFFECT OF COMPRESSIVE STRAIN ON ELECTRIC RESISTENCE

Robert OLEJNIK [a*] , Petr SLOBODIAN [a], Pavel RIHA [b] , Dusan KIMMER [c] , Petr SAHA [a]

[a] *Tomas Bata University in Zlin, Faculty of Technology, Polymer centre, Czech Republic*
[b] *Institute of Hydrodynamics, Academy of Sciences, Prague, Czech Republic*
[c] *SPUR a.s., T. Bati 299, 764 22 Zlín, Czech Republic*
**e-mail: rolejnik@volny.cz*

Abstract

Multi-wall carbon nanotube networks were prepared by process of filtration of CNT aqueous dispersions. CNT dispersions were prepared with help of surfactant system (Sodium dodecyl sulfate with amylalcohol) by ultrasonication. Three types of MWCNT tubes were used. The first were pure CNT material delivered by supplier. The other were chemically treated in aim to prepare CNT oxidised forms (1. acid solution of $KMnO_4$, 2. mixture of acids H_2SO_4 + HNO_3). It was found that chemical modification significantly changes properties of prepared carbon nanotube networks ("Buckypaper"). There were observed differences in porous structure between all of the forms analysed by SEM microscopy. Further, apparent density of prepared "Buckypapers" changes in respect of used CNT material leading to different porosity of Buckypapers. Electrical resistance is also affected by process of MWCNT oxidation together with its temperature dependence. Effect of compressive strain on electric resistance of multi-wall carbon nanotube networks was further tested. It was found that resistance is sensitive to compressive strain both in the course of strain growth and when loading/unloading cycles are imposed.

Keywords: Carbon nanotube network; Compression; Electrical resistence; Stress sensor;

1 INTRODUCTION

(CNT) network structures show a great potential for developing high-performance polymer composites and enhanced sensors. CNT networks can proportionally transfer their unique properties into reinforced composite materials and films for sensors and bring substantial improvements in structural strength, electrical and thermal conductivity, electromagnetic interference shielding and other properties [1,2].

The first carbon nanotube network was fabricated by Walters *et al.,* who dispersed nanotubes into a liquid suspension and then filtered through fine filtration mesh [3].

The fabrication of CNT network based polymer composite described above is rather laborious. A novel idea is to circumvent the laborious technology and to suggest a way leading to continuous and technologically easier manufacturing of CNT network based polymer composites. The novel process consists of using the non-woven polystyrene (PS) filter on which CNT collect and form a network during CNT suspension filtration, as integrating and supporting element. The CNT slightly infiltrate into the filter and adhere to it, finally forming CNT layer. The obtained CNT/PS composite is compression moulded above PS melting temperature when PS filter transforms into flexible PS polymer film.

2 MULTIWALL CARBON NANOTUBE NETWORKS AND COMPOSITES

The purified MWNT of acetylene type (Sun Nanotech Co. Ltd., China) are used for the preparation of aqueous paste: 1.6 g of MWNT and ~ 50 ml of deionized water are mixed with the help of a mortar and pestle. The paste is diluted in deionized water with sodium dodecyl sulfate (SDS) and 1-pentanol. Then NaOH solved in water is added to adjust pH to the value of 10 [4]. The final nanotube concentration in the dispersion is 0.3 wt.%, concentration of SDS and 1-pentanol 0.1M and 0.14M, respectively [5]. The dispersion is sonicated in Dr. Hielscher GmbH apparatus (ultrasonic horn S7, amplitude 88 μm, power density 300 W/cm^2, frequency 24 kHz) for 2 hours.

3 EXPERIMENTAL TECHNIQUES

The structure of both principal MWNT networks prepared from pristine tubes and their oxidized form are investigated with a scanning electron microscope (SEM)

Pure MWNT are also analyzed via transmission electron microscopy (TEM) using microscope JEOL JEM 2010 at the accelerating voltage of 160 kV. The sample for TEM is fabricated on 300 mesh copper grid with a carbon film (SPI, USA) from MWNT dispersion in acetone prepared by ultrasonication, which is deposited on the grid and dried.

The MWNT networks and composites are tested for deformation using a simple set-up.

4 RESULT

4.1 Free-standing entangled MWCNT networks

To examine the length, thickness, waviness, multi-wall arrangement and possible structural defects of MWNT, TEM analysis is used. The diameter of individual nanotubes is determined to be between 10 and 60 nm, their length from tenth of micron up to 3 μm. The used $KMnO_4$ oxidation procedure of MWCNT crude material leads to significant tubes degradation.

The both types of MWNT aqueous dispersions (using MWCNT pristine tubes and their oxidized forms) are filtered thought PU non-woven membrane to form intertwined networks. As follows from Fig. 1 (left), Prepared MWNT layer is then peeled of the filter achieving self-standing MWNT entangled network. The SEM micrograph of PS filter prepared by technology of electrospinning is shown in Fig. 1 (right). The prepared MWCNT layer is not peeled of the filter and remains as a part of PS/MWNT composite.

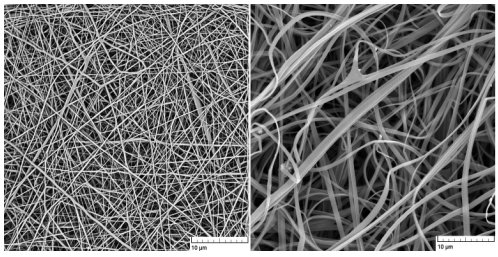

Fig. 1 SEM micrograph of PU (left) and PS non-woven filtering membrane at the same magnification (displayed scaler 10 □m).

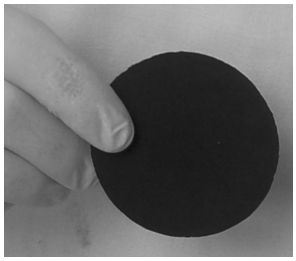

Fig. 2 Free-standing randomly entangled MWCNT network (disk diameter 75 mm, thickness 0.15 mm).

The upper surfaces of both principal MWNT networks were studied, and their SEM micrographs can be seen in Fig. 3: a) made of pure MWCNT (MWCNT-N), b) oxidized form (MWCNT-$N_{(KMnO4)}$). The pictures show some differences between both structures; the surface of the buckypaper made of oxidized tubes seems to be smoother, with more densely packed tubes and a smaller diameter of inter-tube pores. Functionalized nanotubes are better individualized from the bundles and aggregates because they are shorter and also because functional groups tend to push away individual nanotubes from each other [6].

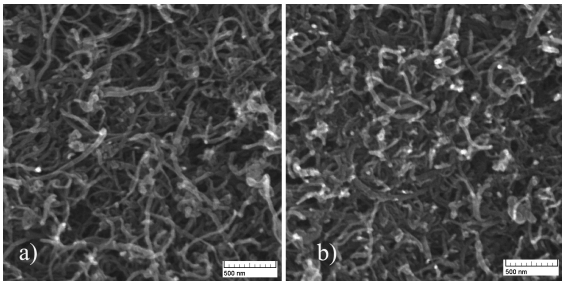

Fig. 3 SEM image of the surface of entangled MWCNT network of buckypaper made of a) pure, and b) oxidized MWCNT.

4.2. Effect of compressive strain/stress on electric resistance of multi-wall carbon nanotube networks

The resistance/compressive strain dependence is shown in Fig. 4 (compressive strain as well as compression is defined as positive deformation and loading, respectively). The measurement show that compression causes a decrease in MWNT network resistance, as clearly visible in the figure. The plotted resistance values, R, are normalized with respect to the initial resistance, R_i, recorded at the start of the test at no load. For each network thickness, i.e. 0.23 and 0.38 mm, four samples are investigated. Their resistance is measured after each compression step to the preset deformation and for the subsequent unloaded state. The resistance in the unloaded states is reduced similarly to the resistance of compressed samples.

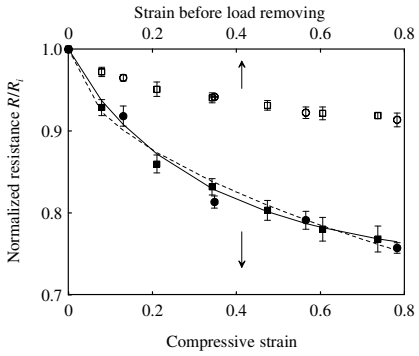

Fig. 4 Normalized resistance vs. strain dependence of entangled carbon nanotube network. The network thickness is 0.23 mm (squares) and 0.38 mm (circles). The full and open symbols denote the network with and without load, respectively.

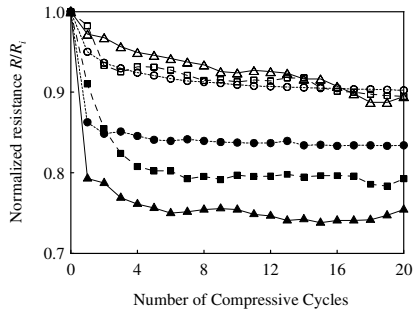

Fig. 5 Normalized resistance of the entangled carbon nanotube network vs. the number of compression/relaxation cycles; network thickness 0.38 mm. The applied compressive strain: 0.21 (circles), 0.47 (squares) and 0.74 (triangles). Full and open symbols denote the network with and without load, respectively.

The observed effect of repeated compression on the network resistance is presented in Fig. 5. As can be seen, with increasing number of deformation cycles the resistance of MWNT network first declines more steeply but after several cycles the decrease is very slight, and eventually no resistance change is observed. It indicates that the network rearrangement becomes steady what is favorable for MWNT network use as the sensing element of compressive stress sensor when the network is suitably deformed in advance.

Electrical properties of manufactured structures are followed also in the course of twelve compression and relaxation cycles with cyclic accumulation of residual strain (compression as well as compressive strain is defined as positive loading and deformation, respectively). The measured data are shown in Fig. 9 as a plot of conductivity values σ vs. applied compressive stress *τ*. Compression causes a conductivity change during both the up-stress and down-stress periods due to specific deformation of porous structure. According to [21], the local contact forces increase during compression, allowing a better contact of nanotubes, which in turn leads to the decrease of contact resistance between crossing nanotubes; in release the dependence is just the opposite. At the same time, the possible effect of the distance between contacts on CNT tangle resistance is considered in [7]. The distance between contacts may decrease during compression owing to evoked relative motion of nanotubes, which corresponds to a lower intrinsic resistance of nanotube segments between contacts. Last but not least, compression may also bend the nanotubes sideways, which results in more contacts between nanotubes [8]. Since the contact points may act as parallel resistors, their increasing number causes an enhancement of MWNT network conductivity.

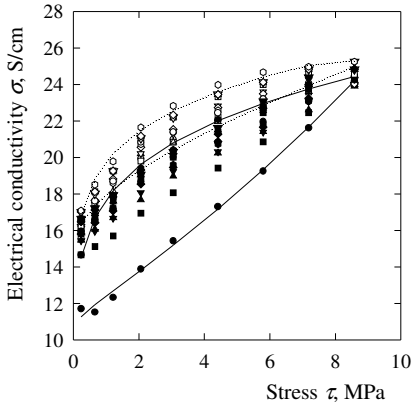

Fig. 6 Electrical conductivity-compressive stress loops for MWCNT network subjected to 12 successive compression/expansion cycles (network thickness 0.42 mm). The solid lines (first loading and unloading cycle) and dotted lines (twelfth cycle).

Mechanical properties of manufactured structures are also followed in the course of twelve compression and relaxation cycles with cyclic accumulation of residual strain (compression as well as compressive strain is defined as positive loading and deformation, respectively). The results in the form of compressive stress vs. strain dependence are presented in Fig. 7.

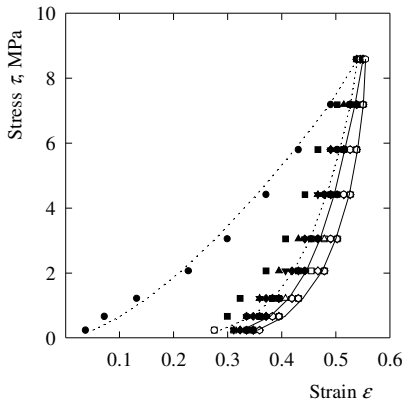

Fig. 7 Stress-strain loops in cyclic compression test for MWCNT network subjected to 12 compression/expansion cycles (the network thickness 0.42 mm). The dotted lines (first loading and unloading cycle) and solid lines (twelfth cycle) represent the power law fitting

The oxidation of MWNT modifies electrical conductivity of MWNT networks under compression. It follows from Fig. 8 where the stress dependent conductivity of pristine and oxidized MWNT networks is plotted for 4 compression and relaxation cycles. Compression causes a conductivity change during both the up-stress and down-stress periods due to specific deformation of porous structure. Nevertheless, the conductivity of nanotube network prepared from chemically functionalized MWNT in $KMnO_4/H_2SO_4$ oxidizing system is lower and less deformation affected than pristine MWNT network. It shows a stabilizing character of oxidation process.

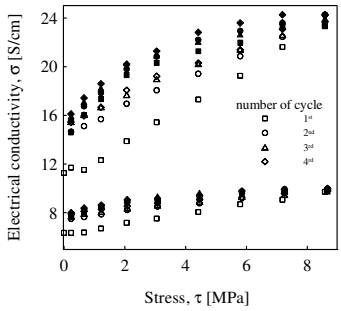

Fig. 8 Electrical conductivity-compressive stress loops for MWCNT and MWCNT ($KMnO_4$) network subjected to four successive compression/expansion cycles (the network thicknesses were 0.41 mm and 0.40 mm).

REFERENCES

[1] E.T. Thostenson, C.Y. Li, T.W. Chou, Nanocomposites in context, Compos. Sci. Technol. 65 (2005) 491-516.

[2] Q. Cao, J.A. Rogers, Ultrathin films of single-walled carbon nanotubes for electronics and sensors: A review of fundamental and applied aspects, Adv. Mater. 21 (2009) 29-53.

[3] D.A. Walters, M.J. Casavant, X.C. Quin, C.B. Huffman, P.J. Boul, L.M. Ericson, E.H. Haroz, M.J. O'Connel, K. Smith, D.T. Colbert, R.E. Smalley, In-plane-aligned membranes of carbon nanotubes, Chem. Phys. Lett. 338 (2001) 14-20.

[4] Rasheed A, Howe JY, Dadmun MD, Britt PF. The efficiency of the oxidation of carbon nanofibers with various oxidizing agents, Carbon 2007;45(5):1072-1080.

[5] Ham HT, Choi YS, Chung IJ. An explanation of dispersion states of single-walled carbon nanotubes in solvents and aqueous surfactant solutions using solubility parameters, Colloid Interf Sci 2005;286(1):216-223.

[6] Wang XB, Li SQ, Xu Y, Wan L, You HJ, Li Q et al. Radical functionalization of single-walled carbon nanotubes with azo(bisisobutyronitrile). Appl Surf Sci 2007;253(18): 7435-7437.

[7] A. Allaoui, S.V. Hoa, P. Evesque, J. Bai : Scripta Mater. 61, 628 (2009).

[8] O. Yaglioglu, A.J. Hart, R. Martens, A.H. Slocum, Method of characterizing electrical contact properties of carbon nanotube coated surfaces, Rev. Sci. Instrum. **77** (2006) 095105/1-3.

Increased Sensitivity of Multiwalled Carbon Nanotube Network by PMMA Functionalization to Vapors with Affine Polarity

R. Olejnik,[1,2] P. Slobodian,[1,2] P. Riha,[3] M. Machovsky[1]

[1]*Polymer Centre, Faculty of Technology, T. Bata University in Zlin, 760 01 Zlin, Czech Republic*
[2]*Centre of Polymer Systems, University Institute, T. Bata University, Nad Ovcirnou 3685, 760 01 Zlin, Czech Republic*
[3]*Institute of Hydrodynamics, Academy of Sciences, 166 12 Prague, Czech Republic*

Received 15 March 2011; accepted 10 October 2011
DOI 10.1002/app.36366
Published online in Wiley Online Library (wileyonlinelibrary.com).

ABSTRACT: Multiwalled carbon nanotube network (MWCNT-N)/poly(methyl methacrylate) (PMMA) composite is prepared by solution radical polymerization. The entangled multiwall carbon nanotube network (MWCNT-N) is obtained by vacuum filtration and functionalized by allyl isocyanate to form polymerizable vinyl groups on a nanotube surface. The solution polymerization binds PMMA covalently to these groups and yields MWCNT-N/PMMA composite manifesting electrical conduction and selective chemical vapor sensing. The latter property is evaluated in terms of affinity of organic solvent vapor and PMMA polarities. It is found that the affinity of acetone polarity with polarity of PMMA improves significantly the sensitivity of the composite to this solvent while the sensitivity to methanol is the same and to *iso*-pentane even decreased in comparison with the corresponding property of MWCNT-N. The composite selective response is favorable for a possible composite use as a sensing element and/or vapor switch. © 2012 Wiley Periodicals, Inc. J Appl Polym Sci 000: 000–000, 2012

Key words: poly(methyl methacrylate) nanocomposites; carbon nanotube networks; electrical resistance; vapor sensing; VOC

INTRODUCTION

Carbon nanotube (CNT)/polymer composites are a type of highly promising materials, where specific properties of CNT can be effectively availed serving for a new multifunctional material with enhanced mechanical, thermal, or electrical properties. Recently, there are efforts to apply CNT in polymer composites not as particular filler but as an entangled network. The novel composites may be used not only as a conductive material[1,2] but also as flame retardant,[3,4] electrode,[5] actuator,[6] strain[7] or pressure sensor,[8,9] organic vapor sensor,[9] etc.

Both principal types of CNT—the multiwalled and single-walled nanotubes—show remarkable sensitivity to the change of chemical composition of the surrounding environment. Gas and vapor adsorption as well as desorption usually proceeds at high rates and amounts.[10] This property is favorable for their use in the form of membranes,[11] adsorbents,[12] or gas sensors.[13,14]

The molecules are adsorbed on CNT surface by van der Waals attracting forces. CNT macroscopic forms like aggregates contain four different adsorption sites: internal, interstitial channels, external grooves, and surfaces.[12] The adsorbed molecules influence the electrical properties of isolated CNT and also the resistance of inter-tube contacts.[15,16] The electrical resistance of CNT aggregates or network structures is predominantly determined by contact resistance of crossing tubes rather than by resistance of CNT segments. The tubes are usually much shorter than sensor dimension and inter-tube contacts act as parallel resistors between highly conductive CNT segments. The significant effect which has influence on the macroscopic CNT electrical resistance is a vapor adsorption at the contacts between nanotubes forming non-conductive layers between them.[13] Thus the resistance measurement is a simple and convenient method to register CNT response to vapor action.

Carbon nanotube/PMMA composites can be used as resistive gas sensors for detection of volatile organics compounds. Several principles of sensing mechanisms can be employed as the change of intrinsic resistance of individual tubes fixed in PMMA matrixes by exposure to reducing methanol vapors[17] or in the form of thin polymeric film with percolating CNT network.[18,19] Also a pure network of CNT can be used. In this case, the conductive

Correspondence to: P. Slobodian (slobodian@ft.utb.cz).

PMMA/CNT composite is prepared by dispersion of spray layer by layer of PMMA microbeads decorated by CNT.[20] Here analyzed molecules lead to easy disconnection of conducting path created by CNT network bridging PMMA microbeads.

The aim of this paper is to prepare a pure MWCNT network and MWCNT-N/PMMA composite and test their vapor sensing ability when exposed to solvents of different polarities and vapor pressure. A selection of solvents covering a broad range of polarities thus enables to reveal MWCNT-N and the composite properties which are suitable for its possible application as a sensing element and/or vapor switch.

EXPERIMENTAL

Materials and procedures

The purified MWCNT of acetylene type were supplied by Sun Nanotech Co., China (diameter 10–30 nm, length 1–10 μm, purity >90% and volume resistance 0.12 Ω cm according to supplier). The complete information about the used pristine MWCNT can be found in our paper,[21] where the results of TEM analysis are presented, so that the diameter of individual nanotubes was determined within the range of 10–60 nm (100 measurements), the average diameter and standard deviation 15 ± 6 nm, and the length from tenths of micron up to 3 μm. The tube wall consists of about 15–35 rolled layers of graphene, with the interlayer distance of ca. 0.35 nm.

MWCNT aqueous paste was prepared using a mortar and pestle (1.6 g of MWCNT and ~ 50 ml of deionized water), then diluted by deionized water and SDS (sodium dodecyl sulfate) and 1-pentanol were added, pH was adjusted to the value of 10 using aqueous solution of NaOH.[22] The final nanotubes concentration in the suspension was 0.3 wt %, concentrations of SDS and 1-pentanol were 0.1 *M* and 0.14 *M*, respectively.[23] The dispersion was homogenized using Dr. Hielscher GmbH apparatus (ultrasonic horn S7, amplitude 88 μm, power density 300 W/cm^2, frequency 24 kHz) for 2 h at the temperature of ca. 50°C. MWCNT networks were prepared by dispersion vacuum filtration through nonwoven polyurethane porous membrane (SPUR a.s, Czech Republic). The membrane was made by electrospinning from PU dimethyl formamide (DMF) solution. For more details of PU chemical composition and particular process characteristics see Refs. 8 and 24. The formed disk-shaped MWCNT network was washed several times by deionized water and methanol in situ, then removed and dried between filter papers at room temperature.

MWCNT-N/PMMA composite was prepared by solution radical polymerization. MWCNT-N was initially functionalized by allyl isocyanate (3 wt % of DMF anhydrous allyl isocyanate solution) at 70°C for 18 h to synthesize free polymerizable vinyl groups on CNT surface. The functionalized network was then put to polymerization glass reactor containing solution of methyl methacrylate (MMA) in methylethyl ketone (MEK) (40 wt %) with a solved azobisisobutyronitrile (AIBN) as radical initiator (1 wt % calculated on total monomer content). The networks made from functionalized and pristine nanotubes were polymerized at 70°C for 20 h. The networks were repeatedly immersed into MEK after polymerization for 30 min to dissolve un-grafted molecules (concentration of MWCNT-N in MEK was around 0.1 wt %) and dried at 40°C for 2 days. Pure PMMA was prepared under the same condition of polymerization as composites, that is, MMA in MEK (40 wt %) polymerized at 70°C for 20 h.

Measurement and characterization

The structure of networks was investigated by a scanning electron microscope (SEM) made by Vega LMU (Tescan s.r.o., Czech Republic). The network was deposited on the carbon targets and covered with a thin Au/Pd layer. For the observations, the regime of secondary electrons was chosen.

Pure MWCNT were also analyzed via transmission electron microscopy (TEM) using microscope JEOL JEM 2010 at the accelerating voltage of 160 kV. The sample for TEM was prepared on 300 mesh copper grid with a carbon film (SPI) from MWCNT dispersion in acetone which was prepared by ultrasonication, deposited on the grid and dried.

Thermogravimetric analysis (TGA) of the samples was carried out using thermogravimeter Setaram Setsyt Evolution 1200. The samples were examined under inert atmosphere of helium (5.5 purity, SIAD TP); the gas flow was 30 cm^3/min at the pressure of 101.325 kPa (i.e., 30 sccm) for all experiments. A platinum crucible was used for the sample, the weight of which was about 4 mg. The temperature was continually increased from the ambient temperature up to 1200°C at the rate of 20°C/min. The calorimetric analysis of MWCNT-N/PMMA composite was performed using differential scanning calorimeter (Perkin-Elmer). The reason was to check thermal properties of synthesized PMMA on CNT surface. To maximize the response from the polymer, the composite was annealed at temperature below PMMA glass transition temperature T_g and again gradually heated.[25] The exact procedure was following. The composite was annealed at 220°C for 5 min, cooled to 100°C at the cooling rate of 10°C/min, isothermal relaxation at 100°C for 1000 min was performed, cooled to 50°C at the cooling rate of 10°C/min and for 1 min annealed at 50°C. The proper

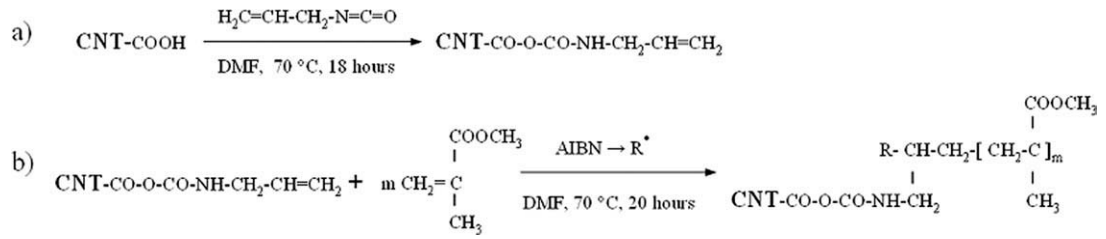

Figure 1 Synthetic route used to prepare MWCNT-N/PMMA composite. a) Reaction of carboxylic group of CNT with binder (allyl isocyanate); b) radical polymerization-incorporation of free vinyl group bonded to the surface of CNT into PMMA growing chain. R denotes radical created from initiator of polymerization AIBN—azobisisobutyronitrile (isobutyronitrile-free radical).

measurement was done in the course of increasing temperature up to 220°C at the heating rate 10°C/min. The similar measurement to illustrate the physical aging phenomenon in pure PMMA was performed when PMMA specimen was annealed at 90°C for 60 and 600 h before DSC up scan.

The electrical resistance of network stripes cut out from the manufactured MWCNT-N and MWCNT-N/PMMA disks (length 15 mm, width 5 mm, thickness ca. 0.3 mm) was measured along the specimen length by the two-point technique using multimeter Sefram 7338. The stripe was placed on a planar holder with Cu electrodes fixed on both sides of the specimen. Time-dependent electrical resistance measurements were performed during adsorption and desorption cycles. In the former case, the holder with the specimen was quickly transferred into an airtight conical flask full of vapors of the respective solvent (*iso*-pentane, acetone, and methanol), a layer of which was at the bottom. The measurements were conducted in saturated vapors at atmospheric pressure, temperature 25°C and relative humidity 60%.[26,27] After 6 min of measurement, the holder was promptly removed from the flask and for the next 6 min the sample was measured in the mode of desorption. This was repeated five times in consecutive cycles.

RESULTS

Structure and properties

A principle of synthetic route used to prepare MWCNT/PMMA nanocomposite is presented in Figure 1. There are two steps of MWCNT functionalization when natural groups presented on surface of CNT (created by CNT postproduction air oxidation) like carboxylic groups (presented in the scheme) but also hydroxyls react with a binder (allyl isocyanate) and create a covalent bond with CNT. Thereafter, a free vinyl group of functionalized CNT is incorporated into growing PMMA chain in the course of radical polymerization of MMA monomer in solution. R in Figure 1 represents the isobutyronitrile-free radical created by thermal decomposition of used radical initiator (AIBN—azobisisobutyronitrile).

The prepared free-standing MWCNT-N of disk shape is shown in Figure 2a. The disk was uniform, smooth, and crack-free, with significant structural integrity allowing easy manipulation. The typical thickness was in the range of 0.15–0.65 mm according to the volume of aqueous MWCNT dispersion used in filtration. The second part of Figure 2 shows SEM micrograph of MWCNT-N surface (Buckypaper) made of entangled tubes. The network porosity $\phi = 0.67$ was calculated through the relation $\phi = 1 - \rho_{net}/\rho_{MWCNT}$, where $\rho_{net} = 0.56 \pm 0.03$ g/cm^3 denotes the measured apparent density of the nanotube network and $\rho_{MWCNT} = 1.7$ g/cm^3 denotes density of nanotubes. The density of nanotube network, ρ_{net}, was calculated from the data obtained by weighting and measuring the network strips. The density of nanotubes was determined by means of the rule of mixing from the measured densities of PMMA/CNT composites (0, 0.5, 1.0 wt % of CNT) prepared by precipitation of their methyl-ethyl ketone solutions pouring into water.[28] Both principal materials are electrical conductive with measured electrical resistivity of MWCNT-N 0.078 ± 0.003 Ω cm and 0.094 ± 0.008 Ω cm for MWCNT-N/PMMA composite.

MWCNT-N was functionalized by allyl isocyanate to synthesize free polymerizable vinyl groups on CNT surface and bind PMMA to these groups. The

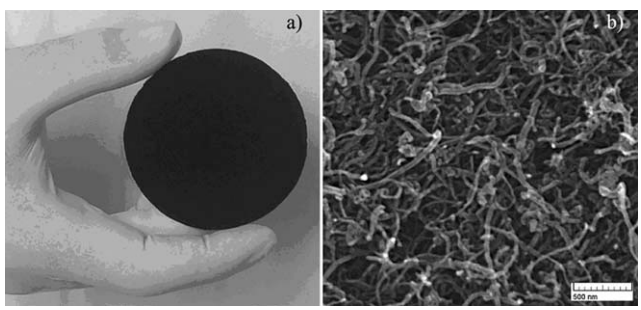

Figure 2 Free-standing randomly entangled MWCNT network (disk diameter 75 mm, thickness 0.15 mm) (a), and SEM image of the surface of entangled MWCNT-N network made of pure MWCNT (b).

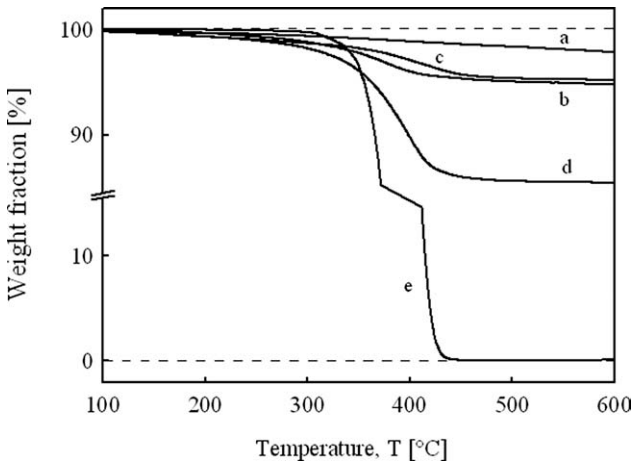

Figure 3 Thermogravimetric analysis of pristine MWCNT (a), allyl isocyanate functionalized MWCNT-N (b), MWCNT-N/PMMA network nanocomposite prepared by only solution polymerization (c), MWCNT-N/PMMA network prepared by solution radical polymerization of allyl isocyanate functionalized MWCNT-N (d), and PMMA (e).

reason was to change MWCNT-N affinity to molecules of organic solvent vapors. The quantity of organic molecules bound to the network was determined by means of thermogravimetric (TG) analysis. The results are presented in Figure 3 where MWCNT-N made of pristine nanotubes shows hardly any degradation in the range of temperatures used (up to 700°C); only very small mass loss of ca. 3 wt % was observed at the highest temperature. This is probably caused by decomposition of amorphous carbon contained in the original material together with functional groups like O—C=O or C—O, also included in crude material. On the other hand, the main chain of PMMA starts to decay at the temperature of about 300°C and is totally decomposed at some 450°C (curve e). The decomposition for PMMA-grafted composite is between 260 and 530°C with maximum at 400°C (curve c) and for allyl functionalized MWCNT-N between 320 and 550°C (curve b). The amount of bonded organic molecules to MWCNT-N was determined as the difference in residual weights of MWCNT-N and composite. The calculated value was about 3 wt % for both allyl isocyanate functionalized MWCNT-N and MWCNT-N/PMMA composite prepared by solution polymerization and 13 wt % for MWCNT-N/PMMA network nanocomposite prepared by solution polymerization of allyl isocyanate functionalized MWCNT-N.

The organic molecules in case of the allyl functionalized composite originate from covalently bonded allyl isocyanate molecules by reaction of isocyanate group with functional groups presented on the surface of CNT. In the case of grafted composite, the CNT surface is functionalized by the radicals originated during polymerization process. The free radicals created either from the initiator or as a growing polymer macro-radicals are able to react with CNT structure by opening the π-bonds in carbon nanotubes and creating a covalent bond between CNT and the radicals (radical addition).[29,30] In the case of MWCNT-N/PMMA network composite prepared by solution polymerization of allyl isocyanate functionalized MWCNT-N, the loss value represents the molecules covalently bonded to CNT surface by radical addition and/or incorporation of free allyl groups attached to CNT surface. Also some portion of isobutyronitrile groups originated from radical initiator AIBN should be expected to be covalently bonded to CNT surface again by process of radical addition.[29] The detected value around 13 wt % is lower in comparison with 45 wt % of PS,[31] or 47 wt % of PMMA[32] for the same technique using isocyanate-based binding elements followed by radical polymerization. The cause is probably less functional groups on CNT surface like acid groups (—COOH) and hydroxyl groups (—OH) capable of reaction with isocyanate groups. Even though the pristine CNT have some functional groups appearing immediately after the CNT production, another groups originate at the proper CNT oxidation when they are exposed to air environment.[33] In this work, pure and non-treated tubes were used contrary to oxidized CNT (by mixture of sulfuric and nitric acids) in[31,32] what means a limited number of sites for potential isocyanate-based linking.

The TEM images of MWCNT structure from MWCNT-N/PMMA composite are presented in Figure 4. The TEM micrographs clearly confirm the presence of PMMA adhering to the MWCNT surface in the form of so-called polymeric "brushes."[31] The polymeric material is found to create discontinuous coverage, part a, or a continuous layer, part b. The approximate thickness is around 1.6 nm in part a and 3–4 nm in part b, which is similar to published values of 4–5 nm.[31,34]

Differential scanning calorimetry analysis of MWCNT-N/PMMA indicates the presence of PMMA bonded to CNT when glass transition region of PMMA defined by a glass transition temperature is reached (Fig. 5). There was measured a broad transition peak during composite heating which overlaps the instrument baseline between ~110 and 155°C (T_g, onset ~ 120°C) after 1000 h of relaxation at 100°C. The measured enthalpy of transition from glass to melt was ~ 0.3 J/g. The annealing was chosen to increase the amount of thermal response during composite heating by the effect of "physical aging phenomenon"[25] occurring in non-crystalline solids like amorphous PMMA. Also it was found that the transition enthalpy increases with time of annealing which suggests again that organic material determined by TG analyses is mostly PMMA. The glass transition temperature of PMMA is usually reported to be

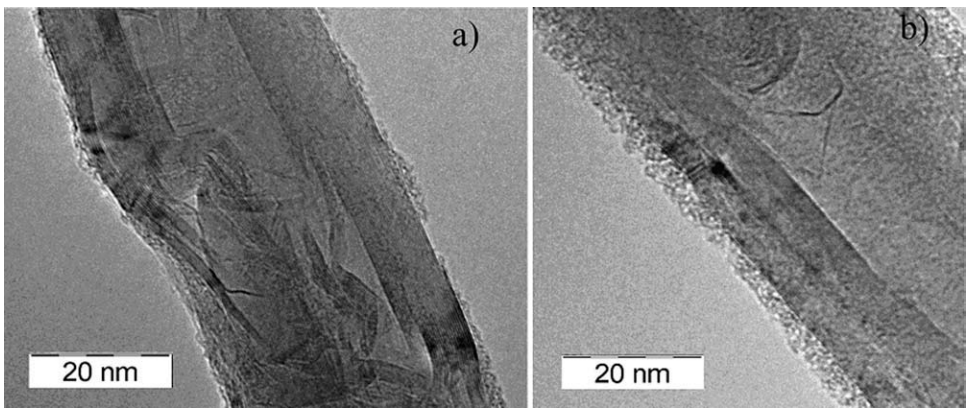

Figure 4 TEM analyses of individual MWCNT tube from MWCNT-N/PMMA network prepared by solution radical polymerization of allyl isocyanate functionalized MWCNT-N, PMMA "brushes" on MWCNT surface.

around 105°C (determined as the transition peak maximum) and transition extension reaches some 16°C. The difference in thermal properties of bulk PMMA compared to PMMA in the composite can be explained by the polymer segment immobilization on the surface of CNT. This phenomenon is usually reported to change thermal properties of polymeric materials such as an increase in T_g and broadening of T_g region.[35] The same phenomenon of physical aging occurs in pure PMMA presented in figure by full symbols (T_g, onset ~96°C, enthalpy of transition 2.1 J/g after 600 h of annealing at 90°C).

The chemical treatment of MWCNT network by allyl isocyanate and subsequent polymerization significantly changes network structure. It is shown in the micrographs of treated MWCNT-N and MWCNT-N/PMMA composite in Figure 6. The surface of the functionalized network seems smooth with grains which indicates that some nanotubes were deposited in agglomerates rather than individually during the network formation. On other hand, the surface of MWCNT-N/PMMA composite is wrinkled and large aggregates can be seen. The reason is probably local network shrinkage in the course of polymerization process when the contraction of PMMA during polymerization of MMA affects also network structure. The effect of polymerization on the composite structure is obvious from the micrographs of the network cross-section in Figure 7. The functionalized MWCNT-N consists of entangled tubes whereas the structure of MWCNT-N/PMMA is distorted by a local shrinkage. Moreover, PMMA seems to form porous texture rather than a continuous polymeric matrix.

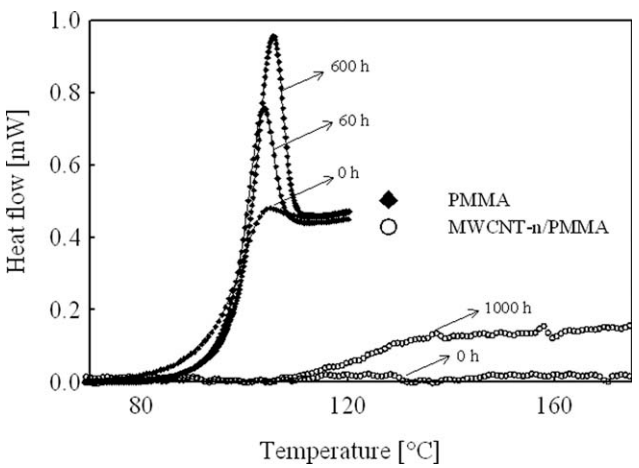

Figure 5 Differential scanning calorimetry analysis of PMMA and MWCNT-N/PMMA composite prepared by solution radical polymerization of allyl isocyanate functionalized MWCNT-N. The enhancement of glass transition response measured at DCS up-scan by process of physical aging of specimens at annealing temperatures below T_g. PMMA annealed at 90°C for 60 and 600 h and the composite at 100°C for 1000 h.

The SEM pictures of upper surface of pure MWCNT-N and MWCNT-N/PMMA composite were used for determination of the pore size distribution by means of the recently proposed digital image analysis technique.[36] The distributions are plotted in Figure 8 and show that the pure MWCNT-N has pores between 9.4 and 611 nm while

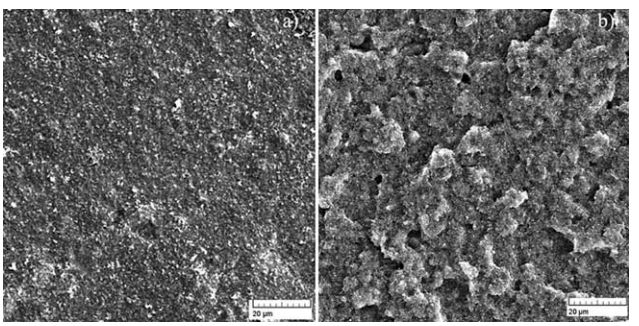

Figure 6 SEM analyses of the upper surfaces of MWCNT-N (a) and MWCNT-N/PMMA nanocomposite (b) prepared by solution radical polymerization of allyl isocyanate functionalized MWCNT-N.

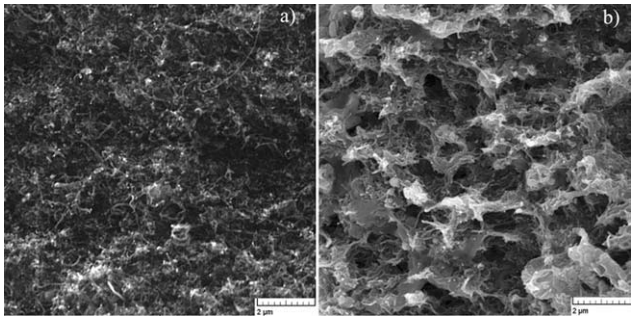

Figure 7 SEM analyses of the fracture surface of MWCNT-N (a) and MWCNT-N/PMMA nanocomposite (b) prepared by solution radical polymerization of allyl isocyanate functionalized MWCNT-N.

MWCNT-N/PMMA composite has larger pores in the range between 28 and 1840 nm.

Vapor sensing properties

Iso-pentane (*i*-PE), acetone, and methanol were used for the investigation of vapor sensing properties of nanotube networks. The chosen solvents cover a broad range of Hansen solubility parameters. The values for acetone are very close to PMMA values while *i*-PE is non-polar and methanol is on the other hand polar solvent but both do not solve PMMA. The data are presented in Table I and Figure 9. The parameters are defined by

$$\delta_t{}^2 = \delta_d{}^2 + \delta_p{}^2 + \delta_h{}^2 \tag{1}$$

where δ_t is the total Hildebrand solubility parameter, and δ_d, δ_p, and δ_h denotes the dispersion, the polar, and the hydrogen bonding component, respectively. The fractional parameters for the Teas triangular graph are defined as

$$\begin{array}{ll} f_d = \delta_d/\left(\delta_d + \delta_p + \delta_h\right), & f_p = \delta_p/\left(\delta_d + \delta_p + \delta_h\right), \\ f_h = \delta_h/\left(\delta_d + \delta_p + \delta_h\right), & f_d + f_d + f_h = 100. \end{array} \tag{2}$$

The values of fractional parameters for acetone are very similar to the value for PMMA, that is, acetone: $f_d = 47.1\%$, $f_p = 31.6\%$, and $f_h = 21.3\%$) and PMMA: $f_d = 50.8\%$, $f_p = 28.7\%$, and $f_h = 20.5\%$. The parameters for *i*-PE are $f_d = 100.0\%$, $f_p = 0.0\%$, and $f_h = 0.0\%$ and for methanol $f_d = 30.4\%$, $f_p = 24.8\%$, and $f_h = 44.9\%$. The networks were exposed to vapor of solvent at the saturated vapor pressure p_i and the corresponding volume fraction x_i,

$$x_i = p_i/p_{\mathrm{A}} \tag{3}$$

where p_A denotes the air pressure. The saturated vapor pressure p_i of the used solvents systematically decreases with increasing δ_t (Table I).

The adsorption of solvent molecules by the network increases its electrical resistance and thus the network resistance measurement is a simple and convenient method to register CNT response to vapor action. The vapor network sensitivity may be defined as

$$S = \left(R_g - R_a\right)/R_a = \Delta R/R_a \tag{4}$$

where R_a represents the stripe resistance in the air, and R_g the resistance of network stripe exposed to vapor.

The average sensitivity values for five different MWCNT-N and MWCNT-N/PMMA networks in the course of adsorption/desorption 6-min cycles when exposed to acetone vapors are shown in Figure 10. The mechanism of macroscopic resistance increase can be explained by formation of a non-conducting layer between nanotubes which degrades the quality of inter-tube contact. Desorption cycle starts by a rapid sensitivity decrease followed by a slower decrease to a constant value within the time of cycle. The organic molecules are removed in the course of desorption and the specimen resistance recovers the initial value. The data show higher vapor detection sensitivity of MWCNT-N/PMMA composite (the average sensitivity is 33.3 ± 3.1) than MWCNT network (15.6 ± 0.8). The increased sensitivity of composite is probably due to PMMA which increases the affinity of the composite structure to acetone vapors. The data demonstrates also good reversibility and reproducibility of adsorption/desorption cycles in case of the composite. On the other hand, the residual sensitivity change can be

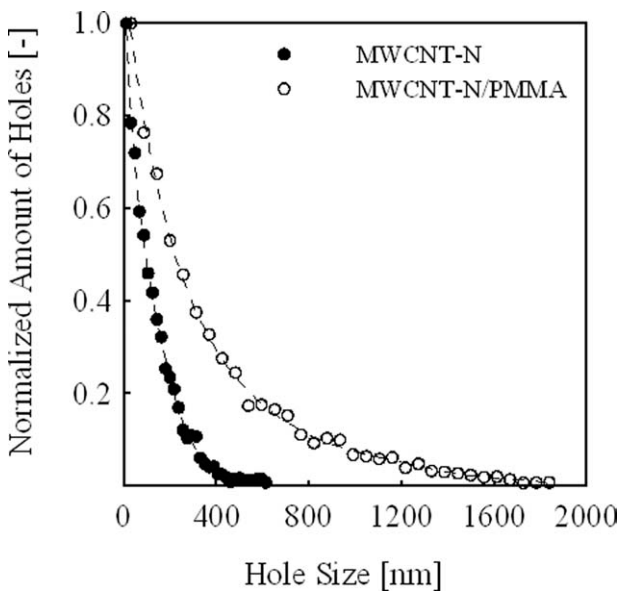

Figure 8 The pore size distribution of pure MWCNT-N and MWCNT-N/PMMA composite prepared by solution radical polymerization of allyl isocyanate functionalized MWCNT-N.

TABLE I
Properties of Tested Organic Solvents and PMMA: Hansen Solubility Parameters δ_d, δ_p, δ_h, Total Hildebrand Solubility Parameter δ_t, Saturated Vapor Pressures p_i, and Corresponding Volume Fractions at 25°C and Atmospheric Pressure x_i

Organic solvent	δ_d (MPa$^{1/2}$)	δ_p (MPa$^{1/2}$)	δ_h (MPa$^{1/2}$)	δ_t (MPa$^{1/2}$)	p_i (kPa)	x_i (vol. %)
PMMA	18.6	10.5	7.5	22.6	–	–
iso-pentane	13.7	0	0	13.7	91.37	90.2
Acetone	15.5	10.4	7.0	20.0	30.46	30.1
Methanol	15.1	12.3	22.3	29.6	16.76	16.5

observed in case of MWCNT-N. The change is probably caused by destruction of some contacts between crossing nanotubes in MWCNT network.[13] The error bars show higher scatter of data for MWCNT-N/PMMA composite than for MWCNT-N. The reason is probably the variability of composite texture compared to pure MWCNT network.

The comparison of network sensitivity for three different solvents (*iso*-pentane, acetone, and methanol) in the typical (third) adsorption/desorption cycle of the cycle sequence is presented in Figure 11. The reached sensitivity values after 6 min of adsorption are listed in Table II together with the ratios of the composite (S_2) to pure MWCNT network sensitivity (S_1). As follows from Figure 11 and Table II, MWCNT-N/PMMA composite is less sensitive when exposed to vapors of *iso*-pentane compared to sensitivity of pure MWCNT-N. The corresponding relation S_2/S_1 is 0.6. Nearly the same response for MWCNT-N and MWCNT-N/PMMA composite is observed for methanol, $S_2/S_1 = 1.1$. However, the significant ratio S_2/S_1 change is found when the composite is exposed to acetone vapor, $S_2/S_1 = 2.1$.

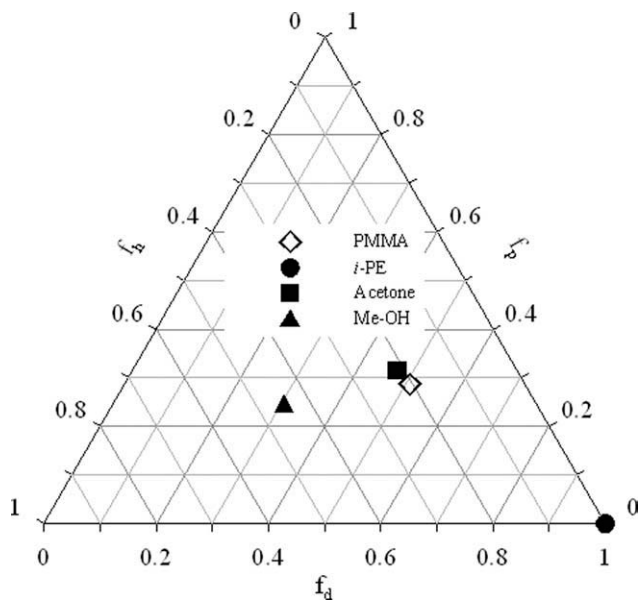

Figure 9 The triangular graph of dispersion, polar, and hydrogen bonding fractional solubility parameters, f_d, f_p, f_h, for used solvents and PMMA.

The main reason is the affinity of PMMA to acetone but the influence of the higher network porosity of composite compared to the one of pure MWCNT-N network cannot be ruled out.

As follows from Figure 11, the network sensitivity depends on the type of network, the vapor pressure and the polarity of the solvent. Figure 12 demonstrates that the maximal sensitivity of pure MWCNT-N increases with volume fraction of vapors x_i despite solvent different polarities. A completely different behavior holds for MWCNT-N/PMMA composite. The composite maximal sensitivities are significantly influenced by the origin of vapors, i.e., their affinity to PMMA. In this respect, the affinity of acetone polarity with polarity

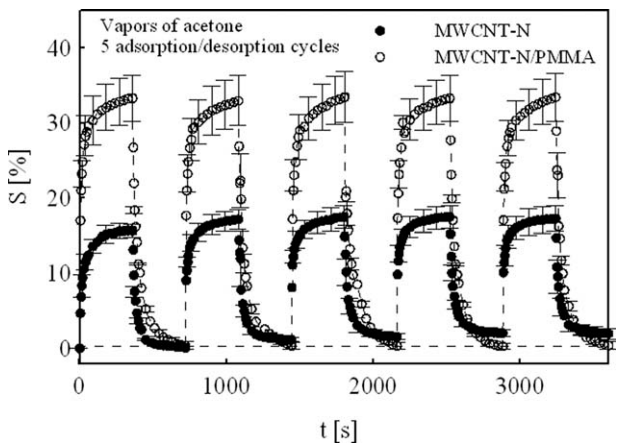

Figure 10 Five adsorption/desorption cycles for MWCNT-N (filled symbols) and MWCNT-N/PMMA nanocomposite (open symbols) prepared by solution radical polymerization of allyl isocyanate functionalized MWCNT-N exposed to vapor of acetone ($n = 5$).

TABLE II
Sensitivities of Both CNT Networks Exposed to Saturated Vapors of Three Different Organic Solvents

Organic solvent	S_1 (%) MWCNT-N	S_2 (%) MWCNT-N/PMMA	S_2/S_1
iso-pentane	20.3 ± 0.6	12.6 ± 1.4	0.6
Acetone	15.6 ± 0.8	33.3 ± 3.1	2.1
Methanol	13.6 ± 0.3	14.7 ± 1.8	1.1

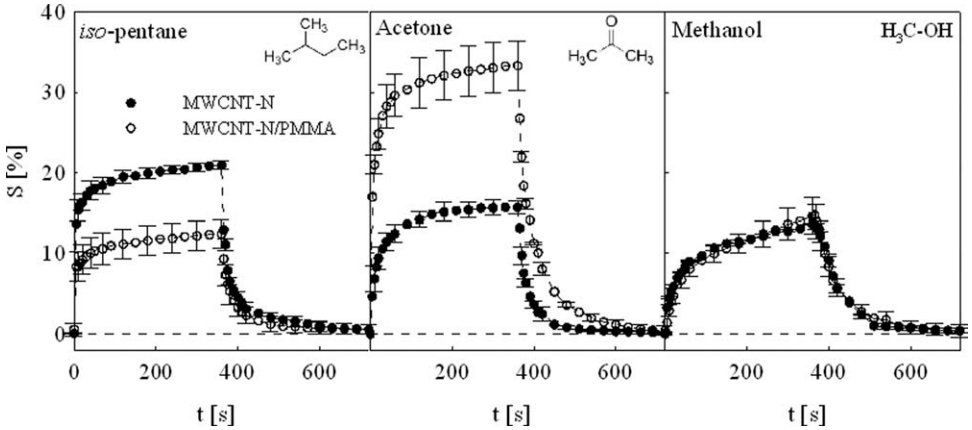

Figure 11 One adsorption/desorption cycle for MWCNT-N (filled symbols) and MWCNT-N/PMMA nanocomposite (open symbols) prepared by solution radical polymerization of allyl isocyanate functionalized MWCNT-N exposed to three different organic solvents: *iso*-pentane (a), acetone (b), and methanol (c).

of PMMA improves significantly the selectivity of the composite network to this solvent while the composite sensitivity to methanol is the same and to *iso*-pentane even lower in comparison with the MWCNT-N sensitivity.

CONCLUSION

Multiwall carbon nanotubes were used to prepare the entangled network and the entangled network/PMMA composite whose response to three organic solvent vapors (*iso*-pentane, acetone, and methanol) was monitored by measuring their electrical resistance change. The resistance response of samples to physisorption and desorption of organic vapors during the test cycles was reversible, reproducible, sensitive, and selective. The possible mechanism of resistance change may involve formation of nonconducting layer between nanotubes in solvent vapors which degrades the quality of inter-tube contact. The nanotube PMMA functionalization improves their sensitivity for acetone vapors. The improvement is caused by affinity of acetone vapors polarity with polarity of PMMA in the composite structure. The potential composite use may be for cheap and easy to prepare micro-sized sensing elements and vapor switches.

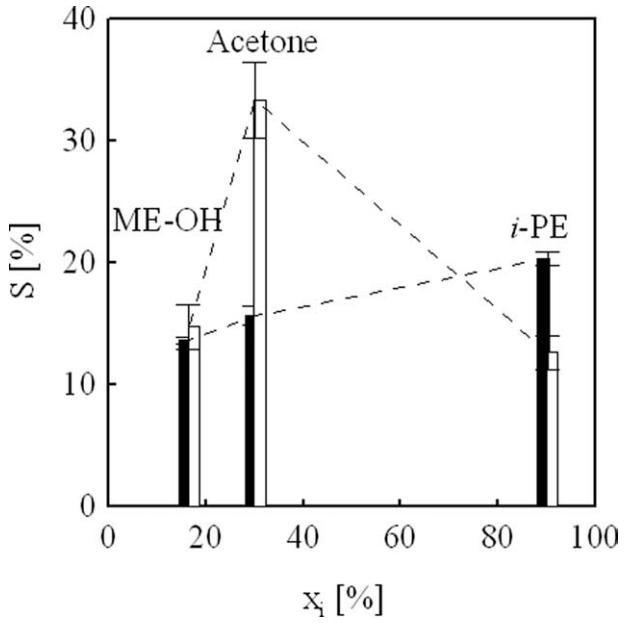

Figure 12 Dependence of sensitivity of MWCNT-N and MWCNT-N/PMMA composite prepared by solution radical polymerization of allyl isocyanate functionalized MWCNT-N on the volume fraction of organic solvent during adsorption/desorption cycle. Black columns are for the pure MWCNT-N sensitivity S_1 and white columns for MWCNT-N/PMMA composite sensitivity S_2.

This project was supported by the internal grant of TBU in Zlín No. IGA/12/FT/11/D funded from the resources of specific university research. This article was also created with the support of Operational Programme Research and Development for Innovations co-funded by the European Regional Development Fund (ERDF) and national budget of the Czech Republic within the framework of the Centre of Polymer Systems project (reg.number: CZ.1.05/2.1.00/03.0111), by the Czech Ministry of Education, Youth and Sports project (MSM 7088352101) and by the Fund of the Institute of Hydrodynamics AV0Z20600510.

The authors would like to thank Dr. Radko Novotny of Palacky University, Olomouc, Czech Republic, for conducting of TEM analyses and Prof. Martin Zatloukal of TBU for performing SEM digital image analysis.

References

1. Cheng, Q. F.; Bao, J. W.; Park, J.; Liang, Z.Y.; Zhang, C.; Wang, B. Adv Funct Mater 2009, 19, 3219.
2. Wang, D.; Song, P. C.; Liu, C. H.; Wu, W.; Fan, S. S. Nanotechnology 2008, 19, 1.
3. Wu, Q.; Zhu, W.; Zhang, C.; Liang, Z.Y.; Wang, B. Carbon 2010, 48, 1799.

4. Fu, X.; Zhang, C.; Liu, T.; Liang, R.; Wang, B. Nanotechnology 2010, 21, 235701.
5. Meng, C. Z.; Liu, C. H.; Fan, S. S. Electrochem Commun 2009, 11, 186.
6. Yun, Z. H.; Shanov, V.; Schulz, M. J.; Narasimhadevara, S.; Subramaniam, S.; Hurd, D.; Boerio, F. J. Smart Mater Struct 2005, 14, 1526.
7. Kang, I. P.; Schulz, M. J.; Kim, J. H.; Shanov, V.; Shi, D. L. Smart Mater Struct 2006, 15, 737.
8. Slobodian, P.; Riha, P.; Lengalova, A.; Olejnik, R.; Saha, P. J Exp Nanosci 2011, 6, 294.
9. Olejnik, R.; Slobodian, P.; Riha, P.; Saha, P. Polym Test (Submitted).
10. Hussain, C. M.; Saridara, C.; Mitra, S. J Chromatogr A 2008, 1185, 161.
11. Smajda, R.; Kukovecz, A.; Konya, Z.; Kiricsi, I. Carbon 2007, 45, 1176.
12. Agnihotri, S.; Mota, J. P. B.; Rostam-Abadi, M.; Rood, M. J. J Phys Chem B 2006, 110, 7640.
13. Romanenko, A. I.; Anikeeva, O. B.; Kuznetsov, V. L.; Buryakov, T. I.; Tkachev, E. N.; Usoltseva, A. N. Sensor Actuat A-Phys 2007, 138, 350.
14. Qureshi, A.; Kang, W. P.; Davidson, J. L.; Gurbuz, Y. Diam Relat Mater 2009, 18, 1401.
15. Tournus, F.; Latil, S.; Heggie, M. I.; Charlier, J. C. Phys Rev B 2005, 72, 075431.
16. Mowbray, D. J.; Morgan, C.; Thygesen, K. S. Phys Rev B 2009, 79, 195431.
17. Li, Y; Wang, H. C.; Yang, M. J. Sensor Actuat B-Chem 2007, 121, 496.
18. Shang, S. M.; Li, L.; Yang, X. M.; Wei, Y. Y. Compos Sci Technol 2009, 69, 1156.
19. Abraham, J. K.; Philip, B.; Witchurch, A.; Varadan, V. K.; Reddy, C. C., Smart Mater Struct 2004, 13, 1045
20. Feller, J. F.; Lu, J.; Zhang, K.; Kumar, B.; Castro, M.; Gatt, N.; Choi, H. J. J Mater Chem 2011, 21, 4142.
21. Slobodian, P.; Riha, P.; Lengalova, A.; Saha, P. J Mater Sci 2011, 46, 3186.
22. Ham, H. T.; Choi, Y. S.; Chung I. J. Colloid Interf Sci 2005, 286, 216.
23. Chern, C. S.; Wu, L. J. J Polym Sci Part A: Polym Chem 2001, 39, 3199.
24. Kimmer, D.; Slobodian, P.; Petras, D.; Zatloukal, M.; Olejnik, R.; Saha P. J Appl Polym Sci 2009, 111, 2711.
25. Slobodian, P.; Riha, P.; Lengalova, A.; Hadac, J.; Saha, P.; Kubat, J. J Non-Cryst Solids 2004, 344, 148.
26. Niu, L.; Luo, Y. L.; Li, Z. Q. Sensor Actuat B-Chem 2007, 126, 361.
27. Slobodian, P.; Riha, P.; Lengalova, A.; Svoboda, P.; Saha, P. Carbon 2011, 49, 2499.
28. Slobodian, P.; Kralova, D.; Lengalova, A.; Novotny, R.; Saha, P. Polym Compos 2010, 31, 452.
29. Wang, X. B.; Li, S. Q.; Xu, Y.; Wan, L.; You, H. J.; Li, Q.; Wang, S. M. Appl Surf Sci 2007, 253, 7435.
30. Kim, S. T.; Choi, H. J.; Hong, S. M. Colloid Polym Sci 2007, 285, 593.
31. Ha, J. U.; Kim, M.; Lee, J.; Choe, S.; Cheong, I. W.; Shim, S. E. J Polym Sci Part A Polym Chem 2006, 44, 6394.
32. Olejnik, R.; Liu, P. B.; Slobodian, P.; Zatloukal, M.; Saha, P. Novel Trends Rheol III 2009, 1152, 204.
33. Rasheed, A.; Howe, J. Y.; Dadmun, M. D.; Britt, P. F. Carbon 2007, 45, 1072.
34. Kim, M. H.; Hong, C. K.; Choe, S.; Shim, S. E. J Polym Sci Part A Polym Chem 2007, 45, 4413.
35. Slobodian, P.; J Therm Anal Calorim 2008, 94, 545.
36. Sambaer, W.; Zatloukal, M.; Kimmer, D. Polym Test 2010, 29, 82.

THE EFFECT OF CHANGE SELECTIVITY FOR SENSING ELEMENT MADE FROM MULTI-WALL CARBON NANOTUBE NETWORK TREATED BY PLASMA

Robert OLEJNIK [a], Petr SLOBODIAN [a], Uroš CVELBAR [b]

[a] Centre of Polymer Systems, Faculty of Technology, Tomas Bata University in Zlin

T.G.Masaryka 555, 760 05 Zlín, Czech Republic, EU, rolejnik@volny.cz, slobodian@ft.utb.cz

[b] *Jozef Stefan Institute, Jamova cesta 39, 1000 Ljubjana,Slovenia, EU,* uros.cvelbar@ijs.si

Abstract

Multiwall carbon nanotubes (MWCNT) network called “Buckypaper” was made by the vacuum filtration method from MWCNT aqueous suspension. In this way we created multi-wall carbon nanotube (MWCNT) networks featured by randomly entangled pure nanotubes. These networks were applied as gas sensors for organic vapors of ethanol and heptane, polar and nonpolar solvents, respectively. The gas response was investigated by electrical resistance measurements. The surface sensitivity and selectivity was then modified by low-temperature reactive surface plasma treatment in different gases. With plasma treatment, we first created the functional groups on the nanotubes surface and latter etch them. These processes changed surface selectivity for detection of organic vapors. The results showed that the MWCNT network electrical resistance increased when exposed to organic solvent vapors. This is reversible process, when removed from the vapors. Therefore, the MWCNT networks show the potential to be used as improved sensing elements for sensitive and selective organic vapor detection in near future.

Keywords: carbon nanotube network, sensor, buckypaper, electrical resistance, plasma treatment

INTRODUCTION

Single-wall carbon nanotubes (SWCNTs) or multi-wall carbon nanotubes (MWCNTs) show remarkable sensitivity to the change of chemical composition of the surrounding environment. This property can be used in order to design new membranes [1], adsorbents [2], gas sensors [3,4,8] and pressure sensors [9,10]. Gas and vapor adsorption as well as desorption usually occurs on the surface at high rates of functional groups [5]. The gas molecules are normally adsorbed on the carbon nanotube (CNT) surface by van der Waals attracting forces, which provide remarkable changes in CNT electrical resistance. The application of this principle can be used for development of CNT-based electrochemical biosensors and gas sensors with a useful ability to selectively detect various gases and organic vapors. Whereas, conductivity measurements can be then a simple and convenient method to register their response to gas molecule adsorption/desorption.

Previous research [6,7] demonstrated that physisorbed molecules influence the electrical properties of isolated CNTs and also inter-tube contacts. The resistance of macroscopic CNT objects like aggregates or network structures used in gas sensors are predominantly determined by contact resistance of crossing tubes, rather than by resistance of CNT segments. Here, the tubes are much shorter than sensor dimensions and inter-tube contacts act as parallel resistors between highly conductive CNT segments.

The dominating process influencing macroscopic resistance is probably gas or vapor adsorption in the space between nanotubes, which forms non-conductive layers between the tubes. This process decreases both the quantity and quality of contacts between nanotubes and consequently increases macroscopic resistance [3].

Functionalizing the carbon nanotubes with a number of functional groups is known to increase their chemical reactivity and can be used as a starting point for further chemical modification. Several methods such as chemical,electrochemical , polymer wrapping, and plasma treatment have been applied to modify

the CNT surface. The method of special interest was found to be plasma treatment, due to easy application and great efficiancy. The functionalization of CNTs was made by using hydrogen, nitrogen, ammonia, O_2/Ar, O_2, CF_4, or SF_6 plasmas. [11]

The presented work we describe preparation of resistive gas sensors with a simple method which is used to modify MWCNTs with reactive plasma. The plasma modified materials are then tested for sensitivity to saturated vapors of two different organic solvents. Finally, reversibility of adsorption/desorption cycles is tested for acetone.

EXPERIMENTAL

The purified MWCNT are produced in a high-yield catalytic process based on chemical vapor deposition were supplied by Bayer MaterialScience, Germany (diameter 5-20 nm, length 1-10 μm, purity >99% and number of walls 3-15. The MWCNT aqueous paste was prepared using a mortar and pestle (0.5 g of MWCNT and ~ 5 ml of deionized water), then homogenized using Dr. Hielscher GmbH apparatus (ultrasonic horn S7, amplitude 88 μm, power density 300 W/cm^2, frequency 24 kHz) for 2 hours and the temperature of ca 50°C. Then were added 3 ml Triton X-100 and 1-M aqueous solution of NaOH for adjusted pH to the value of 10. The dispersion was homogenized using Dr. Hielscher GmbH apparatus (ultrasonic horn S7, amplitude 88 μm, power density 300 W/cm^2, frequency 24 kHz) for 1 hour and centrifuged for 15 min at 3000 rpm. The sediment was removed.

MWCNT networks, “Buckypaper” (MWCNT-N), were prepared by dispersion vacuum filtration thought polyurethane submicron size porous membrane. The formed disk-shaped network was washed several times by deionized water and methanol in situ, then removed and dried between filter papers at RT. The resulting buckypaper was cut in the shape of strips. The strips were then treated by low temperature reactive plasma. The plasma was generated in an inductively coupled radiofrequency discharge at 27.12 MHz in a commercially available gas of O_2, CO_2, N_2, H_2, Ar, SO_2 or CF_4 , at the pressure 50 Pa. Whereas, the base pressure of vacuum system was 1 Pa.

After the plasma modification, the strips made of CNT networks were exposed to the vapors of two different solvents; ethanol and heptane. The chosen solvents were characterized by their polarity. The specimens were exposed to saturated vapors of solvents at defined experimental conditions: 25 °C, atmospheric pressure and 6 minute adsorption/desorption cycles.

RESULTS

Fig. 1 represents SEM analyses of upper surfaces of prepared CNT networks. The surface of CNT networks is very smooth, clean without fragments in the space between the network.

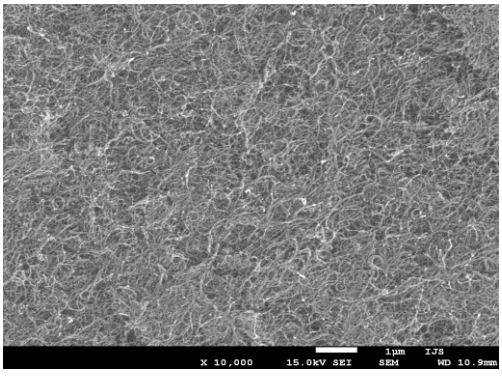

Fig. 1 SEM analyses of CNT networks made by vacuum filtration

Fig. 2 represents the change of sensitivity of CNT networks treated by seven different gases. The modification created different functional groups on multiwall carbon nanotube surface. Each functional group has different affinity for polar and nonpolar organic vapors represent by ethanol and heptanes.

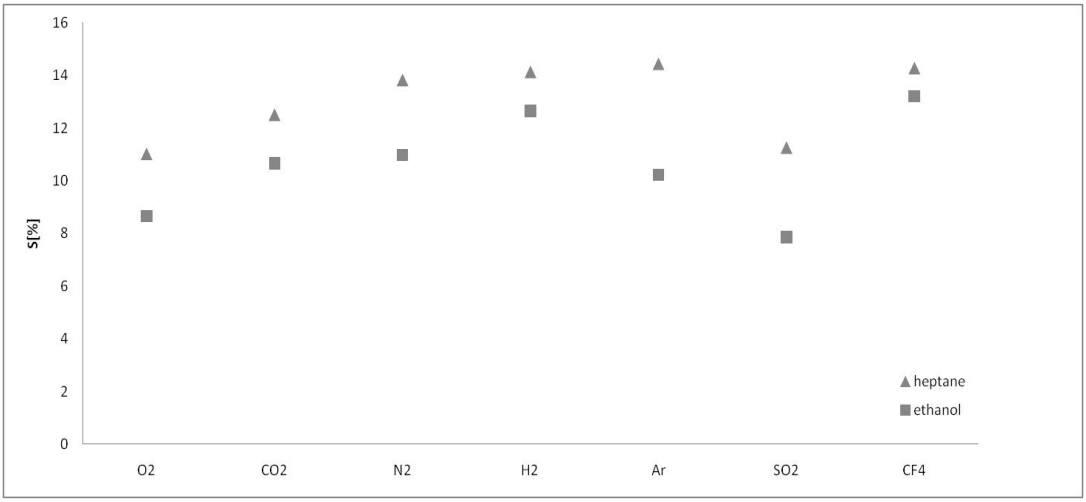

Fig. 2 The sensitivity of Multiwall carbon nanotubes network exposed to vapors of two different organic solvents and treated by plasma in seven gases at 50pa and 3 minutes.

The typical adsorption/desorption behavior of CNT network exposed to/disposed from organic vapors is presented in Fig. 3. The graph illustrates a time-dependent change of parameter S representing sensitivity of the nanotube networks. The curves show specific course of adsorption/desorption, with an obvious on/off effect. An initial sharp increase in sensitivity is followed by a slower phase. Simultaneously, desorption is represented by a rapid decrease reaching a constant value in some cases, in others followed by further, slower decrease. The sensitivity is defined by eq. 1 where R_a represents specimen resistance in air and R_g resistance of the specimen exposed to gas/vapor, ΔR stands for the resistance change.

$$S = \frac{R_g - R_a}{R_a} = \frac{\Delta R}{R_a} \tag{1}$$

Table 1 presents properties of tested organic solvents. Hildebrand solubility parameter, δ_t, and pressures, p_i, and saturated vapor volume fractions, x_i. It was found that x_i has the similar value for both solvents so the sensitivity depend on their polarity.

solvent	δ_d [Mpa$^{1/2}$]	δ_p [Mpa$^{1/2}$]	δ_h [Mpa$^{1/2}$]	δ_t [Mpa$^{1/2}$]	p_i [kPa]	x_i [vol. %]
heptane	15.3	0	0	15.3	6.13	6.0
ethanol	15.8	8.8	19.4	26.5	7.86	7.1

Table 1 Properties of tested organic solvents: Hansen solubility parameters, δ_d, δ_p, δ_d total Hildebrand solubility parameter, δ_t, saturated vapor pressures, p_i, and corresponding volume fractions, x_i, at 25°C.

Fig. 3 Represents response to three consecutive cycles in saturated vapors of ethanol measured in 6-minute intervals. Experimental data also demonstrate good reversibility of adsorption/desorption processes.

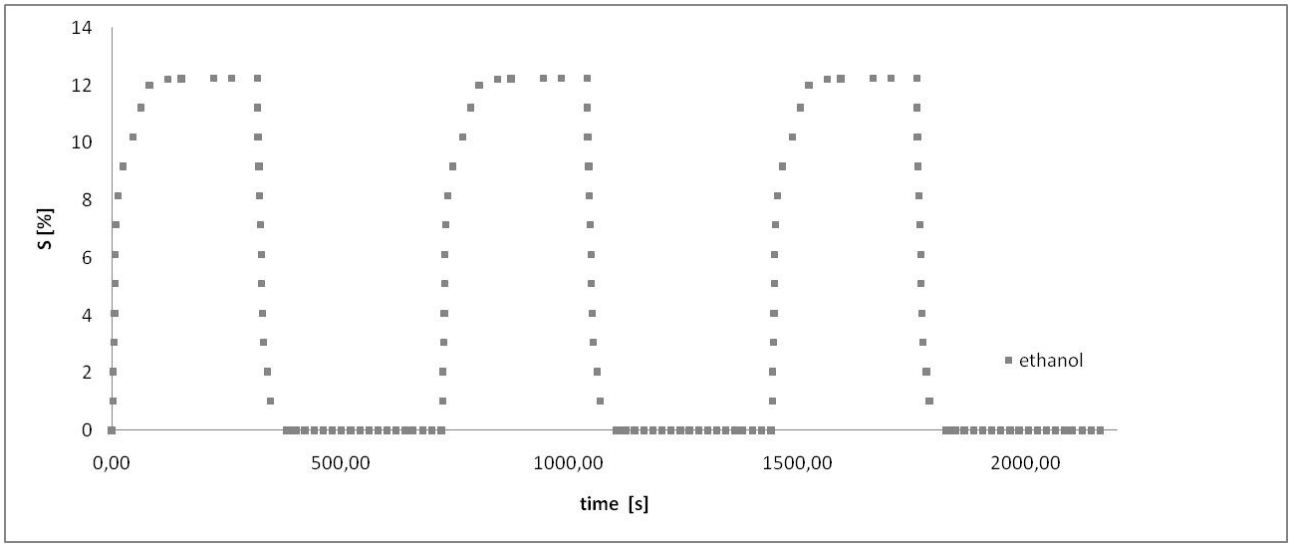

Fig. 3 Three adsorption/desorption cycles of Multiwall carbon nanotubes network exposed to vapors of ethanol.

Conclusions

Multiwall carbon nanotubes were used to prepare CNT network (buckypaper) by vacuum filtration method. Their response to adsorption/desorption cycles were determined as a change of macroscopic resistance. The response to adsorption/desorption was measured as a change of resistance. The surface of buckypaper was treated by RF plasma in different atmospheres, which functionalized their surfaces and changed affinity for the polar and nonpolar organic vapors. The lowest response was found to be 7.86 % in SO_2 plasma, and highest 13.20 in CF_4 for ethanol. Whereas,the lowest response was 11.00 % in O_2 plasma, and the highest 14.44 in Ar for heptane. The sensitivity had limited efficiency, since only the upper most layers of bucky paper underwent surface modificationHowever, we found that CNT network has good sensitivity and assumed selectivity defined by pressures of saturated vapors of used organics solvents. And more, we found that measured response had a good reversibility.

Acknowledgement

This article was created with support of Operational Programme Research and Development for Innovations co-funded by the European Regional Development

Fund (ERDF) and national budget of Czech Republic within the framework of the Centre of Polymer Systems project (reg.number: CZ.1.05/2.1.00/03.0111) and the Czech Ministry of Education, Youth and Sports project (MSM 7088352101). This project was supported by the internal grant of TBU in Zlín No. IGA/3/FT/11/D funded from the resources of specific university research.

REFERENCES

[1] Smajda R, Kukovecz A, Konya Z, Kiricsi I. Structure and gas permeability of multi-wall carbon nanotube buckypapers. Carbon 2007;45(6):1176-1184.

[2] Agnihotri S, Mota JPB, Rostam-Abadi M, Rood MJ. Theoretical and experimental investigation of morphology and temperature effects on adsorption of organic vapors in single-walled carbon nanotubes. J Phys Chem B 2006;110(15):7640-7647.

[3] Romanenko A I, Anikeeva OB, Kuznetsov VL, Buryakov TI, Tkachev EN, Usoltseva AN. Influence of helium, hydrogen, oxygen, air and methane on conductivity of multiwalled carbon nanotubes. Sensor Actuat A-Phys 2007;138(2):350-354.

[4] Qureshi A, Kang WP, Davidson JL, Gurbuz Y. Review on carbon-derived, solid-state, micro and nano sensors for electrochemical sensing application. Diam Relat Mater 2009;18(12):1401-1420.

[5] Hussain CM, Saridara C, Mitra S. Microtrapping characteristics of single and multi-walled carbon nanotubes. J Chromatogr A 2008;1185(2):161-166.

[6] Tournus F, Latil S, Heggie MI, Charlier JC. pi-stacking interaction between carbon nanotubes and organic molecules, Phys Rev B 2005;72(7):Article Number 075431.

[7] Mowbray DJ, Morgan C, Thygesen KS. Influence of O-2 and N-2 on the conductivity of carbon nanotube networks. Phys Rev B 2009;79(19):Article Number 195431.

[8] P. Slobodian, P**.** Riha, A. Lengalova, P. Svoboda and P. Saha, Multi-wall carbon nanotube networks as potential resistive gas sensors for organic vapor detection, Carbon, Volume 49, Issue 7, June 2011, Pages 2499-2507

[9] Slobodian, P, Riha P, Lengalova A, Saha P, Compressive stress-electrical conductivity characteristics of multiwall carbon nanotube networs. Journal of Materials Science. Volume 46, Issue 9 (2011), Page 3186

[10] P. Slobodian, P. Riha, A. Lengalova, P. Svoboda, P. Saha, Multi. Journal of Materials Science. Volume 46, Issue 9 (2011), Page 3186

[11] Uwe Vohrer, Justin Holmes, Zhonglai Li, AunShih Teh, Pagona Papakonstantinou, Manuel Ruether and Werner Blau, Tailoring the Wettability of Carbon Nanotube Powders, Bucky paper and Vertically Aligned Nanofires, Design, Synthesis and Grown of the Nanotubes for Industrial Technology,

Plasma surface modification of entangled multi-wall carbon nanotubes network for organic vapor detection

Robert Olejnik[1,2], Petr Slobodian[1,2], Uroš Cvelbar[2]

[1]Centre of Polymer Systems, University Institute, Tomas Bata University, Nad Ovcirnou 3685, 76001 Zlin, Czech Republic

[2]Polymer Centre, Faculty of Technology, Tomas Bata University in Zlin, T.G.M. 275, 76272 Zlin, Czech Republic

[3]Jozef Stefan Institute, Jamova cesta 39, 1000 Ljubjana, Slovenia

rolejnik@volny.cz

Entangled multiwall carbon nanotubes (MWCNT) network "Buckypaper" was made by the vacuum filtration from MWCNT aqueous dispersion. In this way we created multi-wall carbon nanotube (MWCNT) networks featured by randomly entangled pure nanotubes. These networks were applied as gas sensors for organic vapors of ethanol and heptane, polar and nonpolar solvents, respectively. The gas response was detected by electrical resistance measurements. The surface sensitivity and selectivity was then modified by low-temperature reactive surface plasma treatment in different gases. With plasma treatment, we first created the functional groups on the nanotubes surface and latter etch them. These processes changed surface selectivity for detection of organic vapors. The results showed that the MWCNT network electrical resistance increased when exposed to organic solvent vapors. This is reversible process, when removed from the vapors. Therefore, the MWCNT networks show the potential to be used as improved sensing elements for sensitive and selective organic vapor detection in near future.

Keywords: carbon nanotube network, sensor, buckypaper, electrical resistance, plasma treatment

INTRODUCTION

Single-wall carbon nanotubes (SWCNTs) or multi-wall carbon nanotubes (MWCNTs) show remarkable sensitivity to the change of chemical composition of the surrounding environment. This property can be used in order to design new membranes [1], adsorbents [2], gas sensors [3,4,8] and pressure sensors [9,10]. Gas and vapor adsorption as well as desorption usually occurs on the surface at high rates of functional groups [5]. The gas molecules are normally adsorbed on the carbon nanotube (CNT) surface by van der Waals attracting forces, which provide remarkable changes in CNT electrical resistance. The application of this principle can be used for development of CNT-based electrochemical biosensors and gas sensors with a useful ability to selectively detect various gases and organic vapors. Whereas, conductivity measurements can be then a simple and convenient method to register their response to gas molecule adsorption/desorption.

Previous research [6,7] demonstrated that physisorbed molecules influence the electrical properties of isolated CNTs and also inter-tube contacts. The resistance of macroscopic CNT objects like aggregates or network structures used in gas sensors are predominantly determined by contact resistance of crossing tubes, rather than by resistance of CNT segments. Here, the tubes are much shorter than sensor dimensions and inter-tube contacts act as parallel resistors between highly conductive CNT segments.

The dominating process influencing macroscopic resistance is probably gas or vapor adsorption in the space between nanotubes, which forms non-conductive layers between the tubes. This process decreases both the quantity and quality of contacts between nanotubes and consequently increases macroscopic resistance [3].

Functionalizing the carbon nanotubes with a number of functional groups is known to increase their chemical reactivity and can be used as a starting point for further chemical modification. Several methods such as chemical,electrochemical , polymer wrapping, and plasma treatment have been applied to modify the CNT surface. The method of special interest

was found to be plasma treatment, due to easy application and great efficiancy. The functionalization of CNTs was made by using hydrogen, nitrogen, ammonia, O_2/Ar, O_2, CF_4, or SF_6 plasmas. [11]

The presented work we describe preparation of resistive gas sensors with a simple method which is used to modify MWCNTs with reactive plasma. The plasma modified materials are then tested for sensitivity to saturated vapors of two different organic solvents. Finally, reversibility of adsorption/desorption cycles is tested for acetone.

EXPERIMENTAL

The purified MWCNT are produced in a high-yield catalytic process based on chemical vapor deposition were supplied by Bayer MaterialScience, Germany (diameter 5-20 nm, length 1-10 μm, purity >99% and number of walls 3-15. The MWCNT aqueous paste was prepared using a mortar and pestle (0.5 g of MWCNT and ~ 5 ml of deionized water), then homogenized using Dr. Hielscher GmbH apparatus (ultrasonic horn S7, amplitude 88 μm, power density 300 W/cm^2, frequency 24 kHz) for 2 hours and the temperature of ca 50°C. Then were added 3 ml Triton X-100 and 1-M aqueous solution of NaOH for adjusted pH to the value of 10. The dispersion was homogenized using Dr. Hielscher GmbH apparatus (ultrasonic horn S7, amplitude 88 μm, power density 300 W/cm^2, frequency 24 kHz) for 1 hour and centrifuged for 15 min at 3000 rpm. The sediment was removed.

MWCNT networks, “Buckypaper” (MWCNT-N), were prepared by dispersion vacuum filtration thought polyurethane submicron size porous membrane. The formed disk-shaped network was washed several times by deionized water and methanol in situ, then removed and dried between filter papers at RT. The resulting buckypaper was cut in the shape of strips. The strips were then treated by low temperature reactive plasma. The plasma was generated in an inductively coupled radiofrequency discharge at 27.12 MHz in a commercially available gas of O_2, CO_2, N_2, H_2, Ar, SO_2 or CF_4 , at the pressure 50 Pa. Whereas, the base pressure of vacuum system was 1 Pa.

After the plasma modification, the strips made of CNT networks were exposed to the vapors of two different solvents; ethanol and heptane. The chosen solvents were characterized by their polarity. The specimens were exposed to saturated vapors of solvents at defined experimental conditions: 25 °C, atmospheric pressure and 6 minute adsorption/desorption cycles.

RESULTS

Fig. 1 represents SEM analyses of upper surfaces of prepared CNT networks. The surface of CNT networks is very smooth, clean without fragments in the space between the network.

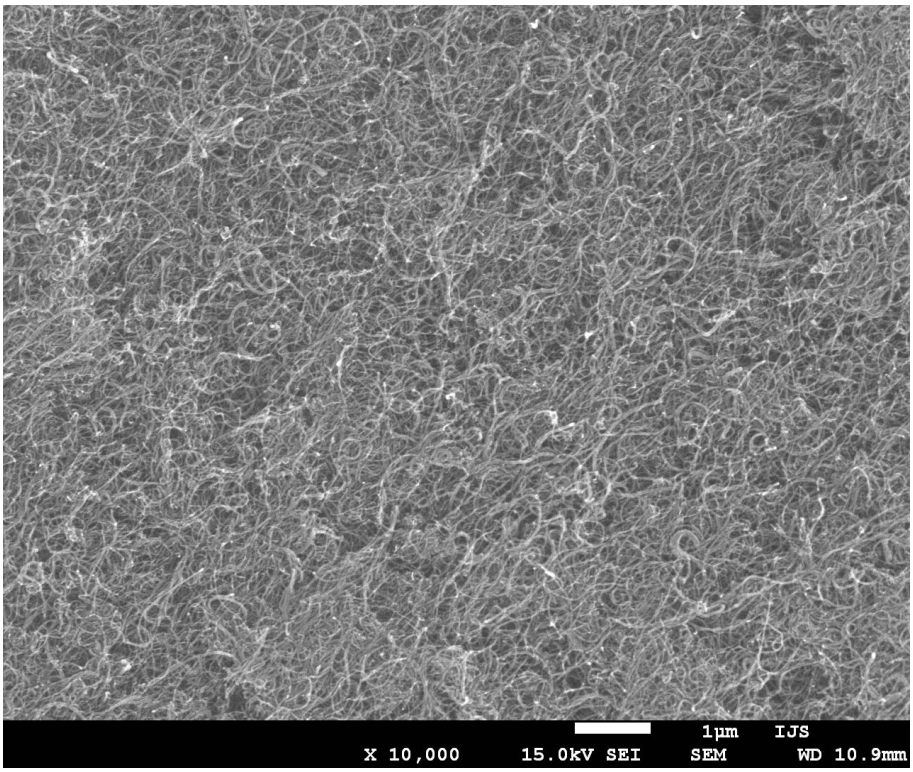

Fig. 1 SEM analyses of CNT networks made by vacuum filtration

Fig. 2 represents the change of sensitivity of CNT networks treated by seven different gases. The modification created different functional groups

on multiwall carbon nanotube surface. Each functional group has different affinity for polar and nonpolar organic vapors represent by ethanol and heptanes.

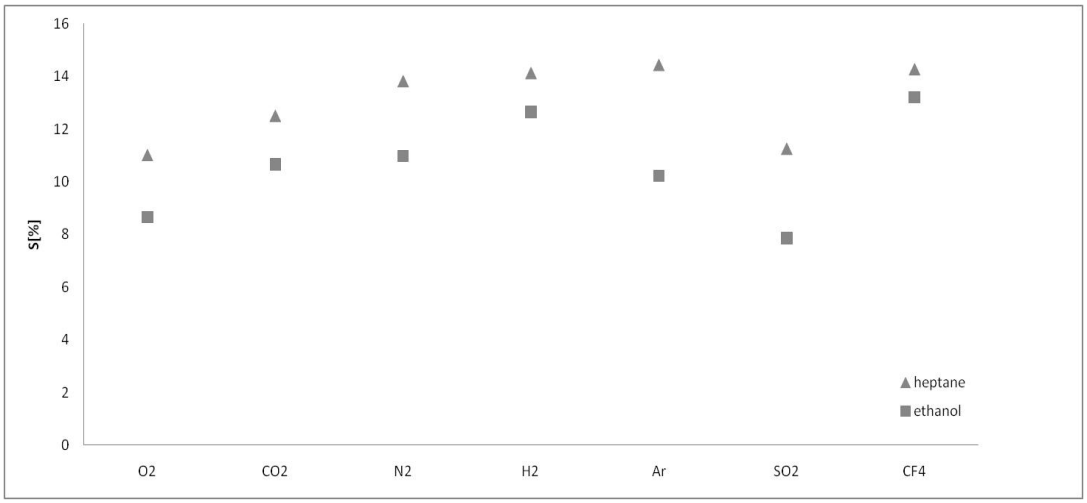

Fig. 2 The sensitivity of Multiwall carbon nanotubes network exposed to vapors of two different organic solvents and treated by plasma in seven gases at 50pa and 3 minutes.

The typical adsorption/desorption behavior of CNT network exposed to/disposed from organic vapors is presented in Fig. 3. The graph illustrates a time-dependent change of parameter S representing sensitivity of the nanotube networks. The curves show specific course of adsorption/desorption, with an obvious on/off effect. An initial sharp increase in sensitivity is followed by a slower phase. Simultaneously, desorption is represented by a rapid decrease reaching a constant value in some cases, in others followed by further, slower decrease. The sensitivity is defined by eq. 1 where R_a represents specimen resistance in air and R_g resistance of the specimen exposed to gas/vapor, ΔR stands for the resistance change.

$$S = \frac{R_g - R_a}{R_a} = \frac{\Delta R}{R_a} \qquad (1)$$

Table 1 presents properties of tested organic solvents. Hildebrand solubility parameter, δ_t, and pressures, p_i, and saturated vapor volume fractions, x_i. It was found that x_i has the similar value for both solvents so the sensitivity depend on their polarity.

solvent	δ_d [Mpa$^{1/2}$]	δ_p [Mpa$^{1/2}$]	δ_h [Mpa$^{1/2}$]	δ_t [Mpa$^{1/2}$]	p_i [kPa]	x_i [vol. %]
heptane	15.3	0	0	15.3	6.13	6.0
ethanol	15.8	8.8	19.4	26.5	7.86	7.1

Table 1 Properties of tested organic solvents: Hansen solubility parameters, δ_d, δ_p, δ_d total Hildebrand solubility parameter, δ_t, saturated vapor pressures, p_i, and corresponding volume fractions, x_i, at 25°C.

Fig. 3 Represents response to three consecutive cycles in saturated vapors of ethanol measured in 6-minute intervals. Experimental data also demonstrate good reversibility of adsorption/desorption processes.

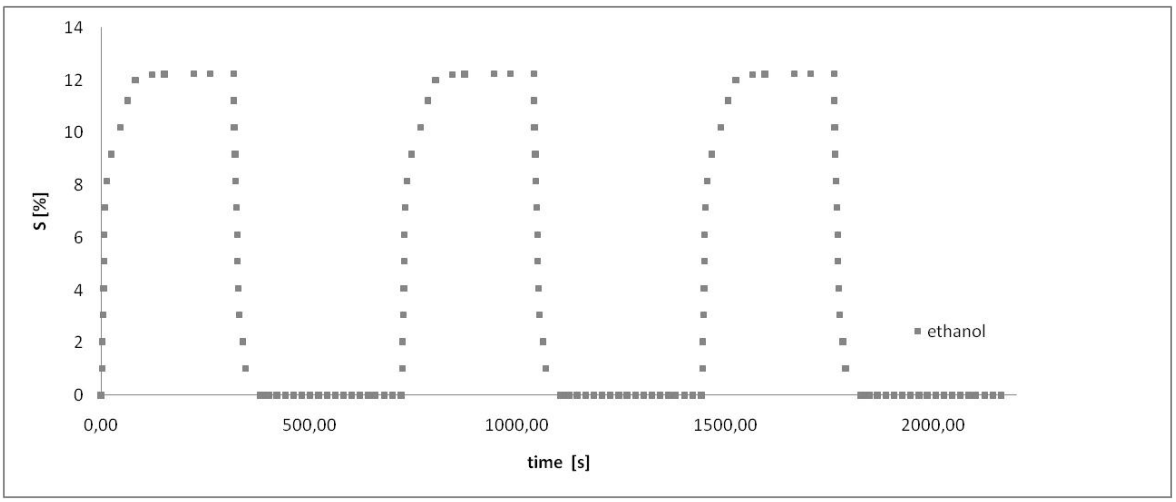

Fig. 3 Three adsorption/desorption cycles of Multiwall carbon nanotubes network exposed to vapors of ethanol.

Conclusions

Multiwall carbon nanotubes were used to prepare CNT network (buckypaper) by vacuum filtration method. Their response to adsorption/desorption cycles were determined as a change of macroscopic resistance. The response to adsorption/desorption was measured as a change of resistance. The surface of buckypaper was treated by RF plasma in different atmospheres, which functionalized their surfaces and changed affinity for the polar and nonpolar organic vapors. The lowest response was found to be 7.86 % in SO_2 plasma, and highest 13.20 in CF_4 for ethanol. Whereas,the lowest response was 11.00 % in O_2 plasma, and the highest 14.44 in Ar for heptane. The sensitivity had limited efficiency, since only the upper most layers of bucky paper underwent surface modificationHowever, we found that CNT network has good sensitivity and assumed selectivity defined by pressures of saturated vapors of used organic solvents. And more, we found that measured response had a good reversibility.

Acknowledgement

This project was supported by the internal grant of TBU in Zlín No. IGA/3/FT/11/D funded from the resources of specific university research. This article was also created with support of Operational Programme Research and Development for Innovations co-funded by the European Regional Development Fund (ERDF) and national budget of Czech Republic within the framework of the Centre of Polymer Systems project (reg.number: CZ.1.05/2.1.00/03.0111) and by the Czech Ministry of Education, Youth and Sports project (MSM 7088352101). Thank you Janez Trtnik for technical support.

REFERENCES

[1] Smajda R, Kukovecz A, Konya Z, Kiricsi I. Structure and gas permeability of multi-wall carbon nanotube buckypapers. Carbon 2007;45(6):1176-1184.
[2] Agnihotri S, Mota JPB, Rostam-Abadi M, Rood MJ. Theoretical and experimental investigation of morphology and temperature effects on adsorption of organic vapors in single-walled carbon nanotubes. J Phys Chem B 2006;110(15):7640-7647.
[3] Romanenko A I, Anikeeva OB, Kuznetsov VL, Buryakov TI, Tkachev EN, Usoltseva AN. Influence of helium, hydrogen, oxygen, air and methane on conductivity of multiwalled carbon nanotubes. Sensor Actuat A-Phys 2007;138(2):350-354.
[4] Qureshi A, Kang WP, Davidson JL, Gurbuz Y. Review on carbon-derived, solid-state, micro and nano sensors for electrochemical sensing application. Diam Relat Mater 2009;18(12):1401-1420.
[5] Hussain CM, Saridara C, Mitra S. Microtrapping characteristics of single and multi-walled carbon nanotubes. J Chromatogr A 2008;1185(2):161-166.
[6] Tournus F, Latil S, Heggie MI, Charlier JC. pi-stacking interaction between carbon nanotubes and organic molecules, Phys Rev B 2005;72(7):Article Number 075431.
[7] Mowbray DJ, Morgan C, Thygesen KS. Influence of O-2 and N-2 on the conductivity of carbon nanotube networks. Phys Rev B 2009;79(19):Article Number 195431.
[8] P. Slobodian**,** P**.** Riha, A. Lengalova, P. Svoboda and P. Saha, Multi-wall carbon nanotube networks as potential resistive gas sensors for organic vapor detection, Carbon, Volume 49, Issue 7, June 2011, Pages 2499-2507
[9] Slobodian, P, Riha P, Lengalova A, Saha P, Compressive stress-electrical conductivity characteristics of multiwall carbon nanotube networs. Journal of Materials Science. Volume 46, Issue 9 (2011), Page 3186
[10] P. Slobodian, P. Riha, A. Lengalova, P. Svoboda, P. Saha, Multi. Journal of Materials Science. Volume 46, Issue 9 (2011), Page 3186
[11] Uwe Vohrer, Justin Holmes, Zhonglai Li, AunShih Teh, Pagona Papakonstantinou, Manuel Ruether and Werner Blau, Tailoring the Wettability of Carbon Nanotube Powders, Bucky paper and Vertically Aligned Nanofires, Design, Synthesis and Grown of the Nanotubes for Industrial Technology,

Thin sensitive layer base on Multiwalled carbon nanotube/polypyrrole composite as a potential gas sensor

ROBERT OLEJNIK[1,2a], PETR SLOBODIAN[1,2b], SHAWQI ALMAJDALAWI[1c]

[1] Faculty of Technology

Tomas Bata University in Zlin

náměstí T. G. Masaryka 275, 762 72 Zlín

CZECH REPUBLIC

[2]Centre of polymer systems

Nad Ovčírnou 3685, 760 01 Zlín

CZECH REPUBLIC

[a]rolejnik@volny.cz, [b]slobodian@ft.utb.cz,[c]shawqimajd@gmail.com

Abstract: - Multi-walled carbon nanotubes networks (MWCNTs) and MWCNT/polypyrrole composite were used as a sensitive layer for organic vapour detection. The sensor detects volatile organic compounds (VOC). The gas sensing is measured by means of macroscopic electrical resistance. The selected solvents have different vapour pressure polarity and donor acceptor behaviour. The electrical resistance of MWCNTs increases when exposed to organic solvent vapours, and reversible reaction is observed when the MWCNT is removed from the vapours. On the other hand, MWCNT/PPy composite creates the donor acceptor interaction between organic vapours molecule. This composite has positive response for electron acceptor vapours such as toluene and hexane and negative response for electron donor such as methanol and acetone

Key-Words: - Carbon nanotube/polypyrrole composite, thin layer, sensing element, interdigitate electrode

1 Introduction

Gas sensors, or chemical sensors, are attracting interest because of their widespread applications in industry, environmental monitoring, space exploration, biomedicine, and pharmaceutics. Gas sensors with high sensitivity and selectivity are required for leakage detections of explosive gases such as hydrogen, and for real-time detections of toxic or pathogenic gases in industries. There is also a strong demand for the ability to monitor and control our ambient environment, especially with the increasing concern of global warming. Researchers from NASA are seeking the use of high-performance gas sensors for the identification of atmospheric components of various planets. In addition, nerve-gas sensing for homeland security is also at the centre of public concern [1]. Generally, there are several basic criteria for good and efficient gas sensing systems: (i) high sensitivity and selectivity; (ii) fast response time and recovery time; (iii) low analyst consumption; (iv) low operating temperature and temperature independence; (v) stability in performances. Commonly used gas sensing materials include vapour-sensitive polymers, semiconductor metal oxides, and other porous structured materials such as porous silicon [2–4]. Since the most common gas sensing principle is the adsorption and desorption of gas molecules on sensing materials, it is quite understandable that by increasing the contact interfaces between the analytes and sensing materials, the sensitivity can be significantly enhanced. The recent

ISBN: 978-1-61804-119-7

development of nanotechnology has created huge potential to build highly sensitive, low cost, portable sensors with low power consumption. The extremely high surface-to-volume ratio and hollow structure of nanomaterials is ideal for gas molecules adsorption and storage. Therefore, gas sensors based on nanomaterials, such as carbon nanotubes (CNTs), nanowires, nanofibres, and nanoparticles, have been widely investigated. Since carbon nanotubes were firstly discovered by Iijima in 1991 [5], they have drawn the most research interests because of their unique geometry, morphology, and properties. Their preparation, properties (such as electronic, mechanical, thermal, and optical properties), and applications on various fields are all being studied intensely. Theoretical and simulation works have also been conducted to understand this nanoscale material and related phenomenon [6].

Polyppyrole is one representant of conductive polymer, which could be used as a sensing layer. There are a lot of method of preparation the composite layer for example coating or polymerization in present of carbon nanotubes.[10]

In this work, a new type of gas sensing element is presented. The sensing element was made by drop deposition method of aqueous dispersion of multi-walled carbon nanotubes and MWCNT/Ppy composite. The drop was evaporated and the network was created. The dispersion was located on the active surface of interdigitated electrode. The interdigitated electrode was made by the etching method. The response for four different solvent was measured . Responses to adsorption/desorption cycles were determined as the change of macroscopic resistance. MWCNTs and MWCNT/Ppy have good sensitivity and assumed selectivity defined by pressures of saturated vapors of the used organics solvents and also MWCNT/PPy specific react with electron donor and acceptor organic molecules. Finally, it was found that measured response has good reversibility.

2 Problem Formulation

Organic vapours sensing elements could be used in many industrial, medical and commercial applications. Most gas or vapours sensors which are available today operate by measuring the impedance of capacitor coated with gas responsive polymer or ceramic.[11]

Carbon nanotubes as a gas sensor have strong interest for researchers and practical application. Carbon nanotubes have specific response for specific gases or vapors. [12].We used MWCNT and MWCNT/PPy nanocomposite as sensing layers. There are several methods to integrate CNTs to different gas sensor structures. Li et al. developed a resistive gas sensor by simply casting SWCNTs on interdigitated electrodes (IDEs) [9]. This method was used in this work. A board with 35 μm Cu layer was used. The interdigitated electrodes pattern was printed on the board by etching with resistance paint. The pattern was etched for 15 minutes by $FeCl_3$ at room temperature and paint was removed by toluene. Finally, the electrodes were cleaned by absolute ethanol. The aqueous dispersion of carbon nanotubes and MWCNT/PPy was then drop-deposited onto the electrode area. A network of carbon nanotubes and layer of MWCNT/PPy subsequently formed after the evaporation of water. The interdigitated electrodes with both networks were exposed to four different solvents: methanol, acetone, toluene and hexane.

3 Problem Solution

MWCNTs produced by chemical vapour deposition of acetylene were supplied by Sun Nanotech Co. Ltd., China (diameter 10-30 nm, length of 1-10 μm, purity of ≥90% and volume resistivity 0.12 Scm

Carbon nanotubes were used into aqueous pastes using a mortar and a pestle (1.6 g MWCNT and ~ 50 ml deionized water), and diluted with deionized water. Consequently, sodium dodecyl sulfate (SDS) and 1-pentanol were added, and pH was adjusted to 10 using an aqueous solution of 0.1 M NaOH [7]. The final concentration of nanotubes in the suspension was 0.3 wt.%, concentrations of SDS and 1-pentanol were 0.1M and 0.14M, respectively [8]. The dispersion was homogenized using Dr. Hielscher GmbH apparatus (ultrasonic horn S7, amplitude 88 μm, power density 300 W/cm^2,

ISBN: 978-1-61804-119-7

frequency 24 kHz) for 2 hours under a temperature of about 50°C. By this way was prepared the aqueous dispersion. 5 µl of the solution was used for preparation of sensitive layer on the interdigitated electrode surface

0.37g of Carbon nanotube supplied by Sun Nanotech Co. Ltd., China was dispersed in 100 ml H_2O 1.84 g of surfactant CTAB was added and then sonicated by using Dr. Hielscher GmbH apparatus (ultrasonic horn S7, amplitude 88 µm, power density 300 W/cm^2, frequency 24 kHz) for 3 hours. 4mL of the monomer pyrrole was added to the above solution with continuous stirring for 30 min. 100 ml of cooled APS solution was added drop by drop to the solution to start the polymerization with stirring. The temperature of the reaction was kept between 0 – 5 °C. The polymerization process was ended after 2 hours of addition APS solution. 5 µl of the solution was used for preparation of sensitive layer on the interdigitated electrode surface.
The aqueous dispersion of carbon nanotubes and MWCNT/PPy was then drop-deposited onto the electrode area. A network of carbon nanotubes and layer of MWCNT/PPy subsequently formed after the evaporation of water. The interdigitated electrodes with both networks were exposed to four different solvents: methanol, acetone, toluene and hexane.

The SEM analysis fig. 1 well describes the morphology of carbon nanotubes network and multiwall carbon nanotubes/polypyrrole nanocomposite respectively. These materials were drop deposited on the interdigitated electrode after that was measured the resistivity change for four different organic vapors: methanol, acetone, toluene and hexane. The typical adsorption/desorption behavior of CNT network and CNT/PPy composite exposed to/disposed from four different organic vapours is presented in Fig. 3. Fig.2 illustrates the maximum change of parameter S representing sensitivity of both created sensitive layers. The observed behaviour for carbon nanotubes network is probably caused by the physical adsorption of the organic molecules in the space between the carbon nanotubes network and increase the resistance to stable value. On the other hand, desorption causes a decrease in resistance by increasing the amount of contacts in the network of carbon nanotubes.

The sensitivity is defined by this equation $S=(R_g - R_a) /R_a$. Where R_a represents specimen resistance in air and R_g the resistance of specimen exposed to gas/vapor, ΔR denotes the resistance change.

In the case of CNT/PPy nanocomposite is behaviour of sensitive layer influence by physical adsorption or desorption and chemical interaction between polypyrrole and organic molecules which are adsorbed on the surface. Fig. 3 shows the sensitivity response in four consecutive cycles. One adsorption/desorption cycle consists of 6 minutes adsorption and 6 minutes desorption. Experimental data also demonstrates good reversibility of adsorption/desorption processes.

4 Conclusion

The interdigitated electrode pattern was printed on the board by etching resistant paint. The pattern was etched for 15 minutes by $FeCl_3$ at room temperature and paint was removed by acetone. A resistive gas sensor was made by simply casting MWCNTs on interdigitated electrodes. The aqueous dispersion of carbon nanotubes was then drop-deposited onto the electrode area. The network response in adsorption/desorption cycles was determined as a change of macroscopic resistance and interaction between molecules and polypyrrole which was formed on the carbon nanotubes surface. The CNT/PPy composite layer specific react with different kind molecules. This composite has positive response for electron acceptor vapours such as toluene and hexane and negative response for electron donor such as methanol and acetone. These capabilities of these sensing elements predetermine for using as a synthetic nose or sensing array with specific response.
MWCNT network and MWCNT/PPy composite has good sensitivity and assumed selectivity defined by pressures of saturated vapours of the used organics solvent. Finally it was found that measured response has good reversibility and sensitivity.

Acknowledgement

The work was supported by the Operational Program of Research and Development for Innovations co-funded by the European Regional Development Fund (ERDF), the National budget of Czech Republic within the framework of the Centre of Polymer Systems project (Reg. No.: CZ.1.05/2.1.00/03.0111). This article was also supported by the internal grant of TBU in Zlin No.

IGA/FT/2012/022 funded from the resources of Specific University Research.

References:

[1] J. Li, in: Carbon Nanotubes: Science and Applications, edited by M. Meyyappan, CRC Press, Boca Roton, Fla USA (2006)
[2] Z. M. Rittersma: Sensors and Actuators A Vol. 96 (2002) p. 196
[3] R. Fenner and E. Zdankiewicz: IEEE Sensors J. Vol. 1 (2001) p. 309
[4] E. Traversa: Sensors and Actuators B Vol. 23 (1995) p. 135
[5] S. Iijima: Nature vol. 354 (1991) p. 56
[6] M. Meyyappan: Carbon nanotubes: Science and Applications (CRC Press, Boco Raton, Fla, USA (2004)
[7] H.T. Ham, Y.S. Choi, I.J. Chung: Colloid Interf. Sci. Vol. 286 (2005) p. 216
[8] C.S. Chern, L.J. Wu: Polym. Sci. Part A : Polym. Chem. Vol. 39 (2001) p. 3199
[9] J. Li, Y. Lu, Q. Ye, et. al.: Nano letters Vol. 3 (2003) p. 929
[10] Junhua Fan, Meixiang Wan, Doaben Zhu, Baohe Chang, Zhenwei Pan, Sishen Xie, Synthesis, Journal of Applied Polymer Science, Vol. 74,(1999) p. 2605-2610
[11] Keat Ghee Ong, Kefeng Zeng, Craing A. Grimes, IEEE sensors journal, vol. 2, no. 2, april 2002
[12] M. Lucci, A. Reale, A. Di Carlo, S. Orlanducci, E. Tamburri, M. L. Terranova, L. Davoli, C. Di Natala, A. Damico, R. Palesse, Sensors and actuators B vol. 118 (2006) p. 226-231

APPENDIX

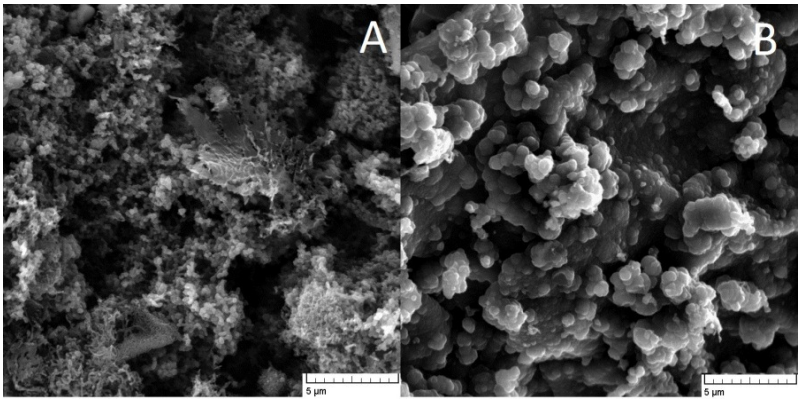

Fig.1 A)SEM analysis of MWCNT/Ppy composite created by evaporation dispersion on the surface of interdigitated electrode B) SEM analysis of CNT network on the surface of interdigitate electrode.

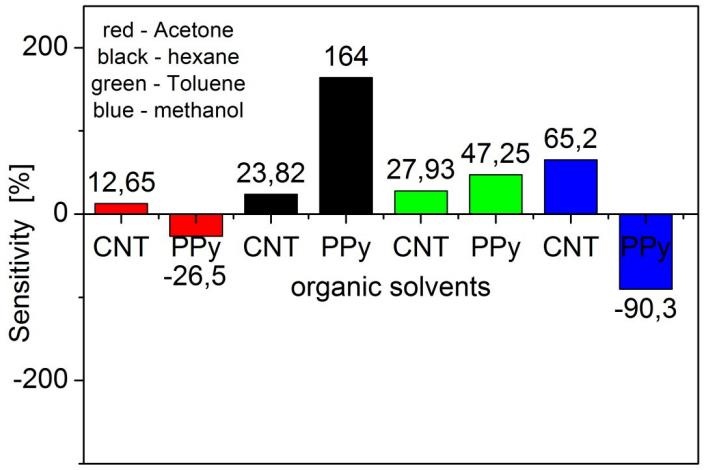

Fig. 2 The maximum *S* values for four different organic solvent and for carbon nanotubes network and CNT/PPy composite sensitive layer.

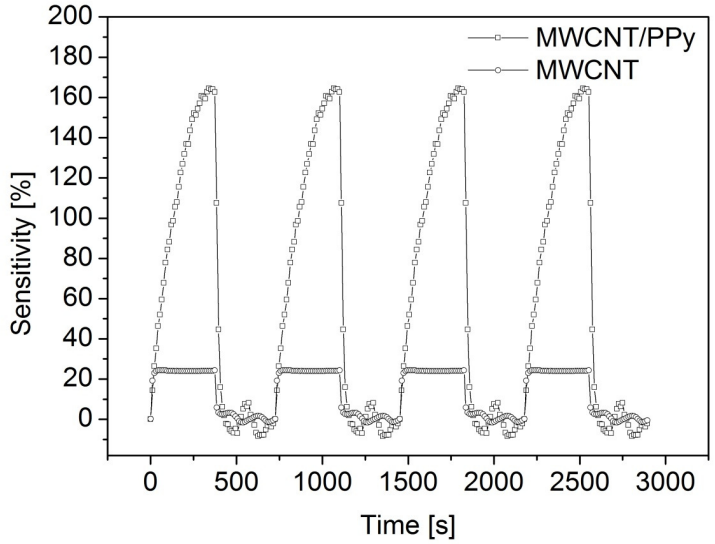

Fig. 3 Sensitivity change of CNT network and CNT/PPy nanocomposite exposed to saturated hexane vapors in four adsorption/desorption cycles.

ISBN: 978-1-61804-119-7

Characterization of Carbon Nanotube Based Polymer Composites Through Rheology

Robert Olejnik[a*], Pengbo Liu[a,b], Petr Slobodian[a], Martin Zatloukal[a], Petr Sáha[a]

[a]*Tomas Bata University in Zlín, Faculty of Technology, T.G.M. 275, 762 72 Zlín, Czech Republic*

rolejnik@volny.cz

[b]*Sichuan University, State Key Laboratory of Polymer Materials Engineering of China*

Abstract. Poly(methyl methacrylate)/Multi-wall carbon nanotubes (MWCNT) nanocomposites were prepared by solution method. Here the dispersions of MWCNT in PMMA solutions were sonicated for appropriate time followed by dispersions coagulation. Both types of CNT materials were used such as pure MWCNT and the same MWCNT after their adequate surface treatment. The aim of treatment was to covalently attach organic material onto surface of CNT to process their better dispersion in polymeric matrix leading to more effective CNT reinforcement effect. The state of CNT dispersion was characterized thought rheology measurements with help of parameters like elasticity and viscosity of the melt. Also the effect of sonication onto pure PMMA matrix was determined.

Keywords: carbon nanotubes, polymer composites, rheology
PACS: 81.05.Qk, 81.05.Tp

EXPERIMENTAL

At the first step MWCNT were oxidized in mixture of sulfuric and nitric acids [1]. In the next step 4,4′-methylenebis(phenyl isocyanate) (MDI) and methacrylamide were used to synthesize so called "CNT-mer" [2] forming active polymerizable vinyl groups on CNT surface which are able to incorporate CNT into growing PMMA polymer chain during consequential radical solution polymerization.

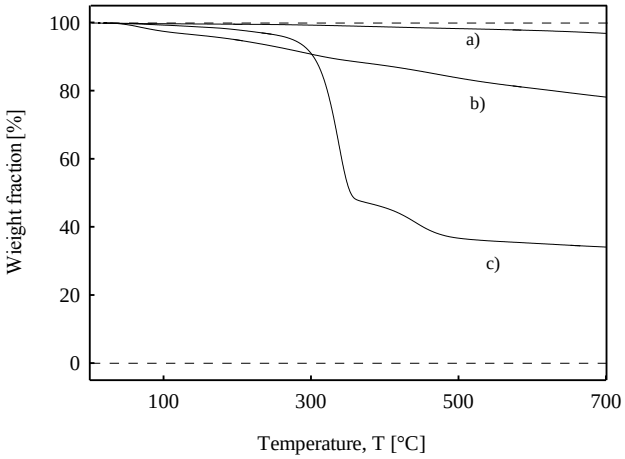

FIGURE 1. Thermogravimetric analysis of as-received MWCNT (a), oxidized MWCNT (b) and MWCNT grafted by the MDI binding agent and PMMA (c).

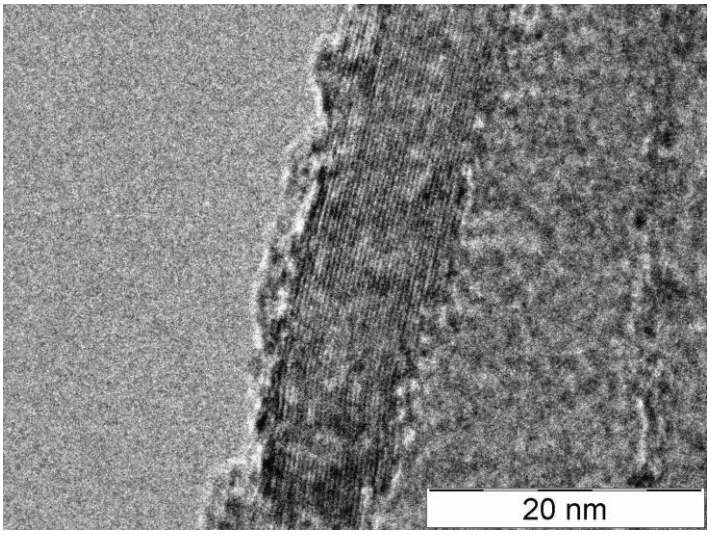

FIGURE 2. TEM morphology of MWCNT surface treated tube. The image shows one wall of MWCNT tube assembled from ~25 of individual graphitic layers with distance between particular layer ~0.35 nm covered by grafted organic layer with thickness ~3.5nm.

Prepared surface treated filler was separated by ultracentrifugation and finally mixed into PMMA commercial polymer (DELPET 80N, Asahi Kasei Corporation) by solution method as was announced above. The CNT dispersion in methylethyl ketone (MEK) with concentration from 0.1, 0.5, 1.0 to 2.0 wt. % of CNT were prepared by sonication using thermostatic ultrasonic bath (Bandelin electronic DT 103H) at 70°C for 4 or 8 hours followed by additional 2 hours using ultrasonic homogenized (Dr. Hielscher GmbH apparatus with ultrasonic horn, S7) at 60°C. The coagulation was performed by pouring of prepared dispersions into mixer filled by antisolvent - water.

The states of prepared composites were characterized thought rheology measurements using the Advanced Rheometric Expansion System (ARES 2000) Rheometrics rheometer in terms of complex viscosity and recoverable shear. In the first step, the effect of sonication time on the complex viscosity of PMMA has been investigated (see Figure 3). It is clearly visible that increase in the sonication time leads to decrease in complex viscosity which can be taken as evidence that the PMMA degradates during the sonication process. In the second step, the effect of CNT content in the PMMA melt on its elasticity (recoverable shear) has been investigated (see Figure 4). Obviously, the increase in the CNT level in the PMMA matrix leads to increase in the PMMA melt elasticity. Finally, the effect of the CNT surface modification, which is described above, on the PMMA melt elasticity has been analyzed through recoverable shear (see Figure 5). In this case, the surface modified CNT in the PMMA matrix enhances the melt elasticity more than no surface modified CNT which suggest that the suggested CNT surface modification might be good tool to improve the interaction between CNT and PMMA polymer matrix.

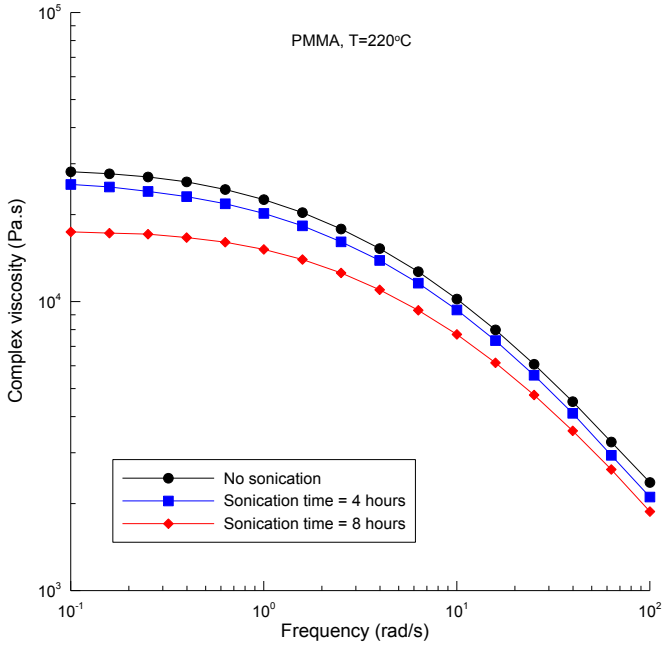

FIG. 3 Effect of the sonication time on the frequency dependent complex viscosity for PMMA polymer melt.

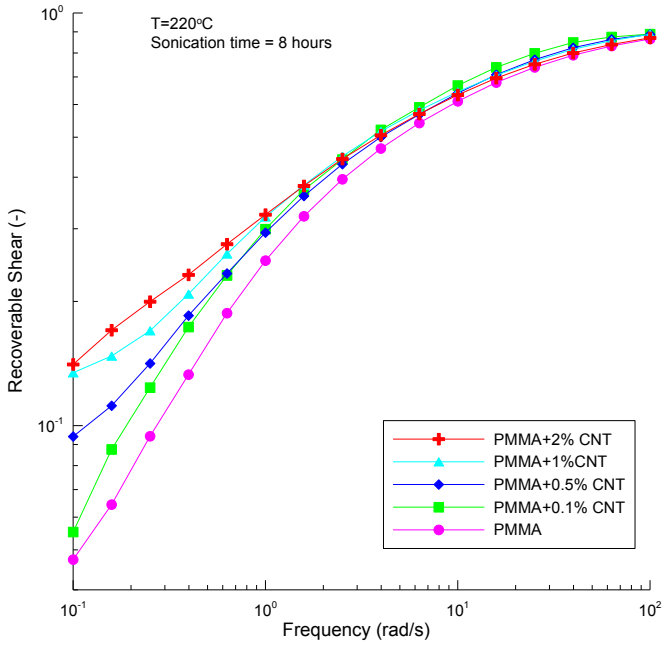

FIG. 4 Effect of the CNT content in the PMMA melt on the recoverable shear.

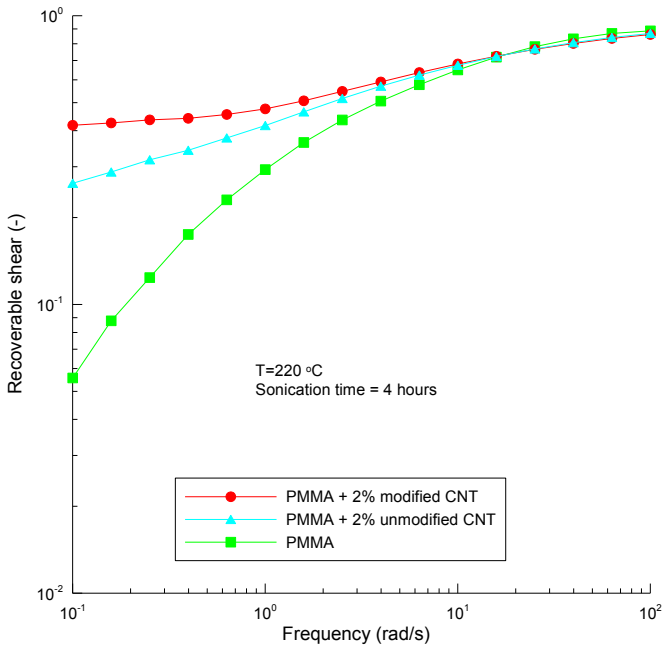

FIG. 5 Effect of the CNT surface modification on the recoverable shear for CNT+PMMA composite.

Conclusion

Based on the rheological evaluation of the tested polymer samples, it has been found that, firstly, sonication of the PMMA can leads to degradation. Secondly, the increase of the CNT content in the CNT+PMMA may leads to enhanced melt elasticity and finally, modification of the CNT surface can increase the CNT+PMMA melt elasticity more than surface no modified CNT.

ACKNOWLEDGMENTS

The financial support by project MSM 7088352101 is gratefully acknowledged.

REFERENCES

1. A. Rasheed, J.Y. Howe, M.D. Dadmun, P.F. Britt, **45**, 1072-1080 (2007).
2. J.U. Ha, M. Kim, J. Lee, S. Choe, I.W. Cheong, S.E. Shim, *J. Polym. Sci.: Part A-Polym. Chem.* **44**, 6394-6401 (2006).

Improved selectivity of oxidized multiwall carbon nanotube network for detection of ethanol vapor

DANIEL Matejik [1,a], ROBERT Olejnik [1,b], PETR Slobodian [1,c] and PETR Saha[1]

[1]Centre of Polymer Systems, Faculty of Technology, Tomas Bata University in Zlín, nám. T.G.Masaryka 555, 760 05 Zlín, Czech Republic

[a]matejikdaniel@gmail.com, [b]rolejnik@volny.cz,[c]slobodian@ft.utb.cz

Keywords: Carbon nanotube network, sensor, Buckypaper, Electrical resistance

Abstract

Two kinds of Multiwall carbon nanotubes (MWCNT) networks "Buckypaper" were made by the vacuum filtration method of MWCNT aqueous suspension. The first one was prepared from pure CNT and the second from its oxidized form by acidic $KMnO_4$ as oxidizing agent. The CNT oxidation increase content of oxygen bonded to the surface of CNT decreasing their hydrophobic character. The sensitivity of MWCNT networks to two kind of organic solvent vapors (ethanol and hepane) has been investigated by resistance measurements. The solvents had different polarities given by Hansen solubility parameters and nearly the same volume fractions of saturated vapors at the condition of experiment. CNT oxidation significantly increases the sensitivity of CNT resistive sensor to vapors of ethanol and decrease response to heptane vapors. The present paper demonstrates the effective way how to add proper selectivity for organic vapor detection.

Introduction

Carbon nanotubes (CNTs) have raised much interest during the recent years due to their inherent extraordinary electrical and mechanical properties [1]. Both principal types of CNT - MWCNT (multi-wall) and show remarkable sensitivity to the change of chemical composition of the surrounding environment. Gas and vapor adsorption as well as desorption usually proceeds at high rates and amounts [2]. This property is favorable for their use in the form of membranes [3], adsorbents [4] or gas sensors [5,6]. It was found that so called "Buckypaper", network prepared from entangled CNT by vacuum filtration can detect organic vapor in air [7].

The oxidation of CNTs has gained a lot of attention in an attempt to purify and also enhance the chemical reactivity of the graphitic network. Typically, through the above harsh treatments, the pristine CNTs can be effectively purified and oxygen-containing groups, mainly carboxyl and hydroxyl, have been found to decorate the graphitic surface [1]. The quality of dispersions for filtration, porosity of prepared buckypaper anyhow tube-tube interactions can by purposely influenced by the proper surface functionalozation such as for example oxidation. There was found that the increasing oxygen content on the surface of CNT leads to buckypaper with more uniform pore structure and dense morphology with lower porosity. It indicates better tube dispersion in the aqueous suspension during filtration process when tubes are deposited as more individualized tubes or as a smaller CNT agglomerates [8].

Even if carbon nanotubes are presently used in indication of gases [9,10], the sensors are quite expensive and difficult to produce. Simpler and cheaper ways to detect gases can be reflected in practical application of described principle. Finally, the present work describes increased sensitivity and achieved selectivity to vapors of ethanol by CNT oxidation.

Experimental

MWCNTs produced by chemical vapor deposition were supplied by Bayer Material Science AG, Germany (diameter 5-20nm, length 1-10μm, C-purity > 99% and bulk density 140-230kg/m^3) [11].

MWCNT networks, "Buckypaper" (MWCNT-N), were prepared by CNT dispersions vacuum filtration thought polyurethane submicron size porous membrane. The formed disk-shaped networks were washed several times by deionized water and methanol in situ, then removed and dried between filter papers at RT. The method of CNT network preparation was several times optimized in aim to achieve uniform and smooth network.

The oxidized material was prepared by following procedure: glass reactor, 300 cm^3 of 0.5M H_2SO_4, 1.5g of $KMnO_4$ and 0.5g of MWCNTs, the dispersion sonicated at 40°C using UP-400S Dr. Hielsher GmbH Apparatus (ultrasonic horn H7, amplitude μm, power density 300W/ cm^3, frequency 24 kHz) for one hour at 50% power of the apparatus and in 50% pulse mode, the product was filtered and washed with concentrated HCl to remove MnO_2.

Results

Fig. 1 represents SEM analyses of upper surfaces of prepared CNT networks on the course of CNT dispersion optimalization. 2a) presents paper fabricated from CNT dispersion prepared by only sonication, 2b) milling of CNT agglomerates before sonication and finally 2c) when milled and sonicated dispersion was centrifuged. Part 2b) represents upper surfaces of CNT network made from $KMnO_4$ oxidized tubes. For next testing of CNT-N structures for gas detection only papers c) and d) were used.

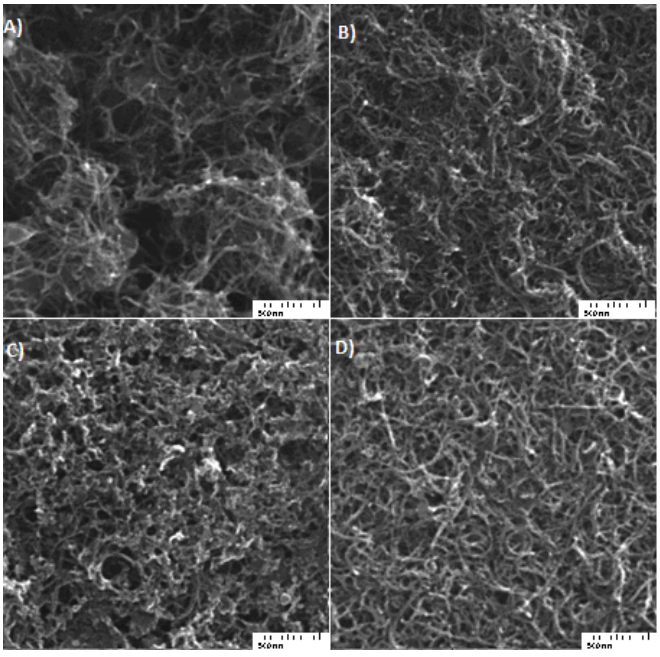

Fig. 1 Upper surfaces of prepared CNT networks made by SEM analyses.

The strips made of CNT networks were exposed to the vapors of two different solvents, adsorbates, (heptane, ethanol). The conditions were 25 °C and each adsorption/desorption cycles was 6 minute long. Saturated vapor pressures, p_i, define corresponding volume fractions, x_i. according Eq. 1. where p_A represents air pressure. Calculated values of x_i at experimental conditions are 7.71 % vol. % for ethanol and 6.0 % vol. % for heptane.

$$x_i = \frac{p_i}{p_A} \tag{1}$$

The data in Fig. 2 a) represent two adsorption to/desorption from cycles for specimens made of pure CNT networks exposed to ethanol and heptane. Then Fig. 1 part b) demonstrate analogical data for network made of oxidized tubes. Over all, the adsorption of organics molecules increase resistance with time, which is presented in the figure as sensitivity or gas response, *S*, defined by Eq. 2.:

$$S = \frac{R_g - R_a}{R_a} = \frac{\Delta R}{R_a} \tag{2}$$

Here R_a represents specimen resistance in air and R_g resistance of the specimen exposed to gas/vapor, ΔR stands for the resistance change. It demonstrates that MWCNT network is sensitive to heptane and ethanol vapors. The curves also presents specific course of adsorption to/desoption form which is reversible and repeatable (5 different specimens were tested for each composition). Finally, part d) presents achieved selectivity of the sensor; when significant increase in sensitivity to ethanol was measured in contrast to decrease of *S* to heptane.

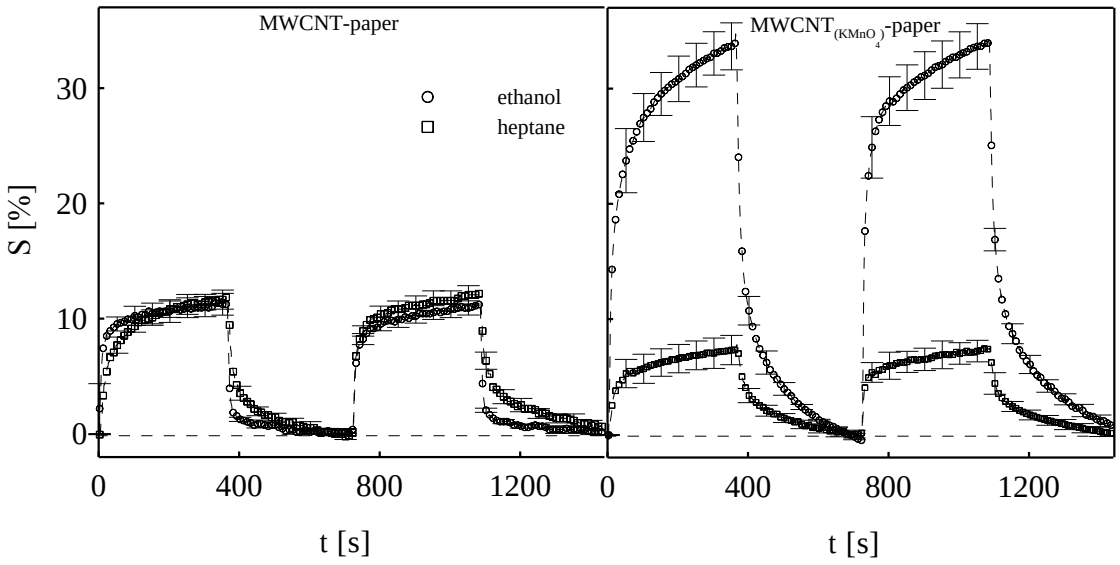

Fig. 2 Two adsorption/desorption cycles for MWCNT-N (open symbols) and MWCNT-N($KMnO_4$) (filled symbols) exposed to vapors of heptane and ethanol.

The increased sensitivity is probably caused by CNT oxidation when there should be better affinity of the tubes to more polar ethanol in contrary to nonpolar heptane (Hildebrand solubility parameter, δ_t: heptan = 7,5 $Mpa^{1/2}$, ethanol = 26,5 $Mpa^{1/2}$). X-ray spectroscopy (EDX) proved increase of oxygen content on the surface of CNT from 4.86 at. % on MWCNT-N to 21.26% on MWCNT-N($KMnO_4$).

Conclusions

Multiwall carbon nanotubes were used in their pure and oxidized form to prepare entangled networks (buckypaper) whose response to two organic solvent vapors was measured on the base of

electrical resistance. The results show that the prepared materials are capable to detect vapors in the air. The CNT network can be considered as potential material for application as cheap and easy to prepare micro-sized vapor sensing element, which is sensitive, selective, reversible and reproducible. The sensor sensitivity to ethanol vapors was effectively improved by CNT proper oxidation by acidic $KMnO_4$.

Acknowledgment

This project was supported by the internal grant of TBU in Zlín No. IGA/3/FT/11/D funded from the resources of specific university research. This article was also created with support of Operational Programme Research and Development for Innovations co-funded by the European Regional Development Fund (ERDF) and national budget of Czech Republic within the framework of the Centre of Polymer Systems project (reg.number: CZ.1.05/2.1.00/03.0111) and by the Fund of the Institute of Hydrodynamics AV0Z20600510.

Reference

[1] V. Datsyuka, M. Kalyvaa, K. Papagelisb, J. Partheniosa, D. Tasisb, A. Siokoua, I. Kallitsisa,c, C. Galiotisa, *Chemical oxidation of multiwalled carbon nanotubes.* Carbon 46 (2008) 833-840.

[2] Hussain C.M., Saridara C., Mitra S., *Microtrapping characteristics of single and multi-walled carbon nanotubes*. J Chromatogr A 2008;1185(2):161-166.

[3] Smajda R., Kukovecz A., Konya Z., Kiricsi I., *Structure and gas permeability of multi-wall carbon nanotube buckypapers.* Carbon 2007;45(6):1176-1184.

[4] Agnihotri S., Mota J.P.B., Rostam-Abadi M., Rood M.J., *Theoretical and experimental investigation of morphology and temperature effects on adsorption of organic vapors in single-walled carbon nanotubes*. J Phys Chem B 2006;110(15):7640-7647.

[5] Romanenko A.I., Anikeeva O.B., Kuznetsov V.L., Buryakov T.I., Tkachev E.N., Usoltseva A.N., *Influence of helium, hydrogen, oxygen, air and methane on conductivity of multiwalled carbon nanotubes.* Sensor Actuat A-Phys 2007;138(2):350-354.

[6] Qureshi A., Kang W.P., Davidson J.L., Gurbuz Y., *Review on carbon-derived, solid-state, micro and nano sensors for electrochemical sensing application*. Diam Relat Mater 2009;18(12):1401-1420.

[7] P. Slobodian, P. Riha, A. Lengalova, P. Svoboda, P. Saha, *Multi-wall carbon nanotube networks as potential resistive gas sensors for organic vapor detection*, Carbon (2011) 49 2499-2507.

[8] Kastanis D., Tasis D., Papagelis K., Parthertios J., Tsakiroglou C., Galiotis C., *Oxidized multi-walled carbon nanotube film fabrication and characterization*, Adv Compos Lett 16(6) (2007) 243-248.

[9] Niu L., Luo Y.L., Li Z.Q., A *highly selective chemical gas sensor based on functionalization of multi-walled carbon nanotubes with poly(ethylene glycol)*. Sensor Actuat B-Chem 2007;126(2):361-367.

[10] Lobotka P., Kunzo P., Kovacova E., Vavra I., Krozanova Z., Smatko V., Stejskal J., Konyushenko E.N., Omastova M., Spitalsky Z., Micusik M., Krupa I., *Thin polyaniline and polyaniline/cabon nanocomposite films for gas sensing*, Thin Solid Films 519 (2011) 4123-4127

[11] Baytubes, Bayer MaterialSience, on line (cit.1.4.2011) <http://www.baytubes.com/jp/downloads/datasheet_baytubes_c_150_hp.pdf>

ELECTRICALLY CONDUCTIVE HIGH ELASTIC POLYURETHANE/CARBON NANOTUBE ENTANGLED NETWORK FILM COMPOSITE WITH STRAIN SENSING POTENTIAL

Petr SLOBODIAN[a,b*], Robert OLEJNIK[a,b], Petr Saha[a,b]

[a]*Polymer Centre, Faculty of Technology, Tomas Bata University in Zlin, T.G.M. 275, 76272 Zlin, Czech Republic*

[b]*Centre of Polymer Systems, University Institute, Tomas Bata University, Nad Ovcirnou 3685, 76001 Zlin, Czech Republic*

**e-mail: slobodian@ft.utb.cz*

Abstract

Actual development in science of carbon nanotube (CNT) structures demonstrates their potential in the field of sensing technology as novel types of sensors [1] or as a part of so called self sensing structural composites [2,3]. These revolutionary materials are capable to detect deformation which is directly connected with macroscopic resistance change of CNT based sensoric unit. Over all, it is usually found that these materials are enough sensitive to strain or stress, sensing can be performed in real-time [4,5] and the process is reversible although some irreversibility fractions are also detected as hysteresis loops in cyclic loading tests [6,1] or as a residual part of sensitivity which remains after specimen is unloaded [3,5,7].

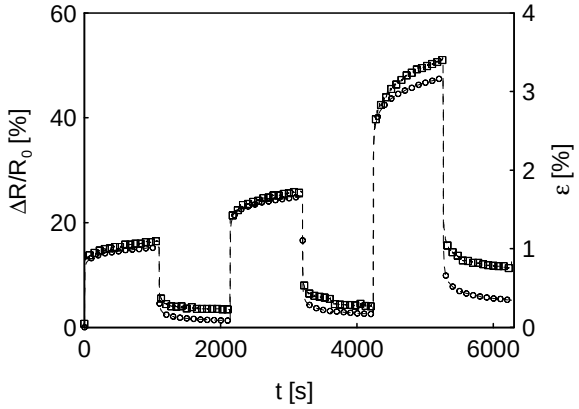

Fig. 1 Response of the relative resistance change and strain of MWNT/TPU composite to the stepwise increase of tensile stress. The strain values are denoted by circles, the relative resistance change by squares.

Thermoplastic polyurethane elastomer (TPU)/MWCNTs network (Buckypaper) composite was prepared and tested as tensile strain sensing element by its macroscopic resistance change measurements. In the first step MWCNT aqueous dispersion was filtered thought TPU filtering membrane prepared by technology of electrospinning. The filtering membrane remains as a part of final composite when this filter-supported CNT network is attached to the surface of TPU tensile test specimens by technology of compression molding and the filter is transformed to TPU adhesive film. In the present contribution the principle of strain sensing by macroscopic resistance change of TPU/MWCNT network composite is reflected. It was found that macroscopis resistance change of this sensoric unit is sensitive, repeatable and reproducible. The capability of our structure to remain its electrical properties at extreme deformation was also tested. The testing has shown as much as 400 % composite extension and more than 270-fold resistance increase. Moreover, the composite resistance is well recoverable upon removal of the load. It indicates favorable properties of the composite for its use as a highly deformable strain sensing element, a strain-electric signal transducer, electromagnetic field shielding and lightning protection.

ACKNOWLEDGMENT

This article was created with support of Operational Programme Research and Development for Innovations co-funded by the European Regional Development Fund (ERDF) and national budget of Czech Republic within the framework of the Centre of Polymer Systems project (reg.number: CZ.1.05/2.1.00/03.0111) and the Czech Ministry of Education, Youth and Sports project (MSM 7088352101).

REFERENCES

[1] P. Slobodian, P. Riha, R. Olejnik. *Electromechanical sensors based on carbon nanotube networks and their polymer composites*, in New Developments and Applications in Sensing Technology, 1st Edition., Springer, **2011**, 337 p., ISBN: 978-3-642-17942-61.

[2] E. Bilotti, R. Zhang, H. Deng, M. Baxendale, T. Peijs, *Fabrication and property prediction of conductive and strain sensing TPU/CNT nanocomposite fibres,*JOURNAL OF MATERIALS CHEMISTRY 20(42) **2010**, 9449-9455.

[3] G.T. Pham, Y.B. Park, Z. Liang, C. Zhang, B. Wang, *Processing and modeling of conductive thermoplastic/carbon nanotube films for strain sensing*, COMPOSITES PART B-ENGINEERING 39(1) **2008**, 209-216.

[4] E.T Thostenson, T.W. Chou, *Real-time in situ sensing of damage evolution in advanced fiber composites using carbon nanotube networks*, NANOTECHNOLOGY 19(21) **2008**, Article Number: 215713.

[5] I.P. Kang, M.J. Schulz, J.H. Kim, V. Shanov, D.L. Shi, *A carbon nanotube strain sensor for structural health monitoring*, SMART MATERIALS & STRUCTURES 15(3) **2006**, 737-748.

[6] M.D. Rein, O. Breuer, H.D. Wagner, Sensors and sensitivity: *Carbon nanotube buckypaper films as strain sensing devices Sensors and sensitivity: Carbon nanotube buckypaper films as strain sensing devices*, COMPOSITES SCIENCE AND TECHNOLOGY 71(3) **2011**, 373-381.

[7] P. SLOBODIAN, P. RIHA, A. LENGALOVA, R. OLEJNIK, P. SAHA. *Effect of compressive strain on electric resistance of multi-wall carbon nanotube networks Journal of experimental nanoscience*, **2011**, Volume 6 Issue 3, 294. June 2011

Effect of functionalized nanotubes with HNO_3 on electrical sensory properties of carbon nanotubes/polyurethane composite under elongation

SLOBODIAN PETR [a,b], OLEJNIK ROBERT [a,b], RIHA PAVEL [c], SAHA PETR [a,b]

[a]Polymer Centre, Faculty of Technology
Tomas Bata University in Zlin
T.G.M. 275, 762 72 Zlin
CZECH REPUBLIC

[b]Centre of Polymer Systems, University Institute,
Tomas Bata University
Nad Ovcirnou 3685, 760 01 Zlin
CZECH REPUBLIC

[c]Institute of Hydrodynamics
Academy of Sciences
Pod Patankou 166 12 Prague
CZECH REPUBLIC

slobodian@ft.utb.cz http://web.ft.utb.cz/

Abstract: Thermoplastic polyurethane elastomer PU/MWCNT-N network (Buckypaper) composite was prepared and tested as tensile strain sensing element by measurement of its macroscopic resistance. In the first step MWCNTs aqueous dispersion was filtered thought PU filtering membrane prepared by technology of electrospinning. The filtering membrane remains as a part of final composite when this filter-supported MWCNT-N network is attached to the surface of PU tensile test specimens by technology of compression molding and the filter is transformed to form of PU adhesive film. The composite can sustain large deformation and the stain can be effectively detected by resistance measurement in real time of deformation. The response is sensitive, reversible and repeatable. Finally, the sensitivity of PU/MWCNT-N sensoric unit was significantly improved by CNT oxidation by HNO_3 acid. This enhancement was quantified by Gauge factor, GF. Its value, for example, increase from 9.5 at tensile strain ~9% for pure network to 23.1 for network made of oxidized tubes measured at the same strain.

Key-Words: Carbon nanotubes, Oxidation, Flexible composites, Strain sensor, Gauge factor, Resistance

1 Introduction

Actual development in science of carbon nanotube (CNT) structures demonstrates their potential in the field of sensing technology as novel types of sensors [1] or as a part of so called self sensing structural composites [2,3] for applications like "health monitoring" of the composites structures. These revolutionary materials are capable to detect deformation which is directly connected with macroscopic resistance change of CNT based sensoric unit. Over all, it is usually found that these materials are enough sensitive to strain or stress, sensing can be performed in real-time [4,5] and the process is reversible although some irreversibility fractions are also detected as hysteresis loops in cyclic loading tests [6,1] or as a residual part of sensitivity which remains after specimen is unloaded [3,5,7].

ISBN: 978-1-61804-046-6

2 Problem Formulation

The purpose of this study is to investigate the change of electrical resistance of PU/MWCNT-N composite in extension/relaxation. The macroscopic resistance change of the composite is monitored by a two-point technique under tensile loading. The changes in resistance are apparently due to straining of the CNT network, which may include nanotube slippage, delamination and damage; the network cracking may cause breaks of portion of electric circuit with the applied stress. Finally, the effect of CNT oxidation by HNO_3 onto sensory properties is focused. This chemical functionalization is capable significantly influence properties of prepared CNT entangled structure (Buckypaper). The different state of CNT deagglomeration in aqueous dispersion can lead to different porosity of prepared CNT networks. Incorporation of oxygenated functional groups change contact resistance between crossing tubes. Both variables can play important role in sensory unit sensitivity defined by Gauge factor.

3 Problem Solution

Purified MWCNT produced by chemical vapor deposition of acetylene were supplied by Sun Nanotech Co. Ltd., China. According to the supplier, the nanotube diameter is 10-30 nm, length 1-10 μm, purity >90% and (volume) resistivity 0.12 Ωcm. Further details on the nanotubes and the results of TEM analysis can be found in our paper [8]. The oxidized material was prepared in a glass reactor with a reflux condenser filled with 250 cm^3 of 5M HNO_3 with 2g of MWCNTs and refluxed at 140°C for 2 hours, then filtered, washed and dried. Both types of nanotubes were used for the preparation of aqueous pastes: 1.6 g of MWCNT and ~50 ml of deionized water were mixed with the help of a mortar and pestle. The paste was then diluted in deionized water with sodium dodecyl sulfate (SDS) and 1-pentanol. Consequently, NaOH aqueous solution was added to adjust pH to the value of 10. The final nanotube concentration in the suspension was 0.3 wt.%, concentration of SDS and 1-pentanol 0.1M and 0.14M, respectively. The suspension was sonicated in Dr. Hielscher GmbH apparatus (ultrasonic horn S7, amplitude 88 μm, power density 300 W/cm^2, frequency 24 kHz) for 2 hours and the temperature of ca 50°C.

The polyurethane non-woven porous membranes for MWCNT dispersion filtration was prepared by electrospinning from polyurethane dimethyl formamide solution. The thermoplastic polyurethane elastomer Desmopan DP 2590A was supplied by Bayer MaterialScience. The ultimate strength 48.9 MPa, strain at break 4.422 and density 1.205 g/cm^3 were specified by supplier. The adequate PU compression molding temperature was selected to be 175°C according DSC measurement (Perkin-Elmer Pyris 1) performed at heating rate 10°C/min. The conditions of electrospinning were: PU weight concentration 16 wt%, the solution electrical conductivity adjusted to 30 μS/cm using natrium chloride, the electric voltage 75 kV (Matsusada DC power supply), the temperature 20-25°C, the relative humidity 25-35 %. The membrane was prepared within the framework of cooperation with SPUR a.s, Czech Republic (for detailed scheme of experimental equipment see reference [9]).

The resistance change of the composite is monitored by a two-point technique under different tensile loading. The experimental set-up is placed into the thermostatic box (Lovibond) and the experimental temperature is 25°C. The longitudinal composite resistance is measured by means of Wheatstone bridge (the resistance of the bridge resistors R_1 = 120 Ω, R_3 = 119 Ω, R_2 = 0-1000 Ω and supply voltage 5V) and the multimeter METEX M-3860D and voltage supply METEX AX 502. Two electrical Cu contacts are fixed to the MWCNT network by a screw mechanism.

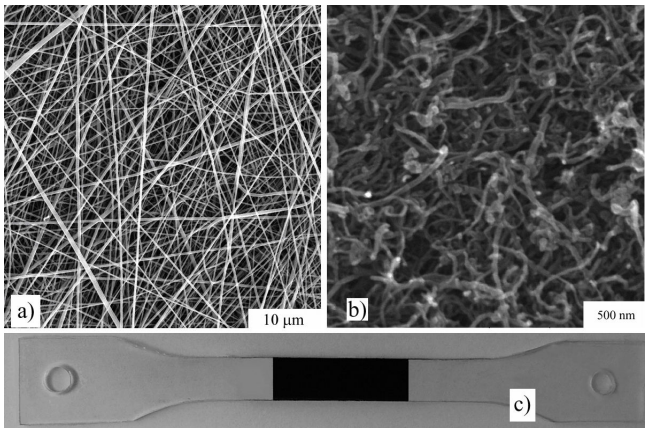

Fig.1, SEM micrograph of polyurethane non-woven filtering membrane (a); Part b represents SEM micrograph of the surface of entangled MWCNT network prepared from pure MWCNT material; c) Photograph of PU dog bone shape of tensile test specimen with the fixed stripe of PU/MWCNT-N layer (black).

The results of scanning electron microscope (SEM) analysis of PU non-woven filtering membrane prepared by the electrospinning process are shown in Figure 1 part a). It was investigated with SEM made by Vega LMU

(Tescan s.r.o., Czech Republic). The network sample was deposited onto carbon targets and covered with a thin Au/Pd layer. For the observations the regime of secondary electrons was chosen. PU fibres are straight with relatively smooth surface of submicron size and the diameter between 0.05-0.39 μm (average diameter 0.14±0.09 μm). The main pore size is around 0.2 μm. The structure of upper surface of MWCNT entangled network made of pure MWCNT is presented in part b). The prepared network structures were uniform, smooth and crack-free. The porosities of MWCNT networks were calculated to be $\phi = 0.67$ for buckypaper prepared from pure MWCNT and $\phi = 0.63$ for HNO_3 oxidised tubes using relation $\phi = 1-\rho_{WCNT-N}/\rho_{CNT}$, where $\rho_{MWCNT-N} = 0.56$ g/cm^3 (pure CNT) and $\rho_{MWCNT-N} = 0.63$ g/cm^3 (oxidised CNT) both denoting the measured apparent density of the nanotube networks. The measured average density of nanotubes $\rho_{CNT} = 1.7$ g/cm^3. Electrical resistivity 0.084 Ωcm and the contact resistance [10] of the network 3.1 kΩ were calculated for network prepared from pure CNT. Adequate values for MWCNT-$N_{(HNO3)}$ were calculated to be 0.203 Ωcm and 9.6 kΩ.

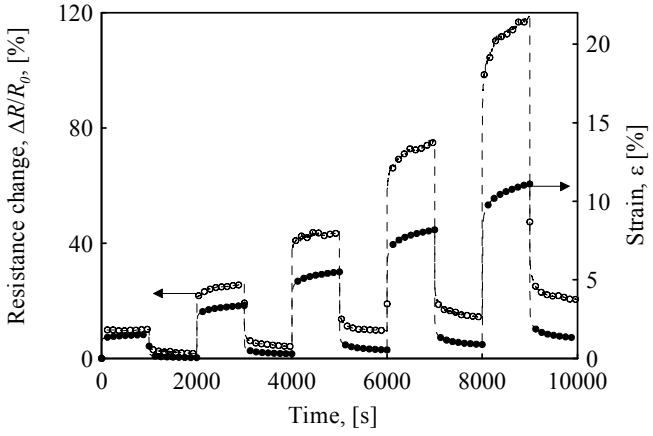

Fig.2, Response of the relative resistance change of PU/MWCNT-N composite to the five consecutive extension/relaxation cycles (creep and reversal creep) with stepwise increase of tensile strain (for composite prepared from pure CNT). The relative resistance changes are denoted by open circles, strain values by full circles.

The measurement evaluating the effect of strain on the PU/MWCNT-N composite resistance was performed during the extension/relaxation cycles with increasing strain in each cycle. The measured data are presented in Figure 2. The results are presented in terms of the percentage of relative resistance change, defined $\Delta R/R_0 = (R-R_0)/R_0$, where R_0 is the electrical resistance of the measured sample before the first elongation, and R is the resistance while elongating. The deformation increase test specimen resistance and this change can be monitored in real-time. It was found that the extension/relaxation is reversible and repeatable. Further, the increasing strain obviously enhances composite plastic deformation. Consequently, the residual strain increases in the off-load state with increasing number of cycles as well as the residual resistance change.

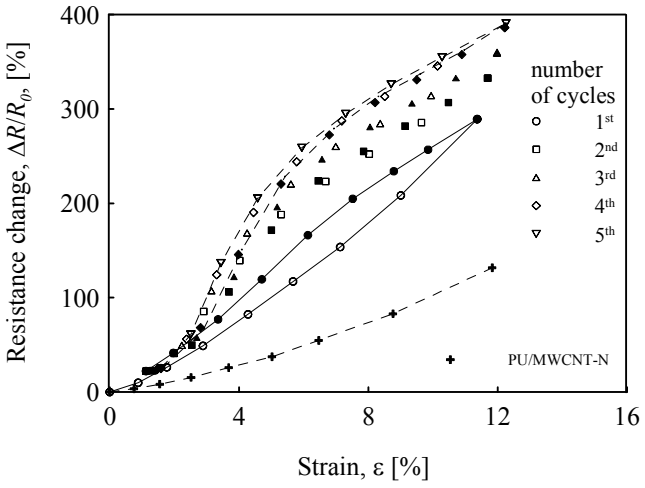

Fig.3, The dependence of relative resistance change-on applied strain for 5 consecutive tensile deformation cycles measured for PU/MWCNT-$N_{(HNO3)}$ composite. The crosses represent data for PU/MWCNT-N during the first loading. Each data were collected 120 s after appropriate step loading/unloading in creep equipment.

The relative resistance change on the course of 5 consecutive loading/unloading cycles for PU/MWCNT-$N_{(HNO3)}$ composite and the first loading of PU/MWCNT-N are for comparison presented in Fig. 3. Mechanical strain, ε, is relative change in length, here in percentage. Extension/relaxation again causes a resistance change during both the up-strain and down-strain periods due to specific deformation of porous structure. Stress-strain hysteresis loops for former material reach a steady-state cyclic regime within the fifth cycle. The sensitivity of PU/MWCNT-N sensoric unit is significantly improved by tubes oxidation. The sensitivity of strain gauge is usually

ISBN: 978-1-61804-046-6

measured by a gauge factor (GF) which is defined as the relative resistance change divided by the applied strain, GF = $(\Delta R/R_0)/\varepsilon$. The calculated data for the first loading of both principal materials are presented in Fig. 4. GF increases with strain for both materials and is in average 2.5 higher for composite made of oxidized tubes comparing with composite made of pure MWCNT.

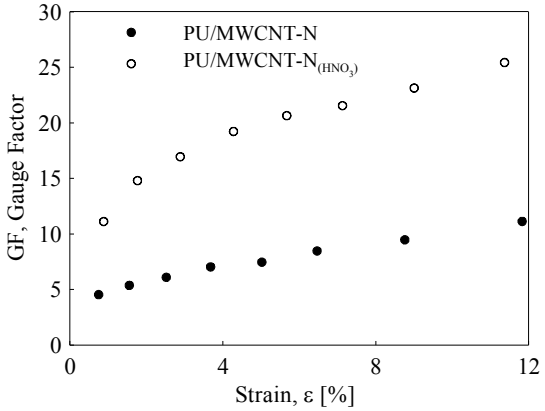

Fig.4, Dependence of the Gauge factor of PU/ MWCNT-N composites on strain for both principal composites made of pure and HNO_3 oxidised MWCNTs.

4 Conclusion

Highly deformable composite composed of a network of electrically-conductive entangled carbon nanotubes bonded to an elastic polyurethane base was introduced. The composite is prepared by the innovative procedure which eliminates the laborious process used usually, i.e. peeling off the nanotube network from the common micro-porous (polycarbonate, nylon) filter followed by the network polymeric impregnation to increase its compactness. The tests show that the prepared composite structure can be effectively used for detection of tensile strain by easy resistance measurement. It can monitor deformation in real time of experiment; the response is sensitive, reversible and repeatable. The MWCNT oxidation by HNO_3 significantly increases sensitivity defined by Gauge factor.

The favorable combination of mechanical and electrical properties open new opportunities for the composite to be used as a highly deformable strain sensing element, a strain-electric signal transducer, electromagnetic field shielding and lightning protection.

Acknowledgement. This work was supported by the Operational Program of Research and Development for Innovations co-funded by the European Regional Development Fund (ERDF), the National budget of Czech Republic within the framework of the Centre of Polymer Systems project (reg.number: CZ.1.05/2.1.00/03.0111), the Czech Ministry of Education, Youth and Sports project (MSM 7088352101). This article was also supported by the internal grant of TBU in Zlín No. IGA/3/FT/11/D funded from the resources of specific university research and by the Fund of Institute of Hydrodynamics AV0Z20600510.

References:

[1] P. Slobodian, P. Riha, R. Olejnik. *Electromechanical sensors based on carbon nanotube networks and their polymer composites*, *in New Developments and Applications in Sensing Technology*, 1st Edition., Springer, 2011, 337 p., ISBN: 978-3-642-17942-61.

[2] E. Bilotti, R. Zhang, H. Deng, M. Baxendale, T. Peijs, Fabrication and property prediction of conductive and strain sensing TPU/CNT nanocomposite fibres, *Journal of material chemistry,* 20(42) 2010, 9449-9455.

[3] G.T. Pham, Y.B. Park, Z. Liang, C. Zhang, B. Wang, Processing and modeling of conductive thermoplastic/carbon nanotube films for strain sensing, *Composites part B- engineering,* 39(1) 2008, 209-216.

[4] E.T Thostenson, T.W. Chou, Real-time in situ sensing of damage evolution in advanced fiber composites using carbon nanotube networks, *Nanotechnology,* 19(21) 2008, Article Number: 215713.

[5] I.P. Kang, M.J. Schulz, J.H. Kim, V. Shanov, D.L. Shi, A carbon nanotube strain sensor for structural health monitoring, *Smart materials and structures,* 15(3) 2006, 737-748.

[6] M.D. Rein, O. Breuer, H.D. Wagner, Sensors and sensitivity: Carbon nanotube buckypaper films as strain sensing devices Sensors and sensitivity: Carbon nanotube buckypaper films as strain sensing devices, *Composites science and technology,* 71(3) 2011, 373-381.

[7] P. Slobodian, P. Riha, A. Lengalova, R. Olejnik, P. Saha. Effect of compressive strain on electric resistance of multi-wall carbon nanotube networks, *Journal of experimental nanoscience*, 6(3) 2011, 294-304.

[8] P. Slobodian, P. Riha, A. Lengalova, P. Saha, Compressive stress-electrical conductivity

characteristics of multiwall carbon nanotube networks, *Journal of Material Science*, 46 (2011), 3186-3190.

[9] D. Kimmer, P. Slobodian, D. Petras, M. Zatloukal, R. Olejník, P. Saha, Polyurethane/Multiwalled Carbon Nanotube Nanowebs Prepared by an Electrospinning Process, *Journal of Applied Polymer Science*, 111(2009), 2711-2714.

[10] A. Allaoui, S.V. Hoa, P. Evesque, J. Bai, Electronic transport in carbon nanotube tangles under compression: The role of contact resistance, *Scripta Materialia*, 61 (2009) 628-631.

Improved electro-mechanical properties of carbon nanotubes network embedded in elastic polyurethane by oxidation

DAVID PETRAS[a],PETR SLOBODIAN[a,b], ROBERT OLEJNIK[a,b], PAVEL RIHA[c]
[a]Polymer Centre, Faculty of Technology
Tomas Bata University in Zlin
T.G.M. 275, 762 72 Zlin
CZECH REPUBLIC

[b]Centre of Polymer Systems, University Institute,
Tomas Bata University
Nad Ovcirnou 3685, 760 01 Zlin
CZECH REPUBLIC

[c]Institute of Hydrodynamics
Academy of Sciences
Pod Patankou 166 12 Prague
CZECH REPUBLIC

slobodian@ft.utb.cz http://web.ft.utb.cz/

Abstract: - The functionalization of multi-walled carbon nanotubes using $KMnO_4$ oxidation has affect on the electrical resistance of nanotube network/polyurethane composite subjected to elongation. The effect was tested in the course of elongating/relaxing cycles. The results show a multiple increase of electro-mechanical properties of the composite with $KMnO_4$ oxidized nanotubes than the composite with pristine nanotubes.

Key-Words: - Carbon nanotubes, Oxidation, Flexible composites, Strain sensor, Resistance

1 Introduction

The oxidation of carbon nanotubes (CNT) became a frequent way to enhance their chemical reactivity and extend application potentiality. Typically, the nanotube wet oxidation by the potassium permanganate ($KMnO_4$) produces carboxylic acid groups (-COOH) on nanotube surface as well as a significant amount of other oxygenated functional groups such as hydroxyl (-OH) and carbonyl (=O) groups [1,2]. The oxidation enhances gas sensing properties of nanotubes toward organic vapors which can be attributed to better affinity of vapors to the oxidized form of nanotubes [3]. Moreover, it was found that the nanotube network made from oxidized nanotubes has more uniform pore structure and dense morphology with lower porosity in comparison with networks formed by pristine nanotubes [4]. The network structure results from fine nanotube aqueous dispersion, and thus deposition of individual nanotubes and/or only small nanotube agglomerates on filtrating membrane since the presence of oxygen-containing groups facilitates the exfoliation of nanotube bundles and increases the solubility in polar media [1,2].

2 Problem Formulation

The purpose of this study is to investigate the effect of oxidation of multiwalled carbon nanotubes on the enhancement of electromechanical properties of nanotube network/polyurethane composite when elongating/relaxing cycles are imposed. To oxidize multiwalled carbon nanotubes (MWCNT), $KMnO_4$ oxidation is used. Incorporation of oxygenated functional groups changes the contact resistance between crossing tubes as well as the overall electric resistance of the composite. However, also the straining of MWCNT network, which may include nanotube slippage, delamination and damage affects

the composite resisitance. Moreover the network cracking may cause breaks of portion of electric circuit with the applied stress. The resistance change of the composite is monitored by a two-point technique.

3 Problem solution

Multiwalled carbon nanotubes BAYTUBES C70 P produced by chemical vapor deposition were supplied by the Bayer MaterialScience AG, Germany (C-purity > 95 wt.%, outer mean diameter ~13 nm, inner mean diameter ~4 nm, length > 1 μm and declared bulk density of MWCNT of agglomerates of micrometric size 45-95 kg/m^3). The oxidized MWCNTs were prepared in a glass reactor with a reflux condenser filled with 250 cm^3 of 0.5M H_2SO_4, into which 5g of $KMnO_4$ (potassium permanganate) as oxidizing agent and 2g of MWCNTs were added. The dispersion was sonicated at 85°C for 15 hours using thermostatic ultrasonic bath (Bandelin electronic DT 103H). The dispersion was filtered and MWCNTs washed with concentrated HCl to remove MnO_2.

Two aqueous (deionized water) dispersions of pristine nanotubes and oxidized by $KMnO_4$ were prepared with concentration of 0.03 wt.% each. The dispersions were sonicated in Dr. Hielscher GmbH apparatus (ultrasonic horn S7, amplitude 88 μm, power density 300 W/cm^2, frequency 24 kHz) for 2 hours and the temperature of ca 50°C. Sodium dodecyl sulfate (SDS) and 1-pentanol surfactant system was used with concentration of components 0.1 M and 0.14 M, respectively and with adjusted pH by aqueous solution of NaOH to the value of 10. MWCNT network (buckypaper) (MWCNT-N) was prepared by nanotube dispersion vacuum filtration thought polyurethane (PU) membrane prepared by technology of electrospinning in cooperation with the SPUR Company a.s. (Czech Republic) [5]. The other network was prepared from treated MWCNTs in the same way as MWCNT-N. The network is thereinafter denoted MWCNT-$N_{(KMnO4)}$.

For preparation of PU non-woven filter, dimethyl formamide/methyl isobutyl ketone (DMF/MIBK, 1:3) solution of thermoplastic polyurethane elastomer Desmopan DP 2590A supplied by Bayer MaterialScience was used. The parameters during electrospinnig process were as follows: PU weight concentration 16 wt.%, the solution electrical conductivity adjusted to 20 μS/cm using sodium chloride, an electric voltage of 75 kV (Matsusada DC power supply), a temperature of 20-25°C, and a relative humidity of 25-35 %.

MWCNT networks were washed several times by deionized water and methanol in situ and dried between two glass micro-fiber filter papers at 40°C for 24 hours. Polyurethane filter and MWCNT network form the layered structure which was melt welded (at 175 °C) onto the surface of PU tensile test specimen (dog-bone shaped) for extension/resistance tests. The shape and dimension of the test specimen are chosen according to standard EN ISO 3167, with a thickness ~ 1 mm. The partial infiltration of MWCNTs into the filter pores creates an effective interlocking of MWCNT network layer with PU filter which even strengthens when the porous filter is transformed into the polymeric film in the course of compression melt welding. The final sensing active area of test specimen consists of bulk polyurethane body with adhered pure CNT entangled network.

Pristine and $KMnO_4$ oxidized MWCNTs were analyzed via transmission electron microscopy (TEM) using microscope JEOL JEM 2010 at the accelerating voltage of 160 kV. The sample for TEM was fabricated on 300 mesh copper grid with a carbon film (SPI, USA) from MWCNT dispersion in acetone prepared by ultrasonication, which was deposited on the grid and dried. The structure of MWCNT networks, PU filtering membrane and MWCNT/PU composites were analyzed by scanning electron microscope (SEM) Vega LMU, produced by Tescan Ltd. The samples were deposited on carbon targets and covered with a thin Au/Pd layer. For the observations the regime of secondary electrons was chosen. The content of oxygen in each form of MWCNT networks was detected with help of X-ray spectroscopy (EDX) which is among accessories of SEM microscope. Thermogravimetric analyses (TGA) of the samples were carried out using thermogravimeter Setaram Setsyt Evolution 1200. The samples were examined under inert atmosphere of helium (5.5 purity, SIAD TP); the gas flow was 30 cm^3/min at the pressure of 101.325 kPa (i.e. 30 sccm) for all experiments. A platinum crucible was used for the sample, the weight of which was about 4 mg. The temperature was increased from ambient up to 1200 °C at the rate of 20 °C/min.

A detailed view of the structure of individual pristine nanotubes and the cluster of nanotubes obtained by means of TEM is shown in Fig. 1a and b, respectively. The nanotube outer and inner diameter is about 20 nm and 4-10 nm, respectively. The multi-wall consists of about 15 rolled layers of graphene. There are also defects obstructing nanotube interior which are commonly seen in MWCNT structures. When the cluster of pristine nanotubes is compared with the cluster of wet

ISBN: 978-1-61804-119-7

oxidized nanotubes in Fig. 1c, the change of the tube length is visible.

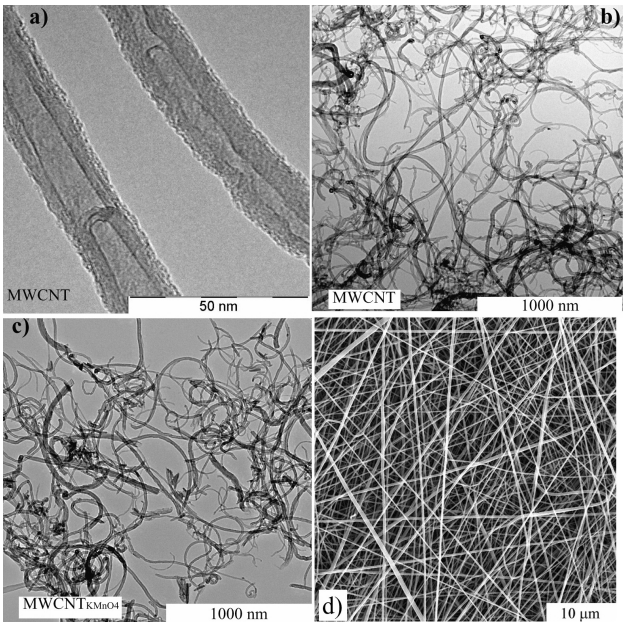

Fig 1. a,b) TEM micrographs of pristine nanotubes, c) KMnO4 wet oxidized nanotubes and d) PU non-woven filtering membrane.

The electrical resistance of MWCNT network is mainly affected by the resistance of inter-tube contacts and the number of contacts, since the conductive nanotubes are short (max. several micrometers) and cannot create a continuous conductive path. However, according to our measurement, the oxidation also increases the network resistance [4].

The measured resistivity of MWCNT network structures was 0.068±0.005 Ωcm for MWCNT-N and 0.317±0.010 Ωcm for MWCNT-$N_{(KMnO4)}$.The resistance of the nanotube contact in the network, $R_{contact}$, calculated by means of the following model [6],

$$R_{contact} = \frac{\rho_{net} A^2}{m} \frac{\pi}{16d} \varphi R \qquad (1)$$

are 3.1±0.4 kΩ (MWCNT-N) and 18.2±0.8 kΩ (MWCNT-$N_{(KMnO4)}$) for the average nanotube diameter of 13 nm. The letters m, A and d in Eq. (1) denote the weight of the sample, its cross section perpendicular to electrical current direction and average CNT diameter, respectively. R denotes the resistance of the whole network and φ the volume fraction of MWCNT defined as $\varphi = 1-\phi$, where ϕ denotes the porosity specified above for MWCNT-N and MWCNT-$N_{(KMnO4)}$. The value of $R_{contact}$ is more than five times higher for oxidized nanotubes in comparison to pristine ones.

In the course of CNT dispersion filtration, the PU filter pores allow partial infiltration of nanotubes into the filter at the beginning of filtration. When the pores are filled with nanotubes, the filter cake (nanotube entangled network) is formed above the filter surface. This partial infiltration of MWCNTs into the filter pores creates an effective interlocking of MWCNT network layer with PU filter which even strengthens when the porous filter is transformed into the polymeric film in the course of compression molding at 175 °C.

The extension of MWCNT/PU composites affects their electrical resistance change with strain. Fig. 2 shows seven extension/relaxation cycles in the course of step increase of tensile strain for PU composite with MWCNT-N and MWCNT-$N_{(KMnO4)}$, respectively. The resistance change is defined as: $\Delta R/R_0 = (R- R_0)/R_0$, where R_0 is the electrical resistance of the measured sample before the first elongation, and R is the resistance while elongating. ε denotes the percentage of mechanical strain, which is the relative change in length.

Figs. 2 and 3 show waveforms of the applied deformation and resistance change response for MWCNT-N/PU and MWCNT-$N_{(KMnO4)}$/PU composites. It is obvious from the comparison of waveforms that in case of MWCNT-N/PU composite the strain sinusoid and the resistance change sinusoid are identical for the strain varying between 2.6 and 8.4 % with frequency 0.07 Hz and the resistance change varying between 10.9 % and 26.6 %, Fig. 7. On the other side, when MWCNT-$N_{(KMnO4)}$/PU composite is subjected to similar cyclic deformation as the composite with pristine nanotubes (strain varies between 2.0 % and 7.9 % with frequency 0.05 Hz), the response of resistance change differs from the strain sinusoid. The resistance change is greater than in case of the composite with pristine nanotubes (the relative resistance change varies between 104.9 % and 247.8 %) and the resistance increase is faster than strain stimulation and vice versa. The short oxidized nanotubes probably lose contacts with other ones more easily with the composite elongation than the longer pristine nanotubes. On the other hand, the readjustment of oxidized nanotube network and formation of nanotube intercontacts with decreasing strain is slower than in case of composite with pristine nanotubes.

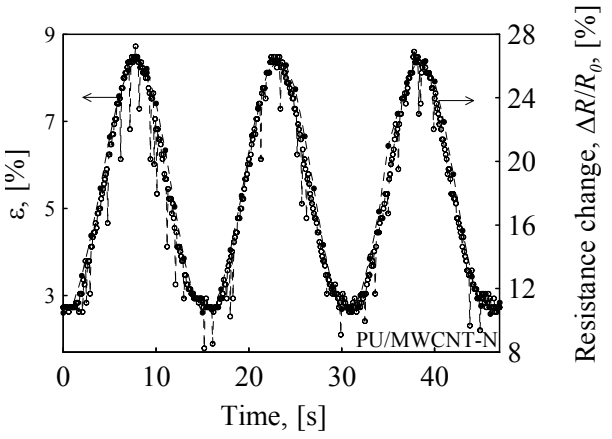

Fig. 2 Relative resistance change, $\Delta R/R_0$, induced by sinusoidal deformation for MWCNT-N/PU composite. The frequency of strain variation is 0.07 Hz. The strain values are denoted by solid circles, the relative resistance change by open circles.

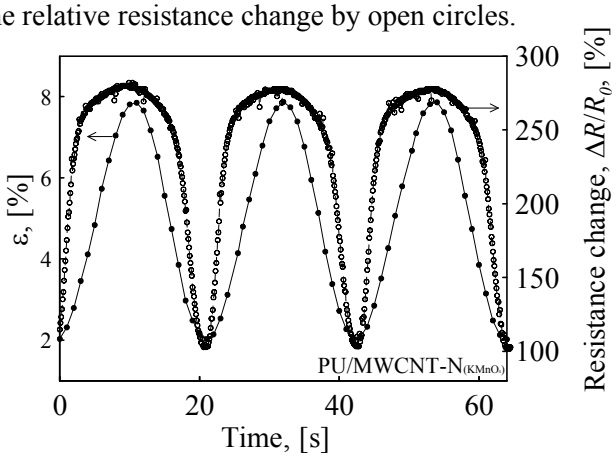

Fig. 3 Relative resistance change, $\Delta R/R_0$, induced by sinusoidal deformation for MWCNT-$N_{(KMnO4)}$/PU composite. Frequency of strain variation is 0.05 Hz. Symbols see Fig. 2.

4 Conclusion

We have introduced a highly deformable composite based on the functionalized multi-walled carbon nanotube network embedded in polyurethane and tested its electrical resistance in extension/relaxation cycles. The composite is prepared by taking a non-woven polyurethane filtering membrane, enmeshing it with carbon nanotubes and melding them into one. This innovative procedure eliminates the laborious process that is usually used, i.e. peeling off the nanotube network from the common micro-porous (polycarbonate, nylon) filter followed by the network polymeric impregnation to increase its compactness. Testing has shown a considerable difference in the resistance change of tested composites with pristine and oxidized nanotubes. The resistance change for oxidized nanotubes is 10 times greater than in case of the composite with pristine nanotubes and the resistance increase is faster than strain stimulation. This is a substantial increase of electro-mechanical properties of the composite achieved by chemical oxidation of nanotubes. The favorable combination of mechanical and electrical properties of the MWCNT-$N_{(KMnO4)}$/PU composite indicates a possible further uses as, for instance, a strain-electric signal transducer, electromagnetic field shielding and lightning protection.

Acknowledgement

This article was supported by the internal grant of TBU in Zlin No. IGA/FT/2012/022 funded from the resources of Specific University Research and by the Fund of Institute of Hydrodynamics AV0Z20600510. The work was also supported by the Operational Program of Research and Development for Innovations co-funded by the European Regional Development Fund (ERDF), the National budget of Czech Republic within the framework of the Centre of Polymer Systems project (Reg. No.: CZ.1.05/2.1.00/03.0111).

References:

[1] K. Hernadi, A. Siska, L. Thien-Nga, L. Forro, I. Kiricsi. Reactivity of different kinds of carbon during oxidative purification of catalytically prepared carbon nanotubes. *Solid State Ionics* 141(1) 2001, 203-209.

[2] A. Rasheed, J.Y. Howe, M.D. Dadmun, P.F. Britt. The efficiency of the oxidation of carbon nanofibers with various oxidizing agents. *Carbon* 45, 2007, 1072-1080.

[3] C.M. Hussain, C. Saridara, S. Mitra. Microtrapping characteristics of single and multi-walled carbon nanotubes. *Journal of Chromatography A* 1185(2) 2008, 161-166.

[4] P. Slobodian, P. Riha, A. Lengalova, P. Svoboda, P. Saha. Multi-wall carbon nanotube networks as potential resistive gas sensors for organic vapor detection. *Carbon* 49(7) 2011, 2499-2507.

[5] D. Kimmer, P. Slobodian, D. Petras, M. Zatloukal, R. Olejnik, P. Saha. Polyurethane multiwalled carbon nanotube nanowebs prepared by an electrospinning process. *Journal of Applied Polymer Science* 111(6) 2009, 2711-2714.

[6] D. Allaoui, S.V. Hoa, P. Evesque, J. Bai. Electronic transport in carbon nanotube tangles under compression: The role of contact resistance. *Scripta Materialia* 61 (6) 2009, 628-631.

Plasma treatment as a way of increasing the selectivity of carbon nanotube networks for organic vapor sensing elements

Robert Olejnik[1,2a], Petr Slobodian[1,2b], Uros Cvelbar[3c] Pavel Riha[4d] and Petr Saha[1,2,e]

[1]Tomas Bata University in Zlin, Faculty of Technology, náměstí T. G. Masaryka 275, 762 72 Zlín Czech Republic

[2]Centre of polymer systems, Nad Ovčírnou 3685, 760 01 Zlín, Czech Republic

[3]Josef Stefan instutite F4, Jamova cesta 39,1000 Ljubjana, Slovenia
[2]Institute of Hydrodynamics, Academy of Sciences, Pod Paťankou 30/5, 16612 Prague 6, Czech Republic

[a]rolejnik@volny.cz, [b]slobodian@ft.utb.cz, [c]uros.cvelbar@ijs.si, [d]riha@ih.cas.cz, [e]saha@ft.utb.cz

Keywords: Carbon nanotube networks, plasma, sensing element, interdigitated electrode

Abstract. Multi-walled carbon nanotubes networks (MWCNTs) were used as a layer for organic vapor detection. The sensor detects volatile organic compounds (VOC). The gas sensing by MWCNTs is measured by means of macroscopic electrical resistance. The selected solvents had different polarities and volume fractions of saturated vapors. The electrical resistance of MWCNTs increases when exposed to organic solvent vapors, and a reversible reaction is observed when the MWCNT is removed from the vapors. The MWCNTs were modified by means of plasma treatment. For modifications RF plasma in O_2 at 50 Pa and an afterglow configuration were used. The modified MWCNTs show an increase in sensitivity caused by creating carboxylic groups on the surface of the carbon nanotubes. It leads, for example, to enhancement of the sensitivity from usual 30 % for heptane at RT to more than 200% after plasma treatment in O_2 for 10s.

Introduction

Gas sensors, or chemical sensors, are attracting interest because of their widespread applications in industry, environmental monitoring, space exploration, biomedicine, and pharmaceutics. Gas sensors with high sensitivity and selectivity are required for leakage detections of explosive gases such as hydrogen, and for real-time detections of toxic or pathogenic gases in industries. There is also a strong demand for the ability to monitor and control our ambient environment, especially with the increasing concern of global warming. Researchers from NASA are seeking the use of high-performance gas sensors for the identification of atmospheric components of various planets. In addition, nerve-gas sensing for homeland security is also at the center of public concern [1]. Generally, there are several basic criteria for good and efficient gas sensing systems: (i) high sensitivity and selectivity; (ii) fast response time and recovery time; (iii) low analyst consumption; (iv) low operating temperature and temperature independence; (v) stability in performances. Commonly used gas sensing materials include vapor-sensitive polymers, semiconductor metal oxides, and other porous structured materials such as porous silicon [2–4]. Since the most common gas sensing principle is the adsorption and desorption of gas molecules on sensing materials, it is quite understandable that by increasing the contact interfaces between the analytes and sensing materials, the sensitivity can be significantly enhanced. The recent development of nanotechnology has created huge potential to build highly sensitive, low cost, portable sensors with low power

consumption. The extremely high surface-to-volume ratio and hollow structure of nanomaterials is ideal for gas molecules adsorption and storage. Therefore, gas sensors based on nanomaterials, such as carbon nanotubes (CNTs), nanowires, nanofibres, and nanoparticles, have been widely investigated. Since carbon nanotubes were firstly discovered by Iijima in 1991 [5], they have drawn the most research interests because of their unique geometry, morphology, and properties. Their preparation, properties (such as electronic, mechanical, thermal, and optical properties), and applications on various fields are all being studied intensely. Theoretical and simulation works have also been conducted to understand this nanoscale material and related phenomenon [6].

In this work, a new type of gas sensing element is presented. The sensing element was made by drop deposition method of aqueous dispersion of multi-walled carbon nanotubes. The drop was evaporated and the carbon nanotubes network was created. The dispersion was located on the active surface of interdigitated electrode. The interdigitated electrode was made by the etching method. The interdigitated electrode with carbon nanotubes network was treated with an afterglow RF plasma in O_2 at 50pa. The plasma treated process was optimized and the most effective treatment time was found. The plasma response to adsorption/desorption cycles were determined as a change of macroscopic resistance. MWCNTs have good sensitivity and assumed selectivity defined by pressures of saturated vapors of the used organics solvents. Finally, it was found that measured response has good reversibility.

Experimental

MWCNTs produced by chemical vapor deposition of acetylene were supplied by Sun Nanotech Co. Ltd., China (diameter 10-30 nm, length of 1-10 μm, purity of ≥90% and volume resistivity 0.12 Scm according to the supplier).

Carbon nanotubes were used into aqueous pastes using a mortar and pestle (1.6 g MWCNT and ~ 50 ml deionized water), and diluted with deionized water. Consequently, sodium dodecyl sulfate (SDS) and 1-pentanol were added, and pH was adjusted to 10 using an aqueous solution of 0.1 M NaOH [7]. The final concentration of nanotubes in the suspension was 0.3 wt.%, concentrations of SDS and 1-pentanol were 0.1M and 0.14M, respectively [8]. The dispersion was homogenized using Dr. Hielscher GmbH apparatus (ultrasonic horn S7, amplitude 88 μm, power density 300 W/cm^2, frequency 24 kHz) for 2 hours under a temperature of about 50°C.

There are several methods to integrate CNTs to different gas sensor structures. Li et al. developed a resistive gas sensor by simply casting SWCNTs on interdigitated electrodes (IDEs) [9]. This method was used in this work. A board with 35 μm Cu layer was used. The interdigitated electrodes pattern was printed on the board by etching with resistance paint. The pattern was etched for 15 minutes by $FeCl_3$ at room temperature and paint was removed by toluene. Finally, the electrodes were cleaned by absolute ethanol. The aqueous dispersion of carbon nanotubes was then drop-deposited onto the electrode area. A network of carbon nanotubes subsequently formed after the evaporation of water. The interdigitated electrode was then treated by low temperature reactive plasma. The plasma was generated in an inductively coupled radiofrequency discharge at 27.12 MHz in a commercially available gas of O_2, at the pressure 50 Pa for 5s, 10s, 15s and 30s.

Results

The typical adsorption/desorption behavior of CNT network exposed to/disposed from heptane organic vapors is presented in Fig. 1. The graph illustrates a time-dependent change of parameter S representing sensitivity of the nanotube networks. The curves show specific course of adsorption/desorption, with an obvious on/off effect. An initial sharp increase in sensitivity is followed by a slower phase. Simultaneously, desorption is represented by a rapid decrease reaching a constant value in some cases, in others followed by further, slower decrease.

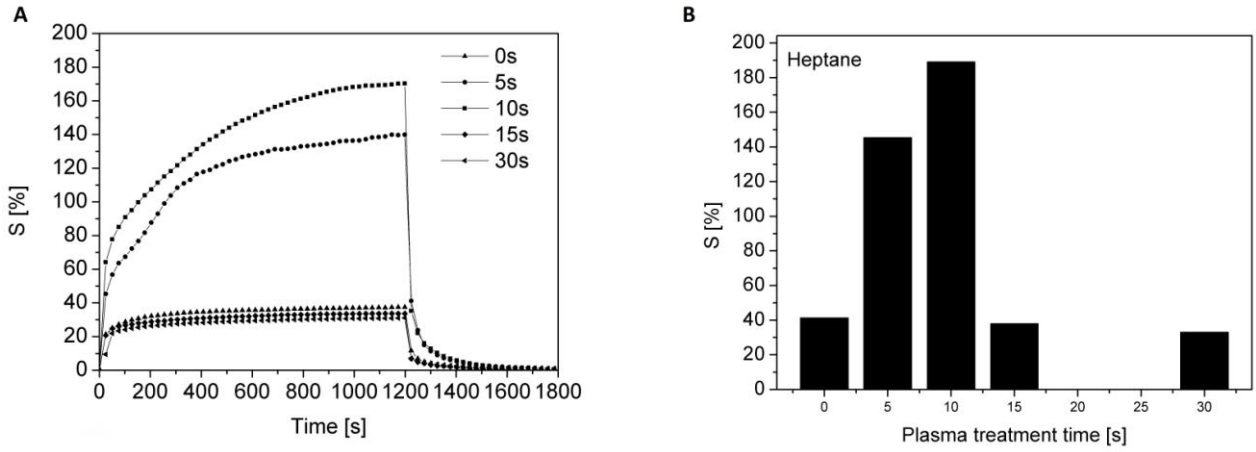

Fig. 1 A) Adsorption/desorption cycle for MWCNT network created by evaporation dispersion on the surface of interdigitated electrode exposed to heptane vapors. The curves in the graph represents four different plasma treatment times in 0_2 at 50 pa. 0 sec represents the control sample. B) The maximum *S* values for adsorption of heptane vapors for different plasma treatment times.

solvent	δ_d [Mpa$^{1/2}$]	δ_p [Mpa$^{1/2}$]	δ_h [Mpa$^{1/2}$]	δ_t [Mpa$^{1/2}$]	p_i [kPa]	x_i [vol. %]
heptane	15.3	0	0	15.3	6.13	6.0

Table 1. Properties of tested organic solvent: Hansen solubility parameters, δ_d, δ_p, δ_d total Hildebrand solubility parameter, δ_t, saturated vapor pressure, p_i, and corresponding volume fraction, x_i, at 25°C aand atmospheric pressure .

The observed behavior is probably caused by the physical adsorption of the heptane molecules in the space between the carbon nanotubes network and increase the resistance to stable value. On the other hand, desorption causes a decrease in resistance by increasing the amount of contacts in the network of carbon nanotubes.

The sensitivity is defined by Eq. 1 where R_a represents specimen resistance in air and R_g the resistance of specimen exposed to gas/vapor, ΔR denotes the resistance change.

$$S = \frac{R_g - R_a}{R_a} = \frac{\Delta R}{R_a} \tag{1}$$

Table 1 presents properties of tested organic solvent. Fig. 2 shows the sensitivity response in five consecutive cycles. One adsorption/desorption cycle consists of 20 minutes adsorption and 10 minutes desorption. Experimental data also demonstrates good reversibility of adsorption/desorption processes.

Conclusions

The interdigitated electrode pattern was printed on the board by etching resistant paint. The pattern was etched for 15 minutes by $FeCl_3$ at room temperature and paint was removed by acetone. A resistive gas sensor was made by simply casting MWCNTs on interdigitated electrodes. The aqueous dispersion of carbon nanotubes was then drop-deposited onto the electrode area.

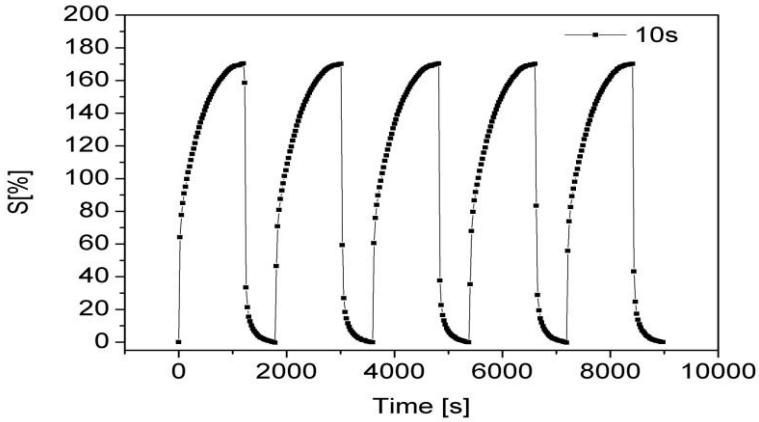

Fig. 2 Sensitivity change of treated MWCNT network exposed to saturated heptane vapors in five adsorption/desorption cycles.

The network of carbon nanotubes subsequently formed after the water evaporation. The surface of carbon nanotubes network was treated with RF plasma in O_2 atmospheres, which functionalized their surfaces and it was found that the most effective treatment time is 10s.

The network response in adsorption/desorption cycles was determined as a change of macroscopic resistance. MWCNT network has good sensitivity and assumed selectivity defined by pressures of saturated vapors of the used organics solvent. Finally it was found that measured response has good reversibility and sensitivity.

Acknowledgement

The work was supported by the Operational Program of Research and Development for Innovations co-funded by the European Regional Development Fund (ERDF), the National budget of Czech Republic within the framework of the Centre of Polymer Systems project (Reg. No.: CZ.1.05/2.1.00/03.0111). This article was also supported by the internal grant of TBU in Zlin No. IGA/FT/2012/022 funded from the resources of Specific University Research and by the Fund of Institute of Hydrodynamics AV0Z20600510.

References

[1] J. Li, in: *Carbon Nanotubes: Science and Applications*, edited by M. Meyyappan, CRC Press, Boca Raton, Fla, USA (2006)

[2] Z. M. Rittersma: Sensors and Actuators A Vol. 96 (2002) p. 196

[3] R. Fenner and E. Zdankiewicz: IEEE Sensors J. Vol. 1 (2001) p. 309

[4] E. Traversa: Sensors and Actuators B Vol. 23 (1995) p. 135

[5] S. Iijima: Nature Vol. 354 (1991)p. 56

[6] M. Meyyappan: *Carbon Nanotubes: Science and Applications* (CRC Press, Boca Raton, Fla, USA (2004)

[7] H.T. Ham, Y.S. Choi, I.J. Chung: Colloid Interf. Sci. Vol.286 (2005) p. 216

[8] C.S. Chern, L.J. Wu: Polym. Sci., Part A: Polym. Chem. Vol. 39 (2001) p. 3199

[9] J. Li, Y. Lu, Q. Ye, et al.: Nano Letters Vol. 3 (2003) p. 929

Electromechanical sensors based on carbon nanotube networks

Petr Slobodian[1], Pavel Riha[2], Robert Olejnik[1], David Petras[1,3] , Michal Machovsky[1] and Petr Saha[1]
[1]Polymer Centre, Faculty of Technology,
Tomas Bata University in Zlín, Czech Republic
[2]Institute of Hydrodynamics,
Academy of Sciences, Prague, Czech Republic
[3]SPUR a.s.,
Zlin, Czech Republic
slobodian@ft.utb.cz, riha@ih.cas.cz, rolejnik@volny.cz, Petras.David@seznam.cz, saha@utb.cz

Abstract

The network of entangled multiwall carbon nanotubes and composite consisting of PS filter-supported nanotube network are introduced as conductors whose conductivity is sensitive to compressive stress both in the course of monotonic stress growth and when loading/unloading cycles are imposed. The testing has shown as much as 100% network conductivity increase at the maximum applied stress. It indicates favorable properties of multiwall carbon nanotube network for its use as a stress-electric signal transducer. To model the conductivity-stress dependence, it is hypothesized that compression increases local contact forces between nanotubes, which results in more conductive contacts. The lack of detailed knowledge of the mechanism as well as an unclear shift from individual contacts to the whole network conductance behavior is circumvented with a statistical approach. In this respect, good data representation is reached using Weibull distribution for the description of nanotube contact resistance distribution.

Keywords: Carbon nanotube network, compression, electrical conductivity, stress sensor

1. Introduction

Recent technological progress heavily relies on the use of materials that can offer advanced structural and functional capabilities. In this respect, entangled carbon nanotube (CNT) network structures show a great potential for developing high-performance polymer composites and enhanced sensors. CNT networks can proportionally transfer their unique properties into reinforced composite materials and films for sensors and bring substantial improvements in structural strength, electrical and thermal conductivity, electromagnetic interference shielding and other properties [1,2].

The first carbon nanotube network was fabricated by Walters *et al.,* who dispersed nanotubes into a liquid suspension and then filtered through fine filtration mesh [3]. Consequently, pure nanotubes stuck to one another and formed a thin freestanding entangled structure, later dubbed buckypaper.

A recent study [4] investigated the mechanical behavior of entangled mats of carbon nanotubes and several other fibers during compression and cyclic tests. The obtained hysteresis loop between loading and unloading was linked with mat morphology and motion, friction and rearrangement of fibers during compaction. However, the electric resistance of freely poured CNT networks at compression has only been measured in [5] on a tangle whose thickness was about 2.5 mm and the maximum strain ca 0.8. The obtained data were analyzed to get an estimate of the resistance of the CNT tangle and the contact resistance between nanotubes.

Though the above mentioned paper [5] brings essential information on CNT resistance compressive stress dependence, the CNT tangles prepared in the discussed study differ from the networks prepared from fluid suspensions and deposited on filtration mesh [3]. Thus the aim of this paper is to study the electrical conductivity of multiwall carbon nanotube (MWCNT) networks prepared by filtration to the thickness of several hundred micrometers, which have a potential for the use as sensing elements.

2. Experimental

Purified MWCNT of acetylene type were supplied by Sun Nanotech Co. Ltd., China. According to the supplier, the nanotube diameter is 10-30 nm, length 1-10 μm, purity >90% and volume resistance 0.12 Ωcm. The nanotubes were used for the preparation of aqueous paste: 1.6 g of MWCNT and ~50 ml of deionized water were mixed with the help of a mortar and pestle. The paste was then diluted in deionized water with sodium dodecyl sulfate (SDS) and 1-pentanol. Consequently, NaOH aqueous solution was added to adjust pH to the value of 10 [6]. The final

nanotube concentration in the suspension was 0.3 wt.%, concentration of SDS and 1-pentanol 0.1M and 0.14M, respectively [7]. The suspension was sonicated in Dr. Hielscher GmbH apparatus (ultrasonic horn S7, amplitude 88 μm, power density 300 W/cm2, frequency 24 kHz) for 2 hours and the temperature of ca 50°C.

For making entangled MWCNT network on a polyurethane porous membrane [8], a vacuum filtration method was used. The formed disk-shaped network was washed several times by deionized water and methanol in situ, then removed and dried between filter papers. The thickness of the obtained disks was typically 0.15-0.46 mm (Fig. 1a).

The structure of MWCNT network was investigated with a scanning electron microscope (SEM) made by Vega Easy Probe (Tescan s.r.o., Czech Republic). The sample taken from the disk was first deposited onto carbon targets and covered with a thin Au/Pd layer. For the observations the regime of secondary electrons was chosen.

Pure MWCNT were also analyzed via transmission electron microscopy (TEM) using microscope JEOL JEM 2010 at the accelerating voltage of 160 kV. The sample for TEM was fabricated on 300 mesh copper grid with a carbon film (SPI, USA) from MWCNT dispersion in acetone which was prepared by ultrasonication, deposited on the grid and dried.

The MWCNT/PS composite is prepared by flow filtration of aqueous MWCNT dispersion through polystyrene (PS) filtrating membrane. The start-up phase when the nanotubes are infiltrated into the PS filter mesh is followed by sedimentation of MWCNT. PS filter-supported filtrate is several times washed by deionized water and methanol in situ. Then the composite is placed between filter papers moisten in acetone and dried between two iron plates at the room temperature for one day. The final drying continued without iron plates at 40 °C throughout another day. The thickness of the non-woven PS filter is typically 0.5 mm and the MWCNT entangled network 0.02-0.4 mm. PS filter-supported MWCNT network composite can be used either without adjustment or the hot compression molding at 190°C converts PS fiber membrane to a film with fixed MWCNT network.

The PS membrane is prepared by electrospinning from solution. PS is solved in a mixture of methyl isobutyl ketone and dimethyl formamide with the volume ratio 3:1 (PS weight concentration is 15 wt%). The nanofiber layer is made using NanoSpider (Elmarco, s.r.o.) equipped by the steel rotation electrode with needles and the steel cylinder collecting electrode (details in [8]). Then the porous layer is subjected to hot pressing at pressure 0.6 MPa and temperature 80°C.

The MWCNT networks were tested for deformation using a simple set-up. The network stripe (length 10 mm and width 8 mm, the loading area between glass plates was 8x8 mm) cut out from the manufactured disks of entangled CNT was stepwise compressed between two glasses to the maximum value with 20 s delay of strain reading in each step. Then the down-stress curve was measured in the same manner. The conductivity characteristic of network stripes was simultaneously measured with deformation. Two electrical contacts were fixed to the stripe by silver colloid electro-conductive paint Dotite D-550 (SPI Supplies) and the electrical conductivity was measured lengthwise by the two-point technique using multimeter Sefram 7338.

3 Results and discussion

3.1. Experimental results

The structure of the upper surface of entangled nanotubes can be seen in Fig. 1b as SEM micrograph.

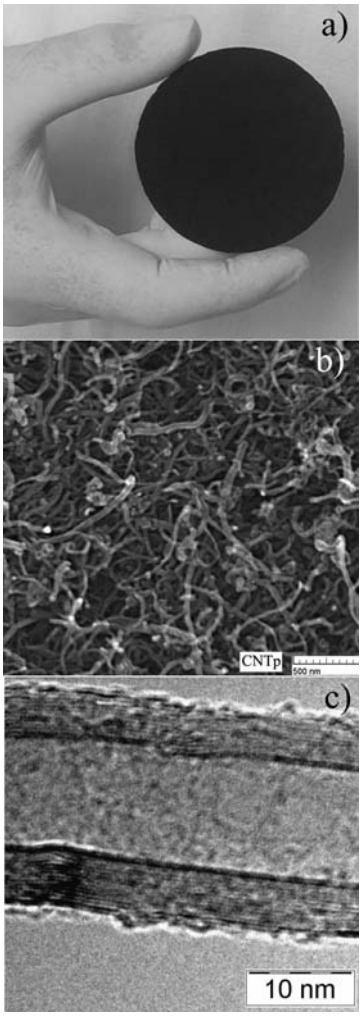

Figure 1: a) Free-standing randomly entangled MWCNT network (disk diameter 75 mm, thickness 0.15 mm), b) SEM image of the surface of entangled MWCNT network of buckypaper, c) detailed view of one individual MWCNT tube (consists of about 15 rolled graphene layers with the interlayer distance of ca 0.35 nm) analyzed by HRTEM.

After filtration of MWCNT suspension the network was dried, which caused its shrinkage by about 7%. The porosity was calculated from relation $\phi = 1 - \rho_{net} / \rho_{MWCNT}$, where ρ_{net} = 0.56±0.03 g/cm^3 denotes the measured apparent density of the nanotube network. The values correspond to those given in literature; for instance, ρ_{net} = 0.54 g/cm^3 is given in [9]. The measured average density of nanotubes ρ_{MWCNT} =1.7 g/cm^3 is very close to the theoretical value, i.e. 1.8 g/cm^3 [8]. Also the calculated porosity $\phi = 0.67$ corresponds well to the published values for MWCNT networks [10].

Mechanical properties of manufactured structures were followed in the course of twelve compression and relaxation cycles with cyclic accumulation of residual strain (compression as well as compressive strain is defined as positive loading and deformation, respectively). The results in the form of compressive stress vs. strain dependence are presented in Fig. 2.

The accumulation of residual strain is often called ratcheting and the minimum strain in each cycle is defined as ratcheting strain, ε_r. In MWCNT network a ratcheting strain appears after the first compression cycle, probably due to the initial deformation of porous structure and blocked reverse motion of nanotubes inside the compact network, as hypothesized in [5]. Thus the ability of the network to be repeatedly highly compressed is reduced. Moreover, during successive cycles of loading and unloading the ratcheting rate per cycle decreases and an asymptotic value of ε_r is obtained, as demonstrated in Fig. 3. Then stress-strain hysteresis loops reach a steady-state cyclic regime.

The measured data on MWCNT conductivity are shown in Fig. 4 as a plot of conductivity values σ vs. applied compressive stress τ. Compression causes a conductivity change during both the up-stress and down-stress periods due to specific deformation of porous structure. According to [5], the local contact forces increase during compression, allowing a better contact of nanotubes, which in turn leads to the decrease of contact resistance between crossing nanotubes; in release, the dependence is just opposite. At the same time, the possible effect of the distance between contacts on CNT tangle resistance is considered in [5]. The distance between contacts may decrease during compression owing to evoked relative motion of nanotubes, which corresponds to a lower intrinsic resistance of nanotube segments between contacts. Last but not least, compression may also bend the nanotubes sideways, which results in more contacts between nanotubes [4]. Since the contact points may act as parallel resistors, their increasing number causes an enhancement of MWCNT network conductivity.

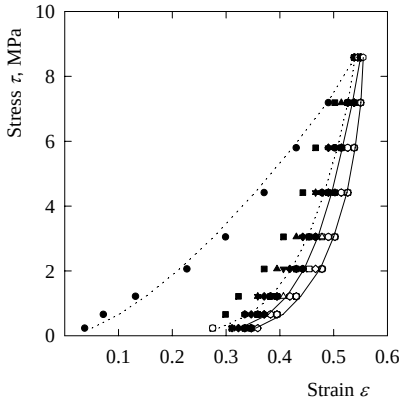

Figure 2: Stress-strain loops in cyclic compression test for MWCNT network subjected to 12 compression/expansion cycles (the network thickness 0.418 mm). The dotted lines (first loading and unloading cycle) and solid lines (twelfth cycle) represent the power law fitting.

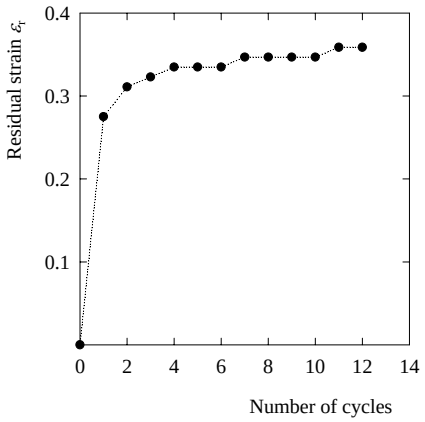

Figure 3: Ratcheting strain versus number of cycles.

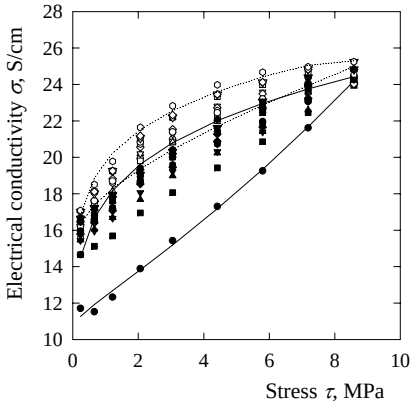

Figure 4: Conductivity-compressive stress loops for MWCNT network subjected to 12 successive compression/expansion cycles (network thickness 0.375 mm). The solid lines (first loading and unloading cycle) and dotted lines (twelfth cycle) represent the prediction given by equation (2).

The conductance mechanisms are apparently not reversible in the initial cycle since the down-stress curve indicates residual conductivity increase in the off-load state. Nevertheless, the ongoing compression cycles have a stabilizing effect on the conductivity-compression loops similarly to their effect on mechanical properties. The conductivity enhancement σ_r, defined as the residual minimum conductivity during each cycle, decreases with the increasing number of cycles, and after about 12 cycles, σ_r tends to reach to an asymptotic value, Fig. 5.

The structure of PS non-woven membrane and the cross-section of the MWCNT/PS network composite is shown in Fig.6a,b. The MWCNT network is coherent, conductive system which, combined with PS fibrous membrane, increases its rigidity and at the same time keeps its electrical properties. The PS membrane porosity allows infiltrating MWCNT into the membrane during the initial part of filtration till the pores are blocked and pure nanotubes network is formed. The composite sheet prepared by double-sided filtration is shown in Fig. 6c. The bulk composite can be prepared by overlaying several PS filter-supported networks and their hardening by hot compression molding.

The results of tensile test are shown in Fig. 7. The initial tensile modulus for MWCNT network is about 600 MPa and the ultimate tensile strength 1 MPa. The test of PS filter-supported MWCNT/PS composite shows a change of mechanical properties in comparison with pure MWCNT network. The PS reinforcement increases the tensile modulus to 1300 MPa and the ultimate tensile strength to 10.3 MPa. The corresponding values for tensile modulus and ultimate strength for PS are 1700 MPa and 13.1 MPa, respectively.

The significant property of new MWCNT/PS composite is its sensitivity to compressive strain. The effect of compression is shown in Fig. 8. The plotted resistance values, *R*, are normalized with respect to the initial resistance, R_0, recorded at the start of the test. The resistance is measured in each compression step at the preset deformation and for the subsequent unloaded state. The resistance mechanism is apparently not reversible in the initial cycles since there is resistance decrease in off-load state. Nevertheless, the ongoing compression cycles have stabilizing effect on the resistance and after about 20 cycles no resistance change is observed, Fig. 9.

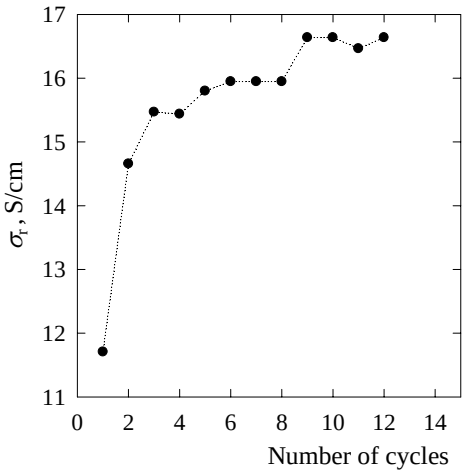

Figure 5: Conductivity enhancement in each cycle vs. number of cycles.

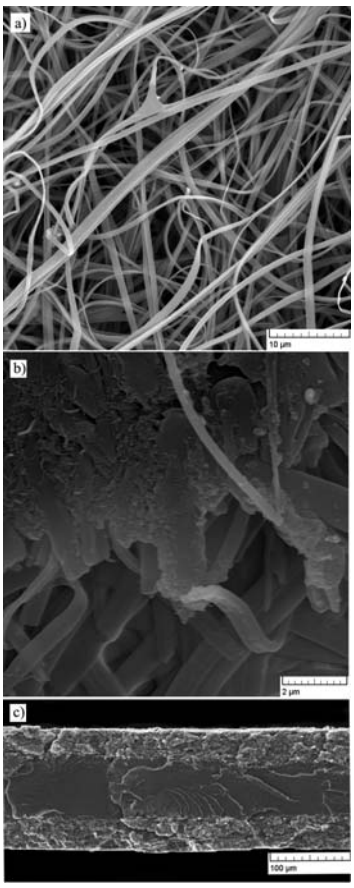

Figure 6: a) SEM analyses of PS filtrating membrane prepared by electrospinning, b) SEM micrograph of cross-section of PS fibrous membrane with infiltrated MWCNT, c) and the cross-section of compressed composite consisting of PS matrix (middle) and two MWCNT network layers (up and below the matrix).

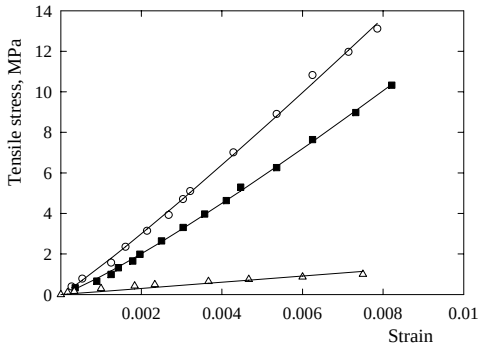

Figure 7: The comparison of tensile properties of PS filter-supported MWCNT network (squares), MWCNT network (triangles) and PS (circles) in tensile test. The lines represent the power law fitting.

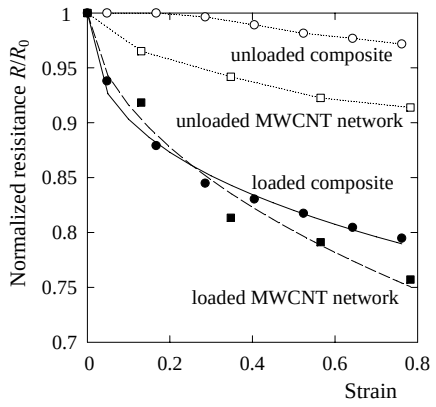

Figure 8: Normalized resistance vs. strain for loaded and unloaded MWCNT/PS composite (circles) and MWCNT network (squares).

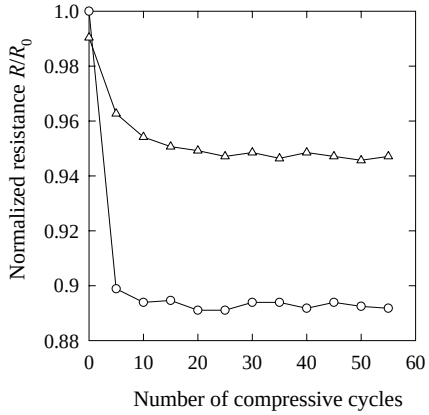

Figure 9: Normalized resistance vs. number of cycles at the load 3.9 MPa (circles) and 0.4 MPa (triangles) for MWCNT/PS composite (right).

3.2. Stochastic model of MWCNT network conductivity

The conductivity of MWCNT network subjected to compressive stress is considered to be governed by the aforementioned mechanisms ranging from the contact resistance between nanotubes through nanotube conduction to the network architecture. The complexity of network ability to conduct an electric current limits the application of classical electricity concepts for finding a relation between local contacts and the macroscopic network response to compressive strain. For this reason, we translate the results of experimental observation into a probabilistic scheme. Within the framework of this scheme, we assume that the distribution of local conductive points enables to describe the joint probability for the total network conductivity change under compressive stress τ by the cumulative distribution function or unreliability function $F(\tau)$ for the two-parameter Weibull distribution

$$\Pr(\tau) = F(\tau) = 1 - \exp\left[-(\tau/\tau_0)^m\right] \quad (1)$$

where $F(\tau)$ is an increasing function, $0 \le F(\tau) \le 1$, and describes the probability of network conductivity change $\Pr(\tau)$ under the stress no greater than τ. The two Weibull parameters are the shape parameter m and the scale parameter τ_0.

The assumption that the probability of the whole network conductivity follows the Weibull distribution is substantiated in Fig. 10. The figure shows that all the experimental points very closely follow a straight line when plotted in Weibull coordinates $\ln\tau$ vs. $\ln(\ln(1/(1-P_i)))$, where $P_i = (i-0.5)/n$ and i ranges from 1 to n, which is the number of tests. The goodness-of-fit to the straight line is reflected in the value of the correlation coefficient r = 0.99.

The tendency of the measured increase of the macroscopic, i.e. network conductivity with compressive stress is bound to the probability of network conductivity change $\Pr(\tau)$ under stress no greater than τ. Consequently, the following relation of the network conductivity $\sigma(\tau)$ to function $F(\tau)$ links appropriately the model prediction with the observed stress-dependent network conductivity increase

$$\sigma(\tau) = \alpha + \left(1 - \exp\left[-(\tau/\tau_0)^m\right]\right) \quad (2)$$

The reasonably good description of the measured data by the predictive relation (2), shown in Fig. 4 justifies the probability model chosen here for the MWCNT network conductivity change under compression.

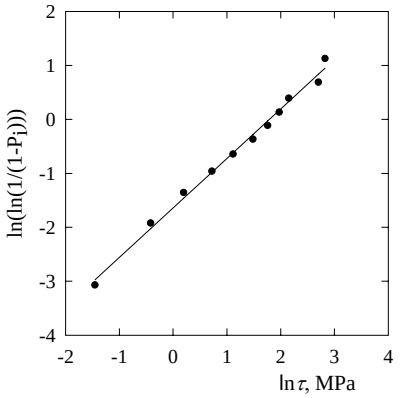

Figure 10: Weibull plot for compressive stress compressing conductive MWCNT network.

4 Conclusions

The conductivity-compression characteristics for entangled carbon nanotube network structures of buckypaper produced by filtering a nanotube suspension has not been studied in details so far. Thus the primary aim of this study was to find out the effect of compression on network electric conductivity when a simple and repeated loading is exerted. The measurements have shown over 100% network conductivity increase at the maximum applied compressive stress. It indicates a good potentiality of MWCNT entangled network for a compression sensing element. The conversion of compressive stress into the conductivity increase is achieved by deformation of porous structure. The structure recovering mechanism projects into the ratcheting strain. The rate of this strain decreases with the increasing number of cycles and an asymptotic value of this residual strain is reached. During successive cycles of loading and unloading the network rearrangement becomes steady and MWCNT network reaches stable stress-strain hysteresis loop shape. This mechanical stabilization is reflected also in conductivity data. The conductivity-stress loop is stable during the same number of cycles as the mechanical cyclic behavior. It shows that the entangled carbon nanotube network structure of buckypaper can be used as the sensing element of compressive stress sensor especially when the network is suitably deformed in advance.

The PS filter-supported entangled multiwall carbon nanotube network composite is also a conductive flexible polymeric material. The combined mechanical and electrical properties open new opportunities for the composite use as pressure sensing elements, polymer composite conductors as well as materials for electromagnetic interference shielding and lightning strike protection. A hot press molding process can produce solid bulk composites consisting of multiple-layers of PS filter-supported MWCNT network.

5 Acknowledgements

This project was supported by the internal grant of TBU in Zlín No. IGA/12/FT/10/D and Ministry of Education, Youth and Sports of the Czech Republic (MSM 7088352101), the Grant Agency of the Academy of Sciences of the Czech Republic (GAAV IAA200600803) and by the Fund of the Institute of Hydrodynamics AV0Z20600510.

6 References

[1] T. Thostenson, C.Y. Li and T.W. Chou, Nanocomposites in context, *Composite Science and Technology*, 65, pp 491-516 (2005).

[2] Q. Cao and J.A. Rogers, Ultrathin films of single-walled carbon nanotubes for electronics and sensors: A review of fundamental and applied aspects, *Advanced Materials*, 21, pp 29-53 (2009).

[3] D.A. Walters, M.J. Casavant, X.C. Quin, C.B. Huffman, P.J. Boul, L.M. Ericson, E.H. Haroz, M.J. O'Connel, K. Smith, D.T. Colbert and R.E. Smalley, In-plane-aligned membranes of carbon nanotubes, *Chemical Physical Letters*, 338 pp 14-20 (2001).

[4] A. Allaoui, S.V. Hoa, P. Evesque, J. Bai, Electronic transport in carbon nanotubes tangles under compression: The role of contact resistance, *Scripta Mater*. 61 (2009) 628-631.

[5] D. Poquillon, B. Viguier, E. Andrieu, Experimental data about mechanical behaviour during compression tests for various matted fibres, *J. Mat. Sci*. 40 (2005) 5963-5970.

[6] H.T. Ham, Y.S. Choi, I.J. Chung, An explanation of dispersion states of single-walled carbon nanotubes in solvents and aqueous surfactant solutions using solubility parameters, *Colloid Interf. Sci.* 286 (2005) 216-223.

[7] C.S. Chern, L.J. Wu: Microemulsion polymerization of styrene stabilized by sodium dodecyl sulfate and short-chain alcohols, *Polym. Sci., Part A: Polym. Chem*. 39, 3199 (2001)

[8] D. Kimmer, P. Slobodian, D. Petráš, M. Zatloukal, R. Olejník, P. Sáha, Polyurethane/MWCNT nanowebs prepared by electrospinning process, *J. Appl. Polym. Sci.* 111 (2009) 2711-2714.

[9] X.L. Xie, Y.W. Mai, X.P. Zhou, Dispersion and alignment of carbon nanotubes in polymer matrix: A review, *Mater. Sci. Eng.* R 49 (2005) 89-112.

[10] R.L.D. Whitby, T. Fukuda, T. Maekawa, S.L. James, S.V. Mikhalovsky, Geometric control and tuneable pore size distribution of buckypaper and buckydiscs, *Carbon* 46 (2008) 949-956.

Composites Science and Technology 81 (2013) 54–60

Contents lists available at SciVerse ScienceDirect

Composites Science and Technology

journal homepage: www.elsevier.com/locate/compscitech

Enhancing effect of $KMnO_4$ oxidation of carbon nanotubes network embedded in elastic polyurethane on overall electro-mechanical properties of composite

P. Slobodian [a,b,*], P. Riha [c], R. Olejnik [a,b], U. Cvelbar [d], P. Saha [a,b]

[a] Polymer Centre, Faculty of Technology, T. Bata University, T.G.M. 275, 76272 Zlin, Czech Republic
[b] Centre of Polymer Systems, University Institute, T. Bata University, Nad Ovcirnou 3685, 76001 Zlin, Czech Republic
[c] Institute of Hydrodynamics, Academy of Sciences, Pod Patankou 5, 166 12 Prague 6, Czech Republic
[d] Jozef Stefan Institute F4, Jamova cesta 39, 1000 Ljubjana, Slovenia

ARTICLE INFO

Article history:
Received 21 November 2012
Received in revised form 25 March 2013
Accepted 28 March 2013
Available online 10 April 2013

Keywords:
A. Carbon nanotubes
A. Nanocomposites
B. Electrical properties
C. Deformation
Nanotube oxidation

ABSTRACT

The effect of functionalization of multiwalled carbon nanotubes using $KMnO_4$ oxidation and oxygen plasma treatment on the electrical resistance of nanotube network/polyurethane composite subjected to elongation has been studied. The layered composite is prepared by taking a non-woven polyurethane filtering membrane which is made by electrospinning, enmeshing it with carbon nanotubes and melding them into one. The testing has shown tenfold composite resistance increase for the composite prepared from $KMnO_4$ oxidized nanotubes in comparison to the network prepared from pristine nanotubes. The evaluated sensitivity of the treated composite in terms of the gauge factor increases linearly with strain from values around five at the start of deformation to nearly 45 at the strain 12%. This is a substantial increase, which put the composite prepared from $KMnO_4$ oxidized nanotubes among ranges the materials and strain gauges with the highest sensitivity of electrical resistance measurement.

1. Introduction

The oxidation of carbon nanotubes (CNTs) became a frequent way to enhance their chemical reactivity and extend application potentiality. Typically, the nanotube wet oxidation by the potassium permanganate ($KMnO_4$) produces carboxylic acid groups (—COOH) on nanotube surface as well as a significant amount of other oxygenated functional groups such as hydroxyl (—OH) and carbonyl (=O) groups [1,2]. The oxidation enhances gas sensing properties of nanotubes toward organic vapors which can be attributed to better affinity of vapors to the oxidized form of nanotubes [3]. Moreover, it was found that the nanotube network made from oxidized nanotubes has more uniform pore structure and dense morphology with lower porosity in comparison with networks formed by pristine nanotubes [4]. The network structure results from fine nanotube aqueous dispersion, and thus deposition of individual nanotubes and/or only small nanotube agglomerates on filtrating membrane since the presence of oxygen-containing groups facilitates the exfoliation of nanotube bundles and increases their dispersion in polar media [1,2,5].

The oxygen plasma treatment of carbon nanotubes preferentially forms hydroxyl and carboxyl groups on the surface of nanotubes, so that nanotubes can provide a strong affinity to liquid molecules and self-disperse into a liquid medium [6–8]. The plasma treatment has the advantage of being non-polluting and the amount of functional groups grafted on the nanotubes surface can be tailored.

The aim of this paper is to study the effect of nanotube oxidation on electromechanical properties of nanotube network/polyurethane composite both in the course of monotonic elongation and when elongating/relaxing cycles are imposed. In this respect, the main achievement is a multiple increase of gauge factor evaluating electromechanical properties of the composite due to $KMnO_4$ oxidation of nanotubes.

2. Experimental

2.1. Materials

Multiwalled carbon nanotubes (MWCNTs) BAYTUBES C70 P produced by chemical vapor deposition were supplied by the Bayer Material Science AG, Germany (C-purity > 95 wt.%, outer mean diameter ~13 nm, inner mean diameter ~4 nm, length >1 μm and declared bulk density of MWCNT of agglomerates of

* Corresponding author at: Polymer Centre, Faculty of Technology, T. Bata University, T.G.M. 275, 76272 Zlin, Czech Republic. Tel.: +420 576031350; fax: +420 576031444.
E-mail address: slobodian@ft.utb.cz (P. Slobodian).

0266-3538/$ - see front matter © 2013 Elsevier Ltd. All rights reserved.
http://dx.doi.org/10.1016/j.compscitech.2013.03.023

micrometric size 45–95 kg/m^3). The oxidized MWCNTs were prepared in a glass reactor with a reflux condenser filled with 250 cm^3 of 0.5 M H_2SO_4, into which 5 g of $KMnO_4$ (potassium permanganate) as oxidizing agent and 2 g of MWCNTs were added. The dispersion was sonicated at 85 °C for 15 h using thermostatic ultrasonic bath (Bandelin electronic DT 103H). The dispersion was filtered and MWCNTs washed with concentrated HCl to remove MnO_2. Besides MWCNT functionalization by the potassium permanganate, the portion of MWCNTs was treated by low temperature oxygen plasma generated in an inductively coupled radio-frequency discharge at 27.12 MHz in a commercially available O_2 gas at the pressure 50 Pa for 10 min.

Nanotubes were used for the preparation of three aqueous pastes: 1.6 g of MWCNTs (either pristine, $KMnO_4$ oxidized or O_2 plasma oxidized) and ~50 ml of deionized water was mixed with a mortar and pestle. The pastes were then diluted in deionized water with sodium dodecyl sulfate (SDS) and 1-pentanol. Consequently, an aqueous solution of NaOH was added to adjust the pH at value of 10. The final nanotube concentration in suspensions was 0.3 wt.%, concentration of SDS and 1-pentanol 0.1 M and 0.14 M, respectively. The suspensions were sonicated in an apparatus from "Dr. Hielscher GmbH" (ultrasonic horn S7, amplitude 88 μm, power density 300 W/cm^2, frequency 24 kHz) for 2 h and with temperature of ca 50 °C.

MWCNT network (buckypaper) (MWCNT-N) was prepared by nanotube dispersion vacuum filtration thought polyurethane (PU) membrane prepared by technology of electrospinning in cooperation with the SPUR Company a.s. (Czech Republic) [9]. The other networks were prepared from treated MWCNTs in the same way as MWCNT-N. These networks are thereinafter denoted MWCNT-$N_{(KMnO4)}$ and MWCNT-$N_{(O2\ plasma)}$.

For an electrospinning process producing PU non-woven filters, the granulated polyurethane elastomer Desmopan DP 2590A supplied by Bayer Material Science was used. Desmopan DP 2590A is a polyester based thermoplastic polyurethane which is produced using monomers 4,4′-Methylenebis(phenyl isocyanate), polyadipate (1,4-butanediol/adipic acid) and 1,4-butanediol as a chain extender. The limited PU properties provided by the manufacture specify density 1210 kg/m^3, melt temperature 210–230 °C, mold temperature 20–40 °C and strain at break 440%.

The polyurethane granules were dissolved in a mixture of dimethyl formamide/methyl isobutyl ketone (Penta Chemikalie, Czech Republic) with volume ratio 3:1. The polymer weight concentration was adjusted to 16% (w/v) and the mixture electric conductivity to 30 μs/cm by adding NaCl in order to optimize the process. The distance of the steel multijet spinning electrode and the steel plate as the collecting electrode of the electrospinning equipment (SPUR a.s., Czech Republic) was 180 mm, Fig. 1. The total number of nozzles was 18, the length of nozzles 30 mm, the distance between nozzles 20 mm, the nozzle internal diameter 1.2 mm and the outer diameter 2.2 mm. The electric voltage was set to 75 kV (Matsusada DC power supply), the temperature 21 ± 2 °C, the relative humidity 35 ± 2.5% and the flow rate of fresh polymeric solution in one nozzle 1.6 μl/min. The final thickness of PU non-woven filters was about 200 μm.

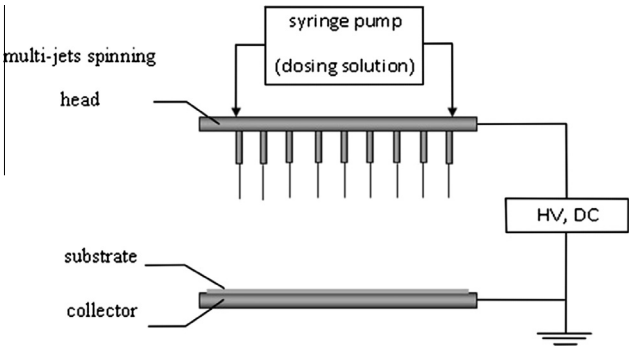

Fig. 1. Schematic diagram of the multijet electrospinning apparatus.

The filtered MWCNT networks were washed several times by deionized water and methanol in situ and dried between two glass microfiber filter papers at 40 °C for 24 h. Polyurethane filter and MWCNT network form the layered structure which was melt welded (at 175 °C) onto the surface of PU tensile test specimen for extension/resistance tests. The partial infiltration of MWCNTs into the filter pores creates an effective interlocking of MWCNT network layer with PU filter which even strengthens when the porous filter is transformed into the polymeric film in the course of compression melt welding.

2.2. Instruments

Pristine, $KMnO_4$, and oxygen plasma-oxidized MWCNTs were analyzed via transmission electron microscopy (TEM) using microscope JEOL JEM 2010 at the accelerating voltage of 160 kV. The sample for TEM was fabricated on 300 mesh copper grid with a carbon film (SPI, USA) from MWCNT dispersion in acetone prepared by ultrasonication, which was deposited on the grid and dried. The structure of MWCNT networks, PU filtering membrane and MWCNT/PU composites were analyzed by scanning electron microscope (SEM) Vega LMU, produced by Tescan Ltd. The samples were deposited on carbon targets and covered with a thin Au/Pd layer. For the observations the regime of secondary electrons was chosen. The content of oxygen in each form of MWCNT networks was detected with help of X-ray spectroscopy (EDX) which is among accessories of SEM microscope. Thermogravimetric analyses (TGA) of MWCNT samples were carried out using thermogravimeter Setaram Setsyt Evolution 1200. The samples were examined under inert atmosphere of helium (5.5 purity, SIAD TP); the gas flow was 30 cm^3/min at the pressure of 101.325 kPa (i.e. 30 sccm) for all experiments. A platinum crucible was used for the sample, the weight of which was about 4 mg. The temperature was increased from ambient up to 1200 °C at the rate of 20 °C/min.

2.3. Measurement of electrical resistance

The purpose of this study is to investigate the change of electrical resistance of different MWCNT network/PU composites in extension. The resistance change of the composite is monitored by a two-point technique by means of Wheatstone bridge (the resistance of the bridge resistors R_1 = 120 Ω, R_3 = 119 Ω, R_2 = 0–1000 Ω and supply voltage 5 V), the multimeter METEX M-3860D and voltage supply METEX AX 502. The time-dependent resistance change of composite was measured by means of the Vernier LabQuest interface system connected to the differential voltage probe and the Wheatstone bridge with sampling frequency 10 and 100 Hz.

For attachment of two copper electrodes to the MWCNT network of the composite samples a screw mechanism was used. The screw tightening was terminated when there was no decrease of network resistance. In that manner, the contact resistance between the network and copper electrodes is controlled and the initial electrical resistance of the system is equally adjusted before the first sample elongation. Initially the network under the screw was pasted by Ag colloid electro-conductive paint Dotite D-550 (SPI Supplies) to decrease the contact resistance. However, the pasting turned out ineffective since no change of the contact resistance was observed. Moreover, the paint crackled and crumbled away in the course of composite elongation.

3. Results

A detailed view of the structure of individual nanotubes and the cluster of nanotubes obtained by means of the transmission electron microscopy (TEM) is shown in Fig. 2a and b, respectively. The nanotube outer and inner diameter is about 20 nm and 4–10 nm, respectively. The multiwall consists of about 15 rolled layers of graphene. There are also defects obstructing nanotube interior which are commonly seen in MWCNT structures [10]. When the cluster of pristine nanotubes is compared with the cluster of wet oxidized nanotubes in Fig. 2c, the change of the tube length is visible. Oxidation of MWCNT by $KMnO_4/H_2SO_4$ mixture causes nanotubes shortening, creation of defect sites and opened ends. Small amount of amorphous carbon after the $KMnO_4$ oxidation process can be also expected [1] although other report shows that oxidation by $KMnO_4$ in an acidic suspension provides nanotubes free of amorphous carbon [2]. Oxidation by $KMnO_4$ can be easily controlled. The disadvantage is that created MnO_2 must be dissolved by concentrated HCl acid [1]. Finally, it is necessary stated that also the used high-energy ultrasound can cause similar effects as oxidation, that is, reduction of nanotube length with ends open by MWCNT shortening [1,2,13]. In our case the energy-dispersive X-ray spectroscopy proves an increase of oxygen content on the surface of MWCNT-$N_{(KMnO4)}$ compared to pristine MWCNT-N from 2.8 at.% to 11.9 at.%; O/C ratio thus increases from 0.03 to 0.14. In the case of plasma treated tubes it is also obvious from TEM analyses that CNT shortening occurred, Fig. 2d. However, the plasma treatment does not increase oxygen content on CNT surface as significantly as $KMnO_4$ oxidation process. The oxygen content is 6.3% and O/C ratio 0.07. These results can be supplemented by additional ones of the thermogravimetric analyses, Fig. 3. As can be seen from the figure, pure MWCNTs show hardly any degradation in the range of temperature up to 700 °C; only very small mass loss of ca 2.5 wt.% was observed at the highest temperature values. This is probably caused by decomposition of amorphous carbon contained in the pristine nanotubes together with functional groups like O—C=O or C—O [11,12]. The similar nanotube degradation as pristine nanotubes show O_2 plasma treated MWCNTs except a slight increase of decomposed material at 700 °C to ca 3.3 wt.%. It confirms only small increase of functional groups attached onto MWCNT surface during plasma treatment. On the other hand $KMnO_4$ oxidized tubes show higher weight loss at 700 °C, ca 9.8 wt.%. The increase is probably caused by a higher content of functional groups, mainly acidic sites but also —OH or C=O groups [13], which are expected to be introduced during oxidation process.

The oxidized nanotubes create smaller entangled bundles (aggregates) in solution than observed for pristine CNTs. Kastanis et al. [14] tested three different oxidizing agents, namely ammonium hydroxide/hydrogen peroxide, sulfuric acid/hydrogen peroxide and hot nitric acid. They found that the increasing oxygen content on the surface of nanotubes leads to MWCNT networks with more uniform pore structure and dense morphology with lower porosity in comparison with pristine MWCNT networks. It indicates better nanotube dispersion in the aqueous suspension during filtration process and network formation when nanotubes

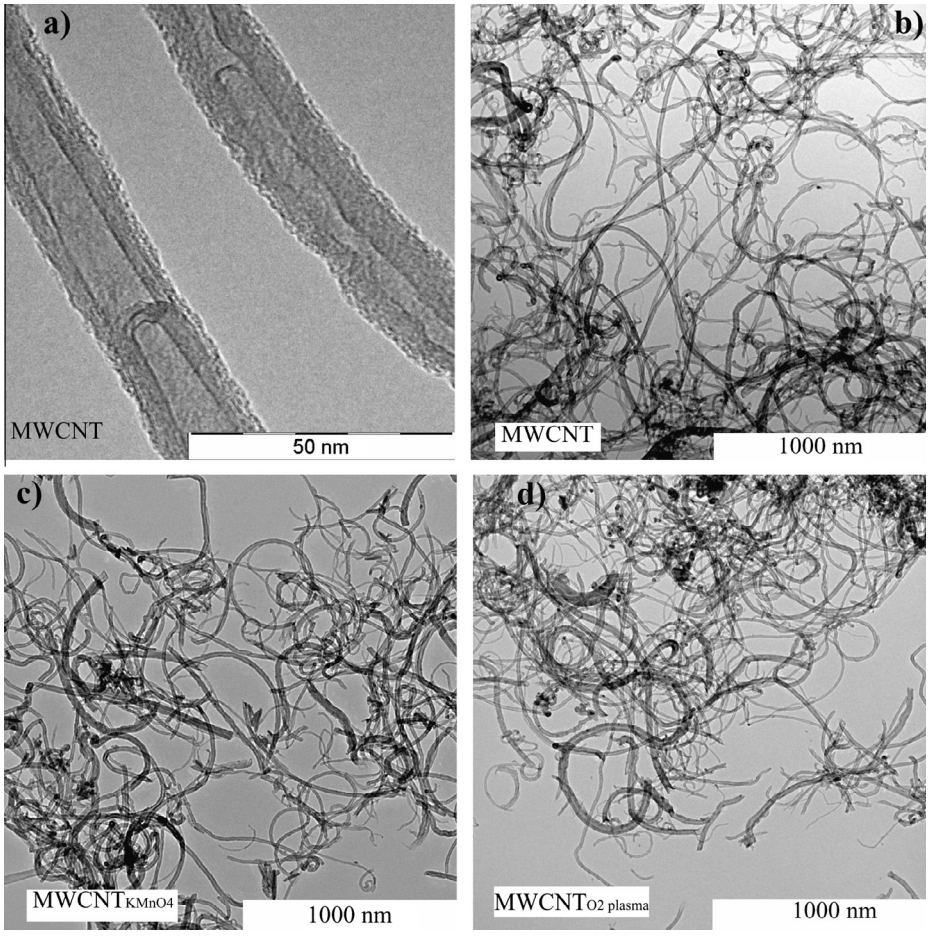

Fig. 2. (a and b) TEM micrographs of pristine nanotubes (BAYTUBES C70 P), (c) $KMnO_4$ wet oxidized nanotubes and (d) O_2 plasma shortened nanotubes.

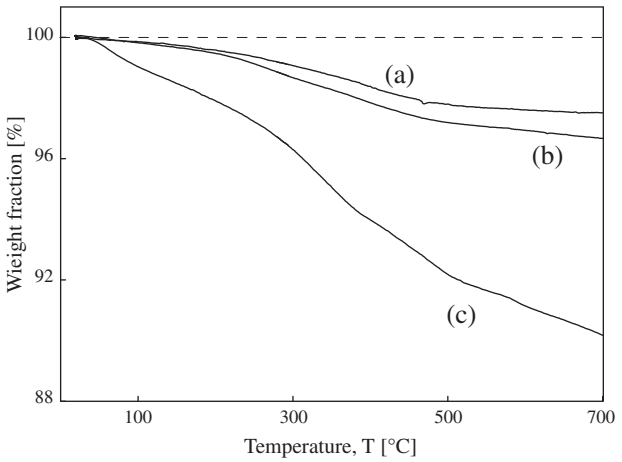

Fig. 3. Thermogravimetric analysis of nanotubes: (a) pristine nanotubes (BAYTUBES C70 P), (b) O_2 plasma shortened and (c) $KMnO_4$ wet oxidized nanotubes.

are deposited individually or as a small CNT bundles. The similar finding was described in our previous paper using different kind of MWCNTs [4].

Fig. 4 shows SEM micrographs of upper surface of entangled MWCNT network of pristine, $KMnO_4$ oxidized and O_2 plasma treated nanotubes. The network of oxidized MWCNT and O_2 plasma treated nanotubes seems to be densely packed than the network of pristine nanotubes. The quantitative difference in MWCNT network structures was determined on basis of the determination of their porosities, ϕ. The calculated porosity values were 0.71 (MWCNT-N), 0.63 (MWCNT-$N_{(KMnO4)}$) and 0.67 (MWCNT-$N_{(O2\ plasma)}$). For the calculation, the relation $\phi = 1 - \rho_{net}/\rho_{MWCNT}$ was used. The ρ_{net} value, the measured apparent density of the network, was 0.38 ± 0.01 g/cm^3 (pristine), 0.48 ± 0.01 g/cm^3 ($KMnO_4$ oxidized) and 0.43 ± 0.02 g/cm^3 (O_2 plasma treated). The measured average density of nanotubes ρ_{MWCNT} = 1.3 g/cm^3.

The electrical resistance of MWCNT network is mainly affected by the resistance of inter-tube contacts and the number of contacts, since the conductive nanotubes are short (max. several micrometers) and cannot create a continuous conductive path [15,16]. However, according to our measurement, the oxidation also increases the network resistance [4].

The measured resistivity of MWCNT network structures was 0.068 ± 0.005 Ω cm for MWCNT-N, 0.317 ± 0.010 Ω cm for MWCNT-$N_{(KMnO4)}$ and 0.071 ± 0.004 Ω cm for MWCNT-$N_{(O2\ plasma)}$. The resistance of the nanotube contacts in the network, $R_{contact}$, calculated by means of the following model [15],

$$R_{contact} = \frac{\rho_{net} A^2}{m} \frac{\pi}{16d} \varphi R \quad (1)$$

is 3.1 ± 0.4 kΩ (MWCNT-N), 18.2 ± 0.8 kΩ (MWCNT-$N_{(KMnO4)}$) and 4.0 ± 0.3 (MWCNT-$N_{(O2\ plasma)}$) for the average nanotube diameter of 13 nm. The letters m, A and d in Eq. (1) denote the weight of the sample, its cross section perpendicular to electrical current direction and average CNT diameter, respectively. R denotes the resistance of the whole network and φ the volume fraction of MWCNT defined as $\varphi = 1 - \phi$, where ϕ denotes the porosity specified above for MWCNT-N, MWCNT-$N_{(KMnO4)}$ and MWCNT-$N_{(O2\ plasma)}$. The value of $R_{contact}$ is more than five times higher for oxidized nanotubes in comparison to pristine ones but only a small increase of the contact resistance was calculated for plasma treated nanotubes compared to the contact resistance of pristine nanotubes. The role may play the content of oxygenated functional groups.

The non-woven filtering membrane made from thermoplastic polyurethane for CNT dispersion vacuum filtration was prepared by technology of electrospinning. The scanning electron microscope (SEM) micrograph of PU filter is shown in Fig. 5a. PU fibers are straight with a relatively smooth surface. The fiber diameter ranges between 0.05 and 0.39 μm (average diameter 0.14 ± 0.09 μm). The main pore size is around 0.2 μm. In the course of CNT dispersion filtration PU filter pores allow partial infiltration of nanotubes into the filter at the beginning of filtration. When the pores are filled with nanotubes, the filter cake (nanotube entangled network) is formed above the filter surface. This partial infiltration of MWCNTs into the filter pores creates an effective mechanical interlocking of MWCNT network layer with PU filter. The final structure of strain sensitive composite is formed in the course of molding at 175 °C when the layer of pure polyurethane stem from the melted PU filtering membrane and the layer of pure MWCNT network is embedded into the polymer. Thus the final structure of the layered composite consists of three layers. The first electrically non-conducting layer is the supporting pure PU layer. The second already conductive interlayer is the particulate MWCNT/PU nanocomposite film which is formed during membrane melting so that the surface nanotubes of the network are enclosed by polymer and embedded in PU layer. The third conductive layer is formed by pure MWCNT network which due to firm link with the polymer is reversibly stretchable. The second and third layers form the sensitive part of layered, longitudinally conductive MWCNT-N/PU composite. The typical thickness of PU layer is 2 mm, the interlayer 3 μm and the pure MWCNT network layer 30 μm.

SEM micrograph of the upper surface of MWCNT-N/PU composite after washing out the pure MWCNT network is shown in Fig. 5b. The cross-section through the same composite with interlayer of embedded MWCNTs into the polyurethane is shown in Fig. 5c.

The sample of different MWCNT-N/PU composite of the size 10 × 50 mm can be easily melt welded onto the surface of PU tensile test specimen (dog-bone shaped) for extension and resistance tests [17], see Fig. 5d. Shape and dimensions of the test specimen

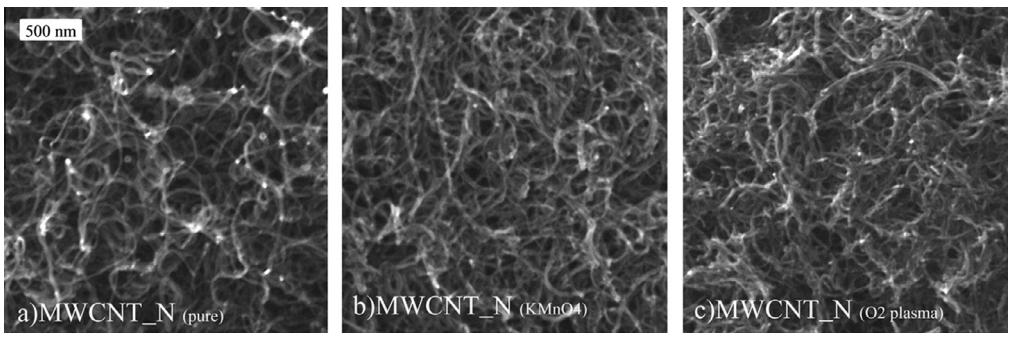

Fig. 4. SEM micrographs of the surface of entangled MWCNT network of pristine MWCNT (a), $KMnO_4$ oxidized MWCNT (b) and O_2 plasma shortened nanotubes (c).

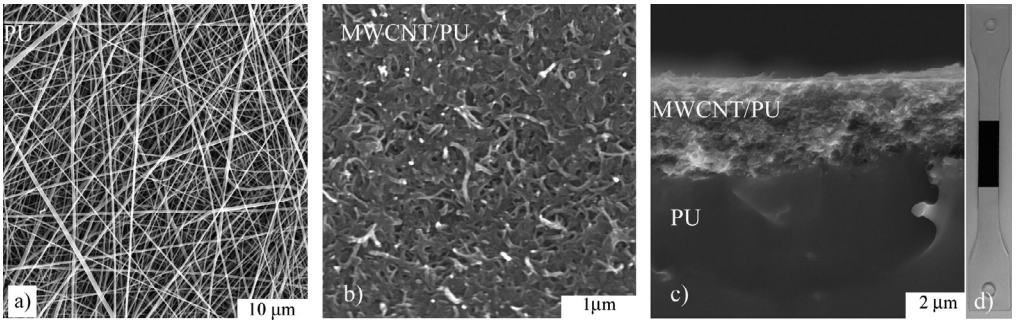

Fig. 5. SEM micrographs (a) polyurethane non-woven filtering membrane; (b) upper surface of MWCNT/PU composite layer after washing out the pure MWCNT network; (c) cross-section through polyurethane base and MWCNT/PU composite layer and (d) Photograph of PU dog-bone shaped specimen, for the tensile test, with the fixed stripe of MWCNT/PU composite (black).

are chosen according to standard EN ISO 3167, with a thickness of 2 mm.

The extension of all kinds of prepared MWCNT/PU composites affects their electrical resistance change with strain. Fig. 6 shows seven extension/relaxation cycles in the course of step increase of tensile strain for PU composite with MWCNT-N and MWCNT-$N_{(KMnO4)}$, respectively. The resistance change is defined as: $\Delta R/R_0 = (R-R_0)/R_0$, where R_0 is the electrical resistance of the measured sample before the first elongation, and R is the resistance while elongating. ε denotes the percentage of mechanical strain, which is the relative change in length. The period of extension/relaxation cycle is 60 s. From Fig. 6 follow considerable difference in the resistance change of tested composites both with respect to the sensitivity to strain and irreversible residual changes. The increasing stress obviously enhances composite irreversible deformation. Consequently, the residual strain and the residual resistance change increases in the off-load state with increasing number of cycles. The residual resistance change is caused by deformation

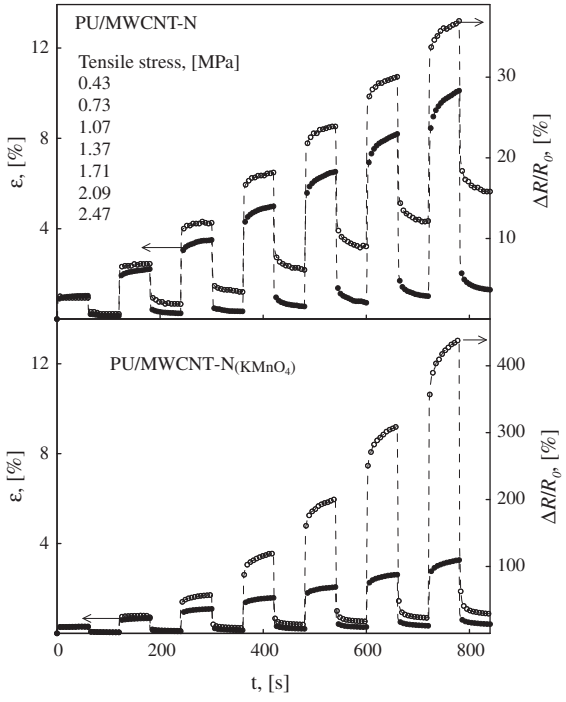

Fig. 6. Response of the relative resistance change, $\Delta R/R_0$, and the strain, ε, of MWCNT-N/PU and MWCNT-$N_{(KMnO4)}$/PU composites to the step increase of tensile stress as indicated in the graph. The strain values are denoted by solid circles, the relative resistance change by open circles.

of conductive structure of MWCNT network which may include nanotube slippage, delamination and buckling. However, in addition to the network deformation, the network cracking may cause breaks of a portion of electric circuit with the applied stress. The residual resistance change is lower in case of MWCNT-N/PU composite than MWCNT-$N_{(KMnO4)}$/PU composite. For example, in case of MWCNT/PU composite the resistance change is around 36% after elongation ~10%, while the corresponding resistance change for MWCNT-$N_{(KMnO4)}$/PU composite is about 438%. On the other hand, the residual resistance change after load remove and 1 min relaxation is 19% and 30% in case of MWCNT-N and MWCNT-$N_{(KMnO4)}$/PU composite, respectively (Fig. 6). However, the corresponding residual resistance change after relaxation is higher, about 51%, in case of MWCNT-$N_{(O2\ plasma)}$/PU composite.

Elongation causes a resistance change during both the up-stress and down-stress periods due to specific deformation of porous structure. The local contact forces between nanotubes decrease probably during elongation, allowing a worse contact of nanotubes and thus increase of their contact resistance. Moreover, the distance between contacts may increase during elongation owing to evoked relative motion of nanotubes, which corresponds to higher intrinsic resistance of nanotube segments between contacts. Last but not least, the elongation may also straighten the nanotubes, which results in a less contacts between nanotubes. Since the contact points may act as parallel resistors, their decreasing number causes an enhancement of MWCNT network resistance. This structure reorganization, i.e. less contact points, probably partly remains when the tensile strength is released, which may be the reason for off-load residual resistance increase. Nevertheless, the ongoing extension cycles have a stabilizing effect on the resistance-elongation dependence as observed during repeated cycles and described below.

Since the pristine and oxidized nanotubes have different porosities (0.71 MWCNT-N, 0.63 MWCNT-$N_{(KMnO4)}$), the structure of networks may have influence on the different strain dependent change of resistance of composites with pristine or oxidized nanotubes. However, this mechanical view does not explain fully the significant difference in the resistance change with elongation. The chemical treatment of nanotubes plays probably a dominant role. We have found by the energy-dispersive X-ray spectroscopy the increase of oxygen content on surface of MWCNT-$N_{(KMnO4)}$ compared to pristine MWCNT-N from 2.8 at.% to 11.9 at.%; O/C ratio increases from 0.03 to 0.14. Thus the number of structural defects may increase after $KMnO_4$ treatment and affect the mechanism of electrical resistance. The oxygen atoms act as acceptors of electrons and change the density of current carriers in surface layers of MWCNTs and thus may decrease electrical conductivity of the composite made of $KMnO_4$ oxidized nanotubes. Moreover, NH groups as proton donors and oxygen in carbonyl

groups of urethane and ester groups as proton acceptors in the polyester-based polyurethane affect formation of hydrogen bonding. Since MWCNT-Ns have hydroxyl, carboxyl, ketone and ether groups on their surface, these groups may play a part in forming hydrogen bonding between the polymer and MWCNT-Ns.

Besides the difference in the residual resistance change of the tested composite, a very significant difference was observed also in the sensitivity to strain. The sensitivity of strain gauge is usually measured by a gauge factor (*GF*) which is defined as the relative resistance change divided by the applied strain, $GF = (\Delta R/R_0)/\varepsilon$. To have a high sensitivity, that is, a high change in resistance for the same strain, higher value of gauge factor is desirable. Using data presented in Fig. 6, *GF* for MWCNT-N/PU slightly increases with deformation reaching nearly constant value $GF = 3.5$ above strain 4%. Gauge factor for MWCNT-N($O_{2\ plasma}$)/PU composite is very similar to the previous case with high strain *GF* about 4.2, Fig. 7. On the other hand, the gauge factor for MWCNT-N($KMnO_4$)/PU composite increases linearly with strain from values of around five at the beginning of deformation to nearly 44 at the strain 10.4%, Fig. 7. The reproducibility (repeatability) of the resistance change measurement is illustrated by taking five measurements on each composite type. Its estimation by the error bars representing standard deviation in Fig. 7 shows a reasonable values.

Figs. 8 and 9 show waveforms of the applied deformation and resistance change response for MWCNT-N/PU and MWCNT-$N_{(KMnO4)}$/PU composites in three cycles. Though the resistance mechanism is apparently not reversible in the initial cycle since the relaxation curve has a residual resistance increase in the off-load state, Fig. 6, the ongoing elongation cycles have a stabilizing effect on the resistance and strain time dependence, Figs. 8 and 9. The initial residual resistance change during each cycle tends to reach immediately the final value and ensures the repeatability of the resistance-strain dependence. It indicates that during initial deformation the nanotube network gets the structure which stays more or less the same regardless the number of deformation cycles. This mechanical stabilization is favorable for the use of the composite as a sensing element of elongation, especially when the network is suitably deformed in advance.

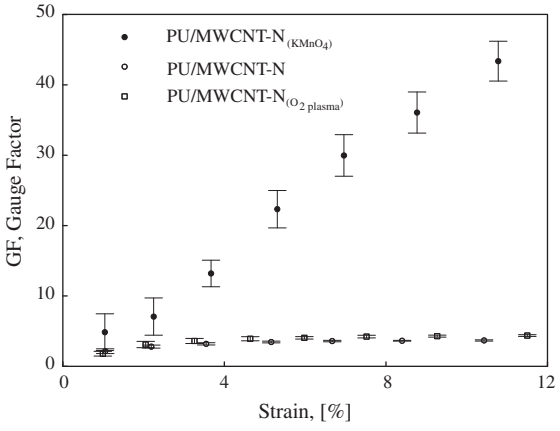

Fig. 7. Strain dependence of gauge factor *GF* of tested composites. The symbols represent means ($n = 5$) and the error bars show the standard deviation.

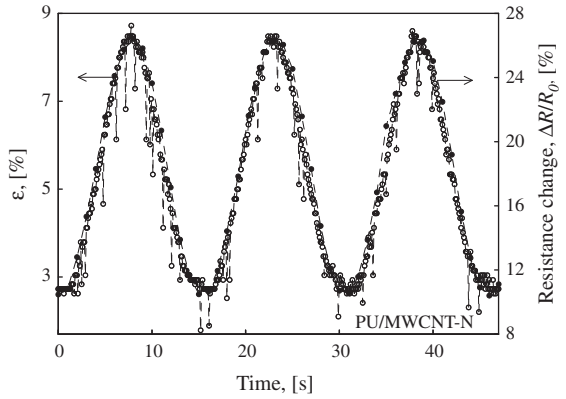

Fig. 8. Relative resistance change, $\Delta R/R_0$, induced by sinusoidal deformation for MWCNT-N/PU composite. The frequency of strain variation is ~0.07 Hz. The strain values are denoted by solid circles, the relative resistance change by open circles.

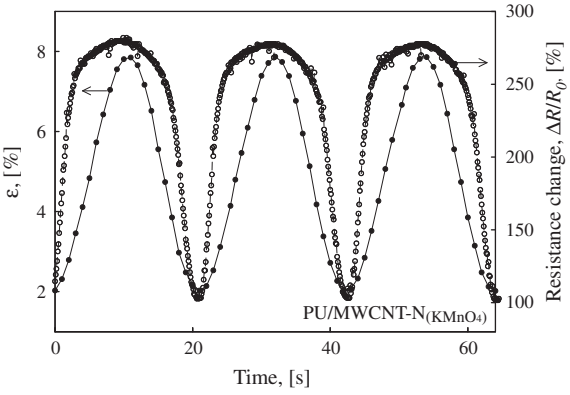

Fig. 9. Relative resistance change, $\Delta R/R_0$, induced by sinusoidal deformation for MWCNT-$N_{(KMnO4)}$/PU composite. The frequency of strain variation is ~0.05 Hz. The strain values are denoted by solid circles, the relative resistance change by open circles.

From the comparison of waveforms in Figs. 8 and 9 is obvious that in case of MWCNT-N/PU composite the strain sinusoid and the resistance change sinusoid are identical for the strain varying between 2.6% and 8.4% with frequency 0.07 Hz and the resistance change varying between 10.9% and 26.6%, Fig. 8. On the other side, when MWCNT-$N_{(KMnO4)}$/PU composite is subjected to similar cyclic deformation as the composite with pristine nanotubes (strain varies between 2.0% and 7.9% with frequency 0.05 Hz), the response of resistance change differs from the strain sinusoid. The resistance

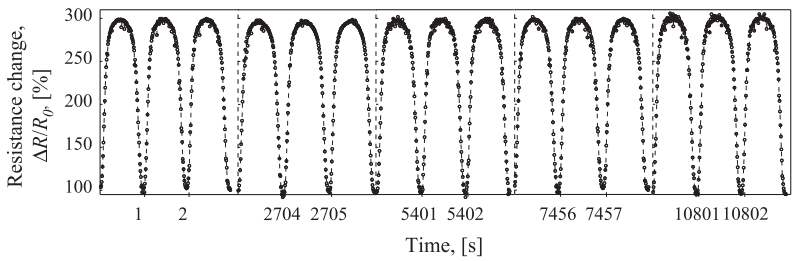

Fig. 10. The cyclic test of MWCNT-$N_{(KMnO4)}$/PU composite in more than 10^4 cycles. The strain varies between 2% and 7.9%, the frequency of strain variation is ~1.0 Hz.

change is greater than in case of the composite with pristine nanotubes (the relative resistance change varies between 104.9% and 247.8%) and the resistance increase is faster than strain stimulation and vice versa. The short oxidized nanotubes probably lose contacts with other ones more easily with the composite elongation than the longer pristine nanotubes. On the other hand, the readjustment of oxidized nanotube network and formation of nanotube intercontacts with decreasing strain is slower than in case of composite with pristine nanotubes.

Fig. 10 demonstrates properties of MWCNT-$N_{(KMnO4)}$/PU composite as well as the properties repeatability under long-lasting cyclic elongation. The frequency of strain cycle is about 1 Hz and more than 10^4 cycles has been monitored. The results show that the resistance change is repetitive and no composite property variation is observed. The composite has reasonable durability and reversibility of the base characteristics complying practical application requirements.

4. Conclusion

Three different kinds of MWCNT/PU composite were prepared to investigate the effect of nanotube oxidation on the modification of their mechanical and electrical properties in the course of monotonic elongation and when elongating/relaxing cycles are imposed. The testing has shown tenfold composite resistance increase for MWCNT network prepared from $KMnO_4$ oxidized nanotubes in comparison to the network prepared from pristine MWCNT and also O_2 plasma oxidized MWCNT network. The evaluated sensitivity of MWCNT-$N_{(KMnO4)}$/PU composite in terms of the gauge factor increases linearly with strain from values around 5 at the start of deformation to nearly 44 at the strain 12%. This is a substantial increase, which put the composite among the materials and strain gauges with the highest sensitivity of electrical resistance measurement. The resistance and sensitivity increase in elongation comes probably from the different porosity of networks and increased content of oxygenated functional groups detached on MWCNT-$N_{(KMnO4)}$ surface which significantly increase contact resistance in CNT junction of network structure. The short oxidized nanotubes probably lose contacts with other ones more easily with the composite elongation than the longer pristine nanotubes. The long-lasting cyclic stretching of MWCNT-$N_{(KMnO4)}$/PU composite shows reasonable durability and reversibility of the composite deformation and electrical resistance complying practical application requirements.

Acknowledgements

The work was supported by the Operational Program of Research and Development for Innovations co-funded by the European Regional Development Fund (ERDF), the National budget of Czech Republic within the framework of the Centre of Polymer Systems project (Reg. number: CZ.1.05/2.1.00/03.0111). The article was written with the support of the Operational Programme, Education for Competitiveness" co-funded by the European Social Fund (ESF) and the national budget of the Czech Republic, within the, Advanced Theoretical and Experimental Studies of Polymer Systems" project (Reg. number: CZ.1.07/2.3.00/20.0104). The Fund of Institute of Hydrodynamics, No. of Project AV0Z20600510, is also acknowledged for support.

References

[1] Hernadi K, Siska A, Thien-Nga L, Forro L, Kiricsi I. Reactivity of different kinds of carbon during oxidative purification of catalytically prepared carbon nanotubes. Solid State Ionics 2001;141(1):203–9.
[2] Rasheed A, Howe JY, Dadmun MD, Britt PF. The efficiency of the oxidation of carbon nanofibers with various oxidizing agents. Carbon 2007;45:1072–80.
[3] Hussain CM, Saridara C, Mitra S. Microtrapping characteristics of single and multiwalled carbon nanotubes. J Chromatogr A 2008;1185(2):161–6.
[4] Slobodian P, Riha P, Lengalova A, Svoboda P, Saha P. Multiwall carbon nanotube networks as potential resistive gas sensors for organic vapor detection. Carbon 2011;49(7):2499–507.
[5] Datsyuk V, Kalyva M, Papagelis K, Parthenios J, Tasis D, Siokou A, et al. Chemical oxidation of multiwalled carbon nanotubes. Carbon 2008;46:833–40.
[6] Kalita G, Adhikan S, Aryal HR, Umeno M, Afre R, Soga T. Fullerene (C_{60}) decoration in oxygen plasma treated multiwalled carbon nanotubes for photovoltaic application. Appl Phys Lett 2008;92:063508.
[7] Chen C, Ogino A, Wang X, Nagatsu M. Plasma treatment of multiwall carbon nanotubes for dispersion improvement in water. Appl Phys Lett 2010;96:131504. 3 pages.
[8] Chen W, Liu X, Liu Y, Bang Y, Kim HI. Preparation of O/W pickering emulsion with oxygen plasma treated carbon nanotubes as surfactants. J Ind Eng Chem 2011;17:455–60.
[9] Kimmer D, Slobodian P, Petras D, Zatloukal M, Olejnik R, Saha P. Polyurethane/multiwalled carbon nanotube nanowebs prepared by an electrospinning process. J Appl Polym Sci 2009;111(6):2711–4.
[10] Harris PJF. Carbon nanotube science: synthesis properties and applications. Cambridge University Press; 2009. p. 123.
[11] Licea-Jimenez L, Henrio PY, Lund A, Laurie TM, Perez-Garcia SA, Nyborg L, et al. Compos Sci Technol 2007;67(5):844–54.
[12] Li Q, Ma Y, Mao C, Wu C. Grafting modification and structural degradation of multi-walled carbon nanotubes under the effect of ultrasonics sonochemistry. Ultrason Sonochem 2009;16(6):752–7.
[13] Zhang J, Zou HL, Qing Q, Yang YL, Li QW, Liu ZF, et al. Effect of chemical oxidation on the structure of single-walled carbon nanotubes. J Phys Chem B 2003;107(16):3712–8.
[14] Kastanis D, Tasis D, Papagelis K, Parthertios J, Tsakiroglou C, Galiotis C. Oxidized multi-walled carbon nanotube film fabrication and characterization. Adv Compos Lett 2007;16(6):243–8.
[15] Allaoui A, Hoa SV, Evesque P, Bai J. Electronic transport in carbon nanotube tangles under compression: The role of contact resistance. Scripta Mater 2009;61(6):628–31.
[16] Yeh CS. A study of nanostructure and properties of mixed nanotube buckypaper materials: fabrication, process modeling characterization, and property modeling. The Florida State University USA, PhD thesis;2007.
[17] Slobodian P, Riha P, Saha P. A highly-deformable composite composed of an entangled network of electrically-conductive carbon-nanotubes embedded in elastic polyurethane. Carbon 2012;50:3446–53.

DEVELOPMENT OF MANUFACTURING PROCESS OF CONDUCTIVE CARBON NANOTUBE NETWORK/POLYSTYRENE COMPOSITES

Pavel Riha[1], Petr Slobodian[2], Robert Olejnik[2], David Petras[2], Petr Saha[2]

[1] *Institute of Hydrodynamics, Academy of Sciences, 166 12 Prague, Czech Republic, riha@ih.cas.cz*

[2]*Polymer Centre, Faculty of Technology, T. Bata University in Zlin, 762 72 Zlin, Czech Republic, slobodian@ft.utb.cz*

ABSTRACT: The composite consisting of filter-supported entangled multiwall carbon nanotube networks were prepared by filtration of nanotube fluid dispersion through a non-woven flexible polystyrene membrane. The nanotubes infiltrate partly into the membrane pores and couple the membrane and the accumulated filtrate layer. The filter-support increases nanotube network mechanical integrity and eliminates the laborious process of peeling off the nanotube network from the usual micro-porous (polycarbonate, nylon) membrane filter followed by the network impregnation to increase its compactness. The composite with embedded nanotube network is shown to be a conductor whose electrical resistance is sensitive to compressive strain. To model the electrical resistance strain dependence, the statistical approach based on Weibull distribution of resistive nanotube contacts is used.

KEYWORDS: carbon nanotube network, non-woven PS membrane, electric resistance, stress sensor.

INTRODUCTION

Recent technology progress relies heavily on the use of materials that can offer advanced structural and functional capabilities. In this respect, entangled carbon nanotube network structures of buckypaper show a great potential for developing high-performance polymer composite materials. The network can proportionally transfer its unique properties into composites and bring substantial improvements in structural strength, electrical and thermal conductivity, electromagnetic interference shielding and other properties in comparison to polymer composites with carbon nanotube particulate filling [1,2]. However, incorporation of conductive nanotube network into a hosting polymer matrix is a difficult task. Traditionally, the network is fixed by a polymer solution (epoxy or bismaleimide resin, polycarbonate solution) to form polymer composites [3,4].

The abovementioned manufacturing of CNT network based polymer composite is rather laborious and may be circumvent by interlocking porous filtrating membrane with entangled CNT. The novel process consists of using the flexible non-woven polystyrene (PS) filter as supporting and integrating element at which, in our case, the multiwall

carbon nanotubes (MWCNT) settle and form a network during MWCNT suspension filtration. The obtained MWCNT/PS composite can be used either without adjustment or hot compressed to increase MWCNT fixing to PS membrane. The repeated layering of MWNT/PS membrane sheets yields bulky forms. The flow processing seems promising for a continuous manufacture of carbon nanotube network/polymer composites since the filter-support ensures itself the composite compactness. The usual peeling off the MWCNT network from the membrane is eliminated as well as the network impregnation by means of polymer solutions to increase its mechanical integrity.

EXPERIMENTAL

The acetylene type MWCNT (diameter 10-30 nm, length 1-10 μm) made by Sun Nanotech Co. Ltd., China, are used for preparation of aqueous paste. The paste is diluted in deionised water with sodium dodecyl sulfate and 1-pentanol and sonicated. For making the entangled MWCNT network on a non-woven PS filtration membrane, the vacuum-filtration method is used. The membrane is prepared by electrospinning from solution. PS is solved in a mixture of methyl isobutyl ketone and dimethyl formamide with the volume ratio 3:1 (PS weight concentration is 15 wt%). The nanofiber layer is made using NanoSpider (Elmarco, s.r.o.) equipped by the steel rotation electrode with needles and the steel cylinder collecting electrode (details in [5]). Then the porous layer is subjected to hot pressing at pressure 0.6 MPa and temperature 80°C.

The MWCNT/PS composite is prepared by flow filtration of aqueous MWCNT dispersion through PS filtrating membrane. The start-up phase when the nanotubes are infiltrated in to the PS filter mesh is followed by sedimentation of MWCNT. PS filter-supported filtrate is several times washed by deionized water and methanol in situ. Then the composite is placed between filter papers moisten in acetone and dried between two iron plates at the room temperature for one day. The final drying continued without iron plates at 40 °C throughout another day. The thickness of the non-woven PS filter is typically 0.5 mm and the MWCNT entangled network 0.02-0.4 mm. PS filter-supported MWCNT network composite can be used either without adjustment or the hot compression molding at 190°C converts PS fiber membrane to a film with fixed MWCNT network.

The structure of MWCNT network as well as the cross-section of PS membrane with infiltrated nanotubes and the compressed PS membrane with MWCNT layers was observed by a scanning electron microscope (SEM) made by Vega Easy Probe (Tescan s.r.o., Czech Republic). The sample is deposited onto carbon targets and covered with a thin Au/Pd layer. The observation is carried out in the regime of secondary electrons. The tensile and compression tests are carried out using a simple set-up. The sample stripe (length 45 and width 8 mm) is stepwise extended with 60 sec delay of strain reading in each step. The compressive deformation is adjusted by means of calibrated steel plates and the corresponding resistance along the stripe length is measured by the two-point technique using multimeter Sefram 7338. The loading area between glass plates is 8x8 mm. The electrical contacts are fixed to the stripes by silver colloid electro-conductive paint Dotite D-550 (SPI Supplies).

RESULTS

The structure of entangled MWCNT network of buckypaper and the cross-section of the PS/MWCNT network composite is shown in Fig.1. The MWCNT network is coherent, conductive system (Fig. 1a) which, combined with PS fibrous membrane, increases its rigidity and at the same time keeps its electrical properties. The upper surface of MWCNT network can be seen in SEM micrograph, Fig. 1b. The PS membrane porosity allows infiltrating MWCNT into the membrane during the initial part of filtration till the pores are blocked and pure nanotubes network is formed, Fig. 1c. The arrow in the figure indicates MWCNT infiltration. The composite sheet prepared by double-sided filtration is shown in Fig. 1d. The bulk composite can be prepared by overlaying several PS filter-supported networks and their hardening by hot compression molding.

The results of tensile test are shown in Fig. 2. The initial tensile modulus for MWCNT network is about 600 MPa and the ultimate tensile strength 1 MPa. The test of PS filter-supported MWCNT/PS composite shows a change of mechanical properties in comparison with MWCNT network. The reinforcement increases the tensile modulus to 1300 MPa and the ultimate tensile strength to 10.3 MPa. The corresponding values for tensile modulus and ultimate strength for PS are 1700 MPa and 13.1 MPa, respectively.

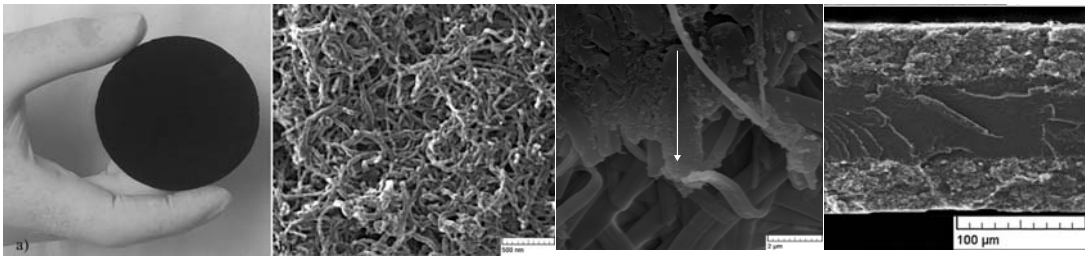

(a) (b) (c) (d)

Fig. 1 Free-standing randomly entangled MWCNT network (disk diameter 75 mm, thickness 0.15 mm) (a), SEM image of the surface of entangled MWCNT network (b), SEM micrograph of cross-section of PS fibrous membrane (bottom) with infiltrated MWCNT (c) and the cross-section of compressed composite consisting of PS matrix (middle) and 2 MWCNT network layers (d).

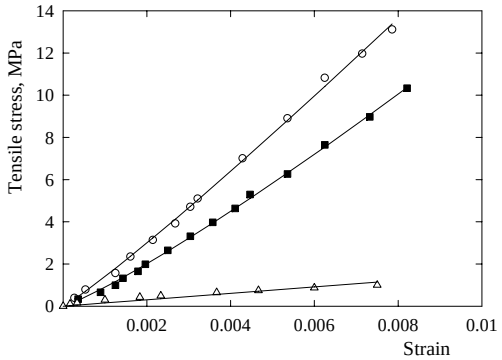

Fig. 2 The comparison of tensile properties of PS filter-supported MWCNT network (squares), MWCNT network (triangles) and PS (circles) in tensile test. The lines represent the power law fitting.

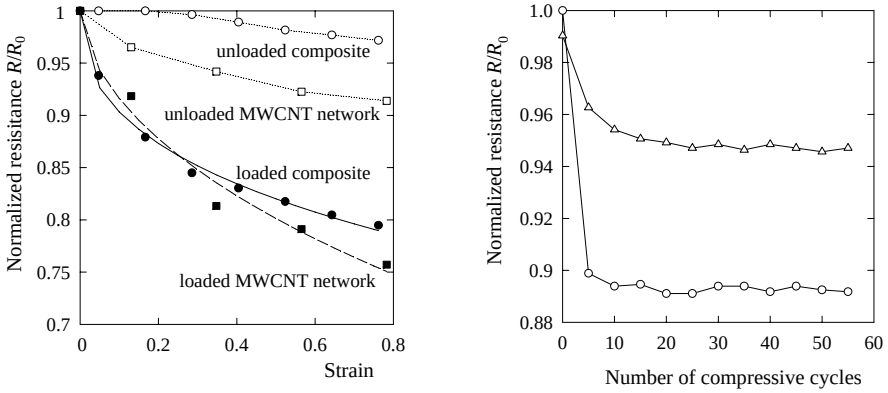

Fig.3 Normalized resistance vs. strain for loaded and unloaded MWCNT/PS composite (circles) and MWCNT network (squares). The solid and dashed stretched exponential line represents Eqn. 2, (left). Normalized resistance vs. number of cycles at the load 3.9 MPa (circles) and 0.4 MPa (triangles) for MWCNT/PS composite (right).

The significant property of new MWCNT/PS composite is its sensitivity to compressive strain. The effect of compression is shown in Fig. 3. The plotted resistance values, *R*, are normalized with respect to the initial resistance, R_0, recorded at the start of the test. The resistance is measured in each compression step at the preset deformation and for the subsequent unloaded state. The resistance mechanism is apparently not reversible in the initial cycles since there is resistance decrease in off-load state. Nevertheless, the ongoing compression cycles have stabilizing effect on the resistance and after about 20 cycles no resistance change is observed.

Stochastic model of MWCNT network resistance

The electric resistance of the MWCNT network subjected to compressive strain is among others affected by the contact resistance between nanotubes, the nanotube inner resistance mechanism and MWCNT network architecture. Owing to the lack of knowledge of these effects, we translate the results of experimental observation into the probabilistic scheme. Within the framework of this scheme, we assume that the distribution of resistive contact points is such that the joint probability for the total network resistance above a particular level under compressive strain γ is described by the reliability function $S(\gamma)$ for the two-parameter Weibull distribution

$$S(\gamma)=\Pr(\Gamma>\gamma)=1-F(\gamma)=\exp\left[-(\gamma/\gamma_0)^m\right] \tag{1}$$

where $F(\gamma)=1-\exp\left[-(\gamma/\gamma_0)^m\right]$ is the cumulative distribution function of Weibull distribution. $S(\gamma)$ is a decreasing function, $1\geq S(\gamma)\geq 0$, and describes the probability of network resistance constancy $\Pr(\gamma)$ under the strain Γ greater than γ (the compressive strain is defined as positive).

The measured dependence of the macroscopic, i.e. network resistance on the compressive strain is in accordance with the chosen probability tendency. Consequently, the following relation of the function $S(\gamma)$ to the normalized network resistance R/R_0,

$$R/R_0 = S(\gamma) = \exp\left[-(\gamma/\gamma_0)^m\right] \quad (2)$$

links appropriately the model prediction with the observed strain dependent network resistance decrease. The reasonably good description of the measured data by the predictive Eqn. 2, shown in Fig. 3 (left) (parameters γ_0=24.9, m=0.41 - solid line, γ_0=6.8, m=0.58 - dashed line), justifies the probability model chosen here for the description of MWCNT/PS composite and MWCNT network resistance change under compression.

FINAL REMARKS

The PS filter-supported entangled multiwall carbon nanotube network composite is a conductive flexible polymeric material. The combined mechanical and electrical properties open new opportunities for the composite use as polymer composite conductors, pressure sensing elements as well as materials for electromagnetic interference shielding and lightning strike protection. A hot press molding process can produce solid bulk composites consisting of multiple-layers of PS filter-supported MWCNT network.

ACKNOWLEDGMENTS

This project was financially supported by the Grant Agency of the Academy of Sciences of the Czech Republic (GAAV IAA200600803), the Fund of Institute of Hydrodynamics AV0Z20600510, the Ministry of Education, Youth and Sports of the Czech Republic (MSM 7088352101) and by the Ministry of Industry and Trade of the Czech Republic (project 2A-1TP1/068).

REFERENCES

1. E.T. Thostenson, C.Y. Li, T.W. Chou, “Nanocomposites in context”, *Composites Science and Technology*, Vol. 65, pp. 491-516 (2005).

2. Q. Cao, J.A. Rogers, “Ultrathin films of single-walled carbon nanotubes for electronics and sensors: A review of fundamental and applied aspects”, *Advanced Materials*, Vol. 21, pp. 29-53 (2009).

3. Z. Wang, Z. Liang, B. Wang, C. Zhang, L Kramer, “Processing and property investigation of single-walled carbon nanotube buckypaper/epoxy resin matrix nanocomposites”, *Composites: Part A*, Vol. 35, pp. 1225-1232 (2004).

4. T.W. Chou, L. Gao, E.T. Thostenson, Z. Zhang, J.H. Byun, “An assessment of the science and technology of carbon nantube-based fibers and composites”, *Composites Science and Technology*, Vol 70, pp. 1-19 (2010).

5. D. Kimmer, P. Slobodian, D. Petráš, M. Zatloukal, R. Olejník, P. Sáha, “Polyurethane/MWCNT nanowebs prepared by electrospinning process”, *Journal of Applied Polymer Science*, Vol. 111, pp. 2711-2714 (2009).

Polyurethane/Carbon nanotube nanocomposite fibers prepared by electrospinning

Robert Olejník[1], Dušan Kimmer[2], Petr Slobodian[1], Pavel Říha[3], Petr Sáha[1]

[1]*Tomas Bata University in Zlín, Faculty of Technology, T.G.M. 275, 762 72 Zlín, Czech Republic*

slobodian@utb.ft.cz

[2]*SPUR a.s., T. Bati 299, 764 22 Zlín, Czech Republic*

[3]*Institute of Hydrodynamics, Academy of Sciences, 166 12 Prague, Czech Republic*

The electrospinning is an effective method that produces polymer nanofibers from polymer solution or melt by applying external electric field. When nanofibers are drawn from a carbon nanotube (CNT)/polymer dispersion, CNT are integrated into the fiber structure. The filled structure may augment mechanical and/or electrical properties of nanofibers.

We have treated multi wall carbon nanotubes (MWCNT) surface (acid oxidation, reaction with 4,4′-methylenebis(phenyl isocyanate) in dimethyl formamide) in order to improve their dispersability and compatibility with polyurethane (PU) matrix. The dispersion of modified nanotubes and PU prepolymer hydroxyl terminated has been homogenized by sonification prior to electrospinning. The structure of fabricated nanofibers as well as CNT distribution were observed by SEM and TEM analyses and compared with pure PU nanofibers.

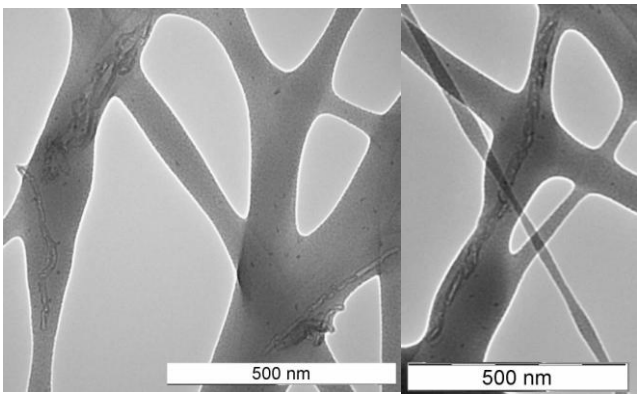

Fig.1 TEM micrographs of fabricated MWCNT/PU nanofibers by electrospinning.

The financial support projects MSM 7088352101 and GAAV IAA200600803 are gratefully acknowledged.

CARBON NANOTUBE NETWORK EMBEDED IN HIGH ELASTIC POLYURETHANE AND ITS USE FOR BODY KINEMATICS AND JOINT FLEXION SENSING

Robert OLEJNIK [1,2,a], Petr SLOBODIAN [1,2,b], Pavel RIHA [3c] and Petr SAHA [1,2,d]

[1]*Tomas Bata University, Faculty of Technology, Polymer Centre, 760 01 Zlin, Czech Republic*

[2]*Tomas Bata University, Centre of Polymer Systems, University Institute, 760 01 Zlin, Czech Republic*

[3]*Institute of Hydrodynamics, Academy of Sciences, 166 12 Prague 6, Czech Republica*

[a]*rolejnik@volny.cz*, [b]*slobodian@ft.utb.cz*, [c]*riha@ih.cas.cz*, [d]*saha@utb.cz*

Abstract

Monitoring of human motion has big relevance not only for medicine but also for technical applications. Joint flexion is one major field where could be body kinematic sensing element applied. The used sensing element is prepared from a highly-deformable polymer composite consist of a network of entangled electrically-conductive carbon nanotubes embedded in elastic polyurethane. The composite is prepared by an innovative procedure in which the non-woven polyurethane filtering membrane prepared by electrospinning technique and the carbon nanotube cake are integrated by compression molding. As an example of the composite use as a strain sensor, human knee flexion and its cyclic movement is monitored, that may be applicable in athletic training as well as in orthopedics,rehabilitation and input device for virtual reality.

Keywords: Carbon nanotubes, polyurethane, strain sensor, resistivity, biomechanics.

Acknowledgement

The work was supported by the Operational Program of Research and Development for Innovations co-funded by the European Regional Development Fund (ERDF), the National budget of Czech Republic within the framework of the Centre of Polymer Systems project (Reg. No.: CZ.1.05/2.1.00/03.0111). This article was also supported by the internal grant of TBU in Zlin No. IGA/FT/2012/022 funded from the resources of Specific University Research and by the Fund of Institute of Hydrodynamics AV0Z20600510.

Improvement of strain sensing element based on the carbon nanotube network by $KMnO_4$ oxidation

Roman Boruta[1a], Petr Slobodian[1,2b],Robert Olejnik [1,2c] Michal Machovský [1d] and Pavel Riha[3e]

[1]Tomas Bata University in Zlin, Faculty of Technology, Polymer Centre, T.G.M. 275, 760 01 Zlin, Czech Republic

[2]Centre of polymer systems, Nad Ovčírnou 3685, 760 01 Zlín, Czech Republic
[3]Institute of Hydrodynamics, Academy of Sciences, 166 12 Prague 6, Czech Republic

[a]roman.boruta@post.cz, [b]slobodian@ft.utb.cz, [c]rolejnik@volny.cz,
[d]machovsky@ft.utb.cz,[e]riha@ih.cas.cz

Keywords: Carbon nanotube networks, strain sensing element, polyurethane

Abstract. The effect of oxidation of multi-walled carbon nanotubes through $KMnO_4$ on the electrical resistance of nanotube network/polyurethane composite subjected to bending has been studied. In this respect, the main achievement is a multiple increase of gauge factor evaluating electromechanical properties of the composite with $KMnO_4$ oxidized nanotubes. It indicates favorable properties of the composite for its use as a highly-deformable strain sensing element.

Introduction

The oxidation of carbon nanotubes (CNT) became a frequent way to enhance their chemical reactivity and extend application potentiality. Typically, the nanotube wet oxidation by the potassium permanganate ($KMnO_4$) produces carboxylic acid groups (-COOH) on nanotube surface as well as a significant amount of other oxygenated functional groups such as hydroxyl (-OH) and carbonyl (=O) groups [1,2]. The oxidation enhances gas sensing properties of nanotubes toward organic vapors which can be attributed to better affinity of vapors to the oxidized form of nanotubes [3]. Moreover, it was found that the nanotube network made from oxidized nanotubes has more uniform pore structure and dense morphology with lower porosity in comparison with networks formed by pristine nanotubes [4]. The network structure results from fine nanotube aqueous dispersion, and thus deposition of individual nanotubes and/or only small nanotube agglomerates on filtrating membrane since the presence of oxygen-containing groups facilitates the exfoliation of nanotube bundles and increases the dispersibility in polar media [1,2].

The aim of this paper is to study the electrical conductivity of multi-walled carbon nanotubes (MWCNTs) network embedded into the polyurethane in the course of bending and when loading/unloading cycles are imposed. MWCNT networks, prepared by filtration to the thickness of several hundred micrometers, show a potential for sensor applications especially when their electrical sensitivity to applied strain $KMnO_4$ oxidation.

Experimental

Multi-walled carbon nanotubes (BAYTUBES C70 P) produced by the chemical vapor deposition were supplied by the Bayer MaterialScience AG, Germany (C-purity > 95 wt.%, outer mean diameter ~13 nm, inner mean diameter ~4 nm, length > 1 μm and declared bulk density of MWCNTs 45-95 kg/m^3). The oxidized MWCNTs were prepared in a glass reactor with a reflux condenser filled with 250 cm^3 of 0.5M H_2SO_4, into which 5g of $KMnO_4$ as oxidizing agent and 2g of MWCNTs were added. The dispersion was sonicated at 85°C for 15 hours using thermostatic

ultrasonic bath (Bandelin electronic DT 103H). The dispersion was filtered and MWCNTs washed with concentrated HCl to remove MnO_2.

Aqueous (deionized water) dispersions of pristine and oxidized nanotubes by $KMnO_4$ were prepared with concentration of 0.03 wt.%. The dispersions were sonicated in Dr. Hielscher GmbH apparatus (ultrasonic horn S7, amplitude 88 μm, power density 300 W/cm^2, frequency 24 kHz) for 2 hours and the temperature of ca 50°C. Sodium dodecyl sulfate (SDS) and 1-pentanol surfactant system was used with concentration of components 0.1 M and 0.14 M, respectively and with adjusted pH by aqueous solution of NaOH to the value of 10. MWCNT network (buckypaper) (MWCNT-N) was prepared by nanotube dispersion vacuum filtration thought polyurethane (PU) membrane prepared by technology of electrospinning in cooperation with the SPUR Company a.s. (Czech Republic) [5]. The other network denoted MWCNT-N($KMnO_4$) was prepared from treated MWCNTs in the same way as MWCNT-N. MWCNT networks were washed several times by deionized water and methanol in situ and dried between two glass micro-fiber filter papers at 40°C for 24 hours. The polyurethane filter and MWCNT network were then compression molded at 175 ^oC to form a layered structure which was subjected to deformation/resistance tests. The resistance was measured lengthwise the composite specimen (40x8 mm) by two points method.

Results

Fig. 1 shows SEM micrographs of upper surface of entangled MWCNT network of pristine and $KMnO_4$ oxidized nanotubes. The network of oxidized MWCNTs seems to be densely packed than the network of pristine nanotubes. The quantitative difference in MWCNT network structures were determined on basis of the measurement of their porosities, ϕ. The calculated porosity values were 0.71 (MWCNT-$N_{(pure)}$) and 0.63 (MWCNT-$N_{(KMnO4)}$) respectively. For the calculation the relation $\phi = 1 - \rho_{net}/\rho_{MWCNT}$ was used, where ρ_{net}, the measured apparent density of the network was 0.38±0.01 g/cm^3 (pristine), 0.48±0.01 g/cm^3 ($KMnO_4$ oxidised). The measured average density of nanotubes was ρ_{MWCNT} = 1.3 g/cm^3. The content of oxygen in each form of MWCNT network was detected with the help of energy-dispersive X-ray spectroscopy (EDX). The oxygen content on the surface of MWCNT increased from 2.8 at.% on pristine nanotubes to 11.9 at.% on $KMnO_4$ oxidized nanotubes.

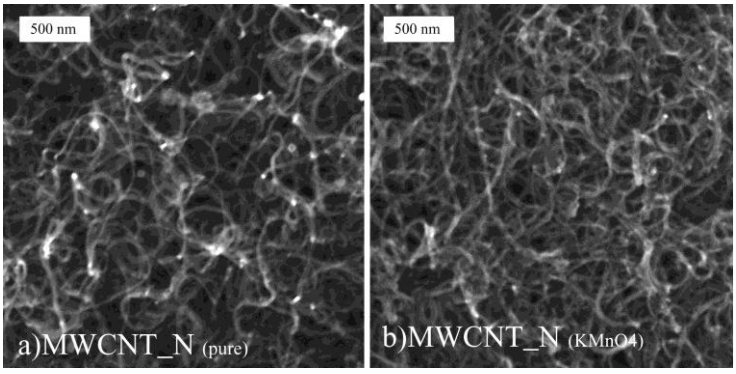

Fig.1 SEM micrographs of the surface of entangled network of pristine MWCNT and $KMnO_4$ oxidized MWCNT.

The deformation of MWCNT/ PU composite affects its electrical resistance. The mechanism of the resistance combines several effects [6]. Among those, the breakage of the formed unbroken MWCNT network apparently plays an important role, as the micrographs in Fig. 2 suggest. To investigate the role of deformation, the composite was subjected to 100 % strain and observed by SEM. The results clearly show a micro-crack structure of MWCNT network surface, Fig. 2b. The transverse cracks are generally wide whereas longitudinal cracks are narrow owing probably to transversal contraction of the testing specimen. The measured Poisson's ratio of PU was from 0.5 at

small strain until 0.29 at 100 % strain. Nevertheless, the transverse cracks contract when the tensile loading is off [6].

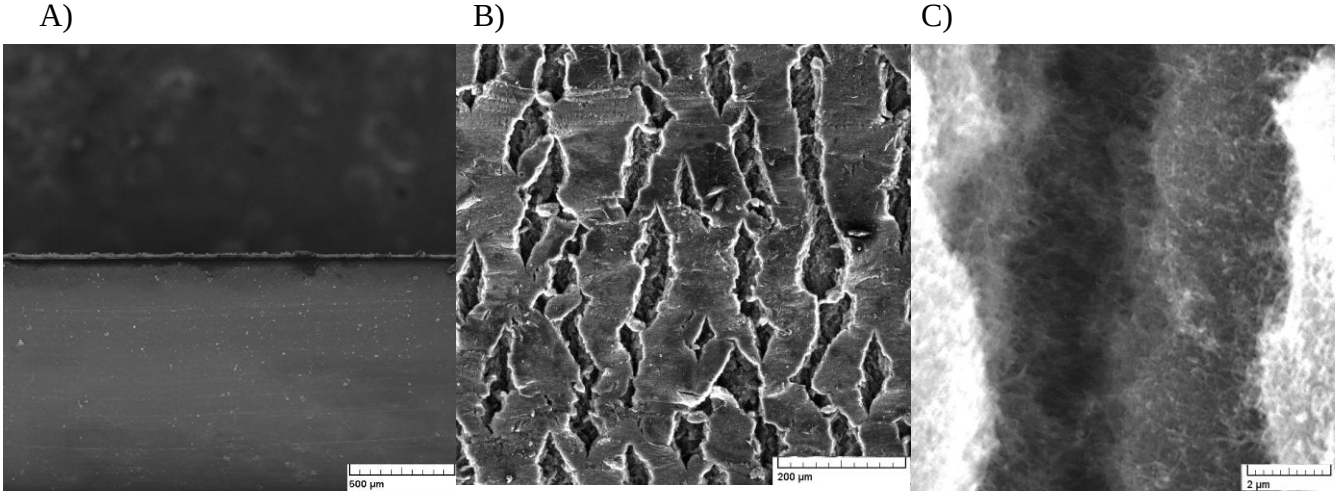

Fig. 2 A) Cross-section of composite consisting of MWNT network (upper part) and PU (lower part) after compression molding (scaler 500 μm). B) SEM micrograph of the micro-cracks on the surface of MWCNT network under 100 % longitudinal strain (scaler 200 μm). C) SEM micrograph of the detail of micro-cracks

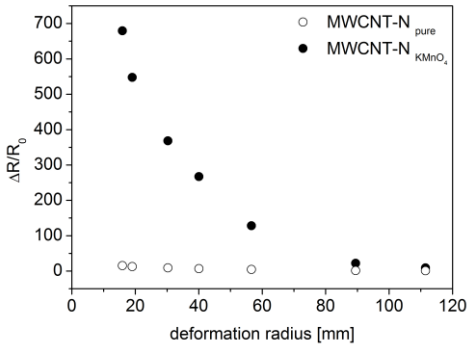

Fig. 3 The normalized resistance change vs. bending radius for the composite with pristine MWCNT (solid circles) and $KMnO_4$ oxidized MWCNT (solid squares).

The cracks are not across whole thickness of MWCNT layer since there are always bonds between the cracks through individual nanotubes [6]. Thus the composite is conductive under imposed loading. It shows Fig. 3, where the dependence of resistance of bending composite specimen on the radius of bending is plotted. The normalized resistance change $\Delta R/R_0$ is related to the initial resistance R_0 of the straight specimen. The resistance change $\Delta R = R - R_0$ is related to the resistance R of the bended specimen at the corresponding radius. The resistance change of pristine MWCNT and oxidized MWCNTs was compared at the radius 40 mm. The change for pristine MWCNTs is about 6.76 % and for the oxidised MWCNTs about 267 %. It corresponds to gauge factor, $GF = \Delta R/R_0/\varepsilon$, for pristine MWCNTs, GF=4.50, and for oxidized MWCNTs, GF=178.The deformation ε of the composite strip was approximately 15.5 %.

The response of the specimen on the cyclic deformation was measured for radius 40 mm. The data for 30 cycles of specimen bending/straightening in Fig. 4 show again the enhancing effect of oxidation. The data are also reasonably repetitive and no material property variation is observed.

The data in Fig. 4 B shows how fast is the time dependent response of the strip of MWCNT/PU composite anchored tightly on one side to the initial deflection of free ending. The measurement demonstrates the composite measuring properties under fast imposed deformation.

A) B)

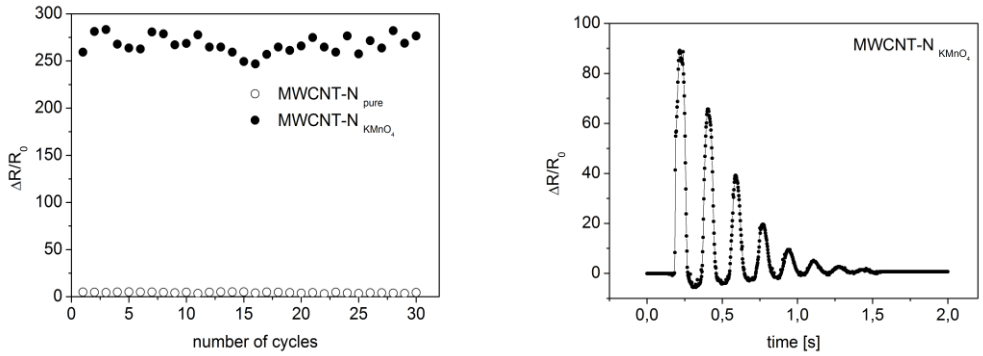

Fig. 4 A) The normalized resistance vs. number of bending/straightening cycles. The solid circles symbols denote pristine MWCNT-$N_{(pure)}$ and the solid squares the oxidized ones. B) Time dependent response of the strip of MWCNT-$N_{(KMnO4)}$ composite anchored tightly on one side to the initial deflection of free ending.

Summary

Multi-walled carbon nanotubes were used in their pure and oxidized form to prepare entangled networks (buckypaper) as a part of MWCNT/PU composite. The response of the composite to deformation was measured by their electrical resistance. The results show that the composite with oxidized network has an enhanced sensitivity to loading. This modified MWCNT/PU composite thus can be considered as a suitable material for application as a cheap and easy to prepare micro-sized strain sensing element.

Acknowledgement

The work was supported by the Operational Program of Research and Development for Innovations co-funded by the European Regional Development Fund (ERDF), the National budget of Czech Republic within the framework of the Centre of Polymer Systems project (Reg. No.: CZ.1.05/2.1.00/03.0111). This article was also supported by the internal grant of TBU in Zlin No. IGA/FT/2012/022 funded from the resources of Specific University Research and by the Fund of Institute of Hydrodynamics AV0Z20600510. We appreciate also support and help provided by the company SPUR a.s. (Czech Republic) during preparation of polyurethane non-woven filters.

References

[1] K. Hernadi, A. Siska, L. Thien-Nga, L. Forro, I. Kiricsi: Solid State Ionics Vol. 141 (2001) p. 203

[2] A. Rasheed, J. Y. Howe, M. D. Dadmun, P. F. Britt: Carbon Vol. 45 (2007) p. 1072

[3] C.M.Hussain, C. Saridara, S.Mitra. J. Chromatogr. A Vol. 1185 (2008) p. 161

[4] P. Slobodian, P. Riha, A. Lengalova, P. Svoboda, P.Saha: Carbon Vol. 49 (2011) p. 2499

[5] D. Kimmer, P. Slobodian, D. Petras, M. Zatloukal, R. Olejník and P. Saha: J. Appl. Polym. Sci. Vol. 111 (2009), p. 2711

[6] P. Slobodian, P. Riha, P. Saha: Carbon (2012). http://dx.doi.org/10.1016/j.carbon.2012.03.008.

Electromechanical properties of carbon nanotube networks under compression

2011 Meas. Sci. Technol. 22 124006

(http://iopscience.iop.org/0957-0233/22/12/124006)

Meas. Sci. Technol. **22** (2011) 124006 (7pp) doi:10.1088/0957-0233/22/12/124006

Electromechanical properties of carbon nanotube networks under compression

Petr Slobodian[1], **Pavel Riha**[2], **Robert Olejnik**[1] **and Petr Saha**[1]

[1] Centre of Polymer Systems, Faculty of Technology, Tomas Bata University in Zlín, Zlín, Czech Republic
[2] Institute of Hydrodynamics, Academy of Sciences, Prague, Czech Republic

E-mail: slobodian@ft.utb.cz, riha@ih.cas.cz, rolejnik@volny.cz and saha@utb.cz

Received 15 February 2011, in final form 17 May 2011
Published 15 November 2011
Online at stacks.iop.org/MST/22/124006

Abstract
The network of entangled multiwall carbon nanotubes and the composite consisting of a polystyrene filter-supported nanotube are introduced as conductors whose conductivity is sensitive to compressive stress both in the course of monotonic stress growth and when loading/unloading cycles are imposed. The testing has shown as much as a 100% network conductivity increase at the maximum applied stress. It indicates the favorable properties of the multiwall carbon nanotube network for its use as a stress-electric signal transducer. To model the conductivity–stress dependence, it is hypothesized that compression increases local contact forces between the nanotubes, which in turn leads to a decrease in the contact resistance between them. The lack of detailed knowledge of the mechanism as well as an unclear shift from individual contacts to the whole network conductance behavior is circumvented with a statistical approach. In this respect, the conductivity/compression data were fitted well using the Weibull distribution for the description of the nanotube contact resistance distribution.

Keywords: carbon nanotube network, compression, electrical conductivity, stress sensor

1. Introduction

Recent technological progress heavily relies on the use of materials that can offer advanced structural and functional capabilities. In this respect, entangled carbon nanotube (CNT) network structures show great potential for developing high-performance polymer composites and enhanced sensors. CNT networks can proportionally transfer their unique properties into reinforced composite materials and films for sensors and bring substantial improvements in structural strength, electrical and thermal conductivity, electromagnetic interference shielding and other properties [1, 2].

The first carbon nanotube network was fabricated by Walters *et al* who dispersed nanotubes into a liquid suspension and then filtered through the fine filtration mesh [3]. Consequently, pure nanotubes stuck to one another and formed a thin freestanding entangled structure, later dubbed buckypaper.

A recent study [4] investigated the mechanical behavior of entangled mats of carbon nanotubes and several other fibers during compression and cyclic tests. The obtained hysteresis loop between loading and unloading was linked with mat morphology and motion, and friction and rearrangement of fibers during compaction. However, the electric resistance of freely poured CNT networks at compression has only been measured in [5] on a tangle whose thickness was about 2.5 mm and the maximum strain about 0.8. The obtained data were analyzed to get an estimate of the CNT tangle resistance and the contact resistance between the nanotubes.

Although the above-mentioned paper [5] brings essential information on CNT resistance compressive stress dependence, the CNT tangles prepared in the discussed study differ from the networks prepared from fluid suspensions and deposited on the filtration mesh [3]. Thus the aim of this paper is to study the compression dependence of the electrical conductivity of the multiwall carbon nanotube (MWCNT) network and the polystyrene (PS) filter-supported multi-wall carbon nanotube network. The former is prepared by the nanotube filtration through the non-woven polyurethane filtration mesh and then the entangled MWCNT sediment is gently peeled off the mesh. The PS filter-supported MWCNT network composite is prepared by nanotube filtration through

the non-woven PS mesh and then both composite portions are integrated by compression molding.

Both materials have a potential for use as pressure sensing elements. Moreover, the measured electromechanical property of the MWCNT/PS composite open new opportunities for the use of the composite as polymer composite conductors as well as material for electromagnetic interference shielding and lightning strike protection.

2. Experimental details

Purified MWCNT produced by the chemical vapor deposition of acetylene were supplied by Sun Nanotech Co. Ltd, China. According to the supplier, the nanotubes have diameter 10–30 nm, length 1–10 μm, purity >90% and electrical resistivity 0.12 Ω cm. The nanotubes were used for the preparation of an aqueous paste: 1.6 g of MWCNT and ∼50 ml of deionized water were mixed with the help of a mortar and pestle. The paste was then diluted in deionized water with sodium dodecyl sulfate (SDS) and 1-pentanol. Consequently, NaOH aqueous solution was added to adjust the pH to the value of 10 [6]. The final nanotube concentration in the suspension was 0.3 wt%, and the concentrations of SDS and 1-pentanol were 0.1 and 0.14 M, respectively [7]. The suspension was sonicated in Dr Hielscher GmbH apparatus (ultrasonic horn S7, amplitude 88 μm, power density 300 W cm^{-2}, frequency 24 kHz) for 2 h at a temperature of about 50 °C.

For making the entangled MWCNT network on a polyurethane porous membrane [8], a vacuum filtration method was used. The formed disk-shaped network was washed several times by deionized water and methanol *in situ*, and then removed and dried between filter papers. The thickness of the obtained disks was typically 0.15–0.46 mm (figure 1(*a*)).

The structure of the MWCNT network was investigated with a scanning electron microscope (SEM) from Vega Easy Probe (Tescan s.r.o., Czech Republic). The sample taken from the disk was first deposited onto carbon targets and covered with a thin Au/Pd layer. For the observations, the regime of secondary electrons was chosen.

Pure MWCNT were also analyzed via transmission electron microscopy (TEM) using the microscope JEOL JEM 2010 at an accelerating voltage of 160 kV. The sample for TEM was fabricated on a 300-mesh copper grid with a carbon film (SPI, USA) from MWCNT dispersion in acetone which was prepared by ultrasonication, deposited on the grid and dried.

The MWCNT/PS composite is prepared by the flow filtration of aqueous MWCNT dispersion through the PS filtrating mesh. The start-up phase when the nanotubes are infiltrated into the PS filter mesh is followed by the sedimentation of the MWCNT. The PS filter-supported filtrate is washed several times by deionized water and methanol *in situ*. Then the composite is placed between filter papers, moistened with acetone and dried between two iron plates at room temperature for 1 day. The final drying continued without iron plates at 40 °C throughout another day. The thickness of the non-woven PS filter is typically 0.5 mm

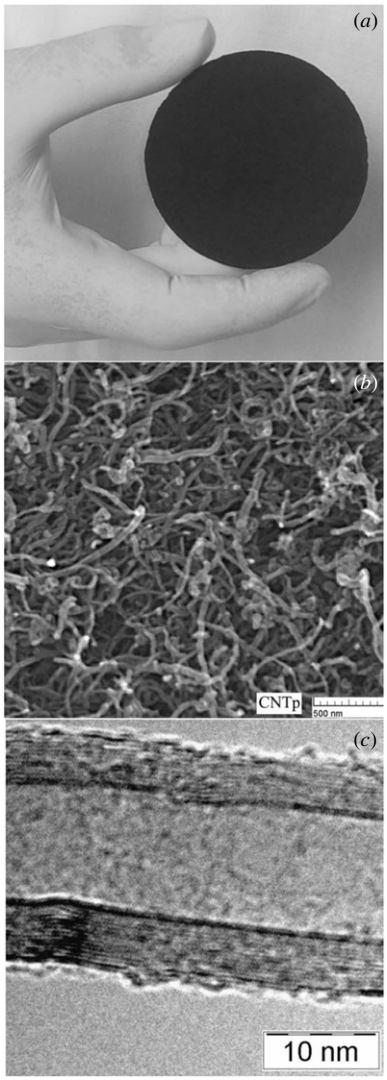

Figure 1. (*a*) Free-standing randomly entangled MWCNT network (disk diameter 75 mm, thickness 0.15 mm), (*b*) SEM image of the surface of the entangled MWCNT network of buckypaper, and (*c*) detailed view of one individual MWCNT tube (consists of about 15 rolled graphene layers with the interlayer distance of about 0.35 nm) analyzed by HRTEM.

and that of the MWCNT entangled network is 0.02–0.4 mm. The PS filter-supported MWCNT network composite can be used either without adjustment or hot compression molding at 190 °C converts the PS fiber membrane to a film with a fixed MWCNT network.

The PS membrane is prepared by electrospinning from the solution. PS is added in a mixture of methyl isobutyl ketone and dimethyl formamide with the volume ratio 3:1 (PS weight concentration is 15 wt%). The nanofiber layer is made using NanoSpider (Elmarco s.r.o.) equipped with a steel rotation electrode with needles and a steel cylinder collecting electrode (details in [8]). Then the porous layer is subjected to hot pressing at pressure 0.6 MPa and temperature 80 °C.

The MWCNT networks were tested for deformation using a simple set-up. The network stripe (length 10 mm and width 8 mm, the loading area between glass plates was 8 mm × 8 mm) cut out from the manufactured disks of the entangled

CNT was compressed stepwise between two glasses to the maximum value with a 20 s delay of strain reading in each step. This period was sufficient to reach a strain stable value for each compression change. Then the stress–strain dependence during the unloading period was measured in the same manner. The conductivity characteristic of network stripes was simultaneously measured with deformation. Two electrical contacts were fixed to the stripe by silver colloid electro-conductive paint Dotite D-550 (SPI Supplies) and the electrical conductivity was measured lengthwise by the two-point technique using a multimeter Sefram 7338. The network connection to electrical leads was outside the compressed 8 mm × 8 mm area so that the contribution of these contacts to the total conductivity was not affected by compression and thus remains constant.

3. Results and discussion

3.1. Experimental results

The structure of the upper surface of entangled nanotubes can be seen in figure 1(*b*) as the SEM micrograph. After the filtration of the MWCNT suspension, the network was dried, which caused its shrinkage by about 7%. The porosity was calculated from the relation $\phi = 1 - \rho_{net}/\rho_{MWCNT}$, where $\rho_{net} = 0.56 \pm 0.03$ g cm^{-3} denotes the measured apparent density of the nanotube network. The values correspond to those given in the literature; for instance, $\rho_{net} = 0.54$ g cm^{-3} as given in [9]. The measured average density of nanotubes $\rho_{MWCNT} = 1.7$ g cm^{-3} is very close to the theoretical value, i.e. 1.8 g cm^{-3} [8]. Also the calculated porosity $\phi = 0.67$ corresponds well to the published values for MWCNT networks [10].

The mechanical properties of manufactured structures were followed in the course of 12 compression and relaxation cycles with a cyclic accumulation of residual strain (compression as well as compressive strain is defined as positive loading and deformation, respectively). The results in the form of compressive stress versus strain dependence are presented in figure 2.

The accumulation of residual strain is often called ratcheting and the minimum strain in each cycle is defined as a ratcheting strain, ε_r. In the MWCNT network, a ratcheting strain appears after the first compression cycle, probably due to the initial deformation of the porous structure and blocked reverse motion of nanotubes inside the compact network, as hypothesized in [5]. Thus the ability of the network to be repeatedly highly compressed is reduced. Moreover, during successive cycles of loading and unloading the ratcheting rate per cycle decreases and an asymptotic value of ε_r is obtained, as demonstrated in figure 3.

The measured data on the MWCNT conductivity are shown in figure 4 as a plot of conductivity values σ versus applied compressive stress τ. Compression causes a conductivity change during both the loading and unloading periods due to a specific deformation of the porous structure. According to [5], the local contact forces increase during compression, allowing a better contact of nanotubes, which in turn leads to a decrease in the contact resistance between

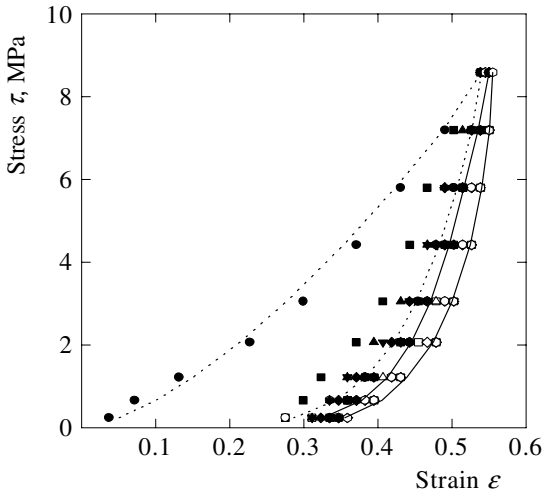

Figure 2. Stress–strain loops in a cyclic compression test for the MWCNT network subjected to 12 compression/expansion cycles (the network thickness 0.418 mm). The dotted lines (first loading and unloading cycle) and solid lines (twelfth cycle) represent the prediction given by equation (1).

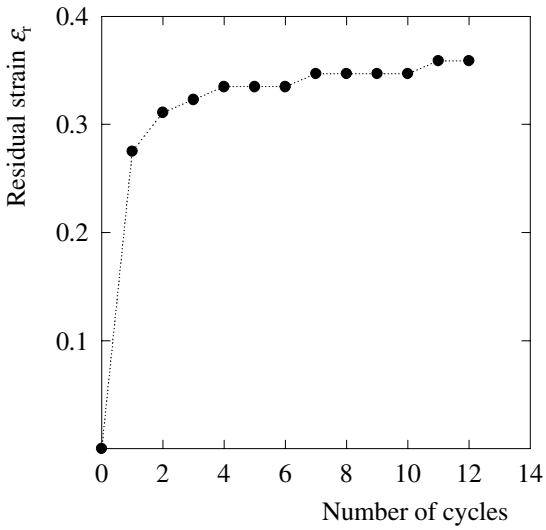

Figure 3. Ratcheting strain versus number of cycles.

crossing nanotubes; in release, the dependence is just opposite. At the same time, the possible effect of the distance between contacts on the CNT tangle resistance is considered in [5]. The distance between contacts may decrease during compression owing to the evoked relative motion of nanotubes, which corresponds to a lower intrinsic resistance of nanotube segments between contacts. Last but not least, compression may also bend the nanotubes sideways, which results in more contacts between nanotubes [4]. Since the contact points may act as parallel resistors, their increasing number causes an enhancement of the MWCNT network conductivity.

The conductance mechanisms are apparently not reversible in the initial cycle since the unloading curve indicates residual conductivity increase in the off-load state. Nevertheless, the ongoing compression cycles have a stabilizing effect on the conductivity–compression loops

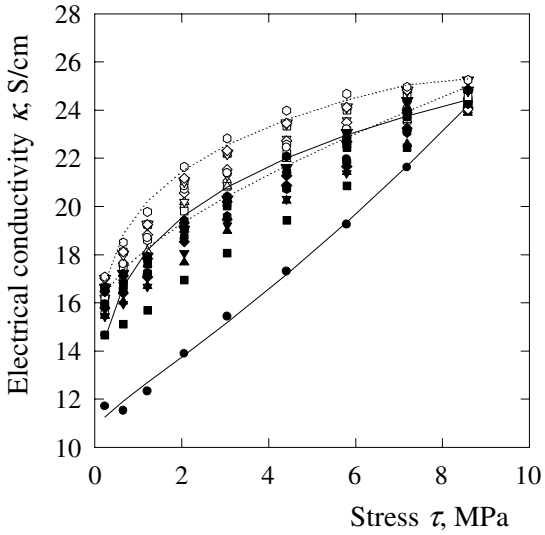

Figure 4. Conductivity–compressive stress loops for the MWCNT network subjected to 12 successive compression/expansion cycles (network thickness 0.375 mm). The solid lines (first loading and unloading cycle) and dotted lines (twelfth cycle) represent the prediction given by equation (8).

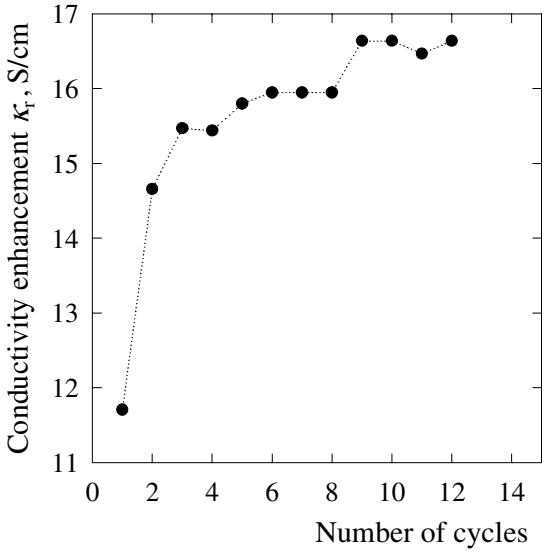

Figure 5. Conductivity enhancement in each cycle versus number of cycles.

similar to their effect on mechanical properties. The conductivity enhancement κ_r, defined as the residual minimum conductivity during each cycle, decreases with increasing number of cycles, and after about 12 cycles, κ_r tends to reach an asymptotic value, figure 5.

The structure of the PS non-woven membrane and the cross-section of the MWCNT/PS network composite are shown in figures 6(*a*) and (*b*). The MWCNT network is a coherent, conductive system which, combined with the PS fibrous membrane, increases its rigidity and at the same time keeps its electrical properties. The PS membrane porosity allows infiltration of MWCNT into the membrane during the initial part of filtration till the pores are blocked and a pure nanotube network is formed. The composite sheet prepared

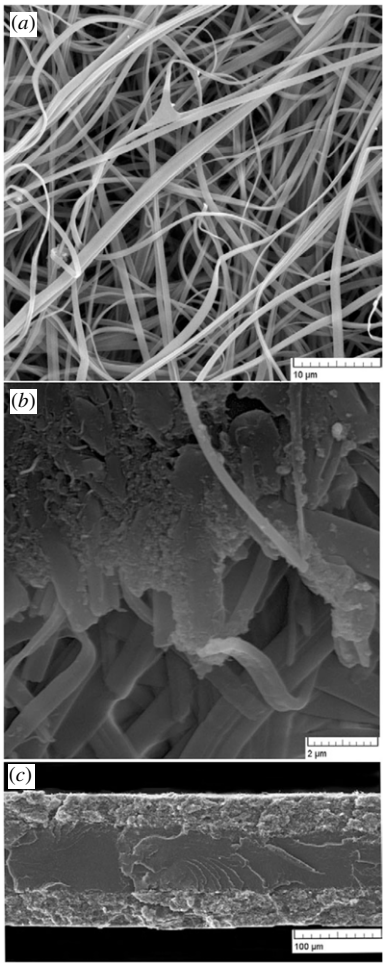

Figure 6. (*a*) SEM analyses of the PS filtrating membrane prepared by electrospinning, (*b*) SEM micrograph of the cross-section of the PS fibrous membrane with infiltrated MWCNT, and (*c*) the cross-section of the compressed composite consisting of the PS matrix (middle) and two MWCNT network layers (above and below the matrix).

by double-sided filtration is shown in figure 6(*c*). The bulk composite can be prepared by overlaying several PS filter-supported networks and their hardening by hot compression molding.

The results of the tensile test are shown in figure 7. The initial tensile modulus for the MWCNT network is about 600 MPa and the ultimate tensile strength is 1 MPa. The test of the PS filter-supported MWCNT/PS composite shows a change in mechanical properties in comparison with a pure MWCNT network. The PS reinforcement increases the tensile modulus to 1300 MPa and the ultimate tensile strength to 10.3 MPa.

The significant property of a new MWCNT/PS composite is its sensitivity to compressive strain. The effect of compression is shown in figure 8. The plotted resistance values, R, are normalized with respect to the initial resistance, R_0, recorded at the start of the test. The resistance is measured in each compression step at the preset deformation and for the subsequent unloaded state. The resistance mechanism is apparently not reversible in the initial cycles since there is a resistance decrease in the off-load state. Nevertheless, the

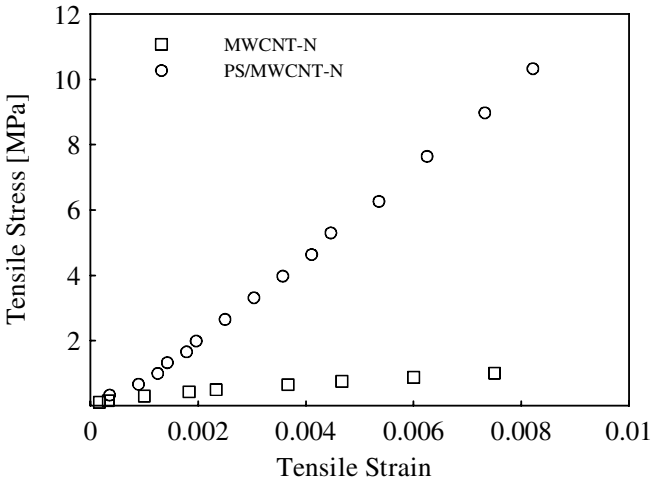

Figure 7. Comparison of the mechanical properties of the MWCNT network (squares) and PS filter-supported MWCNT network (circles) in a tensile test.

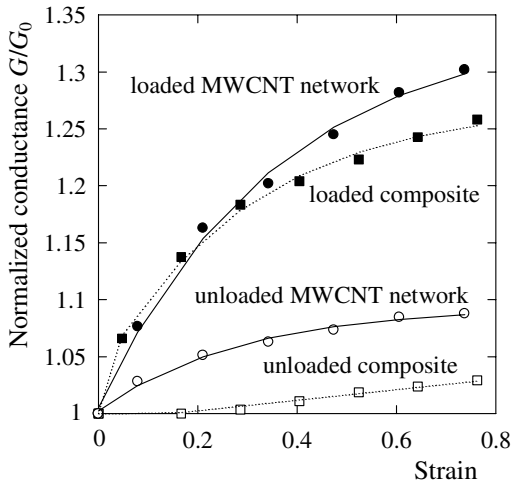

Figure 8. Normalized conductance versus strain for the loaded and unloaded MWCNT/PS composite (squares) and MWCNT network (circles). The solid lines and dotted lines represent the prediction given by equation (8).

ongoing compression cycles have a stabilizing effect on the resistance and after about 20 cycles no resistance change is observed, figure 9.

3.2. Deformation mechanics

The filtering type of MWCNT network is an assembly of entangled, non-bonded and randomly oriented carbon nanotubes. When the compressive load is applied, the data on deformation micromechanics of the wad assembly indicate increased local force between CNT [4], the fiber buckling [11], the slippage with friction at contact points [12, 13] and irreversible fiber rearrangement reflected in the hysteresis stress–strain curves during loading and unloading cycles (figure 2) [5]. However, the existing micromechanics models which relate the compressive stress and deformation of the randomly oriented mats [14, 15] are based on the bending

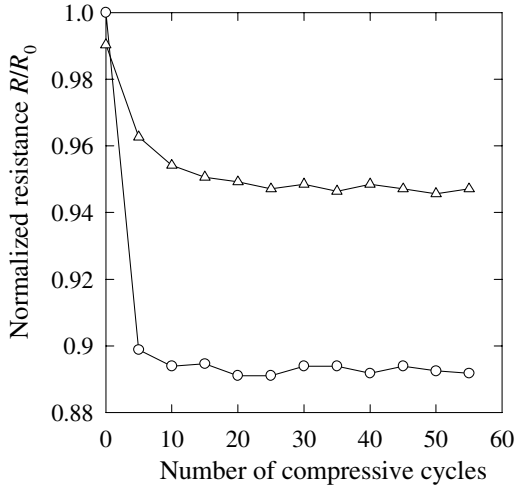

Figure 9. Normalized resistance versus number of cycles at the load 3.9 MPa (circles) and 0.4 MPa (triangles) for the MWCNT/PS composite (right).

deformation of fibers without frictional slippage at contact points. It is a simplifying assumption that the motion of the contacts is affine, that is, it follows the macroscopic strain of the network [13]. To generalize the above assumptions which are restricted to the bonded assembly, we propose on the basis of the above-mentioned known data obtained in [4, 11, 13] that the total compressive stress, which affects the network deformation, is a combination of the elastic bending stress and the friction stress:

$$\sigma = \sigma_e + \sigma_f. \tag{1}$$

The micromechanical analyses of the fiber assembly led to the power-law dependence of the bending stress to the fiber volume fraction with the power-law index n equal to 3 for the random 3D structure [14, 15] and 5 for a planar network structure [15]. This dependence in terms of strain has the form

$$\sigma_b = k_E\left(\varepsilon^n - \varepsilon_r^n\right), \tag{2}$$

where ε denotes the compressive (engineering) strain, ε_r the residual compressive strain and $k_E = kE$, where E denotes the elastic modulus of nanotubes and k an adjustable parameter of the model which accounts for the nanotube orientation distribution, the degree of waviness and loading direction [16].

The friction stress is proportional to the contact force. The contact force increases with compressive nanotube packing. Consequently, the friction stress is assumed to follow proportionally the compressive strain:

$$\sigma_f = \mu(\varepsilon - \varepsilon_r), \tag{3}$$

where μ denotes the friction coefficient.

The hysteresis loops in figure 2 show that the compressive stress increases with a rising rate in the course of loading period. On the other hand, compression decreases abruptly at the beginning of release. To include the possible mechanism in the stress–strain relation (1), a scalar structural parameter λ is used to characterize the instantaneous network structure. A value of unity may reflect the network deformation owing to slippage at the contact points. A decreasing λ value

may correspond to an increasing bending deformation of nanotubes owing to their tightened contacts by compression. The progress of the structural change may be expressed by the first-order kinetic equation as

$$d\lambda/d\varepsilon = -\lambda, \qquad \lambda = \exp(-\varepsilon). \tag{4}$$

Thus the structural parameter determines the relative importance of the friction at contact points with deformation progress as

$$\sigma_f = \mu(\varepsilon - \varepsilon_r)\{\exp[-(\varepsilon - \varepsilon_r)]\}. \tag{5}$$

At the same time, the compression of contacts prevents nanotube slippage and the bending deformation takes place:

$$\sigma_e = k_E\left(\varepsilon^n - \varepsilon_r^n\right)\{1 - \exp[-(\varepsilon - \varepsilon_r)]\}. \tag{6}$$

The power-law index n is considered to be equal to 3 for the loading period of the first cycle when the network is not yet compressed. Afterward, the compressed network is considered planar and $n = 5$.

3.3. Stochastic model of the MWCNT network conductivity

The conductivity of the MWCNT network subjected to compressive stress is considered to be governed by the aforementioned mechanisms ranging from the contact resistance between the nanotubes through nanotube conduction to the network architecture. The complexity of network ability to conduct an electric current limits the application of classical electricity concepts for finding a relation between local contacts and the macroscopic network response to compressive stress. For this reason, we translate the results of experimental observation into a probabilistic scheme. Within the framework of this scheme, we assume that the distribution of local conductive points enables us to describe the joint probability for the total network conductivity change under compressive stress τ by the cumulative distribution function or unreliability function $F(\sigma)$ for the two-parameter Weibull distribution:

$$\Pr(\sigma) = F(\sigma) = 1 - \exp[-(\sigma/\sigma_0)^m], \tag{7}$$

where $F(\sigma)$ is an increasing function, $0 \leqslant F(\sigma) \leqslant 1$, and describes the probability of network conductivity change $\Pr(\sigma)$ under stress no greater than σ. The two Weibull parameters are the shape parameter m and the scale parameter σ_0.

The reason for our choice of the Weibull distribution is that it is a versatile distribution that can take on the characteristics of other types of distributions for the probability of network conductivity change (exponential, Rayleigh, extreme value distributions) based on the value of the shape parameter m. The Weibull distribution also expresses some information about the possible relation of the network conductivity change to stress, namely that the random events (the changes in contacts' resistance) occur continuously and independent of one another with a varying change rate. For all that, this useful probabilistic scheme does not identify the real kinetics between contacts' resistance and the compressive stress since the real events are not random but deterministic governed by the causality principles. The Weibull distribution is commonly used to model time to fail, time to repair and material strength [17, 18].

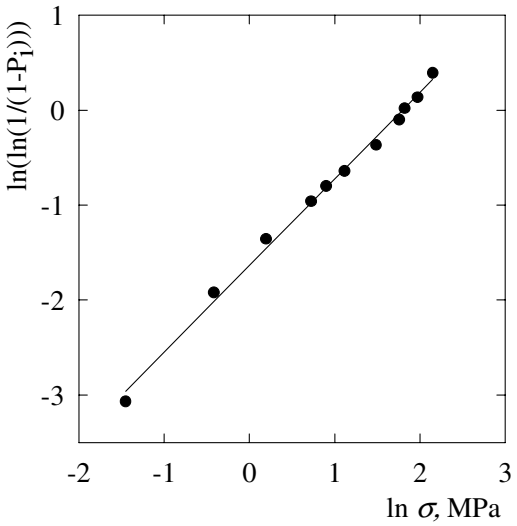

Figure 10. Weibull plot for the compressive stress deforming conductive MWCNT network.

The assumption that the probability of the whole network conductivity follows the Weibull distribution is substantiated in figure 10. The figure shows that all the experimental points very closely follow a straight line when plotted in the Weibull coordinates $\ln\sigma$ versus $\ln(\ln(1/(1 - P_i)))$, where $P_i = (i - 0.5)/n$ and i ranges from 1 to n, which is the number of tests. The goodness-of-fit to the straight line is reflected in the value of the correlation coefficient $r = 0.99$.

The tendency of the measured increase of the macroscopic, i.e. network, conductivity with compressive stress is bound to the probability of network conductivity change $\Pr(\sigma)$ under stress no greater than σ. Consequently, the following relation of the network conductivity $\kappa(\sigma)$ to the function $F(\sigma)$ links appropriately the model prediction with the observed stress-dependent network conductivity increase:

$$\kappa(\sigma) = \alpha + \beta(1 - \exp[-(\sigma/\sigma_0)^m]), \tag{8}$$

where α and β are location parameters.

The reasonably good description of the measured data by the predictive relation (8), shown in figure 4, justifies the probability model chosen here for the MWCNT network conductivity change under compression.

4. Conclusions

The conductivity–compression characteristics for entangled carbon nanotube network structures of buckypaper produced by filtering a nanotube suspension has not been studied in detail so far. Thus the primary aim of this study was to find out the effect of compression on network electric conductivity when a simple and repeated loading is exerted. The measurements have shown an over 100% network conductivity increase at the maximum applied compressive stress. It indicates a good potentiality of the MWCNT entangled network for a compression sensing element. The conversion of compressive stress into the conductivity increase is achieved by the

deformation of the porous structure. The structure recovering mechanism projects into the ratcheting strain. The rate of this strain decreases with increasing number of cycles and an asymptotic value of this residual strain is reached. During successive cycles of loading and unloading the network rearrangement becomes steady and the MWCNT network reaches a stable stress–strain hysteresis loop shape. This mechanical stabilization is also reflected in conductivity data. The conductivity–stress loop is stable during the same number of cycles as the mechanical cyclic behavior. It shows that the entangled carbon nanotube network structure of buckypaper can be used as the sensing element of the compressive stress sensor especially when the network is suitably deformed in advance.

The PS filter-supported entangled multiwall carbon nanotube network composite is also a conductive flexible polymeric material. The combined mechanical and electrical properties open new opportunities for the composite use as pressure sensing elements, polymer composite conductors as well as materials for electromagnetic interference shielding and lightning strike protection. The advantage of the PS filter-supported MWCNT composite is flexibility and easy manipulation. The shape and size of the conductive polymer composite can be easily adjusted. Moreover, the composite conductivity may be affected not only by its compression but also by extension.

The MWCNT networks and PS filter-supported MWCNT composite can be applied in biochips or microfluidic and nano-electromechanical systems that are devices integrating electrical and mechanical components where pressure information is required. However, the materials and data obtained here do not lead directly to sensor and electromechanical systems' production. The engineering research must be conducted before the proof-of-concept measurements will lead to the field operation of reproducible, high-performance and cost-effective MWCNT-based pressure sensors and electromechanical devices.

Acknowledgments

This project was supported by the internal grant of Tomas Bata University in Zlín no IGA/12/FT/10/D funded from the resources of specific university research. This article was also created with support from Operational Programme Research and Development for Innovations co-funded by the European Regional Development Fund (ERDF) and the national budget of the Czech Republic within the framework of the Centre of Polymer Systems project (reg. no: CZ.1.05/2.1.00/03.0111) and by the Grant Agency of the Academy of Sciences of the Czech Republic (GAAV IAA200600803) and by the Fund of the Institute of Hydrodynamics AV0Z20600510.

References

[1] Thostenson T, Li C Y and Chou T W 2005 Nanocomposites in context *Compos. Sci. Technol.* **65** 491–516
[2] Cao Q and Rogers J A 2009 Ultrathin films of single-walled carbon nanotubes for electronics and sensors: a review of fundamental and applied aspects *Adv. Mater.* **21** 29–53
[3] Walters D A *et al* 2001 In-plane-aligned membranes of carbon nanotubes *Chem. Phys. Lett.* **338** 14–20
[4] Allaoui A, Hoa S V, Evesque P and Bai J 2009 Electronic transport in carbon nanotubes tangles under compression: the role of contact resistance *Scr. Mater.* **61** 628–31
[5] Poquillon D, Viguier B and Andrieu E 2005 Experimental data about mechanical behaviour during compression tests for various matted fibres *J. Mater. Sci.* **40** 5963–70
[6] Ham H T, Choi Y S and Chung I J 2005 An explanation of dispersion states of single-walled carbon nanotubes in solvents and aqueous surfactant solutions using solubility parameters *J. Colloid Interface Sci.* **286** 216–23
[7] Chern C S and Wu L J 2001 Microemulsion polymerization of styrene stabilized by sodium dodecyl sulfate and short-chain alcohols *J. Polym. Sci.* A **39** 3199
[8] Kimmer D, Slobodian P, Petráš D, Zatloukal M, Olejník R and Sáha P 2009 Polyurethane/MWCNT nanowebs prepared by electrospinning process *J. Appl. Polym. Sci.* **111** 2711–4
[9] Xie X L, Mai Y W and Zhou X P 2005 Dispersion and alignment of carbon nanotubes in polymer matrix: a review *Mater. Sci. Eng.* R **49** 89–112
[10] Whitby R L D, Fukuda T, Maekawa T, James S L and Mikhalovsky S V 2008 Geometric control and tuneable pore size distribution of buckypaper and buckydiscs *Carbon* **46** 949–56
[11] Yaglioglu O, Hart A J, Martens R and Slocum A H 2006 Method of characterizing electrical contact properties of carbon nanotube coated surfaces *Rev. Sci. Instrum.* **77** 095105
[12] Stankovic S B 2008 Compression hysteresis of fibrous systems *Polym. Eng. Sci.* **48** 676–82
[13] Barbier C, Dendievel R and Rodney D 2009 Role of friction in the mechanics of nonbonded fibrous materials *Phys. Rev.* E **80** 016115
[14] van Wyk C M 1946 Note on the compressibility of wool *J. Textile Inst.* **37** T285–92
[15] Toll S 1998 Packing mechanics of fiber reinforcements *Polym. Eng. Sci.* **38** 1337–50
[16] Masse J P, Slavo L, Rodney D, Brechet Y and Bouaziz O 2006 Influence of relative density on the architecture and mechanical behaviour of a steel metallic wool *Scr. Mater.* **54** 1379–83
[17] Weibull W 1951 A statistical distribution function of wide applicability *J. Appl. Mech. Trans. ASME* **18** 293–7
[18] Xia Z H and Gurtin W A 2007 Modeling of mechanical damage detection in CFRPs via electrical resistance *Compos. Sci. Technol.* **67** 1518–29

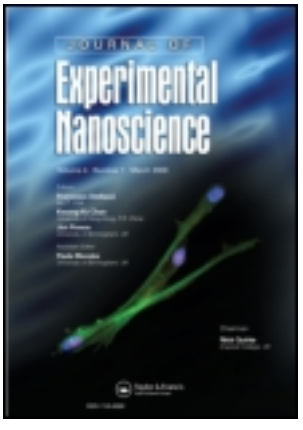

Journal of Experimental Nanoscience
Publication details, including instructions for authors and subscription information:
http://www.tandfonline.com/loi/tjen20

Effect of compressive strain on electric resistance of multi-wall carbon nanotube networks

P. Slobodian [a], P. Riha [b], A. Lengalova [c], R. Olejnik [a], D. Kimmer [d] & P. Saha [a]

[a] Faculty of Technology, Polymer Centre, Tomas Bata University in Zlín, 76272 Zlín, Czech Republic

[b] Institute of Hydrodynamics, Academy of Sciences, 16612 Prague, Czech Republic

[c] Faculty of Humanities, Tomas Bata University in Zlín, 76001 Zlín, Czech Republic

[d] SPUR a.s., T. Bati 299, 76422 Zlín, Czech Republic

Version of record first published: 03 May 2011.

To cite this article: P. Slobodian , P. Riha , A. Lengalova , R. Olejnik , D. Kimmer & P. Saha (2011): Effect of compressive strain on electric resistance of multi-wall carbon nanotube networks, Journal of Experimental Nanoscience, 6:3, 294-304

To link to this article: http://dx.doi.org/10.1080/17458080.2010.506522

Journal of Experimental Nanoscience
Vol. 6, No. 3, June 2011, 294–304

Taylor & Francis
Taylor & Francis Group

Effect of compressive strain on electric resistance of multi-wall carbon nanotube networks

P. Slobodian[a]*, P. Riha[b], A. Lengalova[c], R. Olejnik[a], D. Kimmer[d] and P. Saha[a]

[a]*Faculty of Technology, Polymer Centre, Tomas Bata University in Zlín, 76272 Zlín, Czech Republic;* [b]*Institute of Hydrodynamics, Academy of Sciences, 16612 Prague, Czech Republic;* [c]*Faculty of Humanities, Tomas Bata University in Zlín, 76001 Zlín, Czech Republic;* [d]*SPUR a.s., T. Bati 299, 76422 Zlín, Czech Republic*

(*Received 15 February 2010; final version received 30 June 2010*)

The network of entangled multi-wall carbon nanotubes is shown as a conductor whose resistance is sensitive to compressive strain, both in the course of strain growth and when loading/unloading cycles are imposed. If the compression is applied, the resistance decrease is up to 25% at the maximum applied deformation. The experimental data are analysed using the Weibull distribution model and a contact network model to get an estimate of the contact resistance between carbon nanotubes and the formation of contacts in the course of compression.

Keywords: MWNT network; electric resistance; buckypaper; strain effect

1. Introduction

Recent technology progress relies heavily on the use of materials that can offer advanced structural and functional capabilities. In this respect, entangled carbon nanotube (CNT) network structures of buckypaper show a great potential for developing high-performance polymer composite materials [1,2]. The first CNT network was fabricated when nanotubes were dispersed into a liquid suspension and then filtered through a fine filtrating mesh [3]. Consequently, numerous studies were aimed to reveal various properties of this CNT network for practical use. In spite of that the electrical resistance of entangled CNT network structures affected by compressive strain has not yet been tested. Thus, the aim of this study is to carry out such tests on multi-wall carbon nanotube (MWNT) network structures. The investigation will also involve the resistance dependence on the number of loading/unloading cycles and the measurement of network tensile deformation.

This study has been inspired by a recent paper on the electric resistance of powdery MWNT layer under compression in which the resistance/compression dependence and the contact resistance between nanotubes is thoroughly evaluated [4]. The resistance is

*Corresponding author. Email: slobodian@ft.utb.cz

ISSN 1745–8080 print/ISSN 1745–8099 online

DOI: 10.1080/17458080.2010.506522
http://www.informaworld.com

measured across the layer in a tubular glass cell to which MWNT powder has been poured. The initial layer thickness is *ca* 2.5 mm and the initial CNT volume fraction is about 0.05. Further, the resistance of CNT macroscopic aggregate forming a network structure of buckypaper is measured along the network stripe. The buckypaper is purposely thin (0.1–0.4 mm) and the CNT volume fraction is about 0.5 since the networks are primarily intended as CNT mats for polymer composite fabrication. Moreover, it can be seen from a simple experiment that the cohesion of freely poured CNT layer is negligible in comparison with CNT macroscopic agglomerate, forming a network structure of buckypaper. Consequently, the order of the contact resistance between the nanotubes of CNT network is reduced by two in comparison to the contact resistance of powdery CNT layer as shown in Section 3.2.

2. Experimental

Purified MWNTs of acetylene type were supplied by Sun Nanotech Co. Ltd., China. According to the supplier, the nanotube diameter is 10–30 nm, length 1–10 μm, purity >90% and volume resistance 0.12 Ω cm.

The nanotubes were used for the preparation of aqueous paste: 1.6 g of MWNT and ~50 mL of deionised water were mixed with the help of a mortar and pestle. The paste was diluted in deionised water with sodium dodecyl sulphate (SDS) and 1-pentanol. Then, NaOH dissolved in water was added to adjust pH to the value of 10 [5]. The final nanotube concentration in the dispersion was 0.3 wt% and concentration of SDS and 1-pentanol 0.1 and 0.14 M, respectively [6]. The dispersion was sonicated in a Dr Hielscher GmbH apparatus (ultrasonic horn S7, amplitude 88 μm, power density 300 W/cm^2 and frequency 24 kHz) for 2 h and the temperature of *ca* at 50°C.

Polyurethane (PU) non-woven membranes for MWNT dispersion filtration were prepared by electrospinning from PU dimethyl formamide solution. For more details of PU chemical composition and particular process characteristics, see reference [7]. To make entangled MWNT network on PU porous filtration membrane, the vacuum filtration method was used. The formed network of disk shape was rinsed several times with deionised water (until neutral pH was reached) and methanol *in situ*, then removed and dried between filter papers. The thickness of the disks was typically 0.15–0.4 mm.

The structure of MWNT network was investigated in the regime of secondary electrons with a scanning electron microscope (SEM) Vega LMU made by Tescan Ltd., Czech Republic. The sample was deposited onto the carbon targets and covered with a thin Au/Pd layer.

Pure MWNTs were also analysed *via* transmission electron microscopy (TEM), using microscope JEOL JEM 2010 at the accelerating voltage of 160 kV. The sample for TEM was fabricated on 300 mesh copper grid with a carbon film (SPI, USA) from MWCNT dispersion in acetone prepared by ultrasonication, which was deposited on the grid and dried.

The resistance/compression dependence for network stripes (length 45 and width 10 mm), prepared by cutting from the manufactured discs of entangled CNT network was measured during network compression between glass plates. The length of the compressed part was 35 mm. The gap between the plates, which determined the network compressive deformation, was adjusted by calibrated metal spacers. The electric resistance along the

stripe was measured by the 2-point technique with multi-meter Sefram 7338. The electrical contacts were fixed to the stripes by silver colloid electrically conductive paint, Dotite D-550 (SPI supplies).

The network was also tested for deformation using a simple set-up. The network stripe was stepwise compressed between two glasses to the maximum value with 60 s delay of strain reading in each step.

3. Results and discussion

3.1. *Experimental results*

MWNT aqueous dispersion was filtered through PU non-woven membrane to form an intertwined network. As shown in Figure 1, PU fibres of the membrane are straight with an average diameter of $0.14 \pm 0.09\,\mu m$ and the diameters of the individual fibres range between 0.05 and 0.39 μm. The fibre surface is smooth and the main pore size is around 0.2 μm. The typical thickness of the prepared self-standing MWNT entangled networks Figure 2(a) was about 0.15–0.4 mm. The upper surface of the network can be seen in the SEM micrograph (Figure 2b). Drying caused shrinkage of the network by about 7%. The porosity of the MWNT network was calculated to be $\phi = 0.67$, which was obtained from the relation $\varphi = 1 - \rho_{net}/\rho_{MWNT}$, where $\rho_{net} = 0.56 \pm 0.03\,g/cm^3$ denotes the measured apparent density of the nanotube network ($n = 10$) and $\rho_{MWNT} = 1.7\,g/cm^3$ is the measured average density of MWNT ($n = 3$). The density of nanotubes is very close to the theoretical

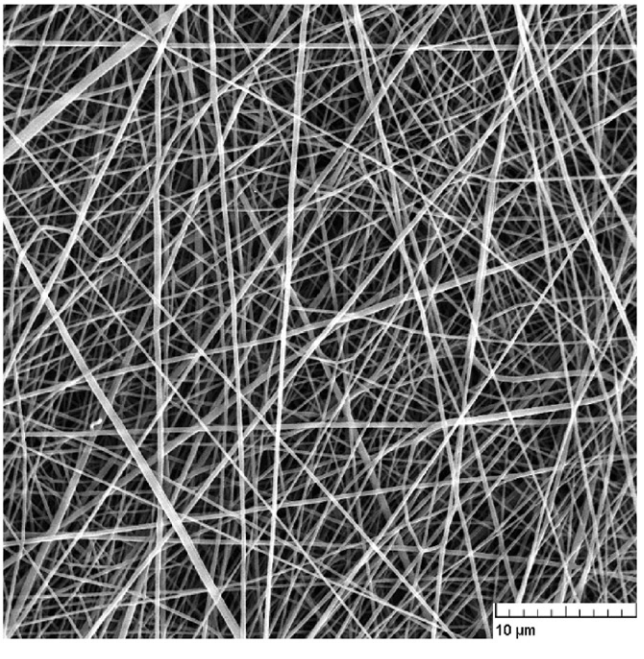

Figure 1. SEM micrographs of PU non-woven filtering membrane.

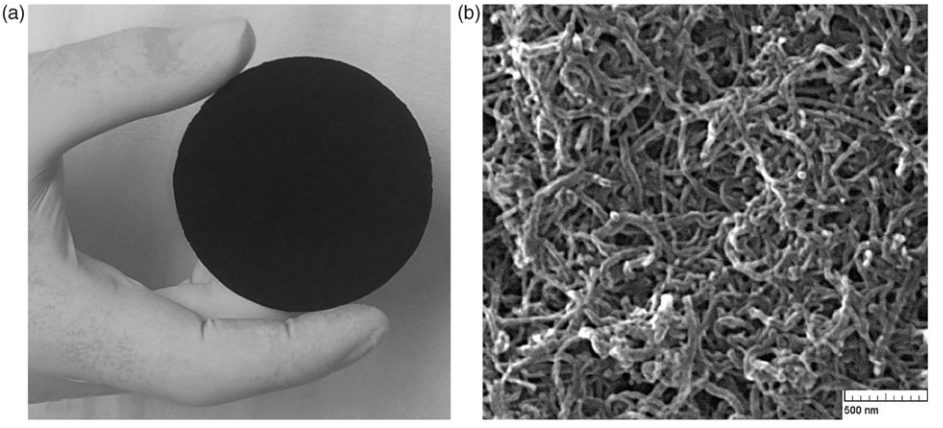

Figure 2. (a) Free-standing randomly entangled MWCNT network (disk diameter 75 mm and thickness 0.15 mm) and (b) SEM image of the surface of entangled MCWNT network of buckypaper.

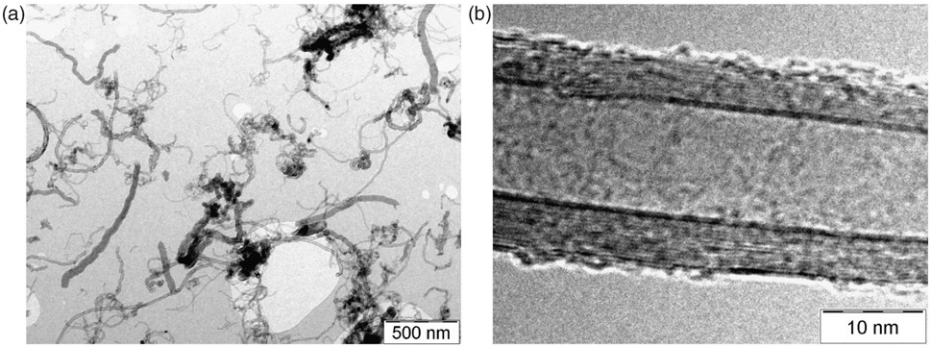

Figure 3. (a) TEM image of MWCNT deposited on the carbon film and (b) HRTEM detailed view of the structure of the nanotube.

value for MWNT, i.e. 1.8 g/cm^3 [8]. Also, the network porosity corresponds to the published values for MWNT networks [9].

To examine the length, thickness, waviness, multi-wall arrangement and possible structural defects of MWNT, TEM analysis was used. The obtained values slightly differ from the properties declared by the manufacturer. A representative sample of nanotubes deposited on copper grid with carbon film is shown in Figure 3(a). From the micrograph, the diameter of individual nanotubes was determined to be between 10 and 60 nm, their length from tenth of micron up to 3 μm. The maximum aspect ratio of the measured MWNT is thus about 300. The observed nanotube wavy morphology can be attributed to their large aspect ratios and low bending stiffness, as well as production-induced distortion (caused by chemical vapour deposition). According to [10,11], increasing waviness tends to increase the resistance of entangled networks of non-straight tubes, but this is not the issue pursued in this article.

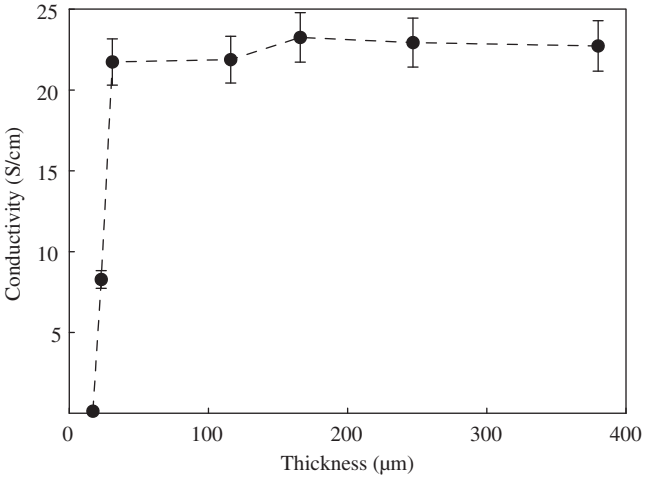

Figure 4. Effect of thickness of the entangled CNT network structures of buckypaper on the electric conductivity.

Figure 3(b) shows the multi-wall arrangement of the nanotube. As can be seen, there are about 15 rolled layers of grapheme, with the interlayer distance of *ca* 0.35 nm. The number of walls was typically from 10 to 35. The outer layer seems to be wrinkled. The surface wrinkles may be of different origin, for instance, owing to adhesion of carbon remnants, the projection of terminating graphene layer in a scroll-like multi-wall arrangement or due to the defects caused by oxidation when MWNT are exposed to the environment after production. The occurrence of some oxygenated functional groups (mostly carboxylic functional groups but also others, such as hydroxyl and carbonyl groups) on MWNT surface was observed by X-ray photoelectron spectroscopy among others [12].

The electric conductivity obtained by the four probe techniques for different network thicknesses is presented in Figure 4. As apparent from the graph, it increases with the network thickness from a very low value of 0.13 ± 0.01 S/cm at the thickness of 17 μm through 8.28 ± 0.01 S/cm at the thickness of 23 μm to almost constant values for the network thickness of above 30 μm. For instance, the measured conductivity for the network thickness of 247 μm was 22.9 ± 1.5 S/cm.

The pivotal property investigated in the research was resistance/compressive strain dependence (compressive strain as well as compression is defined as positive deformation and loading, respectively). The measurements have shown that compression causes a decrease in MWNT network resistance, as clearly visible in Figure 5. The plotted resistance values, R, are normalised with respect to the initial resistance, R_i, recorded at the start of the test at no load. For each network thickness, i.e. 0.23 and 0.38 mm, four samples were investigated. Their resistance was measured after each compression step to the pre-set deformation and for the subsequent unloaded state. The resistance in unloaded states was reduced similarly to the resistance of compressed samples.

Figure 6 shows the strain dependence of normalised change in resistance overlapped with the stress–strain curve to show the correspondence between the two. Both nonlinear

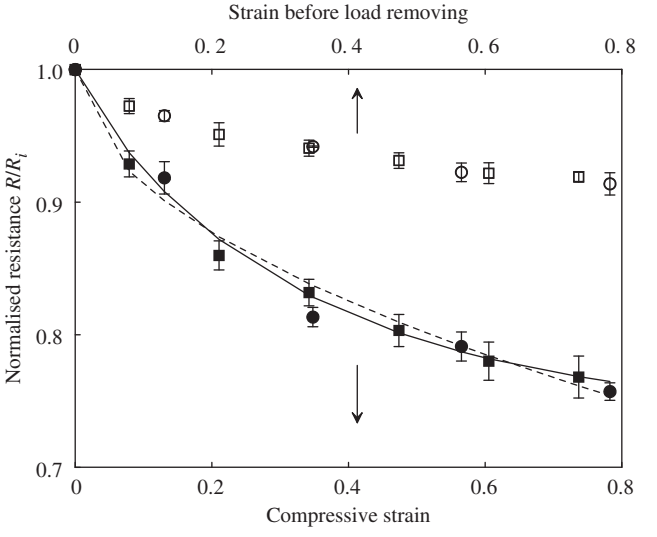

Figure 5. Normalised resistance *vs*. strain dependence of entangled CNT network. The network thicknesses are 0.23 mm (squares) and 0.38 mm (circles). The full and open symbols denote the network with and without load, respectively. Data presented as a mean ± standard deviation, $n = 4$. The solid and broken lines represent the prediction given by Equation (2) and the contact network model [4], respectively.

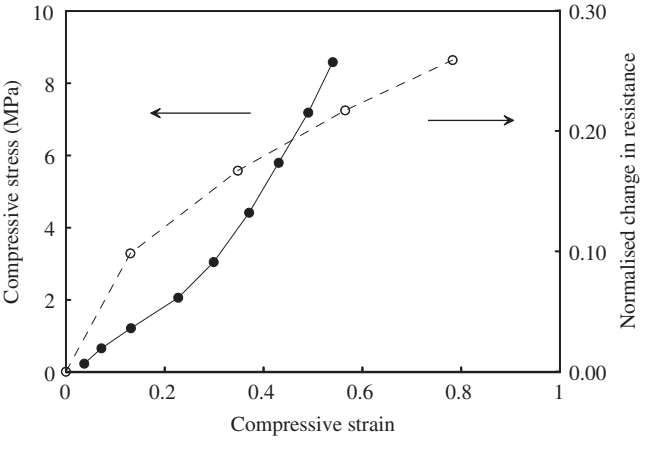

Figure 6. Strain-dependent normalised change in resistance curve overlapped with the stress–strain curve.

curves show that the normalised resistance change $(R_i - R)/R_i$ decreases with increasing compressive stress when strain approaches its maximal limit.

The observed effect of repeated compression on the network resistance is shown in Figure 7. As can be seen, with increasing number of deformation cycles, the resistance of MWNT network first declines more steeply, but after several cycles the decrease is very

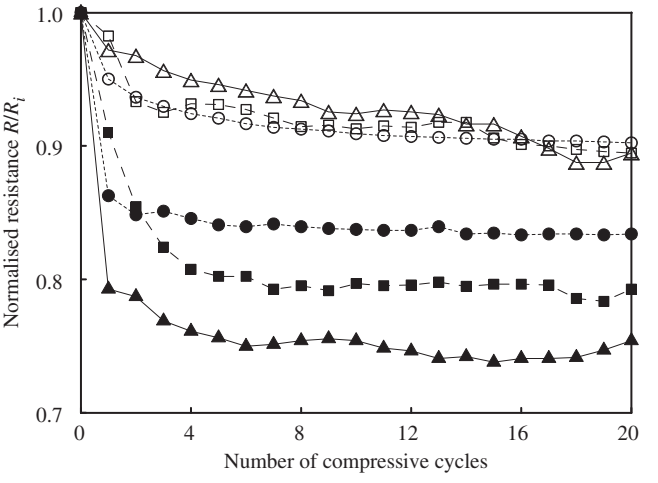

Figure 7. Normalised resistance of the entangled CNT network *vs*. the number of compression/relaxation cycles; network thickness 0.38 mm. The applied compressive strain: 0.21 (circles), 0.47 (squares) and 0.74 (triangles). Full and open symbols denote the network with and without load, respectively.

slight, and eventually no resistance change is observed. It indicates that the network rearrangement becomes steady, which is favourable for MWNT network application in sensing elements of compressive stress sensors when the network is suitably deformed in advance.

3.2. *MWNT network and contact resistance*

The resistance of the CNT network is affected by many factors ranging from nanotube conduction mechanisms through their size to the contact resistance between nanotubes and the network architecture [4,12,13]. Networks investigated in our study are formed by randomly oriented short nanotubes. A similar research was carried out for short single-wall carbon nanotube (SWNT) network with the result that the network resistance is dominated by the contact resistance between nanotubes while the intrinsic resistance of nanotubes is negligible [12]. Moreover, a uniform distribution of the intercontact resistances for unloaded SWNT network was supposed.

In accordance with the evidence given in [4], the local force between nanotubes increases during compression. This allows better contacts between them, which consequently leads to the decrease of contact resistance. Besides electron transfer facilitated this way, the residual resistance decrease shown in Figure 5 suggests an additional mechanism of resistance/strain behaviour. As indicated in [13], compression may also buckle the nanotubes, which results in more contacts between them. Since the contact points act as parallel resistors, their increasing number causes reduction of the overall network resistance. This structure reorganisation, i.e. more contact points, probably partly remains when the compressive strength is released, which may be the reason for off-load resistance decrease.

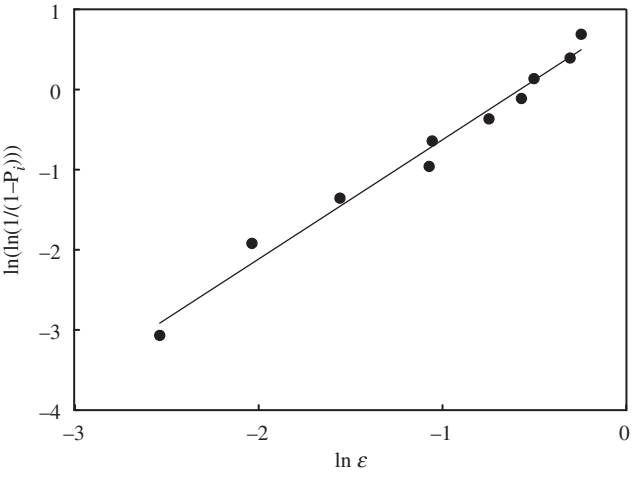

Figure 8. Weibull plot for compressive strain deforming conductive MWCNT network.

If this more complicated picture of network electrical resistance change is assumed rather than the effect of contact resistance between nanotubes only [4,12], the possible distribution of individual intercontact resistances, which is considered to govern the total resistance of the network [4], may change. In this regard, we assume that the distribution of intercontact resistances in compressed MWNT network is such that the joint probability for this total network resistance change under strain ε is described by the cumulative distribution function $F(\varepsilon)$ for the two-parameter Weibull distribution,

$$\Pr(\varepsilon) = F(\varepsilon) = 1 - \exp[-(\varepsilon/\varepsilon_0)^m], \tag{1}$$

where $F(\varepsilon)$ is the cumulative distribution function of the Weibull distribution. $F(\varepsilon)$ an increasing function, $0 \leq F(\varepsilon) \leq 1$, and represents the probability of network resistance change $\Pr(\varepsilon)$ under strain no greater than ε. The two parameters of the Weibull distribution are the shape parameter m and the normalising factor ε_0. The shape parameter describes the spread in strain to change the resistance.

The assumption that the probability of the whole network resistance follows the Weibull distribution is substantiated in Figure 8. The figure shows that all the experimental points very closely follow a straight line when plotted in the Weibull coordinates $\ln(\ln(1/(1 - P_i)))$ *versus* $\ln \varepsilon$, where $P_i = (i - 0.5)/n$ and i ranges from 1 to n, which is the number of tests. The goodness-of-fit to the straight line is reflected in the value of the correlation coefficient $r = 0.99$.

The tendency of the measured reduction in the macroscopic, i.e. network resistance with compressive strain is bound to the probability of network resistance change $\Pr(\varepsilon)$ under strain no greater than ε. Consequently, the following relation of the normalised network resistance R/R_i to function $F(\varepsilon)$ links appropriately the model prediction with the observed strain-dependent network resistance decrease

$$R/R_i = \alpha + \beta F(\varepsilon) = \alpha + \beta(1 - \exp[-(\varepsilon/\varepsilon_0)^m]), \tag{2}$$

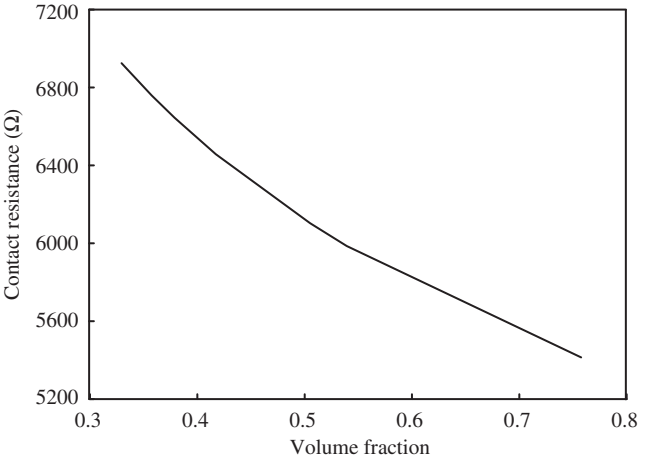

Figure 9. Contact resistance between crossing MWCNT evaluated from data in Figure 5 as a function of MCWNT volume fraction.

where α and β are location parameters and R_i the initial network resistance at the start of experiments at no load. The reasonably good description of the measured data by the predictive relation (2) is shown in Figure 5 (broken line; parameters $\alpha = 1$, $\beta = -0.26$, $m = 0.91$, $\varepsilon_0 = 0.33$).

For data description in Figure 5, we also exploit the contact network model despite its original use to represent the electronic transport properties of carbon nanofibre/epoxy resin composites and CNT tangles of moderate CNT volume fractions (up to 0.2) [4,14]. Moreover, the contact resistance power law model $R_{\text{contact}} = K\varphi^n$ [4] is used here to evaluate the contact resistance between crossing MWNTs in our network (Figure 9), though besides the contact resistance, also an increased number of contacts in the course of compression due to buckling of nanotubes may be expected.

As follows from Figure 5, the contact network model describes the measured resistance data quite well similarly as Equation (2), which may also suggest the dominant effect of local contact resistance between MWNT on the decrease of total resistance of entangled MWNT network structures of buckypaper during compression. The dependence of contact resistance R_{contact} on the network deformation is presented in Figure 9; the deformation is expressed in terms of MWNT volume fraction to be comparable with similar data given in [4]. The data show that the contact resistance between the crossing MWNT in buckypaper (the considered average MWNT diameter is 20 nm) is lower by up to two orders of magnitude in comparison to the contact resistance of powdery CNT layer presented in [4]. The probable reason is a higher MWNT volume fraction and compactness of filtered MWNT network in this study.

4. Final remarks

The resistance/strain relation for entangled CNT network structures of buckypaper produced by filtering a nanotube suspension has not been studied in detail so far. Thus, the

primary aim of this article was to reveal the effect of compression on the network resistance when a simple and repeated loading is exerted. The measurements carried out have shown as much as 20% resistance reduction at the maximum applied deformation. When the compression load is released, the network resistance partially recovers. The recovery depends on the loading extent and history. For instance, the resistance recovery is constant when the preceding network compression was about 0.8 and nearly constant when the sample has been subjected to several compressive cycles.

The overall network resistance change reflects the increase of local contact forces, i.e. better contacts between nanotubes, which reduces the network resistance. Another considered mechanism contributing to the number of conducting contacts in the course of compression is buckling of nanotubes sideways. Since the contact points act as parallel resistors, their higher number results in reduced total network resistance. Both the mechanisms are deterministic physical processes caused by loading applied crosswise on the network sheet. These processes involve both a decrease in the resistance of existing contacts and creation of new ones during compression. However, due to lack of knowledge of these deterministic processes, in this study we apply the probability description of events. It leads to the first approximation model of joint inner mechanisms of compressive strain effect on the overall resistance of network of nanotubes. The choice of the probability model is justified by reasonably good agreement between the resistance/strain dependence given by Equation (2) and shown in Figure 5.

Acknowledgements

This project was financially supported by the Ministry of Education, Youth and Sports of the Czech Republic (MSM 7088352101), the Grant Agency of the Academy of Sciences of the Czech Republic (GAAV IAA200600803) and by the Fund of Institute of Hydrodynamics AV0Z20600510.

References

[1] E.T. Thostenson, C.Y. Li, and T.W. Chou, *Nanocomposites in context*, Compos. Sci. Technol. 65 (2005), pp. 491–516.

[2] Q. Cao and J.A. Rogers, *Ultrathin films of single-walled carbon nanotubes for electronics and sensors: A review of fundamental and applied aspects*, Adv. Mater. 21 (2009), pp. 29–53.

[3] D.A. Walters, M.J. Casavant, X.C. Quin, C.B. Huffman, P.J. Boul, L.M. Ericson, E.H. Haroz, M.J. O'Connel, K. Smith, D.T. Colbert, and R.E. Smalley, *In-plane-aligned membranes of carbon nanotubes*, Chem. Phys. Lett. 338 (2001), pp. 14–20.

[4] A. Allaoui, S.V. Hoa, P. Evesque, and J. Bai, *Electronic transport in carbon nanotube tangles under compression: The role of contact resistance*, Scr. Mater. 61 (2009), pp. 628–631.

[5] H.T. Ham, Y.S. Choi, and I.J. Chung, *An explanation of dispersion states of single-walled carbon nanotubes in solvents and aqueous surfactant solutions using solubility parameters*, Colloid Interface Sci. 286 (2005), pp. 216–223.

[6] C.S. Chern and L.J. Wu, *Microemulsion polymerization of styrene stabilized by sodium dodecyl sulfate and short-chain alcohols*, Polym. Sci. Part A: Polym. Chem. 39 (2001), pp. 3199–3210.

[7] D. Kimmer, P. Slobodian, D. Petráš, M. Zatloukal, R. Olejník, and P. Sáha, *Polyurethane/MWCNT nanowebs prepared by electrospinning process*, J. Appl. Polym. Sci. 111 (2009), pp. 2711–2714.

[8] X.L. Xie, Y.W. Mai, and X.P. Zhou, *Dispersion and alignment of carbon nanotubes in polymer matrix: A review*, Mater. Sci. Eng. R 49 (2005), pp. 89–112.
[9] R.L.D. Whitby, T. Fukuda, T. Maekawa, S.L. James, and S.V. Mikhalovsky, *Geometric control and tuneable pore size distribution of buckypaper and buckydiscs*, Carbon 46 (2008), pp. 949–956.
[10] C. Li, E.T. Thostenson, and T.W. Chou, *Effect of nanotube waviness on the electrical conductivity of carbon nanotube-based composites*, Compos. Sci. Technol. 68 (2008), pp. 1445–1452.
[11] L. Licea-Jimenez, P.Y. Henrio, A. Lund, T.M. Laurie, S.A. Perez-Garcia, L. Nyborg, H. Hassander, H. Bertilsson, and R.W. Rychwalski, *MWNT reinforced melamine-formaldehyde containing alpha-cellulose*, Compos. Sci. Technol. 67 (2007), pp. 844–854.
[12] C.S. Yeh, *A study of nanostructure and properties of mixed nanotube buckypaper materials: Fabrication, process modeling characterization, and property modeling*, Ph.D. diss., The Florida State University, 2007.
[13] O. Yaglioglu, A.J. Hart, R. Martens, and A.H. Slocum, *Method of characterizing electrical contact properties of carbon nanotube coated surfaces*, Rev. Sci. Instrum. 77 (2006), p. 095105.
[14] A. Allaoui, S.V. Hoa, and M.D. Pugh, *The electronic transport properties and microstructure of carbon nanofiber/epoxy composites*, Compos. Sci. Technol. 68 (2008), pp. 410–416.

Polyurethane/Multiwalled Carbon Nanotube Nanowebs Prepared by an Electrospinning Process

Dušan Kimmer,[1] Petr Slobodian,[2] David Petráš,[1] Martin Zatloukal,[2] Robert Olejník,[2] Petr Sáha[2]

[1]*SPUR a.s., T. Bati 299, 764 22 Zlín, Czech Republic*
[2]*Tomas Bata University in Zlín, Faculty of Technology, T. G. M. 275, 762 72 Zlín, Czech Republic*

Received 13 June 2008; accepted 25 August 2008
DOI 10.1002/app.29238
Published online 2 December 2008 in Wiley InterScience (www.interscience.wiley.com).

ABSTRACT: Polyurethane (PU) and PU/multiwalled carbon nanotube (MWCNT) nanocomposite nanofibers, both with diameters of 350 nm, were prepared by an electrospinning process from PU dimethylformamide solutions. The appearance of nanowebs in PU/MWCNT nanofiber structures containing PU fibers with diameters of 20–40 nm was observed. The existence of these structures could have been based on the occurrence of strong secondary electric fields, which were created between individual conducting MWCNTs (distributed in the PU/MWCNT nanocomposites), which started to behave as the local moving nanoelectrodes promoting the creation of additional very fine nanowebs during the electrospinning processes. To our knowledge, this is the first report describing nanowebs from synthetic polymers prepared by an electrospinning process.
 J Appl Polym Sci 111: 2711–2714, 2009

INTRODUCTION

Electrospinning is a unique and attractive methodology for nanoscale fiber production from both synthetic[1,2] and natural sources[3] through the use of an external electric field imposed on a polymer solution[4] or melt.[5] Fibers prepared by electrospinning technology may have almost circular cross sections, smooth surfaces, and diameters ranging from a few nanometers to several micrometers.[6] These fibers have great applicability for drug-delivery media, medical implants, nanocomposites for dental restoration, preservation of bioactive agents, biosensors, molecular separation, filters, tissue engineering, wound dressing, and protective clothing.[6–8] The main weakness of these structures seems to be their poor mechanical properties caused by relaxation processes occurring immediately after fiber formation, at which a certain degree of molecular orientation is lost.[9–12] With the aim to overcome this problem, nanocomposite fibers can be combined with single-walled carbon nanotubes (SWCNTs) or multiwalled carbon nanotubes (MWCNTs) to achieve a significantly enhanced Young's modulus.[12]

Correspondence to: P. Slobodian (slobodian@ft.utb.cz).
Contract grant sponsor: Czech Science Foundation; contract grant number: 106/06P189.
Contract grant sponsor: Czech Ministry of Education and Sport; contract grant number: MSM 7088352101.
Contract grant sponsor: Czech Ministry of Industry and Trade; contract grant number: 2A-1TP1/068.

Recently, weblike structures (containing very fine fibers 5–15 nm in diameter) occurring together with aligned fibers with much higher diameters (100–150 nm) have been identified in natural biopolymers, such as collagen spider silk, denatured collagen, and Bombyx mori silk, reinforced by SWCNTs (produced by electrospinning technology[12–14]). As these structures mimic natural tissue structure, they can be used as scaffolds for biomedical tissue engineering.[6] Such nanowebs structure can also lead to enhanced mechanical properties in fibers prepared via electrospinning.[12,13] Lam[13] explained weblike structure formation during silk electrospinning by the creation of small SWCNT ropes (created from SWCNT cluster breakdown during the dispersion of the SWCNTs by sonication), which were consequently reagglomerated in the silk solution to form a large bundle (with a diameter exceeding that of the nanofiber) and expelled during electrospinning from the polymer jet under extremely high force and velocity, which caused the bundles to open and form nanowebs.

Polyurethane (PU) elastomeric materials pose desirable technological and life-cycle properties. Their physical and mechanical properties can be significantly varied in terms of the amount of soft and hard segments during polymer synthesis. They are resistant to microorganisms and abrasion with high hydrolytic stability. Unfortunately, up to now, there has been no research reported about a procedure that can be used to produce nanowebs from any synthetic polymers such as PU. Thus, the main aim of this study was to investigate whether these structures could be obtained by an electrospinning

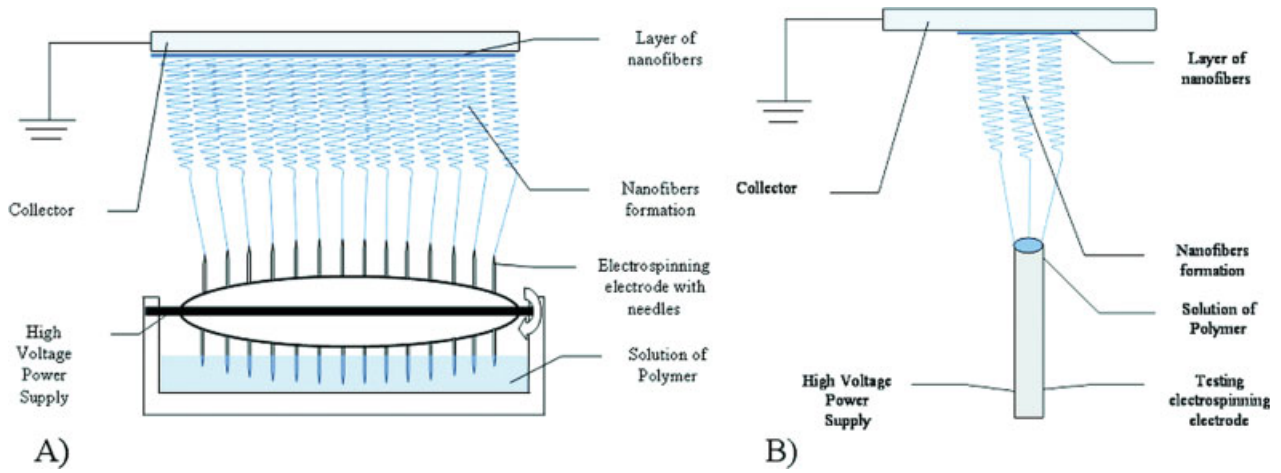

Scheme 1 (A) Scheme of the electrospinning process with the NanoSpider machine with a rotating electrospinning electrode with needles. (B) Scheme of the electrospinning process with one electrospinning electrode for TEM sample preparation. [Color figure can be viewed in the online issue, which is available at www.interscience.wiley.com.]

process applied onto a PU solution and to provide a plausible explanation for the mechanism leading to the development of these structures.

EXPERIMENTAL

Materials

PU solution in dimethylformamide (DMF) was synthesized from monomers such as 4,4′-methylenebis(phenyl isocyanate), polyester diol (number-average molecular weight $\sim 2 \times 10^3$), and 1,4-butandiol at a molar ratio of 6: 1 : 5 at 90°C for 5 h. A prepared solution suitable for electrospinning had a total PU concentration of about 13 wt %, a viscosity of 1.4 Pa s, and a conductivity of 140 μS/cm (adjusted by tetraethylamonium bromide). The dispersion of MWCNTs in PU solution was prepared with help of sonication with a Dr. Hielscher GmbH apparatus (ultrasonic horn S7, amplitude = 88 μm, density of power = 300 W/cm^2, frequency = 24 kHz) for 4 h at 65°C. The MWCNTs (acetylene type, purified) were supplied by Sun Nanotech Co., Ltd. (China; diameter = 10–30 nm, length = 1–10 μm, purity > 90%, volume resistance = 0.12 Ω cm, as reported by the supplier). The MWCNT material was used as received or with a surface modification. The modification was done through a two-step oxidation as described in ref. 15; that is, hydrogen peroxide was applied first, and a nitric and sulfuric acids (1 : 3 volume ratio) mixture was used in the second step. Oxidized MWCNTs were washed and dried before reaction with 4,4′-methylenebis(phenyl isocyanate) in DMF to derive carboxylic and hydroxyl groups from isocyanate ones.[16]

Electrospinning process and analysis

In the first step, pure PU and PU/MWCNT nanofibers were prepared from a PU solution in DMF with a commercially available NanoSpider machine (Elmarco s.r.o. Liberec, Czech Republic) (http://www.elmarco.com/) with one rotational electrode with needles [see Scheme 1(A)]. Consequent structure analyses were done by field emission scanning electron microscopy (FESEM; JSM-6700F, Jeol, Tokyo, Japan). With the aim of analyzing the presence of MWCNT material in the prepared PU/MWCNT nanofibers and also of understanding the PU nanoweb structures in more detail, transmission electron microscopy (TEM; JEM 2010, Jeol, Tokyo, Japan) was used. For an effective detailed structure analysis of the certain part of the PU/MWCNT and nanowebs, it was necessary to prepare a sample containing only a small amount of nanofibers/nanowebs by means of an electrospinning process with one static electrode only, as depicted in Scheme 1(B). The experimental conditions of the electrospinning process with both types of electrodes were the same as the following ones: relative humidity ≈ 29%, temperature ≈ 25°C, electric voltage ≈ 75 kV, distance between electrodes = 18 cm, electrode spin = 7 r/min, and speed of antistatic polypropylene nonwoven fabric collecting nanofibers = 0.16 m/min. The square weight of one prepared nanofiber layer was measured to be about 900 mg/m^2 (rotational electrode).

RESULTS AND DISCUSSION

FESEM analysis of the PU and PU/MWCNT nanofibers prepared by the electrospinning process with a rotating electrode are provided in Figure 1(A,B). It

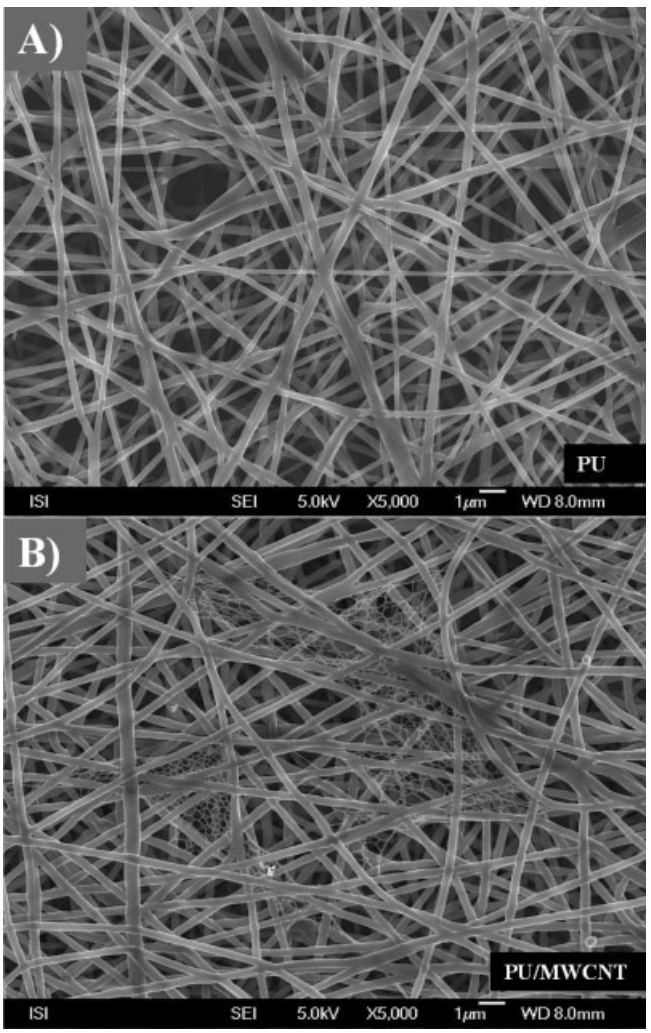

Figure 1 FESEM images of the PU-based nanofibers: (A) without and (B) with MWCNTs (no applied surface modification).

was clearly shown that the presence of the MWCNTs promoted the creation of weblike structures in comparison with the PU nanofibers without MWCNTs. The diameter of the PU nanofibers was about 350 nm, whereas the weblike structures consisted of regularly distributed very fine nanofibers with diameters of just about 20–40 nm, which were strongly embedded in the thicker PU nanofibers [see Fig. 2(A)]. These PU weblike structures were very similar to the Bombyx mori silk nanofibers containing SWCNTs.[12] TEM analysis of the PU/MWCNT nanofibers prepared by the electrospinning process with one static electrode only is provided in Figure 2(B) with the aim of analyzing the creation of the one nanoweb fiber. It was clearly visible that individual and very well aligned MWCNTs (except for a small curvature at the junction point) occurred in the outer surface of the main nanofiber from which nanoweb fiber was created. This observation led us to conclude that the nanoweb formation was based on the occurrence of strong secondary electric fields that were created between individual MWCNTs (or their agglomerated forms) and that started to behave as local moving nanoelectrodes promoting the creation of additional very fine nanowebs during the electrospinning processes.

CONCLUSIONS

PU and PU/MWCNT nanocomposite nanofibers created via an electrospinning process from PU solution were successfully prepared with average diameter around 350 nm. MWCNTs were present inside the PU/MWCNT nanofibers as individual tubes well aligned with nanofibers axes. Finally, so-called nanowebs were observed during the electrospinning process for PU-containing MWCNTs. We suggest that these nanowebs were created because of strong

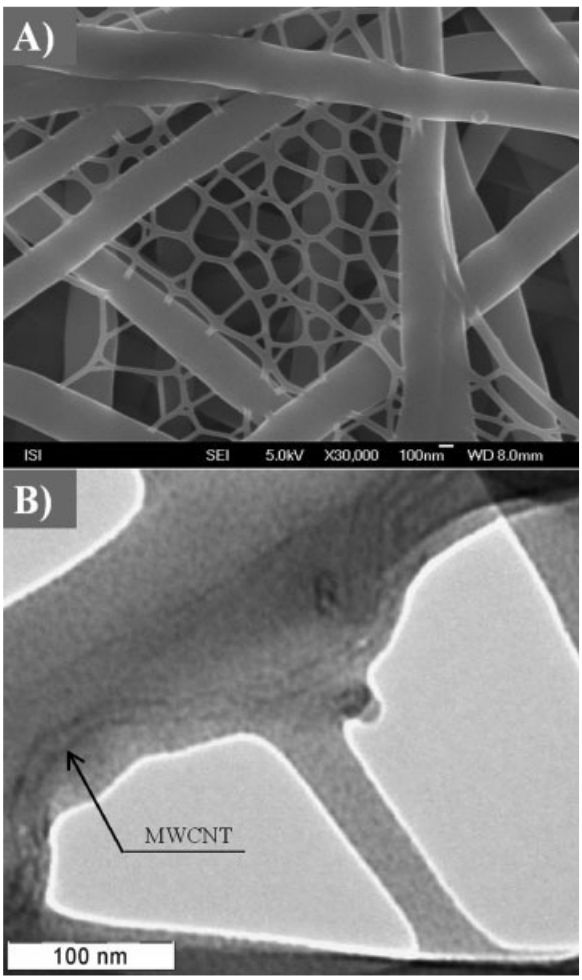

Figure 2 Detailed views of the weblike structures of the PU-based nanofibers with MWCNTs. (A) FESEM image of the weblike structure (MWCNTs with no surface modification). (B) TEM image of the weblike structure (MWCNTs with surface modification); detailed view of the strongly embedded fine fiber of the weblike structure to the thicker PU/MWCNT nanofiber containing an individual MWCNT.

secondary electric fields occurring between MWCNTs during the electrospinning process.

REFERENCES

1. Doshi, J.; Reneker, D. J. Electrostat 1995, 35, 151.
2. Zhuo, H.; Hu, J.; Chen, S.; Yeung, L. J Appl Polym Sci 2008, 109, 406.
3. Matthews, J. A.; Wnek, G. E.; Simpson, D. G.; Bowlin, G. L. Biomacromolecules 2002, 3, 232.
4. Demir, M. M.; Yilgor, I.; Yilgor, E. Polymer 2002, 43, 3303.
5. Casper, C. L.; Stephens, J. S.; Tassi, N. G.; Chase, D. B.; Rabolt, J. F. Macromolecules 2004, 37, 573.
6. Zhang, Y. Z.; Lim, C. T.; Ramakrishna, S.; Huang, Z. M. J Matter Sci-Mater M 2005, 16, 933.
7. Inai, R.; Kotaki, M.; Ramakrishna, S. Nanotechnology 2005, 16, 208.
8. Huang, Z. M.; Zhang, Y. Z.; Kotaki, M.; Ramakrishna, S. Compos Sci Technol 2003, 63, 2223.
9. Lyons, J. M. Melt-Electrospinning of Thermoplastic Polymers: An Experimental and Theoretical Analysis; Drexel University: Philadelphia, 2004.
10. Pedicini, A.; Farris, R. J. Polymer 2003, 44, 6857.
11. Anderson, J. P.; McGrath, K.; Kaplan, D. In Protein-Based Materials; Birkhauser: Basel, Switzerland, 1997; p 371.
12. Ayutsede, J.; Gandhi, M.; Sukigara, S.; Ye, H. H.; Hsu, C. M.; Gogotsi, Y.; Ko, F. Biomacromolecules 2006, 7, 208.
13. Lam, H. Ph.D. Thesis, Drexel University, 2004.
14. Stephens, J. S.; Casper, C. L.; Chase, D. B.; Rabolt, J. F. Polym Prepr (Am Chem Soc Div Polym Chem) 2003, 44, 91.
15. Licea-Jimenez, L.; Henrio, P. Y.; Lund, A.; Laurie, T. M.; Perez-Garcia, S. A.; Nyborg, L.; Hassander, H.; Bertilsson, H.; Rychwalski, R. W. Compos Sci Technol 2007, 67, 844.
16. Ha, J. U.; Kim, M.; Lee, J.; Choe, S.; Cheong, I. W.; Shim, S. E. J Polym Sci Part A: Polym Chem 2006, 44, 6394.

Key Engineering Materials Vol. 543 (2013) pp 410-413

doi:10.4028/www.scientific.net/KEM.543.410

Plasma treatment as a way of increasing the selectivity of carbon nanotube networks for organic vapor sensing elements

Robert Olejnik[1,2a], Petr Slobodian[1,2b], Uros Cvelbar[3c] Pavel Riha[4d] and Petr Saha[1,2,e]

[1]Tomas Bata University in Zlin, Faculty of Technology, náměstí T. G. Masaryka 275, 762 72 Zlín Czech Republic

[2]Centre of polymer systems, Nad Ovčírnou 3685, 760 01 Zlín, Czech Republic

[3]Josef Stefan instutite F4, Jamova cesta 39,1000 Ljubjana, Slovenia

[2]Institute of Hydrodynamics, Academy of Sciences, Pod Paťankou 30/5, 16612 Prague 6, Czech Republic

[a]rolejnik@volny.cz, [b]slobodian@ft.utb.cz, [c]uros.cvelbar@ijs.si, [d]riha@ih.cas.cz, [e]saha@ft.utb.cz

Keywords: Carbon nanotube networks, plasma, sensing element, interdigitated electrode

Abstract. Multi-walled carbon nanotubes networks (MWCNTs) were used as a layer for organic vapor detection. The sensor detects volatile organic compounds (VOC). The gas sensing by MWCNTs is measured by means of macroscopic electrical resistance. The selected solvents had different polarities and volume fractions of saturated vapors. The electrical resistance of MWCNTs increases when exposed to organic solvent vapors, and a reversible reaction is observed when the MWCNT is removed from the vapors. The MWCNTs were modified by means of plasma treatment. For modifications RF plasma in O_2 at 50 Pa and an afterglow configuration were used. The modified MWCNTs show an increase in sensitivity caused by creating carboxylic groups on the surface of the carbon nanotubes. It leads, for example, to enhancement of the sensitivity from usual 30 % for heptane at RT to more than 200% after plasma treatment in O_2 for 10s.

Introduction

Gas sensors, or chemical sensors, are attracting interest because of their widespread applications in industry, environmental monitoring, space exploration, biomedicine, and pharmaceutics. Gas sensors with high sensitivity and selectivity are required for leakage detections of explosive gases such as hydrogen, and for real-time detections of toxic or pathogenic gases in industries. There is also a strong demand for the ability to monitor and control our ambient environment, especially with the increasing concern of global warming. Researchers from NASA are seeking the use of high-performance gas sensors for the identification of atmospheric components of various planets. In addition, nerve-gas sensing for homeland security is also at the center of public concern [1]. Generally, there are several basic criteria for good and efficient gas sensing systems: (i) high sensitivity and selectivity; (ii) fast response time and recovery time; (iii) low analyst consumption; (iv) low operating temperature and temperature independence; (v) stability in performances. Commonly used gas sensing materials include vapor-sensitive polymers, semiconductor metal oxides, and other porous structured materials such as porous silicon [2–4]. Since the most common gas sensing principle is the adsorption and desorption of gas molecules on sensing materials, it is quite understandable that by increasing the contact interfaces between the analytes and sensing materials, the sensitivity can be significantly enhanced. The recent development of nanotechnology has created huge potential to build highly sensitive, low cost, portable sensors with low power consumption. The extremely high surface-to-volume ratio and hollow structure of nanomaterials is ideal for gas molecules adsorption and storage. Therefore, gas sensors based on nanomaterials, such as carbon nanotubes (CNTs), nanowires, nanofibres, and nanoparticles, have been widely investigated. Since carbon nanotubes were firstly discovered by Iijima in 1991 [5], they have drawn

the most research interests because of their unique geometry, morphology, and properties. Their preparation, properties (such as electronic, mechanical, thermal, and optical properties), and applications on various fields are all being studied intensely. Theoretical and simulation works have also been conducted to understand this nanoscale material and related phenomenon [6].

In this work, a new type of gas sensing element is presented. The sensing element was made by drop deposition method of aqueous dispersion of multi-walled carbon nanotubes. The drop was evaporated and the carbon nanotubes network was created. The dispersion was located on the active surface of interdigitated electrode. The interdigitated electrode was made by the etching method. The interdigitated electrode with carbon nanotubes network was treated with an afterglow RF plasma in O_2 at 50pa. The plasma treated process was optimized and the most effective treatment time was found. The plasma response to adsorption/desorption cycles were determined as a change of macroscopic resistance. MWCNTs have good sensitivity and assumed selectivity defined by pressures of saturated vapors of the used organics solvents. Finally, it was found that measured response has good reversibility.

Experimental

MWCNTs produced by chemical vapor deposition of acetylene were supplied by Sun Nanotech Co. Ltd., China (diameter 10-30 nm, length of 1-10 μm, purity of ≥90% and volume resistivity 0.12 Scm according to the supplier).

Carbon nanotubes were used into aqueous pastes using a mortar and pestle (1.6 g MWCNT and ~ 50 ml deionized water), and diluted with deionized water. Consequently, sodium dodecyl sulfate (SDS) and 1-pentanol were added, and pH was adjusted to 10 using an aqueous solution of 0.1 M NaOH [7]. The final concentration of nanotubes in the suspension was 0.3 wt.%, concentrations of SDS and 1-pentanol were 0.1M and 0.14M, respectively [8]. The dispersion was homogenized using Dr. Hielscher GmbH apparatus (ultrasonic horn S7, amplitude 88 μm, power density 300 W/cm^2, frequency 24 kHz) for 2 hours under a temperature of about 50°C.

There are several methods to integrate CNTs to different gas sensor structures. Li et al. developed a resistive gas sensor by simply casting SWCNTs on interdigitated electrodes (IDEs) [9]. This method was used in this work. A board with 35 μm Cu layer was used. The interdigitated electrodes pattern was printed on the board by etching with resistance paint. The pattern was etched for 15 minutes by $FeCl_3$ at room temperature and paint was removed by toluene. Finally, the electrodes were cleaned by absolute ethanol. The aqueous dispersion of carbon nanotubes was then drop-deposited onto the electrode area. A network of carbon nanotubes subsequently formed after the evaporation of water. The interdigitated electrode was then treated by low temperature reactive plasma. The plasma was generated in an inductively coupled radiofrequency discharge at 27.12 MHz in a commercially available gas of O_2, at the pressure 50 Pa for 5s, 10s, 15s and 30s.

Results

The typical adsorption/desorption behavior of CNT network exposed to/disposed from heptane organic vapors is presented in Fig. 1. The graph illustrates a time-dependent change of parameter S representing sensitivity of the nanotube networks. The curves show specific course of adsorption/desorption, with an obvious on/off effect. An initial sharp increase in sensitivity is followed by a slower phase. Simultaneously, desorption is represented by a rapid decrease reaching a constant value in some cases, in others followed by further, slower decrease.

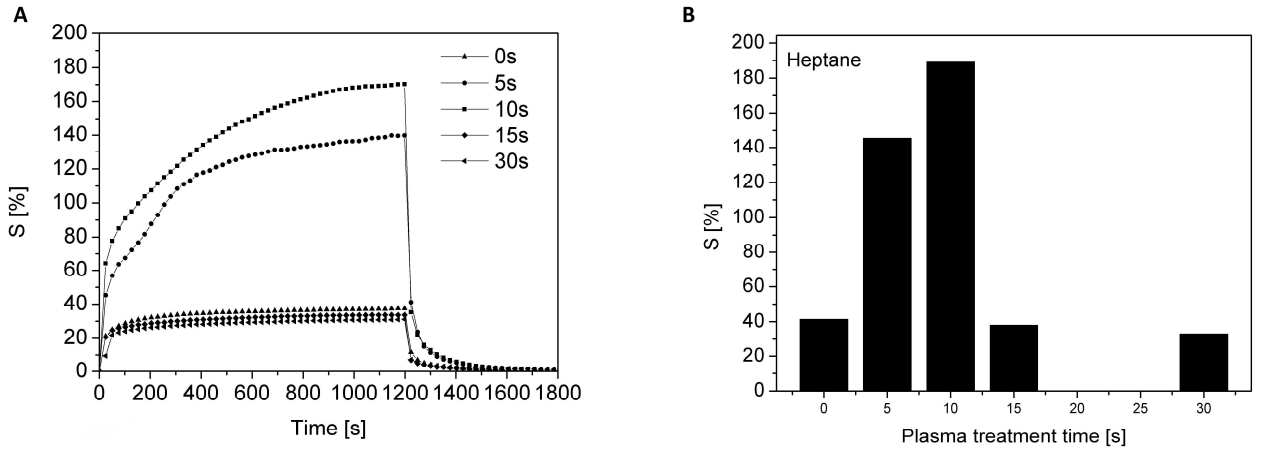

Fig. 1 A) Adsorption/desorption cycle for MWCNT network created by evaporation dispersion on the surface of interdigitated electrode exposed to heptane vapors. The curves in the graph represents four different plasma treatment times in 0_2 at 50 pa. 0 sec represents the control sample. B) The maximum *S* values for adsorption of heptane vapors for different plasma treatment times.

Table 1. Properties of tested organic solvent: Hansen solubility parameters, δ_d, δ_p, δ_d total Hildebrand solubility parameter, δ_t, saturated vapor pressure, p_i, and corresponding volume fraction, x_i, at 25°C aand atmospheric pressure .

solvent	δ_d [$Mpa^{1/2}$]	δ_p [$Mpa^{1/2}$]	δ_h [$Mpa^{1/2}$]	δ_t [$Mpa^{1/2}$]	p_i [kPa]	x_i [vol. %]
heptane	15.3	0	0	15.3	6.13	6.0

The observed behavior is probably caused by the physical adsorption of the heptane molecules in the space between the carbon nanotubes network and increase the resistance to stable value. On the other hand, desorption causes a decrease in resistance by increasing the amount of contacts in the network of carbon nanotubes.

The sensitivity is defined by Eq. 1 where R_a represents specimen resistance in air and R_g the resistance of specimen exposed to gas/vapor, ΔR denotes the resistance change.

$$S = \frac{R_g - R_a}{R_a} = \frac{\Delta R}{R_a} \tag{1}$$

Table 1 presents properties of tested organic solvent. Fig. 2 shows the sensitivity response in five consecutive cycles. One adsorption/desorption cycle consists of 20 minutes adsorption and 10 minutes desorption. Experimental data also demonstrates good reversibility of adsorption/desorption processes.

Conclusions

The interdigitated electrode pattern was printed on the board by etching resistant paint. The pattern was etched for 15 minutes by $FeCl_3$ at room temperature and paint was removed by acetone. A resistive gas sensor was made by simply casting MWCNTs on interdigitated electrodes. The aqueous dispersion of carbon nanotubes was then drop-deposited onto the electrode area.

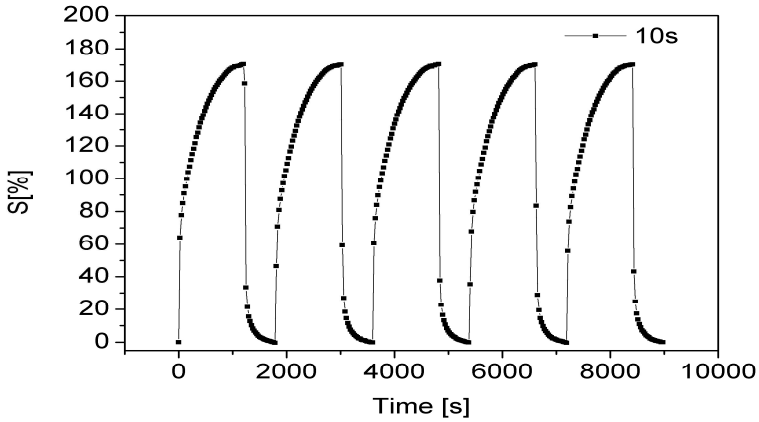

Fig. 2 Sensitivity change of treated MWCNT network exposed to saturated heptane vapors in five adsorption/desorption cycles.

The network of carbon nanotubes subsequently formed after the water evaporation. The surface of carbon nanotubes network was treated with RF plasma in O_2 atmospheres, which functionalized their surfaces and it was found that the most effective treatment time is 10s.

The network response in adsorption/desorption cycles was determined as a change of macroscopic resistance. MWCNT network has good sensitivity and assumed selectivity defined by pressures of saturated vapors of the used organics solvent. Finally it was found that measured response has good reversibility and sensitivity.

Acknowledgement

The work was supported by the Operational Program of Research and Development for Innovations co-funded by the European Regional Development Fund (ERDF), the National budget of Czech Republic within the framework of the Centre of Polymer Systems project (Reg. No.: CZ.1.05/2.1.00/03.0111). This article was also supported by the internal grant of TBU in Zlin No. IGA/FT/2012/022 funded from the resources of Specific University Research and by the Fund of Institute of Hydrodynamics AV0Z20600510.

References

[1] J. Li, in: *Carbon Nanotubes: Science and Applications*, edited by M. Meyyappan, CRC Press, Boca Raton, Fla, USA (2006)

[2] Z. M. Rittersma: Sensors and Actuators A Vol. 96 (2002) p. 196

[3] R. Fenner and E. Zdankiewicz: IEEE Sensors J. Vol. 1 (2001) p. 309

[4] E. Traversa: Sensors and Actuators B Vol. 23 (1995) p. 135

[5] S. Iijima: Nature Vol. 354 (1991)p. 56

[6] M. Meyyappan: *Carbon Nanotubes: Science and Applications* (CRC Press, Boca Raton, Fla, USA (2004)

[7] H.T. Ham, Y.S. Choi, I.J. Chung: Colloid Interf. Sci. Vol.286 (2005) p. 216

[8] C.S. Chern, L.J. Wu: Polym. Sci., Part A: Polym. Chem. Vol. 39 (2001) p. 3199

[9] J. Li, Y. Lu, Q. Ye, et al.: Nano Letters Vol. 3 (2003) p. 929

Key Engineering Materials Vol. 495 (2012) pp 9-12
Online available since 2011/Nov/15 at www.scientific.net

doi:10.4028/www.scientific.net/KEM.495.9

Sensing element made of multi-wall carbon nanotube network for organic vapor detection

Robert Olejnik[1,a], Petr Slobodian[1, b] and Petr Saha[1, c]

[1]Centre of Polymer Systems, Faculty of Technology, Tomas Bata University in Zlin

T.G.Masaryka 555, 760 05 Zlín, Czech Republic

[a]rolejnik @volny.cz,[b]slobodian@ft.utb.cz,[c]saha@utb.cz

Keywords: Carbon nanotube network, sensor, Buckypaper, Electrical resistance

Abstract. Multiwall carbon nanotubes (MWCNT) network "Buckypaper" was made by the vacuum filtration method of MWCNT aqueous suspension. The sensitivity of multi-wall carbon nanotube (MWCNT) networks of randomly entangled pure nanotubes to various organic solvent vapors (tetrahydrofuran, methyl ethyl ketone, and ethanol) has been investigated by resistance measurements. The results demonstrate that the network electrical resistance increases when exposed to organic solvent vapors, and a reversible reaction is observed when the sample is removed from the vapors. The investigated MWCNT networks could be potentially used as sensing elements for sensitive and selective organic vapor detection**.**

Introduction

Single-wall carbon nanotubes (SWCNTs) and multi-wall carbon nanotubes (MWCNTs) show remarkable sensitivity to the change of chemical composition of the surrounding environment. This property is favorable for their use in the form of membranes [1], adsorbents [2] or gas sensors [3,4,8] and pressure sensors [9,10]. Gas and vapor adsorption as well as desorption usually proceeds at high rates and amounts [5]. The molecules are adsorbed on the carbon nanotube (CNT) surface by van der Waals attracting forces, which leads to remarkable changes in CNT electrical resistance. A smart application of this principle can eventually lead to development of CNT-based electrochemical biosensors and gas sensors with a useful ability to detect various gases and organic vapors. Conductivity measurement is then a simple and convenient method to register CNT response to vapor adsorption/desorption.

Previous research [6,7] found that physisorbed molecules influence the electrical properties of isolated CNTs and also inter-tube contacts. The resistance of macroscopic CNT objects like aggregates or network structures used in gas sensors is predominantly determined by contact resistance of crossing tubes, rather than by resistance of CNT segments. Here, the tubes are much shorter than sensor dimensions and inter-tube contacts act as parallel resistors between highly conductive CNT segments.

The dominating process influencing macroscopic resistance is probably gas or vapor adsorption in the space between nanotubes, which forms non-conductive layers between the tubes. This process decreases both the quantity and quality of contacts between nanotubes and consequently increases macroscopic resistance [3].

The present work describes resistive gas sensors prepared in a simple way from MWCNTs. Their sensitivity to saturated vapors of three different organic solvents are tested. Finally, reversibility of adsorption/desorption cycles is tested for tetrahydrofuran.

Experimental

The purified MWCNT of acetylene type were supplied by Sun Nanotech Co. Ltd., China (diameter 10-30 nm, length 1-10 μm, purity >90% and volume resistance 0.12 Ω cm according to supplier). The MWCNT aqueous paste was prepared using a mortar and pestle (1.6 g of MWCNT and ~ 50 ml of deionized water), then diluted by deionized water and SDS (sodium dodecyl sulfate) and 1-pentanol were added, pH was adjusted to the value of 10 using aqueous solution of NaOH. The final nanotubes concentration in the suspension was 0.3 wt. %, concentration of SDS and 1-pentanol 0.1M and 0.14M, respectively. The dispersion was homogenized using Dr. Hielscher GmbH apparatus (ultrasonic horn S7, amplitude 88 μm, power density 300 W/cm2, frequency 24 kHz) for 2 hours and the temperature of ca 50°C. MWCNT networks, "Buckypaper" (MWCNT-N), were prepared by dispersion vacuum filtration thought polyurethane submicron size porous membrane. The formed disk-shaped network was washed several times by deionized water and methanol in situ, then removed and dried between filter papers at RT. The strips made of CNT networks were exposed to the vapors of seven different solvents, adsorbates, (tetrahydrofuran - THF, methyl ethyl ketone – MEK nad ethanol - EtOH) The chosen solvents are characterized by their functional groups such as ketone, ether, alcohol and hydrocarbon. The specimens were exposed to saturated vapors of solvents at defined experimental conditions: 25 °C, atmospheric pressure and 6 minute adsorption/desorption cycles.

Results

The typical adsorption/desorption behavior of CNT network exposed to/disposed from different organic vapors is presented in Fig. 1. The graph illustrates a time-dependent change of parameter S representing sensitivity of the nanotube networks. The curves show specific course of adsorption/desorption, with an obvious on/off effect. An initial sharp increase in sensitivity is followed by a slower phase. Simultaneously, desorption is represented by a rapid decrease reaching a constant value in some cases, in others followed by further, slower decrease. The sensitivity is defined by eq. 1 where Ra represents specimen resistance in air and Rg resistance of the specimen exposed to gas/vapor, ΔR stands for the resistance change.

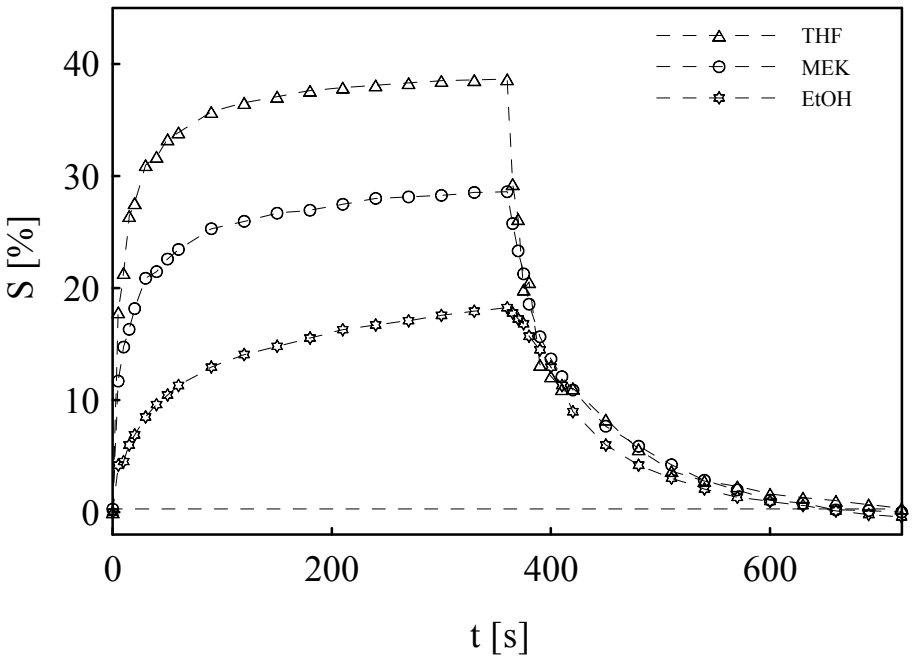

Fig. 1 *One adsorption/desorption cycle of Multiwall carbon nanotubes network exposed to vapors of three different organic solvents*

$$S = \frac{R_g - R_a}{R_a} = \frac{\Delta R}{R_a} \tag{1}$$

Table 1 presents properties of tested organic solvents arranged in order with decreasing S. It demonstrate selectivity of CNT network to different vapors defined by Hildebrand solubility parameter, δt, and pressures, pi, and saturated vapor volume fractions, xi. It was found that S increase nearly proportionally with increase in xi. and selected range of δt influence it fewer.

Table 1 Properties of tested organic solvents: Hansen solubility parameters, δd, δp, δd total Hildebrand solubility parameter, δt, saturated vapor pressures, pi, and corresponding volume fractions, xi, at 25°C and atmospheric pressure and sensitivity S.

solvent	δ_d [$Mpa^{1/2}$]	δ_p [$Mpa^{1/2}$]	δ_h [$Mpa^{1/2}$]	δ_t [$Mpa^{1/2}$]	p_i [kPa]	x_i [vol. %]	S [%]
THF	16.8	5.7	8	19.5	20.66	20.4	38.7
MEK	16	9	5.1	19	12.67	12.5	28.7
EtOH	15.8	8.8	19.4	26.5	7.86	7.1	19.6

Fig. 2 Represents response to three consecutive cycles in saturated vapors of THF measured in 6-minute intervals. Experimental data also demonstrate good reversibility of adsorption/desorption processes.

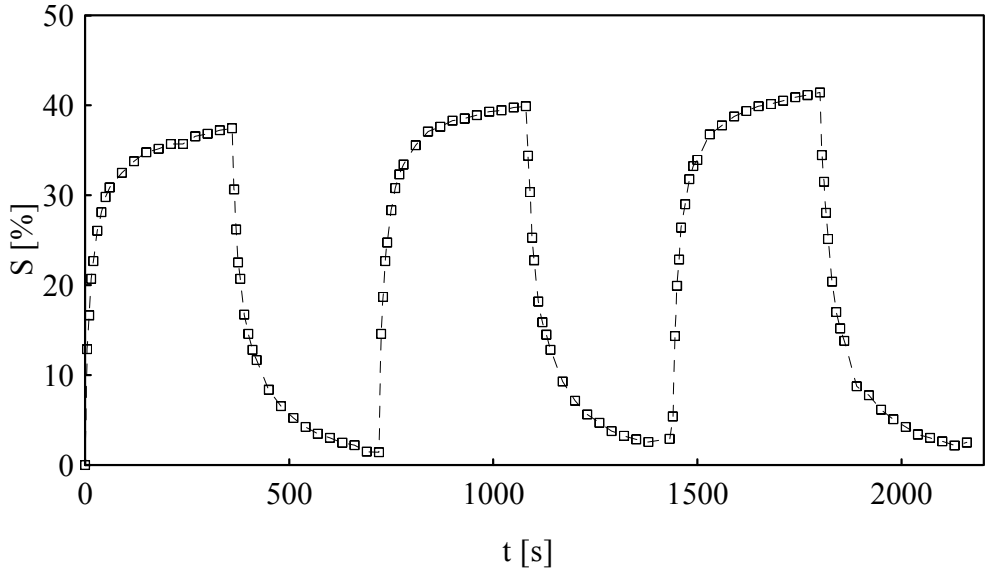

Fig. 2 *Three adsorption/desorption cycles of Multiwall carbon nanotubes network exposed to vapors of THF.*

Conclusions

Multiwall carbon nanotubes were used to prepare CNT network (buckypaper) by vacuum filtration method. Their response to adsorption/desorption cycles were determined as a change of macroscopic resistance. The response to adsorption/desorption was measured as a change of resistance. CNT network has good sensitivity and assumed selectivity defined by pressures of saturated vapors of used organics solvents. Finally it was found that measured response has good reversibility.

Acknowledgement

This project was supported by the internal grant of TBU in Zlín No. IGA/3/FT/11/D funded from the resources of specific university research. This article was also created with support of Operational Programme Research and Development for Innovations co-funded by the European Regional Development Fund (ERDF) and national budget of Czech Republic within the framework of the Centre of Polymer Systems project (reg.number: CZ.1.05/2.1.00/03.0111) and by the Fund of the Institute of Hydrodynamics AV0Z20600510.

References

[1] Smajda R, Kukovecz A, Konya Z, Kiricsi I. Structure and gas permeability of multi-wall carbon nanotube buckypapers. Carbon 2007;45(6):1176-1184.

[2] Agnihotri S, Mota JPB, Rostam-Abadi M, Rood MJ. Theoretical and experimental investigation of morphology and temperature effects on adsorption of organic vapors in single-walled carbon nanotubes. J Phys Chem B 2006;110(15):7640-7647.

[3] Romanenko A I, Anikeeva OB, Kuznetsov VL, Buryakov TI, Tkachev EN, Usoltseva AN. Influence of helium, hydrogen, oxygen, air and methane on conductivity of multiwalled carbon nanotubes. Sensor Actuat A-Phys 2007;138(2):350-354.

[4] Qureshi A, Kang WP, Davidson JL, Gurbuz Y. Review on carbon-derived, solid-state, micro and nano sensors for electrochemical sensing application. Diam Relat Mater 2009;18(12):1401-1420.

[5] Hussain CM, Saridara C, Mitra S. Microtrapping characteristics of single and multi-walled carbon nanotubes. J Chromatogr A 2008;1185(2):161-166.

[6] Tournus F, Latil S, Heggie MI, Charlier JC. pi-stacking interaction between carbon nanotubes and organic molecules, Phys Rev B 2005;72(7):Article Number 075431.

[7] Mowbray DJ, Morgan C, Thygesen KS. Influence of O-2 and N-2 on the conductivity of carbon nanotube networks. Phys Rev B 2009;79(19):Article Number 195431.

[8] P. Slobodian, P**.** Riha, A. Lengalova, P. Svoboda and P. Saha, Multi-wall carbon nanotube networks as potential resistive gas sensors for organic vapor detection, Carbon, Volume 49, Issue 7, June 2011, Pages 2499-2507

[9] Slobodian, P, Riha P, Lengalova A, Saha P, Compressive stress-electrical conductivity characteristics of multiwall carbon nanotube networs. Journal of Materials Science. Volume 46, Issue 9 (2011), Page 3186

[10] P. Slobodian, P. Riha, A. Lengalova, P. Svoboda, P. Saha, Multi. Journal of Materials Science. Volume 46, Issue 9 (2011), Page 3186

Materials and Applications for Sensors and Transducers
10.4028/www.scientific.net/KEM.495

Sensing Element Made of Multi-Wall Carbon Nanotube Network for Organic Vapor Detection
10.4028/www.scientific.net/KEM.495.9

Key Engineering Materials Vol. 495 (2012) pp 83-86
Online available since 2011/Nov/15 at www.scientific.net

doi:10.4028/www.scientific.net/KEM.495.83

Improved selectivity of oxidized multiwall carbon nanotube network for detection of ethanol vapor

Daniel Matejik [1,a], Robert Olejnik [1,b] , Petr Slobodian [1,c] and Petr Saha[1]

[1]Centre of Polymer Systems, Faculty of Technology, Tomas Bata University in Zlín, nám. T.G.Masaryka 555, 760 05 Zlín, Czech Republic

[a]matejikdaniel@gmail.com, [b]rolejnik@volny.cz,[c]slobodian@ft.utb.cz

Keywords: Carbon nanotube network, sensor, Buckypaper, Electrical resistance

Abstract. Two kinds of Multiwall carbon nanotubes (MWCNT) networks "Buckypaper" were made by the vacuum filtration method of MWCNT aqueous suspension. The first one was prepared from pure CNT and the second from its oxidized form by acidic KMnO4 as oxidizing agent. The CNT oxidation increase content of oxygen bonded to the surface of CNT decreasing their hydrophobic character. The sensitivity of MWCNT networks to two kind of organic solvent vapors (ethanol and hepane) has been investigated by resistance measurements. The solvents had different polarities given by Hansen solubility parameters and nearly the same volume fractions of saturated vapors at the condition of experiment. CNT oxidation significantly increases the sensitivity of CNT resistive sensor to vapors of ethanol and decrease response to heptane vapors. The present paper demonstrates the effective way how to add proper selectivity for organic vapor detection**.**

Introduction

Carbon nanotubes (CNTs) have raised much interest during the recent years due to their inherent extraordinary electrical and mechanical properties [1]. Both principal types of CNT - MWCNT (multi-wall) and show remarkable sensitivity to the change of chemical composition of the surrounding environment. Gas and vapor adsorption as well as desorption usually proceeds at high rates and amounts [2]. This property is favorable for their use in the form of membranes [3], adsorbents [4] or gas sensors [5,6]. It was found that so called "Buckypaper", network prepared from entangled CNT by vacuum filtration can detect organic vapor in air [7].

The oxidation of CNTs has gained a lot of attention in an attempt to purify and also enhance the chemical reactivity of the graphitic network. Typically, through the above harsh treatments, the pristine CNTs can be effectively purified and oxygen-containing groups, mainly carboxyl and hydroxyl, have been found to decorate the graphitic surface [1]. The quality of dispersions for filtration, porosity of prepared buckypaper anyhow tube-tube interactions can by purposely influenced by the proper surface functionalozation such as for example oxidation. There was found that the increasing oxygen content on the surface of CNT leads to buckypaper with more uniform pore structure and dense morphology with lower porosity. It indicates better tube dispersion in the aqueous suspension during filtration process when tubes are deposited as more individualized tubes or as a smaller CNT agglomerates [8].

Even if carbon nanotubes are presently used in indication of gases [9,10], the sensors are quite expensive and difficult to produce. Simpler and cheaper ways to detect gases can be reflected in practical application of described principle. Finally, the present work describes increased sensitivity and achieved selectivity to vapors of ethanol by CNT oxidation.

Experimental

MWCNTs produced by chemical vapor deposition were supplied by Bayer Material Science AG, Germany (diameter 5-20nm, length 1-10μm, C-purity > 99% and bulk density 140-230kg/m^3) [11].

MWCNT networks, "Buckypaper" (MWCNT-N), were prepared by CNT dispersions vacuum filtration thought polyurethane submicron size porous membrane. The formed disk-shaped networks were washed several times by deionized water and methanol in situ, then removed and dried between filter papers at RT. The method of CNT network preparation was several times optimized in aim to achieve uniform and smooth network.

The oxidized material was prepared by following procedure: glass reactor, 300 cm^3 of 0.5M H_2SO_4, 1.5g of $KMnO_4$ and 0.5g of MWCNTs, the dispersion sonicated at 40°C using UP-400S Dr. Hielsher GmbH Apparatus (ultrasonic horn H7, amplitude μm, power density 300W/ cm^3, frequency 24 kHz) for one hour at 50% power of the apparatus and in 50% pulse mode, the product was filtered and washed with concentrated HCl to remove MnO_2.

Results

Fig. 1 represents SEM analyses of upper surfaces of prepared CNT networks on the course of CNT dispersion optimalization. 2a) presents paper fabricated from CNT dispersion prepared by only sonication, 2b) milling of CNT agglomerates before sonication and finally 2c) when milled and sonicated dispersion was centrifuged. Part 2b) represents upper surfaces of CNT network made from $KMnO_4$ oxidized tubes. For next testing of CNT-N structures for gas detection only papers c) and d) were used.

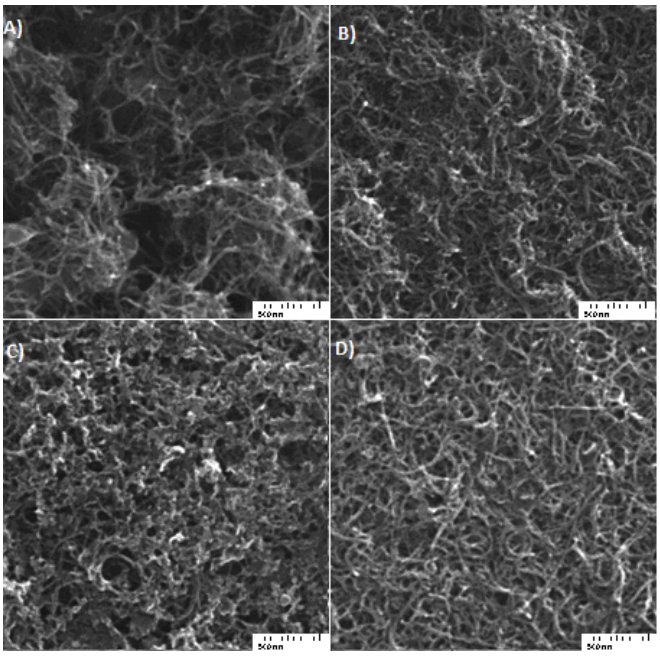

Fig. 1 *Upper surfaces of prepared CNT networks made by SEM analyses.*

The strips made of CNT networks were exposed to the vapors of two different solvents, adsorbates, (heptane, ethanol). The conditions were 25 °C and each adsorption/desorption cycles was 6 minute long. Saturated vapor pressures, p_i, define corresponding volume fractions, x_i. according Eq. 1. where p_A represents air pressure. Calculated values of x_i at experimental conditions are 7.71 % vol. % for ethanol and 6.0 % vol. % for heptane.

$$x_i = \frac{p_i}{p_A} \tag{1}$$

The data in Fig. 2 a) represent two adsorption to/desorption from cycles for specimens made of pure CNT networks exposed to ethanol and heptane. Then Fig. 1 part b) demonstrate analogical data for network made of oxidized tubes. Over all, the adsorption of organics molecules increase resistance with time, which is presented in the figure as sensitivity or gas response, S, defined by Eq. 2.:

$$S = \frac{R_g - R_a}{R_a} = \frac{\Delta R}{R_a} \tag{2}$$

Here R_a represents specimen resistance in air and R_g resistance of the specimen exposed to gas/vapor, ΔR stands for the resistance change. It demonstrates that MWCNT network is sensitive to heptane and ethanol vapors. The curves also presents specific course of adsorption to/desoption form which is reversible and repeatable (5 different specimens were tested for each composition). Finally, part d) presents achieved selectivity of the sensor; when significant increase in sensitivity to ethanol was measured in contrast to decrease of *S* to heptane.

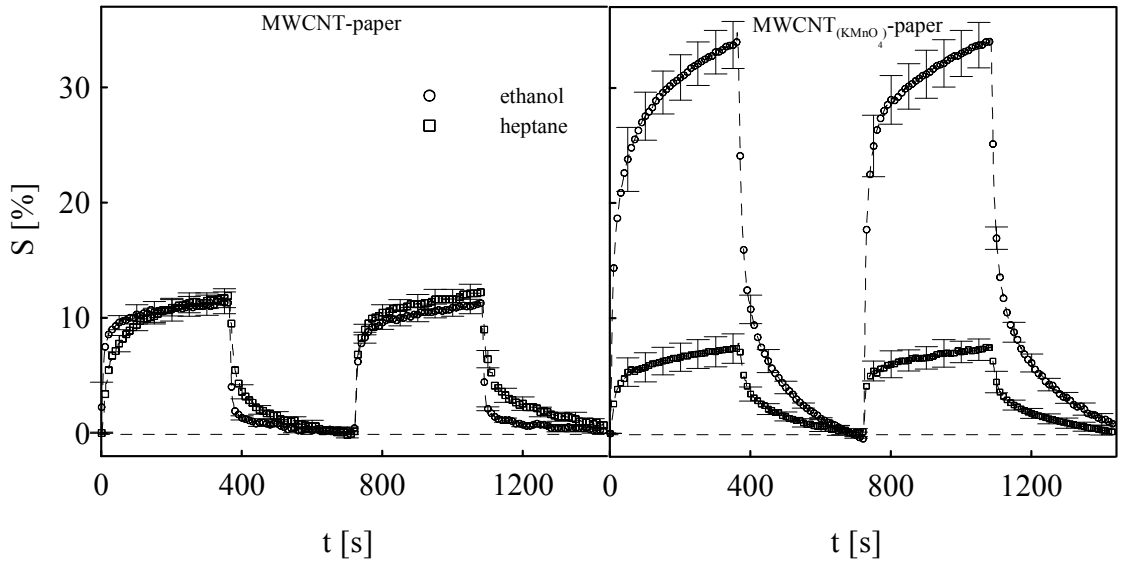

Fig. 2 *Two adsorption/desorption cycles for MWCNT-N (open symbols) and MWCNT-N($KMnO_4$) (filled symbols) exposed to vapors of heptane and ethanol.*

The increased sensitivity is probably caused by CNT oxidation when there should be better affinity of the tubes to more polar ethanol in contrary to nonpolar heptane (Hildebrand solubility parameter, δ_t: heptan = 7,5 $Mpa^{1/2}$, ethanol = 26,5 $Mpa^{1/2}$). X-ray spectroscopy (EDX) proved increase of oxygen content on the surface of CNT from 4.86 at. % on MWCNT-N to 21.26% on MWCNT-N($KMnO_4$).

Conclusions

Multiwall carbon nanotubes were used in their pure and oxidized form to prepare entangled networks (buckypaper) whose response to two organic solvent vapors was measured on the base of electrical resistance. The results show that the prepared materials are capable to detect vapors in the air. The CNT network can be considered as potential material for application as cheap and easy to prepare micro-sized vapor sensing element, which is sensitive, selective, reversible and reproducible. The sensor sensitivity to ethanol vapors was effectively improved by CNT proper oxidation by acidic $KMnO_4$.

Acknowledgment

This project was supported by the internal grant of TBU in Zlín No. IGA/3/FT/11/D funded from the resources of specific university research. This article was also created with support of Operational Programme Research and Development for Innovations co-funded by the European Regional Development Fund (ERDF) and national budget of Czech Republic within the framework of the Centre of Polymer Systems project (reg.number: CZ.1.05/2.1.00/03.0111) and by the Fund of the Institute of Hydrodynamics AV0Z20600510.

Reference

[1] V. Datsyuka, M. Kalyvaa, K. Papagelisb, J. Partheniosa, D. Tasisb, A. Siokoua, I. Kallitsisa,c, C. Galiotisa, *Chemical oxidation of multiwalled carbon nanotubes*. Carbon 46 (2008) 833-840.

[2] Hussain C.M., Saridara C., Mitra S., *Microtrapping characteristics of single and multi-walled carbon nanotubes*. J Chromatogr A 2008;1185(2):161-166.

[3] Smajda R., Kukovecz A., Konya Z., Kiricsi I., *Structure and gas permeability of multi-wall carbon nanotube buckypapers.* Carbon 2007;45(6):1176-1184.

[4] Agnihotri S., Mota J.P.B., Rostam-Abadi M., Rood M.J., *Theoretical and experimental investigation of morphology and temperature effects on adsorption of organic vapors in single-walled carbon nanotubes*. J Phys Chem B 2006;110(15):7640-7647.

[5] Romanenko A.I., Anikeeva O.B., Kuznetsov V.L., Buryakov T.I., Tkachev E.N., Usoltseva A.N., *Influence of helium, hydrogen, oxygen, air and methane on conductivity of multiwalled carbon nanotubes.* Sensor Actuat A-Phys 2007;138(2):350-354.

[6] Qureshi A., Kang W.P., Davidson J.L., Gurbuz Y., *Review on carbon-derived, solid-state, micro and nano sensors for electrochemical sensing application*. Diam Relat Mater 2009;18(12):1401-1420.

[7] P. Slobodian, P. Riha, A. Lengalova, P. Svoboda, P. Saha, *Multi-wall carbon nanotube networks as potential resistive gas sensors for organic vapor detection*, Carbon (2011) 49 2499-2507.

[8] Kastanis D., Tasis D., Papagelis K., Parthertios J., Tsakiroglou C., Galiotis C., *Oxidized multi-walled carbon nanotube film fabrication and characterization*, Adv Compos Lett 16(6) (2007) 243-248.

[9] Niu L., Luo Y.L., Li Z.Q., A *highly selective chemical gas sensor based on functionalization of multi-walled carbon nanotubes with poly(ethylene glycol)*. Sensor Actuat B-Chem 2007;126(2):361-367.

[10] Lobotka P., Kunzo P., Kovacova E., Vavra I., Krozanova Z., Smatko V., Stejskal J., Konyushenko E.N., Omastova M., Spitalsky Z., Micusik M., Krupa I., *Thin polyaniline and polyaniline/cabon nanocomposite films for gas sensing*, Thin Solid Films 519 (2011) 4123-4127

[11] Baytubes, Bayer MaterialSience, on line (cit.1.4.2011) <http://www.baytubes.com/jp/downloads/datasheet_baytubes_c_150_hp.pdf>

Materials and Applications for Sensors and Transducers
10.4028/www.scientific.net/KEM.495

Improved Selectivity of Oxidized Multiwall Carbon Nanotube Network for Detection of Ethanol Vapor
10.4028/www.scientific.net/KEM.495.83